Aus dem Institut für Molekularbiologie und Tumorforschung
Geschäftsführender Direktor: Prof. Dr. Rolf Müller

des Fachbereichs Medizin der Philipps-Universität Marburg

Suppression proinflammatorischer Gene in Makrophagen durch Aszites des Ovarialkarzinoms

Kumulative Dissertation

zur Erlangung des Doktorgrades der Naturwissenschaften

dem Fachbereich Medizin

der Philipps-Universität Marburg

vorgelegt von

Annika Unger

geb. Wortmann

aus Marburg

Marburg, 2018

Angenommen vom Fachbereich Medizin der Philipps-Universität Marburg am: 02. März 2018

Gedruckt mit Genehmigung des Fachbereichs

Dekan: Prof. Dr. Helmut Schäfer
Referent: Dr. Till Adhikary
Korreferent: Prof. Dr. Bernd Schmeck

Inhaltsverzeichnis

Abkürzungsverzeichnis

AA	*Arachidonic acid*
ALA	*α-Linolenic acid*
ANGPTL4	*Angiopoietin-like 4*
BCL	*B-cell lymphoma*
BRCA	*Breast cancer*
CCL	*CC-chemokine ligand 2*
CEFT	Peptidpool aus Cytomegalovirus, Epstein-Barr Virus, Influenza Virus und Tetanus Toxin
CD	*Cluster of differentiation*
C/EBP	CCAAT/*Enhancer binding protein*
ChIP	*Chromatin immunoprecipitation*
CPT1A	*Carnitine palmitoyltransferase I*
CXCL	*Chemokine (C-X-C motif) ligand*
DHA	*Docosahexaenoic acid*
EAE	Experimentelle autoimmune Enzephalomyelitis
EBI3	*Epstein-barr virus induced gene 3*
ECM	*Extracellular matrix*
EMSA	*Elektrophoretic mobility shift assay*
ENPP2	*Ectonucleotide pyrophosphatase/phosphodiesterase 2*
EPA	*Eicosapentaenoic acid*
FACS	*Flourescent activated cell sorting*
GM-CSF	*Granulocyte-macrophage colony-stimulating factor*
H3K4me3	*Trimethylation of lysine 4 on histone H3*
H3K27ac	*Acetylation of lysine 27 on histone H3*
H3K27me3	*Trimethylation of lysine 27 on histone H3*
HGSOC	*High grade serous ovarian carcinoma* (Serös-papilläres Zystadenokarzinom)
ICSBP	*Interferon consensus sequence binding protein*
IDO	Indolamin-2,3-Dioxygenase
IκB	*Inhibitor of nuclear factor κB*
IFN	Interferon
IFNGR	Interferon-gamma Rezeptor
IL	Interleukin
IPA	*Ingenuity Pathway Analysis*

IRF	*Interferon regulatory factor*
ISG15	*Interferon-stimulated gene 15*
JAK	Januskinase
LA	Linolsäure, *Linoleic acid*
LPA	*Lysophosphatidic acid*
LC-MS/MS	*Liquid chromatography–mass spectrometry/mass spectrometry*
LPS	Lipopolysaccharid
LRP5	*Low-density lipoprotein receptor-related protein 5*
LTB4	Leukotrien B4
MCP	*Monocyte chemotactic protein*
MDC	*Myeloid dendritic cell*
MDM	*Monocyte-derived macrophage*
MSDM	*Mendelian susceptibility to mycobacterial disease*
MMP	Matrix-Metalloproteinase
mRNA	*Messenger ribonucleic acid*
NFAT	*Nuclear factor of activated T-cells*
NF-κB	*Nuclear factor kappa-light-chain-enhancer of activated B cells*
NK	Natürliche Killer
NKT	Natürliche Killer-T
PD-1	*Programmed cell death protein 1*
PDK4	Pyruvat Dehydrogenase Kinase 4
PDC	*Plasmacytoid dendritic cell*
PG	Prostaglandin
PPAR	*Peroxisome proliferator-activated receptor*
PPRE	*PPAR response element*
PUFA	*Polyunsaturated fatty acid*
RHD	*REL-homology domain*
RXR	Retinoid-X-Rezeptor
STIC	*Serous tubal intraepithelial carcinoma*
STAT	*Signal transducer and activator of transcription*
TAM	Tumor-assoziierte Makrophagen
TGF	*Transforming growth factor*
T_H	T-Helfer
TLR	*Toll-like* Rezeptor
TP53	Tumor Protein 53
TNF	*Tumor necrosis factor*

TNFSF	*Tumor necrosis factor superfamily*
TSS	*Transcription start site*
TYK	Tyrosinkinase
VCAM	*Vascular cell adhesion molecule*
VEGF	*Vascular endothelial growth factor*
WT	Wildtyp

1 Summary

Since high grade serous ovarian cancer is one of the deadliest cancers in women, efforts to establish new therapies are of great interest. Undoubtedly, the reversion of the suppressive and protumorigenic functions of tumor-associated immune cells would be a significant therapeutic approach.

The interactive network of tumor-associated immune cells and metastatic tumor cells, especially macrophages, is determined to a large extend by the secretome of the peritoneal fluid, which occurs at advanced stages as a malignancy-associated effusion, termed ascites. Published data have shown a correlation of high concentrations of IL-10, IL-6 or TGFβ in ascites with a poor prognosis.

In this thesis, high concentrations of polyunsaturated fatty acids, such as linoleic acid or arachidonic acid, were identified in the ascites as natural agonists of the lipid sensor PPARβ/δ, a member of the nuclear receptor superfamily. In tumor-associated macrophages, high concentrations of these fatty acids, which are stored in intracellular lipid droplets, result in the constitutive overexpression of PPARβ/δ specific target genes. Consistent with this finding, these cells were found to be refractory to synthetic PPARβ/δ agonists *in vitro* but repressible by inhibitory PPARβ/δ ligands. Expression of *ANGPTL4,* one of the major target genes of PPARβ/δ, with functions in metastasis, is associated with a reduced relapse free survival of the patients, underscoring the potential clinical significance of our results.

In human macrophages from healthy donors, we identified two fundamentally different mechanisms of agonist-induced transcriptional regulation of PPARβ/δ target genes. On the one hand, there is the canonical, cell-type-independent induction of different target genes of lipid and glucose metabolism (including *ANGPTL4*) by specific synthetic agonists. On the other hand, a macrophage-specific inverse regulation, which does not require direct PPARβ/δ chromatin binding and mainly affects the regulation of immune functions, could be identified. PPARβ/δ agonists mainly lead to the repression of proinflammatory genes, which might be relevant in view of the predominantly anti-inflammatory effect of the ascites. However, antiinflammatory genes are also repressed by the same ligands. This suggests the induction of a specific, hitherto not described polarisation state of macrophages that is regulated by PPARβ/δ.

In order to gain a better understanding of the protumorigenic macrophages within the tumor microenvironment, the regulation of IL-12, a central cytokine responsible for the proinflammatory functions of macrophages, was investigated in detail. IL-12 is not expressed in TAMs, and is not inducible by Interferon-γ (IFNγ) and lipopolysaccharide in

ascites-treated macrophages from healthy donors. However, the observed reversibility of ascites-mediated suppression by subsequent ascites withdrawal or IFNγ supplementation is potentially interesting from a therapeutical view.

One of the major roles of IL-10 is to repress transcription of *IL12B*, which encodes for the limiting subunit of the IL-12 heterodimer. IL-10 is known to impinge on nuclear translocation of the NF-κB subunits *c*-REL and RELA/p65. Since *IL12B* has been described as an NF-κB target gene, we hypothesized that NF-κB signaling is an important target of ascites-mediated suppression of *IL12B* induction via IL-10. This hypothesis could not be confirmed. The ascites-mediated suppression of *IL12B* indeed coincided with a markedly reduced translocation of *c*-REL and p65/RELA in primary human macrophages *in vitro*. Surprisingly, however, chromatin binding by these factors to a newly identified upstream regulatory binding site was largely unaltered. These findings suggest that besides a possible role for NF-κB, other regulatory mechanisms play an essential role in the suppression of *IL12B* transcription. This conclusion is supported by the finding that another *c*-REL target gene, *CXCL10,* is not repressed by ascites.

Zusammenfassung

Da das seröse Ovarialkarzinom einer der tödlichsten Tumorerkrankungen bei Frauen darstellt, sind neue Therapieansätze von erheblichem Interesse. Eine Reversion der Suppression und protumorigenen Funktionen Tumor-assoziierter Immunzellen wäre dabei zweifellos ein bedeutender therapeutischer Ansatz.

Das interaktive Netzwerk aus Tumor-assoziierten Immunzellen und metastasierenden Tumorzellen, insbesondere Makrophagen, wird maßgeblich über das Sekretom des Aszites bestimmt. Publizierte Daten zeigten bereits eine Korrelation hoher Konzentrationen von IL-10, IL-6 oder TGFβ im Aszites mit einer schlechten Prognose.

Im Rahmen dieser Arbeit konnten mehrfach ungesättigte Fettsäuren wie Linolsäure oder Arachidonsäure im Aszites als natürliche Agonisten des als Lipidsensor fungierenden Kernrezeptors PPARβ/δ identifiziert werden. In Tumor-assoziierten Makrophagen des Aszites führen hohe Konzentrationen dieser Fettsäuren, die in intrazellulären Lipidtröpfchen gespeichert werden, zu einer konstitutiven Überexpression PPARβ/δ-spezifischer Zielgene. Im Einklang mit diesem Befund erwiesen sich diese Zellen als refraktär gegenüber synthetischen PPARβ/δ Agonisten *in vitro,* allerdings reprimierbar durch inhibitorische PPARβ/δ-Liganden. Die Expression von *ANGPTL4,* eines der wichtigsten Zielgene von PPARβ/δ mit Funktionen bei der Metastasierung ist mit einem verkürztem rezidivfreien Überleben der Patientinnen korreliert, was die mögliche klinische Bedeutung unserer Ergebnisse unterstreicht.

In humanen Makrophagen gesunder Spender konnten wir zwei grundsätzlich unterschiedliche Mechanismen einer Agonisten-induzierten transkriptionellen Regulation von PPARβ/δ Zielgenen identifizieren. Zum einen existiert eine kanonische, zelltypunabhängige Induktion verschiedener Zielgene des Lipid- und Glukosemetabolismus (einschließlich *ANGPTL4*) durch spezifische synthetische Agonisten. Zum anderen konnte eine Makrophagen-spezifische inverse Regulation identifiziert werden, die keiner direkten PPARβ/δ-Chromatinbindung bedarf und hauptsächlich die Regulation von Immunfunktionen betrifft. Hierbei führen PPARβ/δ Agonisten hauptsächlich zu einer Repression proinflammatorischer Gene, was im Hinblick auf die vorrangig antiinflammatorische Wirkung des Aszites relevant sein könnte. Allerdings werden durch dieselben Liganden auch antiinflammatorische Gene reprimiert. Dies spricht für die Induktion eines spezifischen, bislang nicht beschriebenen PPARβ/δ–regulierten Polarisierungsstatus der Makrophagen.

Um ein besseres Verständnis der protumorigenen Makrophagen innerhalb des Tumormikromilieus zu erhalten wurde die Regulation von IL-12, einem für die

proinflammatorische Funktion von Makrophagen zentralen Zytokin, näher untersucht. IL-12 ist in TAM nicht exprimiert und ist in Aszites-behandelten Makrophagen gesunder Spender nicht durch proinflammatorische Stimuli, wie Interferon-γ (IFNγ) und Lipopolysaccharid induzierbar. Andererseits könnte die beobachtete Reversibilität der Aszites-vermittelten Suppression durch nachfolgenden Aszitesentzug oder IFNγ Supplementation aus therapeutischer Sicht interessant sein.

Eine wichtige Rolle von IL-10 ist die Repression der Transkription von *IL12B*, das für die limitierende p40 Untereinheit des IL-12 Heterodimers kodiert. IL-10 hemmt bekanntermaßen die Kerntranslokation der NF-κB-Untereinheiten *c*-REL und p65/RELA. Da *IL12B* als NF-κB-Zielgen beschrieben wurde, liegt die Vermutung nahe, dass der NF-κB-Signalweg ein zentrales Ziel der durch Aszites vermittelten, von IL-10 abhängigen Suppression der *IL12B*-Induktion ist. Diese Hypothese konnte allerdings nicht bestätigt werden. Die Behandlung primärer Makrophagen mit Aszites *in vitro* supprimierte zwar die Stimulus-abhängige Transkription von *IL12B* und ging mit einer deutlich verminderten Translokation von *c*-REL und p65/RELA einher. Überraschenderweise erwies sich jedoch die Chromatinbindung dieser Faktoren an eine neu identifizierte, der TSS vorgelagerten Bindestelle des *IL12B* Lokus, als weitgehend unbeeinflusst. Diese Befunde legen nahe, dass neben einer Rolle für NF-κB andere Regulationsmechanismen eine essentielle Rolle bei der Suppression der *IL12B*-Transkription spielen. Diese Schlussfolgerung wird bestärkt durch den Befund, dass ein anderes *c*-REL-Zielgen, *CXCL10*, nicht durch den Aszites reprimiert wird.

2 Einleitung

2.1 Ovarialkarzinom

Das Ovarialkarzinom ist die Haupttodesursache aller gynäkologischen Erkrankungen weltweit (Parkin et al. 2005), (Lengyel 2010), (Jemal et al. 2009). Es betrifft meist Frauen über dem 50. Lebensjahr (Pignata et al. 2011) und beträgt je nach Fortschritt der Erkrankungen zum Zeitpunkt der Diagnose eine 5-Jahres-Überlebensrate von 17-95 % (American Cancer Society, 2017).

Die Besonderheit des Ovarialkarzinoms, im Gegensatz zu anderen Tumorentitäten, liegt darin, dass sich der Tumor sehr leicht über die peritoneale Flüssigkeit ausbreiten kann und es somit zu einer schnellen Progression und Metastasierung kommt. Aufgrund der sich erst in fortgeschrittenem Stadium bemerkbaren Symptome, wird der Krebs in 75 % aller Fälle erst sehr spät diagnostiziert und die Überlebenschancen sinken auf nur 30 % (Lengyel 2010).

Die Klassifizierung des Ovarialkarzinoms unterliegt vielfältigen Faktoren und wird in mehr als fünf verschieden histologische Subtypen unterteilt. Diese unterscheiden sich stark in der Schwere ihrer Ausprägung. Zu den prominentesten Subtypen zählen das Klarzellkarzinom, das endometroide Karzinom, das muzinöse Zystadenokarzinom, das am häufigsten diagnostizierte seröse-papilläre Zystadenokarzinom (high grade serous ovarian carcinoma, HGSOC) und das seröse tubare intraepitheliale Karzinom (serous tubal intraepithelial carcinoma, STIC). Letzteres besitzt ähnliche Eigenschaften wie das HGSOC und wird häufig als Vorläuferstufe des HGSOCs angesehen (Matulonis et al. 2016).

Nebst Punktmutationen von *TP53* (in über 90% aller Fälle) und somatischen Mutationen von *BRCA1* und *BRCA2* spielt die chromosomale Instabilität im HGSOC eine große Rolle. In etwa der Hälfte aller Tumore besteht ein Defekt in der homologen Rekombination (Network 2011).

Die Therapie des HGSOC besteht hauptsächlich in der chirurgischen Entfernung des Tumors mit anschließender Platin-basierter Chemotherapie (Pignata et al. 2011). Der Tumor wirkt zunächst sehr sensitiv gegenüber der Therapie, entwickelt jedoch eine zunehmende Resistenz, welche in den meisten Fällen zu einem Rezidiv der Erkrankung und zu einer niedrigen 5-Jahres-Überlebensrate führt (Bowtell et al. 2015).

2.1.1 Aszites des Ovarialkarzinom

Das Ovarialkarzinom ist gekennzeichnet durch das schnelle Wachstum und die Dissemination des Tumors in den Peritonealraum aufgrund der Akkumulation maligner

Aszitesflüssigkeit (Lengyel 2010). Unter physiologischen Bedingungen werden zwei Drittel der Peritonealflüssigkeit in das lymphatische System reabsorbiert (Feldman and Knapp 1974). Die vermehrte Ansammlung des Aszites im Ovarialkarzinom entsteht höchstwahrscheinlich durch die Dissemination des Tumors und der damit einhergehenden verstärkten Mikrovaskularisierung (Sherer, Eliakim, and Abulafia 2000).

Aufgrund der physiologischen Strömung und Verteilung des Aszites im Peritoneum erfolgt die Metastasierung hauptsächlich an drei Regionen: dem großen Omentum, dem rechten subphrenischen Raum und dem Douglas Raum (Buy et al. 1988).

Neben den Tumorzellen beherbergt der Aszites ein großes Reservoir an löslichen Faktoren, dazu zählen diverse Chemokine, Zytokine, Wachstumsfaktoren und Extrazelluläre Matrix (ECM) Bestandteile (Matte et al. 2012), (G. B. Mills et al. 1988), aber auch Phospholipide wie Lysophosphatidsäure (LPA) (Mukherjee et al. 2012) und dessen Derivate (Shen et al. 2001) sind in hohen Konzentrationen vorhanden. Die Konzentrationen verschiedener Zytokine, darunter IL-10, IL-6 (Reinartz et al. 2014) und Leptin (Matte et al. 2012) korrelieren mit einer schlechten Prognose der Patientinnen. Auch die Expression von *Vascular endothelial growth factor* (VEGF) korreliert mit einer schlechten Prognose aufgrund erhöhter Metastasierung des Tumors (Santin et al. 1999). Hier gibt es bereits erste Erfolge in der Therapie mittels eines humanisierten Antikörpers, Bevacizumab, der mittlerweile standardmäßig in der Therapie angewendet wird (Ferriss et al. 2015).

Neben den löslichen Faktoren besteht der Aszites aus vielen Zellen, die dem Immunsystem entspringen (Worzfeld et al. 2017). Darunter befinden sich Tumor-assoziierte $CD4^+$ / $CD8^+$ T-Zellen, regulatorische T-Zellen (Leffers et al. 2009), natürliche Killerzellen (NK-Zellen) und natürliche Killer-T-Zellen (NKT-Zellen) (Bamias et al. 2007) sowie Zellen monozytären Ursprungs, hauptsächlich Tumor-assoziierte Makrophagen (TAM) (Mantovani et al. 2002), aber auch CCL2-produzierende plasmacytoide dendritische Zellen (PDC) sind in geringer Anzahl vorhanden. Mittels eines anti-CCL2 Antikörpers konnte bereits die Anzahl der regulatorischen T-Zellen, die mit einer schlechten Prognose korrelieren (Giuntoli et al. 2009) minimiert werden (Curiel, Coukos, et al. 2004). Hingegen sind IL-12 produzierende myeloide dendritische Zellen (MDC) nicht im Aszites vorhanden. *In vivo* konnte gezeigt werden, dass durch die Produktion von IL-12 der MDC die Angiogenese gehemmt wird. Der Aszites favorisiert demnach die Anwesenheit von PDC im Gegensatz zu MDC (Curiel, Cheng, et al. 2004).

2.2 Makrophagen

Makrophagen werden den Zellen des angeborenen Immunsystem zugeordnet und entstehen aus hämatopoetischen Vorläuferzellen des Knochenmarks. Eine weitere Population von Makrophagen sind die Gewebsmakrophagen. Diese entstehen sehr früh während der Embryonalentwicklung aus Vorläuferzellen im Dottersack und sind in der Lage sich im Gewebe ständig selbst zu erneuern (Gomez Perdiguero et al. 2014). Makrophagen stellen einen divergenten, adaptiven und plastischen Zelltyp mit vielfältigen Funktionen in der Immunregulation, Gewebshomöostase, Wundheilung, allergischen und chronischen Entzündungsprozessen, der daraus bedingten Krankheitspathogenese und Krebs dar (Sica and Mantovani 2012), (C. D. Mills and Ley 2014). Aus diesem Grund verliert die gängige, binäre Klassifizierung in M1 und M2 Makrophagen, also pro- und antiinflammatorische Makrophagen zunehmend an Bedeutung. Makrophagen werden vielmehr in ein Netzwerk anhand ihrer Herkunft, ihrer Aktivatoren und Marker eingeteilt und koexistieren oft in unterschiedlichen Aktivierungszuständen (Murray et al. 2014), (Sica and Mantovani 2012). *In vitro* werden Makrophagen jedoch häufig in zwei Aktivierungszustände eingeteilt. Mit Hilfe der Zytokine Interleukin-4 (IL-4) und Interleukin-13 (IL-13) werden sie zu einem alternativen Aktivierungszustand und mit Lipopoysacchariden (LPS) und Interferon gamma zu einem starken proinflammatorischen Phänotyp polarisiert (Martinez, Helming, and Gordon 2009), (Chanput et al. 2013). Humane Makrophagen können kein Stickstoffmonoxid als Mechanismus der unspezifischen Immunantwort produzieren (Gross et al. 2014). Somit leiten sie eine starke proinflammatorische Antwort ein, indem sie proinflammatorische Zytokine, wie IL-12 freisetzen und damit eine zytotoxische Antwort von NK- und T-Zellen auslösen (Trinchieri 1995).

2.2.1 Tumor-assoziierte Makrophagen (TAM)

Die Mikroumgebung solider Tumore und die damit verbundenen Entzündungsprozesse spielen in der Tumorigenese eine zentrale Bedeutung und sind Teil der „Hallmarks of cancer“ (Cavallo et al. 2011). Tumor-assoziierte Makrophagen dienen oft der Verbindung von Entzündungsprozessen und Kanzerogenese. Sie sind in der Lage die Tumorzellproliferation und Angiogenese zu steigern, fördern die Matrixreorganisation und reprimieren die Immunantwort. Sie stellen somit ein sehr interessantes therapeutisches Ziel in der Bekämpfung diverser Krebserkrankungen, darunter dem Ovarialkarzinom, dar (Solinas et al. 2009), (Mantovani and Locati 2013), (Mantovani et al. 2002).

Die Hauptsignalwege und Transkriptionsfaktoren, welche in Korrelation mit einem protumorigenen Phänotyp von TAM stehen sind NF-κB, STAT1, STAT3, STAT6, IRF3 und C/EBPβ (Antonio Sica and Bronte 2007). In TAM wird ein funktioneller STAT1/ IRF3 Signalweg beschrieben, der zu einer hohen Expression von IL-10 im Fibrosarkom Modell führt (Subhra K. Biswas et al. 2006). Des Weiteren kommt es in Mäusen zu einem verstärkten Tumorwachstum nach Stat1 Depletion (Kaplan et al. 1998) und einer STAT1 vermittelten funktionellen T-Zell Antwort in TAM (Kusmartsev and Gabrilovich 2005).

Im Ovarialkarzinom konnte gezeigt werden, dass es aufgrund einer hohen Expression der Zytokine IL-10 und *transforming growth factor-ß* (TGF-ß) oder Arginase-1 von TAM zu einer immunsuppressiven Mikroumgebung des infiltrierenden Tumors kommt (Hao et al. 2012), (Santin et al. 2001). Im HGSOC nehmen Tumor-assoziierten Makrophagen einen gemischten Polarisierungszustand ein, bei dem die Anzahl dieser Makrophagen im Aszites, bzw. die hohe Expression antiinflammatorischer Marker wie CD163 und IL-10 negativ mit dem rückfallfreien Überleben der Patientinnen korrelieren (Reinartz et al. 2014).

Jedoch wurde in weiteren eigenen Studien gezeigt, dass TAM im Ovarialkarzinoms ein ähnliches Transkriptom und Polarisierungsmarker wie peritoneale Makrophagen von Patientinnen mit benignen Erkrankungen besitzen. Der einzige Unterschied konnte in der Expression von Genen festgestellt werden, die die extrazelluläre Matrix und somit Wundheilung und Tumorigenese betreffen (Finkernagel et al. 2016).

TAM des HGSOC können anhand der Expression einer Interferon-regulierten Gruppe von Genen in zwei distinkte Gruppen unterteilt werden. Die Gruppe mit verstärktem IFN *Signaling* zeigte einen deutlich verbesserten klinischen Verlauf im Vergleich zu einer Gruppe mit niedriger IFN-Antwort (Adhikary et al. 2017). Des Weiteren konnte bereits gezeigt werden, dass unter 32 Zytokinen allein IFNγ in der Lage ist den immunsuppressiven, protumorigenen IL-12^{low}, IL-10^{high} Phänotyp zu revertieren (Duluc et al. 2009), (Adhikary et al. 2017). Zusammengefasst lässt dies vermuten, dass TAM antiinflammatorischen Peritonealmakrophagen ähneln, wie sie bei nicht an Tumoren erkrankten Patienten anzutreffen sind, und zumindest ein Teil der Population die Fähigkeit besitzen könnte, pro-inflammatorische und anti-tumorigene Transkripte zu exprimieren.

2.3 NF-κB

NF-κB ist einer der wichtigsten Regulatoren in Immunfunktionen und Entzündungsprozessen. NF-κB wurde 1986 erstmals erwähnt von Sen und Baltimore, als κ- light chain bindendes Protein in B-Zellen im *Elektrophoretic-mobility-shift-Assays* (EMSA) (Sen and Baltimore 1986). Heutzutage ist jedoch allgemein bekannt, dass die meisten der fünf Mitglieder der NF-κB Familie ubiquitär exprimiert werden. Zu diesen zählen NF-κB1 (p50), NF-κB2 (p52) und die zugehörigen Vorläuferproteine p105, bzw. p100, RELA (p65), *c*-REL und RELB (Liou and Baltimore 1993). Allen Familienmitgliedern gemeinsam ist eine REL-*homology domain* (RHD). Diese Region dient der Heterodimerisierung mit anderen Familienmitgliedern, der Homodimersierung, der Translokation in den Kern und DNA-Bindung sowie der Interaktion mit den inhibitorischen Proteinen, den IκBs. Darüber hinaus besitzen REL Proteine Transaktivierungsdomänen, die zur Transkription diverser proinflammatorischer Zielgenen führen können (Thanos and Maniatis 1995).

NF-κB unterliegt nicht der Regulation durch *de novo* Synthese, sondern liegt als primärer Faktor inaktiv im Zytoplasma vor und wird nach Aktivierung aufgrund der Ubiquitinierung und proteasomalen Degradierung der inhibitorischen Proteine in den Nukleus an responsive Zielgene transportiert und bindet dort an die Konsensussequenz 5'GGGRAYYYYY-3' (Baeuerle 1994).

Die IκB Familie lässt sich in zwei Gruppen einteilen. Die klassischen, zytoplasmatischen Mitglieder IκBα, IκBβ, IκBε und die atypischen, kernständigen Proteine BCL-3, IκBζ, $I\kappa B_{NS}$, IκBη und IκBL (Annemann et al. 2016). Jeder dieser Faktoren besitzt sich wiederholende Ankyrin Elemente, diese dienen der Proteinstabilität der REL-Proteine und der Interaktion mit der DNA-Bindungsdomäne der NF-κB-Proteine und halten diese in einem transkriptionell inaktiven Zustand. p105 und p100 besitzen als Vorläuferproteine ebenfalls Ankyrin Elemente und sind somit eigene Inhibitoren der aktiven Spaltprodukte p50 und p52 (Hoesel and Schmid 2013).

Da RELA eine hohe „Turn-over" Rate besitzt, was als Sicherheitsmechanismus gegen einen Verlust des Signalweges gedeutet werden kann, besitzt NF-κB neben seiner Funktion in der zellulären Immunität eine entscheidende Rolle als Überlebensfaktor, vor allem auch in Tumorzellen. Aus diesem Grund ist ein kompletter Ausfall des Signalweges für die Zelle nicht von Vorteil und somit meist nicht vorhanden (Piva, Belardo, and Santoro 2006), (Wagner et al. 2015), (Ashall et al. 2009).

Der NF-κB Signalweg ist auch einer der wichtigsten Signalwege während der Polarisierung Tumor-assoziierter Makrophagen zu einem protumorigenen Phänotyp (S.

K. Biswas and Lewis 2010). In vielen Tumoren wurde dieser Gruppe von Transkriptionsfaktoren eine entscheidende Rolle bei der Entstehung von Krebs zugeschrieben. Die Hauptursache scheint ein deregulierter Signalweg zu sein, (Subhra K. Biswas et al. 2006), der über die Überexpression des inhibitorischen p50 Proteins erfolgt und zu einer verminderten IL-12p40 und TNFα Expression (A. Saccani et al. 2006) und erhöhten STAT1-Phosphorylierung führt (Subhra K. Biswas et al. 2006). Aber auch der konstitutive Erhalt des NF-κB Weges könnte von Bedeutung sein (Hagemann et al. 2008). Auch die physikalischen Interaktionen der NF-κB-Transkriptionsfaktoren und die Wechselwirkungen des Signalweges mit anderen Transkriptionsfaktoren wie STAT3 oder p53 ist von zentraler Bedeutung (Hoesel and Schmid 2013).

Im Gegensatz dazu führt die Aktivierung des NF-κB Weges im Ovarialkarzinom zur Aktivierung von NK Zellen aufgrund einer erhöhten Expression von löslichem Interleukin-18 (Bellora et al. 2014). Eine Antitumorresponsivität und Reversibilität protumorigener TAM wurde erzeugt durch eine kombinierte Behandlung von CpG Oligonukleotiden, die eine TLR9 Antwort auslösen, und einem antagonistisch wirkenden anti-IL-10 Rezeptor spezifischen Antikörper (Guiducci et al. 2005).

2.4 Interleukin 12 (IL-12)

Schon während der Entdeckung des Zytokins IL-12 im Jahr 1989 erkannte man seine Besonderheit. Bis dato war es das erste und einzige Zytokin, dass als Heterodimer (IL-12p70), bestehend aus den zwei Untereinheiten p40 und p35, vorlag. Es wurde als NK-Zell-stimulierendes Protein beschrieben und führt zur IFNγ Produktion durch Zielzellen (Kobayashi et al. 1989). Erst nach mehr als zehn Jahren wurde bekannt, dass IL-12 zu einer Gruppe von vier heterodimerisierenden Zytokinen gehört.

Die IL-12 Familie besitzt eine zentrale Rolle in der Immunregulation. Neben seiner Funktion in der Regulation verschiedener T-Zell Populationen hat IL-12 Einfluss auf die Entwicklung dieser Zellen. Während IL-12 und IL-23 allgemein proinflammatorische Zytokine induzieren und die Entwicklung der proinflammatorischen T_H1 und T_H17 Zellen regulieren, üben IL-27 und IL-35 eher eine suppressive Funktion auf das Immunsystem aus indem sie die Polarisierung zu regulatorischen T-Zellen fördern (Vignali and Kuchroo 2012).

IL-23 besteht aus der Untereinheit p19, welche allein biologisch inaktiv ist, und der Untereinheit p40. IL-23 besitzt zwar strukturelle Ähnlichkeiten zu IL-12, hat aber eine differentielle Rolle in der Immunabwehr (McKenzie, Kastelein, and Cua 2006). IL-23 ist der Hauptmediator der IL-17 Produktion von Gedächtnis T-Zellen, führt allerdings nicht zu deren Differenzierung (Bettelli et al. 2006). Exogen überexprimiertes IL-23 führt über

Gedächtnis-T-Zellen zu einem anti-tumoralen Effekt, wohingegen eine endogene Expression von IL-23 die Tumorinzidenz und das Tumorwachstum fördert (Langowski et al. 2006).

STAT3 ist in vielen Tumoren aufgrund verstärkter DNA-Bindung konstitutiv aktiv (Yu and Jove 2004). Über immunsuppressive Faktoren, wie IL-10, wird STAT3 aktiviert und führt zu einem antiinflammatorischen Effekt, indem es die Produktion proinflammatorischer Mediatoren wie IL-12 unterbindet, jedoch die Induktion von IL-23 fördert. Dies funktioniert hauptsächlich über die Aktivierung von IL-23p19 durch RelA. Im Gegensatz dazu wird die durch *c*-Rel induzierte Expression von IL-12p35 in Tumor-assoziierten dendritischen Zellen von Stat3 verhindert (Kortylewski et al. 2009).

IL-12 wird von antigen-präsentierenden Zellen, hauptsächlich von Makrophagen und dendritischen Zellen aufgrund diverser Stimuli, darunter LPS und IFNγ sezerniert. Die Signalkaskade wird von IL-12 durch dessen Bindung an Transmembranrezeptoren ausgeübt. Die p35 Untereinheit von IL-12 bindet an den IL-12 Rezeptor IL-12Rβ2, p40 an den IL-12Rβ1. Neben der Proliferation von NK- und T-Zellen führt die Aktivierung von STAT4 über IL-12 zu der Generierung und Aktivierung von zytotoxischen T-Zellen. Einer der wichtigsten regulatorischen Signalwege der IL-12 (Sanjabi et al. 2000), (Grumont et al. 2001) und IL-23 (Carmody et al. 2007) Transkription ist NF-κB und im speziellen der Transkriptionsfaktor *c*-Rel (Rahim et al. 2005). Sanjabi *et al* konnten zeigen, dass im Gegensatz zu p65 knockout Mäusen *c*-Rel knockout Mäuse drastisch reduzierte *Il12b* mRNA und Proteinlevel aufzeigten (Sanjabi et al. 2000). Auch konnte für die Expression von p35 in $CD8^+$ dendritischen Zellen die Abhängigkeit von *c*-Rel-Komplexen aufgezeigt werden (Grumont et al. 2001). Neben *c*-Rel gilt das Interferon-Konsensus-Sequenz-bindende Protein (Icsbp/Irf8) als weiterer wichtiger Faktor für die *Il12b* Expression, da in Irf8 knockout Mäusen weder *Il12b* Transkription noch Promotoraktivität in Reportergenassays nachgewiesen werden konnte und dies vollständig durch ektopische Irf8 Expression aufgehoben wurde (Wang et al. 2000).

Um eine maximale IL-12p70 Antwort zu erreichen werden jedoch weitere aktivierende Faktoren wie STAT1, IRF1 (Liu et al. 2003) und IRF8 (Wang et al. 2000) benötigt (Wagner et al. 2015). Über einen positiven Rückkopplungsmechanismus wird die IL-12 Antwort zusätzlich gesteigert. Die von IL-12 induzierte IFNγ Produktion durch T-Zellen erhöht die Produktion von IL-12 in antigen-präsentierenden Zellen und verstärkt zusätzlich die T_H1 Antwort (Becskei and Grusby 2007). Im Gegensatz dazu konnte mittels siRNA Experimenten gegen *TYK2*, einer Tyrosinkinase der Januskinase (JAK) Familie und *RELB* eine erhöhte IL-12 Sekretion gemessen werden (Wagner et al. 2015).

Die bedeutende Rolle des IFNγ-Signalweges in der IL-12 Regulation zeigten auch Studien der „*Mendelian susceptibility to Mycobacterial disease*“ (MSDM). Die erhöhte Anfälligkeit gegenüber mykobakteriellen Infektionen konnte u.a. auf genetische Defekte in *IFNGR1*, *IFNGR2*, *STAT1*, *IL12B* und *IL12RB1*, *ISG15* und *IRF8* zurückgeführt werden (Bustamante et al. 2014).

Neben pathogenspezifischen Stimuli, welche die IL-12 Signalkaskade aktivieren, gibt es auch endogene Signale wie den CD40 Liganden, die zur Aktivierung des Signalweges führen. CD40L alleine führt allerdings zur Induktion von IL-10. Erst in Kombination mit weiteren Stimuli wie GM-CSF, IL-4 und IFNγ kommt es zu einer IL-12 Induktion (Conzelmann et al. 2010).

IL-12p70 besitzt eine herausragende Rolle in der Vernetzung des angeborenen und adaptiven Immunsystems. Letztendlich führt die Sekretion des Proteins zu einer T_H1 Differenzierung und zytotoxischen Aktivität von NK- und T-Zellen (Trinchieri 1995). IL-12 spielt in der antitumoralen-Aktivität eine bedeutende Rolle. Viele Arbeiten in Maus-Tumormodellen zeigten ein teils komplett inhibiertes Tumorwachstum nach peritumoraler Injektion von IL-12 in subkutane Renca Tumore (Brunda et al. 1993). In klinischen Studien zeigte IL-12 jedoch noch keine Erfolge aufgrund systemischer Toxizitäten und einer geringen Wirksamkeit, hervorgerufen durch dominantere, immunsuppressive Faktoren im Tumormilieu (Beyer and Schultze 2006), (Portielje et al. 2003), (Haicheur et al. 2000).

IL12-p40 kann als Monomer oder Homodimer (IL-12p80) eine antagonistische Wirkung auf IL-12 haben und immunsuppressiv wirken, indem es kompetitiv an den IL-12 Rezeptor bindet und so einen negativen Rückkopplungsmechanismus ausübt (Cooper and Khader 2007).

Die Synthese von IL-10 und IL-12 unterliegt *in vivo* einem Kreislauf und gegenseitiger Kontrolle. Kommt es jedoch zu einem Ungleichgewicht, hat dies gravierende Folgen auf die Polarisierung und Reaktion von Makrophagen auf das Immunsystem (Segal, Dwyer, and Shevach 1998), (Xiaoyu Hu, Chakravarty, and Ivashkiv 2008).

Wie bereits erwähnt inhibiert IL-10 über STAT3 die Synthese von IL-12. Dies erfolgt durch die Suppression von *IL12B* und *IL12A* auf transkriptioneller Ebene. Diese inhibitorische Aktivität von IL-10 auf die Expression von p40 kann durch Cycloheximid, einem Translationsinhibitor unterbunden werden. Dies trifft allerdings nicht auf p35 zu. Die transkriptionelle Regulation der Untereinheiten von IL-12, p35 und p40 scheint nicht identisch zu sein. Da der Translationsblocker in LPS oder *S.aureus* behandelten Zellen lediglich das *IL12B* und nicht das *IL12A* mRNA Level und die Transkription vollständig

inhibieren konnte, wird p35 vermutlich über bereits vorhandene Transkriptionsfaktoren reguliert, wohingegen die Regulation der *IL12B* Transkription einer *de novo* Proteinsynthese unterliegt (Aste-Amezaga et al. 1998).

Auch Adenosin führt zu einer Suppression von IL-12 über A2A Rezeptor abhängige und unabhängige Mechanismen. In einer Studie wurde gezeigt, dass Adenosin zu einer verstärkten IL-10 Produktion in Maus Makrophagen führt, die Suppression von IL-12 hier jedoch unabhängig von IL-10 erfolgt (HASKO 2000).

2.5 Peroxisomen-Proliferator-aktivierte Rezeptoren (PPAR)

Makrophagen sind nicht nur zentrale Regulatoren von Immunreaktionen durch Sekretion proinflammatorischer Zytokine, sondern besitzen als residente Zellen eine sehr wichtige Rolle in der Wundheilung und im Metabolismus. In diesen alternativ aktivierten Makrophagen steht die Regulation der Homöostase im Vordergrund. Kang und Odegaard et. al beschrieben den Kernrezeptor PPARβ/δ als maßgeblichen Regulator der alternativen Aktivierung von Makrophagen in Kupffer Zellen der Leber und im Fettgewebe (Kang et al. 2008b), (Odegaard et al. 2008).

Peroxisomen-Proliferator-aktivierte Rezeptoren (PPAR) sind lipidregulierte Kernrezeptoren und wurden ursprünglich als Regulatoren der β-Oxidation in Peroxisomen identifiziert (Issemann and Green 1990). PPARs umfassen drei Isoformen: PPARα, PPARβ/δ und PPARγ (Desvergne and Wahli 1999). Allen gemeinsam ist ihre Rolle im Lipid- und Glukosemetabolismus. PPARα wird hauptsächlich in der Leber, im braunen Fettgewebe und Geweben mit hohem Fettsäurekatabolismus wie Herz, Niere, Dünndarmarm und Skelettmuskel exprimiert. PPARβ/δ ist ein ubiquitär exprimierter Faktor, gehäuft kommt er jedoch in Hirn, Gastrointestinaltrakt und Dickdarm vor (Escher et al. 2001), (Braissant et al. 1996). PPARγ wird sowohl im Dickdarm, in der Retina, in den Skelettmuskeln und lymphoiden Organen als auch verstärkt in weißem und braunem Fettgewebe exprimiert (Rosen and Spiegelman 2001).

PPAR bindet zusammen mit dem Heterodimerisierungspartner Retinoid-X-Rezeptor (RXR) an die PPAR Responsiven Elemente (PPREs) in Kontrollregionen der entsprechenden Zielgene. Durch PPARβ/δ kommt es entweder zu einer Liganden-unabhängigen Repression, zu einer Liganden-abhängigen Aktivierung bzw. Derepression oder zu einer Liganden-unabhängigen Aktivierung der Zielgen-Transkription (Adhikary et al. 2011).

Mehrfach ungesättigte Fettsäuren wie Arachidonsäure und Linolsäure wirken als Agonisten aller drei Subtypen. Eicosanoide wie Leukotrien B4 (LTB4) oder 8S-HETE sind physiologische Liganden von PPARα. Prostaglandin J2 ist ein physiologischer

Agonist für PPARγ (Barry M. Forman et al. 1995) und 15-HETE ist ein PPARβ/δ selektiver Agonist (Naruhn et al. 2009), (Kostadinova, Wahli, and Michalik 2005).

Aufgrund der Korrelation erhöhter Fettsäurewerte mit Adipositas, Diabetes, Arteriosklerose und Blutdochdruck, stellen PPARs einen wichtigen Regulator und auch therapeutisch vielversprechende Zielstrukturen in der Bekämpfung metabolischer Erkrankungen dar (B M Forman, Chen, and Evans 1997).

Neben physiologischen Liganden wurden in den letzten Jahren auch selektive synthetische Agonisten hergestellt. Hierzu zählen Rosiglitazon und Pioglitazon, selektiv für PPARγ, die bereits erfolgreich in der Behandlung von Diabetes Mellitus Typ 2 eingesetzt werden. Fibrate wie Bezafibrat und Gemfibrozil für PPARα, die zur Behandlung von Dislipidämien verabreicht werden (Kostadinova, Wahli, and Michalik 2005) und die selektiven Agonisten GW501516, L165,041, GW0742 und GW2433 für PPARβ/δ (Sznaidman et al. 2003), (Peraza et al. 2006), (Sen and Baltimore 1986).

Neben dem Einsatz PPAR selektiver Liganden ist auch der Einsatz inverser Agonisten von therapeutischem Interesse. Inverse Agonisten führen im Vergleich zu Agonisten zur transkriptionellen Repression kanonischer PPAR-Zielgene. Der inverse PPARβ/δ Agonist ST247 ist hochaffin zu PPARβ/δ und führt zu dessen verstärkter Interaktion mit Korepressoren und reprimiert so die basale Expression von PPARβ/δ-spezifischen Zielgenen wie *ANGPTL4* (Naruhn et al. 2011). Des Weiteren vermindert er durch kompetetive Bindung Agonisten-induzierte transkriptionelle Aktivität. Eine verbesserte Bioverfügbarkeit bietet jedoch der der strukturell ähnliche inverse Agonist PT-S264 (Toth et al. 2016).

2.5.1 PPARβ/δ als Immunmodulator

PPARβ/δ besitzt neben seiner Funktion im Glukose- und Lipidmetabolismus, vor allem in der Fettsäureoxidation, zusätzliche Funktionen in der Karzinogenese (T. Adhikary et al. 2013), der Differenzierung und Apoptose und auch eine zentrale Rolle in der Immunregulation, indem er den inflammatorischen Status in Makrophagen kontrolliert (Müller 2017).

Die proinflammatorische Rolle des Rezeptors konnte zum einen in Pparβ/δ knockout Makrophagen gezeigt werden, in denen die proinflammatorischen Zytokine IL-1ß, MMP9 und das Chemoattraktant MCP-1 durch den spezifischen Agonisten GW501516 herunterreguliert werden (C.-H. Lee 2003). Auch in Psoriasis, einer Autoimmunerkrankung der Haut, waren *PPARD* mRNA und Proteinlevel drastisch erhöht (Westergaard et al. 2003), (Romanowska et al. 2010).

Auf der anderen Seite besitzt PPARβ/δ allerdings auch eine antiinflammatorische Rolle, was in mehreren Studien gezeigt werden konnte.

In eigenen Analysen konnte ein Zusammenhang von PPARβ/δ und anti- bzw. proinflammatorischen Signalwegen wie TGFβ und IL-1β gezeigt werden (Kaddatz et al. 2010), (Stockert et al. 2013, 2011). Des Weiteren verringerten PPAR Agonisten die *VCAM1* Expression und reduzierten drastisch die p65 Translokation in endothelialen Zellen (Rival et al. 2002). Auch die Aktivierung von PPARβ/δ in Fibroblasten führte zu einer Inhibition des IL-1 Signalweges (Chong et al. 2009). Die Expression von T_H2 Zytokinen wie IL-13 und IL-4 antiinflammatorischer Adipozyten führte in Kokultur über PPARβ/δ zu einer alternativen Polarisierung adipozytärer Gewebsmakrophagen (Kang et al. 2008a). PPARβ/δ Agonisten mindern außerdem die experimentelle autoimmune Enzephalomyelitis (EAE) im Mausmodell, indem sie die IFNγ und IL-17 Produktion der T_H1 und T_H17 Zellen blockieren, IL-12 und IL-23 inhibieren und gleichzeitig die IL-4 und IL-10 Produktion steigern (Kanakasabai et al. 2010).

2.6 Ziel der vorliegenden Arbeit

Bis zum heutigen Zeitpunkt ist die Rolle löslicher Mediatoren der Tumormikroumgebung bei der Immunsuppression und pro-tumorigenen Polarisierung von Tumor-assoziierten Makrophagen im menschlichen Ovarialkarzinom nur ansatzweise verstanden. Besonders proinflammatorische Signalwege wie der NF-κB Signalweg werden kontrovers in diesem Zusammenhang diskutiert.

Ziel der vorliegenden Arbeit war es den Einfluss spezifischer Faktoren des Aszites auf zwei zentrale Transkriptionsfaktoren zu untersuchen, und zwar den lipidresponsiven Kernrezeptor PPARβ/δ sowie den zytokinregulierten Transkriptionsfaktor NF-κB. Dabei sollten auch die Regulation von Immunfunktionen durch PPARβ/δ sowie die Rolle von spezifischen Mitgliedern der NF-κB-Familie bei der Regulation von IL-12, ein für die Funktion inflammatorischer Makrophagen zentrales Zytokin, näher untersucht werden.

3 Ergebnisse

3.1 Deregulation of PPARβ/δ target genes in tumor-associated macrophages by fatty acid ligands in the ovarian cancer microenvironment

Tim Schumann*, Till Adhikary*, **Annika Wortmann***, Florian Finkernagel, Sonja Lieber, Evelyn Schnitzer, Nathalie Legrand, Yvonne Schober, W. Andreas Nockher, Philipp M. Toth, Wibke E. Diederich, Andrea Nist, Thorsten Stiewe, Uwe Wagner, Silke Reinartz, Sabine Müller-Brüsselbach and Rolf Müller (2015) Oncotarget 6(15): 13416-33
* These authors contributed equally to the paper as first authors.

Eine der häufigsten Begleiterscheinungen des Ovarialkarzinoms ist ein maligner Aszites, der neben Tumorzellen und antiinflammatorischen Mediatoren eine große Anzahl an Immunzellen, insbesondere Tumor-assoziierte Makrophagen beinhaltet. Eine hohe Anzahl an Tumor-assoziierten Makrophagen korreliert mit einer schlechten Überlebensprognose der Patientinnen. Aufgrund sezernierter Chemokine, Zytokine und weiterer antiinflammatorischer Mediatoren besitzt dieser Zelltyp eine hohe Plastizität und einen gemischten pro- als auch antiinflammatorischen Phänotyp.

In dieser Publikation konnte nach Lipidomanalysen gezeigt werden, dass sich im Aszites eine Reihe mehrfach ungesättigter Fettsäuren befinden. Diese Lipide, vorangestellt Linolsäure, wirken als physiologische Liganden für den Transkriptionsfaktor PPARβ/δ, ein Typ II Kernrezeptor, der neben wichtigen Aufgaben im Fettsäuremetabolismus maßgeblich an der Makrophagenpolarisation beteiligt ist.

Tumor-assoziierte Makrophagen besitzen einen divergenten, eher antiinflammatorischen Phänotyp, mit einer hohen Expression des *scavenger rezeptor CD163* und einer niedrigen Expression der Matrixmetalloprotease *MMP9* (Abbildung 1A). Mikroskopisch auffällig ist, dass dieser Phänotyp einem durch einen synthetischen Agonisten (L165,041) für PPARβ/δ induzierbaren Phänotyp in Makrophagen gleicht und nicht durch zusätzliche Gabe des synthetischen Liganden L165,041 verändert wird (Abbildung 1B).

Als *in vitro* Modellsystem zur Aufklärung der Ligandenfunktion in TAM eignen sich hervorragend Monozyten-abgeleitete Makrophagen (MDM), da sie eine vergleichbar hohe messbare DNA-Bindung von PPARβ/δ und seinem Heterodimerisierungspartner RXR an den genomischen *PDK4* Enhancer Bereich besitzen. Im Gegensatz dazu besitzen frisch isolierte Monozyten eine deutlich reduzierte Anwesenheit von PPARβ/δ

und RXR an dieser Region und wurden demzufolge als Modellsystem ausgeschlossen (Abbildung 2A). Im Einklang hiermit war die geringe Expression von *PPARD* in Monozyten.

Zur globalen Analyse der Liganden-abhängigen Effekte von PPARβ/δ in Makrophagen oder Tumor-assoziierten Makrophagen wurden genomweite Studien mittels RNA Sequenzierung durchgeführt. Es konnten direkte, durch Agonisten induzierte oder durch inverse Agonisten reprimierte Zielgene in MDM als auch in Aszites kultivierten TAM identifiziert werden. Hierbei zeigte sich erneut, dass TAM im Vergleich zu MDM nicht responsiv auf synthetische Agonisten sind. Des Weiteren wurde in TAM eine größere Anzahl an Genen gefunden, die durch inverse Agonisten reprimiert werden. Diese Ergebnisse verdeutlichten, dass der Aszites vermutlich hohe Spiegel an physiologischen PPARβ/δ Agonisten beinhaltet (Abbildung 2B, C). Auch ChIP Sequenzierungsdaten unterstützten diese Erkenntnis, da es eine große Übereinstimmung der Bindungsstellen von PPARβ/δ und RXR in MDM und in Aszites kultivierten TAM gab (Abbildung 2E, F). Somit scheint die erhöhte Expression direkter PPARβ/δ-Zielgene in TAM nicht durch veränderte DNA-Bindung des Rezeptors verursacht zu sein. Um zu überprüfen, ob der Verlust der Ligandenregulation in TAM durch Aszites stabil ist, wurden TAM in herkömmlichem Medium kultiviert und der Ligandeneffekt analysiert. Hierbei zeigte sich, dass es lediglich zu einer gering gesteigerten Induktion kanonischer Zielgene von PPARβ/δ (*PDK4* und *ANGPTL4*) in TAM kam. Somit veranlasst der Aszites eine sehr stabile Veränderung der Makrophagen im Hinblick auf die Responsivität synthetischer PPARβ/δ Liganden (Abbildung 2D).

Etwa die Hälfte aller induzierten Gene in kultivierten TAM zeigten auch eine erhöhte und durch Agonisten unbeeinflussbare Expression in *ex vivo* TAM (Abbildung 3A, B, C). Diese Deregulation betraf unter anderem die Expression der kanonischen PPARβ/δ Zielgene *PDK4*, *ANGPTL4* und *CPT1A* (Abbildung 3D) und die Proteinexpression von PDK4 (Abbildung 3E). ANGPTL4 ist in diesem Zusammenhang besonders hervorzuheben, da dessen Expression mit einer schlechten Prognose der Patientinnen mit HGSOC korreliert (Abbildung 3F, G) und es eine zentrale Rolle während der Metastasierung und Invasion spielt.

Weitere Funktionen der induzierten Transkripte in *ex vivo* TAM konnten mittels IPA (*Ingenuity Pathway Analysis*) überwiegend dem Glukose- und Lipidmetabolismus, Entzündungsfunktionen, Zellmigration als auch dem Überleben zugeordnet werden (Abbildung 4A). Deren wichtigste identifizierte Regulatoren sind die PPAR Liganden Bezafibrat, Eicosapentaensäure (EPA), Lipopolysaccharide (LPS), Rosiglitazon und Pirinixinsäure (Abbildung 4B).

Zur Verifizierung der Aszites vermittelten Deregulation von PPARβ/δ Zielgenen in TAM wurden MDM gesunder Spender in Aszites kultiviert und die Expression mehrerer PPARβ/δ Zielgene untersucht. Die in Abbildung 5A und 5B dargestellten Gene zeigten eine deutlich erhöhte Expression nach Aszitesbehandlung (ähnlich der Induktion durch L165,041) im Vergleich zur Kontrollgruppe. Auch hatte die zusätzliche Stimulation mit L165,041 im Aszites keinen Einfluss mehr (Abbildung 5B).

Um zu zeigen, dass die Deregulation der Zielgene im Aszites vornehmlich PPARβ/δ vermittelt ist, wurden Luziferase-Reportergenassays am *PDK4* Enhancer durchgeführt, die der Kontrolle von mutierten oder funktionsfähigen PPREs unterliegen. Hierbei zeigte sich, dass die durch Aszites induzierte Luziferaseaktiviät bei mutierten PPREs deutlich vermindert wurde, wohingegen der Aszites bei den Wildtyp-PPRE-Sequenzen eine sehr starke Reportergenaktivität verursachte (Abbildung 5C).

Nicht nur in humanen Makrophagen, sondern auch in Maus-Knochenmarksmakrophagen konnte eine Aszites vermittelte Deregulation der Pparβ/δ Zielgene *Pdk4* und *Angptl4* nachgewiesen werden. In Mäusen mit Pparβ/δ knockout kam es zu einem Verlust dieser Regulation (Abbildung 5D).

Alle bisher bekannten PPARβ/δ Agonisten sind Fettsäuren oder Fettsäurederivate. Da diese in Makrophagen in intrazelluläre Lipidtröpfchen eingelagert werden und auch noch mehrere Tage nach Wegnahme des Aszites oder der gesondert zugeführten mehrfach ungesättigten Fettsäuren (PUFAs) noch nachweisbar sind, scheint die Deregulation in Makrophagen sehr stabil zu sein (Abbildung 7A-F). Zur genaueren Identifikation der Fettsäuren im Aszites wurden Lipidomanalysen mittels LC-MS/MS durchgeführt. Die gemessene Fettsäure mit der höchsten Konzentration ist Linolsäure (LA), gefolgt von Arachidonsäure (AA), Docosahexaensäure (DHA) und Eicosapentaensäure (EPA). Bis auf EPA und alpha-Linolensäure (ALA) führte jede dieser Fettsäuren zu einer starken Induktion von *PDK4* in humanen Makrophagen *in vitro* (Abbildung 6A, B). Sowohl LA als auch dessen konjugierte Formen konnten bereits innerhalb einer dreistündigen Behandlung dosisabhängig *PDK4* in MDM induzieren (Abbildung 6C). LA induzierte mehrere PPARβ/δ spezifische Zielgene ähnlich stark wie der synthetische Agonist L165,041 und dies lässt sich durch inverse PPARβ/δ Agonisten wie PT-S264 kompetitiv verhindern (Abbildung 6E), was möglicherweise Hinweise auf eine therapeutische Anwendbarkeit dieser Liganden geben könnte.

Der Eigenanteil zur Erstellung dieser Publikation umfasst die Beteiligung an Versuchsplanung, Durchführung und Datenanalyse zu Abbildung 1A, 2A, D-F, Abbildung 3D, 5A, B, Abbildung 6C, E, Abbildung 7C, Abbildung S3, S4, Tabelle S1

Kollaborationspartner am Zentrum für Tumorbiologie und Immunologie: PPARβ/δ selektive inverse Agonisten wurden synthetisiert und zur Verfügung gestellt von Philipp M.Toth und Wibke E. Diederich aus dem Institut für Pharmazeutische Chemie. RNA und ChIP Sequenzierung wurden durchgeführt von Andrea Nist und Thorsten Stiewe aus der Genomics Core Facility. Patientenproben wurden zur Verfügung gestellt von Uwe Wagner und Silke Reinartz, Klinik für Gynäkologie, Gynäkol. Onkologie und Endokrinologie.
Kollaborationspartner der Philipps-Universität Marburg: Lipidomanalysen wurden durchgeführt von Yvonne Schober and W. Andreas Nockher am Institut für Labormedizin und Pathobiochemie, Molekulare Diagonstik.

3.2 The transcriptional PPARβ/δ network in human macrophages defines a unique agonist-induced activation state

Till Adhikary*, **Annika Wortmann***, Tim Schumann*, Florian Finkernagel*, Sonja Lieber, Katrin Roth, Philipp M. Toth, Wibke E. Diederich, Andrea Nist, Thorsten Stiewe, Lara Kleinesudeik, Silke Reinartz, Sabine Müller-Brüsselbach and Rolf Müller (2015) Nucleic Acids Research. 43(10): 5033–5051
* These authors contributed equally to the paper as first authors.

Die Rolle von PPARβ/δ in der Immunregulation ist bis zum heutigen Stand der Forschung noch weitgehend ungeklärt. Bereits bekannt ist jedoch, dass PPARβ/δ spezifische Agonisten eine antiinflammatorische Immunantwort in Makrophagen auslösen können (Daniel S. Straus and Glass 2007). Im Gegensatz dazu führt die Überexpression von PPARβ/δ in der Epidermis zur Psoriasis und erfüllt somit eine proinflammatorische Funktion (Westergaard et al. 2003), (Romanowska et al. 2010).

In dieser hier dargestellten Publikation konnten erstmals immunregulatorische Gene identifiziert werden, die durch PPARβ/δ selektive Agonisten über einen nicht-kanonischen Weg reprimiert werden. Demhingegen konnte auch eine durch Liganden geförderte Regulation proinflammatorischer Gene beobachtet werden. Daraus lässt sich ein besonderer Liganden-gesteuerter Phänotyp humaner Makrophagen postulieren.

Zur Untersuchung PPARβ/δ Liganden-abhängiger Effekte wurden von humanen Monozyten abgeleitete Makrophagen gesunder Spender verwendet, die sowohl eine gut messbare *PPARD* Genexpression, als auch PPARβ/δ Proteinlevel besitzen (Abbildung 1 A, B, Abbildung S1). In diesen Zellen ist die Ligandenregulation, messbar an der PPARβ/δ Zielgenexpression von *PDK4* (Abbildung 1C), gut sichtbar. Die Chromatinbindung von PPARβ/δ und dem Heterodimerisierungspartner RXR an der *PDK4* Enhancer Region (Abbildung S2) legt nahe, dass die Induktion abhängig von direkter DNA-Bindung des Heterodimers ist.

Um eine genauere Einsicht in das durch PPARβ/δ Liganden regulierte Transkriptom und Cistrom zu bekommen wurden genomweite Studien mittels RNA und ChIP Sequenzierung in humanen Makrophagen durchgeführt. Im Transkriptom zeigten sich neben den kanonischen, durch den Agonisten L165,041 induzierte und inverse Agonisten reprimierte Gene (Abbildung 2A) auch eine große Anzahl an invers regulierten Genen, die durch Agonisten reprimiert und durch inverse Agonisten induziert werden (Abbildung 2B). Nach IPA Diseases and Functions Annotation Analyse konnten die durch Agonisten induzierten Gene hauptsächlich der Inhibition des Zelltodes von Immunzellen und der Suppression von Immunzellfunktionen zugeordnet werden.

Allerdings gab es auch eine Gruppe von Genen die durch L165,041 induziert wurden und maßgeblich an der Entstehung von Entzündungsfunktionen wie der Colitis beteiligt sind (Abbildung 2C). Durch die Analyse der Upstream Regulatoren mittels IPA konnten zwei durch L165,041 regulierte Klassen unterschieden werden. Zum einen werden kanonische Zielgene durch bereits bekannte Regulatoren des Lipidmetabolismus wie Pirinixinsäure und Rosiglitazon induziert, zum anderen werden allerdings auch nicht kanonische Zielgene von Immunmodulatoren wie TLR4, LPS, TNF, IFNG, IL1B, IL4, und STAT3 reprimiert (Abbildung 2E).

Um auszuschließen, dass die inverse Regulation aus einem *off target* Effekt resultiert, wurden Knochenmarksmakrophagen (BMDM) von Wildtyp (WT) und Pparβ/δ knockout Mäusen mit dem PPARβ/δ Agonisten GW501516 behandelt. Die kanonischen Zielgene *Angptl4* und *Pdk4* wurden lediglich in WT-Mäusen durch den Agonisten induziert. Auch die inversen Zielgene *Ccl24*, *Tnfsf15* und *Serpinb2* wurden nur in WT-Mäusen durch den Agonisten reprimiert. Zwei weitere Gene (*Ccl8* und *Enpp2*) die einer inversen Regulation in humanen Makrophagen unterlagen, wurden in diesem System nicht durch den Agonisten reguliert, was mutmaßlich an der differentiellen Regulation in Maus und Mensch liegt.

ChIP-Seq Analysen in humanen Makrophagen zeigten eine Anreicherung von PPARβ/δ und RXR an 3372 Regionen innerhalb des Genoms. 130 mit diesen genomischen Regionen assoziierte Transkripte unterliegen der Regulation durch L165,041. Die Bindung von PPARβ/δ und RXR erfolgte an annotierten Transkriptionsstarts, innerhalb von Introns oder vorgelagerten Bereichen (Abbildung 3A-C). Die Funktionen dieser kanonisch regulierten Gene liegen hauptsächlich im Lipidmetabolismus, der Zellmigration, aber auch in der Immunregulation (Abbildung 3E, Abbildung S4, Tabelle 1, Abbildung S6).

Im Gegensatz zur direkten Bindung von PPARβ/δ und RXR an den kanonischen Zielgenen konnte in den nicht kanonisch durch L165,041 reprimierten Genen lediglich eine sehr schwache Bindung von PPARβ/δ und RXR an den entsprechenden Loci nachgewiesen werden (Abbildung 4A, B).

Die Hauptregulatoren dieser inversen Zielgene sind Modulatoren proinflammatorischer Zytokin-Signalwege (Abbildung 4C, Tabelle 1). Einige dieser Gene werden durch STAT1, STAT3, NF-κB, BCL6 und p300 reguliert (Abbildung 4D). Einen weiteren Hinweis für eine Rolle des NF-κB Weges gab einer Behandlung von Makrophagen mit dem Proteasominhibitor MG132 in Kombination mit L165,041. MG132 hemmt den Abbau der inhibitorischen Faktoren des NF-κB Weges, der IκBs. Bei gleichzeitiger Behandlung mit L165,041 wurde die invers regulierte Repression der

Gene, bis auf *IL8*, teilweise aufgehoben. Da die Repression jedoch nicht vollständig aufgehoben wird, sind höchstwahrscheinlich noch andere Signalwege an dieser Regulation beteiligt (Abbildung 4E).

Morphologisch betrachtet ähneln L165,041-differenzierte Makrophagen sehr stark einem IL-4 erzeugten, M2 polarisiertem Phänotyp. Die Funktion dieses Phänotyps entspricht auch einer verminderten Phagozytoserate der mit L165,041 behandelten Makrophagen (Abbildung 6F). Entgegengesetzt entsprechen in Gegenwart von LPS und IFNγ differenzierte, M1-artige Makrophagen eher einem morphologischen Phänotyp der durch inverse Agonisten wie PT-S264 induziert wird (Abbildung 6, Abbildung S5).

Funktionelle Netzwerk-Analysen wie in Abbildung 5 dargestellt zeigen zum einen eine Reihe durch Liganden reprimierte Immunfunktionen aber auch einige Liganden erzeugten proinflammatorische Eigenschaften. Zum Beispiel kommt es zu einer gesteigerten T-Zellaktivität, gemessen an IFNγ produzierenden $CD8^+$ T-Zellen nach Kokultur L165,041-differenzierter MDM, die zuvor einem CEFT Peptidpool ausgesetzt wurden (Abbildung 7A).

IDO1 als geschwindigkeitsbestimmendes Enzym im Aminosäureabbau von Tryptophan zu Kynurenin wurde als inverses Zielgen identifiziert. Eine erhöhte IDO Aktivität führt generell zur Suppression der T-Zell Aktivität. L165,041 führt jedoch in Makrophagen zu einer verminderten *IDO* Expression, IDO Proteinlevel und Kynureninlevel und somit generell zu einer proinflammatorischen Antwort (Abbildung 7B-D, Abbildung S7). In diesem Fall reichte die verminderte Kynureninkonzentration dennoch aus um die T-Zell-Aktivierung zu vermindern. Auch die Expression des PD-1 Liganden (CD274) und des Fcγ-Rezeptors FCGR2B (CD32B) wurden deutlich durch L165,041 reprimiert (Abbildung 7F-H).

Zur Übertragung der gewonnen Erkenntnisse über die inverse Regulation durch L165,041 auf andere Zelltypen wurden zunächst die Trankriptom und Cistrom Daten mit denen der Myofibroblastenzelllinie WPMY-1 und der Brustzellkrebszellinie MDA-MB231 verglichen. Es kam zur Übereinstimmung von 129 regulierten Genen in allen drei Zelltypen, die hauptsächlich im Intermediärstoffwechsel zu finden sind (Abbildung 9A). Allerdings kam es zu keiner Übereinstimmung der invers regulierten Gene (Abbildung 9B). Auch sind diese Zellen refraktär gegenüber der Regulation von *CD52* und *LRP5*, die in Makrophagen durch L165,041 induziert werden (Abbildung 9C, Abbildung S4). Somit gibt es zusammengefasst eine kanonische Regulation bestimmter Transkripte die zelltypunabhängig oder Makrophagen spezifisch ist und eine Makrophagen selektive nicht kanonische Zielgenregulation.

Der Eigenanteil zur Erstellung dieser Publikation umfasst die Beteiligung an Versuchsplanung, Durchführung und Datenanalyse zu Abbildung 3A-C, Abbildung 4A, B, E, Abbildung 7D, Abbildung 9C, Abbildung S2, Abbildung S4, Abbildung S6

Kollaborationspartner am Zentrum für Tumorbiologie und Immunologie: PPARβ/δ selektive inverse Agonisten wurden synthetisiert und zur Verfügung gestellt von Philipp M.Toth und Wibke E. Diederich aus dem Institut für Pharmazeutische Chemie. RNA und ChIP Sequenzierung wurden durchgeführt von Andrea Nist und Thorsten Stiewe aus der Genomics Core Facility. FACS Phänotypisierung und T-Zell Aktivierungsassays von Lara Kleinesudeik und Silke Reinartz, Klinik für Gynäkologie, Gynäkol. Onkologie und Endokrinologie. Video Mikroskopie von Kathrin Roth, Zelluläre Bildgebung Core Facility.

3.3 Chromatin Binding of *c*-REL and p65 Is Not Limiting for Macrophage *IL12B* Transcription During Immediate Suppression by Ovarian Carcinoma Ascites

Annika Unger, Florian Finkernagel, Nathalie Hoffmann, Felix Neuhaus, Barbara Joos, Andrea Nist, Thorsten Stiewe, Alexander Visekruna, Uwe Wagner, Silke Reinartz, Sabine Müller-Brüsselbach, Rolf Müller and Till Adhikary (2018), *Front. Immunol.* 9:1425. doi: 10.3389/fimmu.2018.01425

IL12p40, kodiert durch *IL12B*, ist der limitierende Faktor für funktionelles IL-12 und einer proinflammatorischen Immunantwort. Tumor-assoziierte Makrophagen des Ovarialkarzinoms sind refraktär gegenüber proinflammatorische Stimuli (Gordon and Freedman 2006) und sezernieren p40 nach Stimulation mit LPS und IFNγ nicht oder nur in geringen Mengen (Finkernagel et al. 2016). Sowohl das Verständnis über die Mechanismen der *IL12B* Suppression, als auch die Reversibilität dieses Zustandes sind für therapeutische Ansatzpunkte maßgeblich und sind somit von höchster Priorität in der Aufklärung immunsuppressiver Mechanismus im Ovarialkarzinom.

In dieser Arbeit wurde zunächst der *ex vivo* Zustand von Tumor-assoziierten Makrophagen des Ovarialkarzinoms in Bezug auf die Fähigkeit der *IL12B* Expression untersucht. Es konnte keine *IL12B* mRNA (Abbildung 1A) und auch kein Protein (Abbildung 1B) detektiert werden. Nach zwei Tagen Kultivierung in Aszites, mit zusätzlicher IFNγ Supplementation oder normalem Kulturmedium (R5) konnte in einem Teil der Spenderinnen der supprimierende Effekt signifikant aufgehoben werden (Abbildung 1A). Dies zeigt, dass TAM potentiell reaktivierbar sind und *IL12B* induzieren können. Höchstwahrscheinlich sind lösliche Faktoren im Aszites für die Suppression verantwortlich.

Um herauszufinden, welcher lösliche Faktor des Aszites die IL-12 Suppression in Makrophagen hervorruft, wurde aufgrund vieler Hinweise in der Literatur der Einfluss von IL-10 untersucht (Segal, Dwyer, and Shevach 1998), (Xiaoyu Hu, Chakravarty, and Ivashkiv 2008). IL-10 führte zu einer Reduktion der im Überstand gemessenen IL12p40 Konzentrationen um ca. 50 % (von 10 auf 5 ng/ml, Abbildung 7B), konnte jedoch nicht den Effekt des Aszites einer vollständigen Suppression von IL12p40 erreichen (Inhibition um mehr als 80 % Abbildung 2B).

In weiteren Versuchen ließ sich klären ob der Aszites über Kurzzeitmechanismen die Suppression hervorruft oder ob die Differenzierung der Zellen eine Rolle spielt. Erstaunlicherweise reicht eine kurze Exposition der MDM gegenüber dem Aszites aus um eine vollständige Suppression von IL-12 zu erreichen (Abbildung 2B). Dieser Effekt

ist auf RNA-Ebene durch eine Depletion des Aszites und Ersetzen durch normales Kulturmedium (+ 1 d R5) wieder reversibel (Abbildung 2A). Der Effekt lässt sich auf Proteinebene nur partiell erkennen und ist aufgrund der Spenderdiversität sehr variabel und nicht signifikant (Abbildung 2B). Die durch Langzeitexposition des Aszites vermittelte Suppression führt in einem Teil der Spender zu einer verbesserten *IL12B* Expression und Sekretion nach Aszitesdepletion für einen längeren Zeitraum (Abbildung 2C, D).

Da die TAM einiger Patientinnen durch Stimulation mit IFNγ im Aszites die Fähigkeit besitzen *IL12B* zu induzieren (5 von 8 TAM Proben, Abbildung 1A, B), stellte sich die Frage ob eine Veränderung ihrer Polarisation für diesen Zustand verantwortlich ist. Umgekehrt stellte sich die Frage ob die Veränderung des Phänotyps, bzw. die Expression verschiedener makrophagenspezifischer Marker erheblich für die *IL12B* Suppression ist. In Abbildung S3 sind FACS Messungen der Makrophagenmarker CD163 (Abbildung S3A) und CD206 (Abbildung S3B) dargestellt, die sehr stark in antiinflammatorischen Makrophagen exprimiert sind. Generell ist der Aszites verantwortlich für die hohe Expression dieser Marker in gesunden Spendermakrophagen nach Differenzierung. Allerdings ändert sich die Expression von CD163 nur geringfügig in Gegenwart von Aszites und IFNγ–differenzierten Zellen, bzw. erhöht sich die Expression nicht maßgeblich nach kurzer Aszites Exposition. Dies bedeutet, dass die Reinduzierbarkeit von *IL12B* keine Reduktion der antiinflammatorischen Marker, bzw. die Suppression von IL-12 durch den Aszites keine Induktion von CD163 bedingt.

Aufgrund der aktuellen Literaturlage, die den NF-κB Weg, speziell *c*-REL als maßgeblichen Regulator der *IL12B* Induktion beschreibt, untersuchten wir die Involvierung des NF-κB Weges in unserem experimentellen System der Aszites induzierten IL-12 Suppression.

Die Translokation von *c*-REL und RELA in Aszites differenzierten Zellen war in einem Großteil der Spenderinnen komplett inhibiert, da sehr geringe bis keine detektierbaren nukleären Proteinkonzentrationen gemessen wurden (Abbildung 3A, C). Auch in Zellen, die nur für einen Tag mit Aszites kultiviert wurden ist die Translokation deutlich verringert (Abbildung 3B, D). Diese ist nach Aszites Wegnahme im Vergleich zur Langzeitexposition jedoch teils revertierbar (vergleiche A/C mit B/D).

Aufgrund dieser Ergebnisse untersuchten wir die Funktionalität der zytoplasmatischen NF-κB Inhibitoren, IκBα, IκBβ und IκBε. Entgegen der Annahme einer Stabilität dieser Faktoren welche die reduzierte Translokation verursacht, konnte man einen funktionellen Abbau von IκBβ und IκBε im Aszites feststellen (Abbildung S4A, S5B, C). IκBα unterliegt generell einer schnelleren Abbau-Kinetik und ist zu dem

betrachteten Zeitpunkt in Medium-differenzierten Makrophagen durch positive Rückkopplung stärker exprimiert (Abbildung S4A, S5A).

Um zu überprüfen, ob der Aszites neben *IL12B* auch noch andere NF-κB Zielgene supprimiert, wurde die Induktion von *CXCL10* nach Aszites-Differenzierung oder Kurzzeitbehandlung untersucht. Erstaunlicherweise verursachte der Aszites keine Suppression des *c*-REL Zielgens *CXCL10* (Abbildung S6A, B).

Um einen genaueren Einblick in die Aszites-vermittelte Regulation der REL und p65 induzierten Zielgene zu gewinnen wurden ChIP Experimente durchgeführt.

ChIP Sequenzierungen in *ex vivo* TAM gaben Hinweise auf regulatorische Bereiche des *IL12B* Lokus. Ein Enhancer mark, Histon H3 Lysin4 Monomethylierung (H3K4me1) wurde an vier Regionen innerhalb eines 25 kbp großen Abschnitts des IL12B Lokus detektiert (Abbildung 4A). 1200 bp stromaufwärts der Transkriptionsstartstelle (TSS) befindet sich ein Element mit an Lysin 4 trimethyliertem Histon H3 (H3K4me3), welches im Allgemeinen direkt an TSSs gefunden wird (Abbildung 4A, B). Etwa 20 kbp stromabwäts des annotierten TSS konnte eine H3K27me3-markierte Region gefunden werden (Abbildung 4A, D), die auf die Anwesenheit repressiver Faktoren wie dem *Polycomb repressive complex 2* deutet. Die Besonderheit der H3K4me3 Marks an einer der TSS vorgelagerten Region, nicht aber an der TSS selbst, zeigte sich auch in anderen *c*-REL Zielgenen, wie *CXCL10* und *IL-2* (Abbildung S9).

Da die Sequenzierungsdaten zwei eigentlich konträre Marks (H3K4me3 und H3K27me3) an einem Lokus zeigen, kann man die Besonderheit einer stabilen Repression und gleichzeitig schnellen Aktivierungsmöglichkeit dieser proinflammatorischen Gene vermuten.

Im weiteren Schritt sollte herausgefunden werden, ob der Aszites einen Einfluss auf die Chromatin-Bindung der NF-κB Transkriptionsfaktoren hat. Es wurde gezeigt, dass Aszites-differenzierte Zellen eine verminderte durch LPS/IFNγ induzierte Bindung von REL und RELA ausschließlich am vorgelagerten TSS (-1200 bp) von IL12B aufweisen (Abbildung 5A). Kurzzeit-Aszites behandelte Makrophagen (R5 differentiation + 1 d ascites) wiesen jedoch kein deutlich verändertes Anreicherungsmuster im Vergleich zu den Kontrollzellen auf, und die Bindung der beiden Transkriptionsfaktoren an zwei regulatorische Bereiche des *CXCL10*-Lokus war in keiner der Zellpopulationen nach Stimulation verändert (Abbildung 7D, E). Auch konnten keine wesentlichen Histonmodifikations- Unterschiede innerhalb dieser drei unterschiedlich differenzierten, bzw. behandelten Makrophagengruppen am *IL12B* (Abbildung 4E-G) oder am *CXCL10* Lokus (Abbildung S9 C, D) festgestellt werden. Dies zeigte, dass trotz verminderter

Translokation der beiden Faktoren, eine ausreichende und funktionelle DNA-Bindung von REL und p65 vorhanden war.

Die Vermutung, dass *c*-REL zwar an der Regulation von *IL12B* beteiligt ist, aber nicht ausschließlich für die Induktion verantwortlich ist zeigte sich auch in siRNA Versuchen in humanen Makrophagen und knockout Zellen in BMDM. Trotz verminderter *c*-REL oder *RELA* Proteinkonzentration oder einem kompletten Verlust von *c*-Rel in knockout Mäusen, kam es lediglich zu einer reduzierten *IL12B* oder p40 Induktion (Abbildung 6A, B, S7).

Der Eigenanteil zur Erstellung dieser Publikation umfasst die Beteiligung an Versuchsplanung, Durchführung und Datenanalyse zu Abbildung 1, 2, 3, 4E-G, 5, Abbildung S2, S3, S4, S5, S6, S7, S8, S9C, D, S10

Kollaborationspartner am Zentrum für Tumorbiologie und Immunologie: ChIP-Sequenzierung wurden durchgeführt von Andrea Nist und Thorsten Stiewe aus der Genomics Core Facility. FACS Phänotypisierung von Silke Reinartz, Klinik für Gynäkologie, Gynäkol. Onkologie und Endokrinologie, Patientenproben wurden zur Verfügung gestellt von Uwe Wagner und Silke Reinartz, Klinik für Gynäkologie, Gynäkol. Onkologie und Endokrinologie.

4 Diskussion

Aszites vermittelte Deregulation PPARβ/δ–spezifischer Zielgene

Die Suppression inflammatorischer Immunzellen in der Mikroumgebung des Ovarialkarzinoms ist einer der bedeutendsten Mechanismen dieses Tumors um einen protumorigenen Phänotyp zu generieren und zu erhalten. Eine äußerst wichtige Rolle spielt in diesem Prozess die Akkumulation des Aszites, als Reservoir von Tumor- und Stromazellen, antiinflammatorischer Immunzellen, löslicher Faktoren und vor allem Lipiden.

Lipide haben einen großen Einfluss auf die Tumorigenese und wie in neuesten Studien gezeigt werden konnte, vor allem auf die Metastasierung des Tumors (Pascual et al. 2017). Die innerhalb dieser Arbeit durchgeführten Lipidomanalysen des Aszites von Ovarialkarzinompatientinnen ergaben teils sehr hohe Konzentrationen an mehrfach ungesättigten Fettsäuren, wie Linolsäure, Arachidonsäure, oder Docosahexaensäure. Einer der Hauptregulatoren des Fettsäuremetabolismuses ist der Lipidsensor PPARβ/δ. Da die im Aszites vorhandenen Fettsäuren natürliche Liganden dieses Kernrezeptors darstellen, wurde deren Einfluss auf die PPARβ/δ spezifische Zielgenregulation in Makrophagen gesunder Spender und Tumor-assoziierten Makrophagen des Ovarialkarzinom untersucht.

Neben morphologischer Ähnlichkeiten des durch PPARβ/δ selektive Agonisten erzeugten antiinflammatorischen Phänotyps von MDM und *ex vivo* TAM zeigten RNA Seq Daten eine Überlappung der Agonisten-induzierten Zielgene in MDM und unbehandelten *ex vivo* TAM, was auf eine Deregulation der Zielgene in TAM hinwies.

PPARβ/δ im Immunsystem

Die Funktionen der deregulierten, durch PPARβ/δ-Agonisten induzierten Zielgene konnten neben den bekannten, klassischen Metabolismus- und Migrationsaufgaben auch dem Überleben und Entzündungs- bzw. Immunfunktionen zugeordnet werden. Bei Letzteren wurde LPS als Hauptmediator der Zielgene mit proinflammatorischer Funktion identifiziert.

Immunmodulatorische Funktionen der PPARs wurden bisher überwiegend für PPARα und PPARγ beschrieben. In Makrophagen wurde vor allem die Interaktion Agonisten-abhängiger Effekte mit den Transkriptionsfaktoren NF-κB, STAT, Aktivator Protein 1 (AP1) und NFAT (*nuclear factor of activated T-cells*) beschrieben (Daynes and Jones 2002). PPARα interagiert durch Transrepressions-Mechanismen beispielsweise mit der RHD von p65 und dem Aminoterminus von JUN (Philippe Delerive et al. 1999)

oder kontrolliert die Dauer der Immunantwort indem Agonisten die verstärkte Transkription und Proteinsynthese des inhibitorischen NF-κB Proteins IκBα induzieren (P. Delerive et al. 2000). Der selektive PPARγ Agonist 15d-PGJ_2 inhibiert die IκB Komplex Kinase (IKK) und dadurch die NF-κB DNA Bindung (D S Straus et al. 2000), wodurch es zu einer Hemmung proinflammatorischer Transkripte kommt. Über den Einfluss von PPARβ/δ auf die Immunregulation gibt es bisher nur wenige Informationen, (Rival et al. 2002), (Stockert et al. 2013), (Daynes and Jones 2002), die im Rahmen dieser Arbeit, insbesondere in humanen Makrophagen genauer charakterisiert werden.

Makrophagen-spezifische inverse Regulation inflammatorischer Gene durch PPARβ/δ-Agonisten

Anhand der gewonnenen Erkenntnisse über PPARβ/δ spezifische Funktionen in humanen Makrophagen wurden neue, transkriptionelle Mechanismen der PPARβ/δ spezifischen Zielgenregulation gefunden, die durch die selektiven Agonisten erzeugt werden. PPARβ/δ Agonisten besitzen nicht nur die Fähigkeit die Expression kanonischer Zielgene zu induzieren, sondern führen auch zu einem nicht-kanonischen Mechanismus, der keine oder nur eine sehr schwache direkte PPARβ/δ DNA Bindung benötigt und zur Repression dieser Gene führt. Diese inverse Regulation ist zelltypspezifisch und betrifft hauptsächlich die Regulation in Makrophagen. Nicht verwunderlich ist aufgrund dieser Tatsache, dass die reprimierten Gene überwiegend an der Immunregulation beteiligt sind und vor allem über NF-κB reguliert werden. Mittels gleichzeitiger Behandlung des Agonisten L165,041 und dem Proteasominhibitor MG132, der die Agonisten-induzierte Repression verschiedener NF-κB Zielgene aufhebt, konnte ein Einfluss des NF-κB Weges auf die inverse Regulation durch PPARβ/δ Agonisten vermutet werden. Zu beachten ist allerdings, dass MG132 kein selektiver IKK-Inhibitor ist und der Einfluss anderer Signalwege nicht ausgeschlossen werden kann.

Zusätzlich zur bisher beschriebenen Agonisten-induzierten antiinflammatorischen Rolle von PPARβ/δ in Makrophagen konnte im Rahmen dieser Arbeit auch eine proinflammatorische Funktion von PPARβ/δ aufgezeigt werden, was zur allgemein kontrovers diskutierten Rolle von PPARβ/δ passt. Beispielsweise wird die T-Zellaktivierung durch Agonistenbehandlung gefördert, indem IDO1, das geschwindigkeitsbestimmende Enzym im Tryptophanabbau, und auch das Endprodukt der enzymatischen Kette Kynurenin, in Makrophagen reduziert werden. Des Weiteren kam es zu einer Agonisten vermittelten Anreicherung $IFN\gamma^+$ positiver CD8 Zellen und einer Reduktion der Expression des T-Zell inhibitorischen Faktors CD274 (PD-1).

Die Expression der PPARβ/δ spezifischen Zielgene unterliegt somit einer einzigartigen Regulation, die von hoher klinischer Bedeutung ist. Ein therapeutisch wichtiger Aspekt ist in diesem Zusammenhang die dosisabhängige Repression verschiedener Aszites-induzierbarer Zielgene in MDM durch den inversen Agonisten PT-S264. Durch bereits niedrige Konzentrationen des inversen Agonisten in Gegenwart von Aszites kann die Transkription von z.B. *ANGPTL4*, dessen Expression mit einer schlechten Prognose der Patientinnen korreliert, *in vitro* deutlich verringert werden. Der Einsatz inverser Agonisten stellt somit einen therapeutischen Ansatzpunkt in der Reversion des protumorigenen, immunsuppressiven Mikromilieus in ein funktionelles, antitumorales Netzwerk diverser Immunzellen dar.

Der Einfluss von PPARs auf die Induktion des proinflammatorischen Zytokins IL-12

Die detaillierte Beschreibung der Involvierung der PPARs, vor allem von PPARβ/δ auf viele weitere essentielle proinflammatorische Transkripte in humanen Makrophagen wie *IL12B* wurde bisher jedoch wenig untersucht. IL-12 ist eines der wichtigsten proinflammatorischen Zytokine, die durch NF-κB reguliert werden und ist in TAM nicht exprimiert. Bereits bekannt ist, dass PPARβ/δ Agonisten die Expression von IL-12 supprimieren und somit die experimentelle autoimmune Enzephalomyelitis (EAE) im Mausmodell schwächen (Kanakasabai et al. 2010). PPARγ Agonisten supprimieren die Produktion der limitierenden Untereinheit von funktionellem IL-12, IL-12p40 in LPS-stimulierten Mikrogliazellen (Xu and Drew 2007) und modulieren die CD40 induzierte Sekretion von Il-12 in murinen dendritschen Zellen (Faveeuw et al. 2000). Der PPARα Agonist Fenofibrat inhibiert die Sekretion von IL-12p40 und IL12p70 (Xu, Racke, and Drew 2007).

Reversibilität der *IL12B* Suppression in TAM

U.a. aufgrund des Einflusses von PPARβ/δ Agonisten auf den NF-κB Signalweg im Ovarialkarzinom wurde die transkriptionelle Induktion von *IL12B* im Hinblick auf die Aszites-vermittelte Suppression des Zytokins hin untersucht.

Zunächst stellte sich die Frage, ob der Aszites, bzw. lösliche Faktoren im Aszites für die Suppression in TAM oder auch in Aszites differenzierten Zellen für die Suppression verantwortlich ist. Da TAM nach einer Kultivierung von zwei Tagen in normalem Kulturmedium (R5) wieder in der Lage sind auf transkriptioneller Ebene *IL12B* zu induzieren, spricht dies für eine mögliche Reversibilität dieser Zellen in einen

proinflammatorischen Status. Die Suppression wird daher überwiegend durch lösliche Faktoren des Aszites hervorgerufen.

Des Weiteren konnte der immunsuppressive IL-10^{high}, IL-12^{low} Phänotyp der TAM sowohl in dieser, als auch in anderen Studien durch IFNγ revertiert werden (Duluc et al. 2009), (X Hu, Chakravarty, and Ivashkiv 2008). Auch konnten Arbeiten der eigenen Gruppe zeigen, dass die Prognose von Ovarialkarzinompatientinnen mit verstärktem Interferon *signaling* deutlich besser ist im Vergleich zu Patientinnen mit weniger stark ausgeprägter Interferonantwort (Adhikary et al. 2017).

Der Einfluss von IL-10 auf IL-12

Als einer der Hauptverursacher der *IL12B* Repression kam IL-10 in Frage, da dieses Zytokin eine erheblich Rolle in der Differenzierung zu einem antiinflammatorischen Phänotyp einnimmt und eine proinflammatorische Antwort unterbindet (Ito and Ansari 1999), (A. Sica et al. 2000), (Williams et al. 2004). Zusätzlich korreliert eine hohe IL-10 Konzentration im Aszites mit einer schlechten Prognose der Patientinnen mit HGSOC (Reinartz et al. 2014). Gezeigt wurde auch, dass sich die IL-10 und IL-12 Expression gegenseitig reguliert und ein Ungleichgewicht dieses Mechanismus zu der Entstehung diverser Erkrankungen führt (Segal, Dwyer, and Shevach 1998). Da TAM im Aszites hohen Konzentrationen an IL-10 ausgesetzt sind, war die Annahme, dass dies zu einer Suppression von *IL12B* über eine NF-κB Inhibition in Makrophagen gesunder Spender führt. In unserem System hingegen konnte jedoch keine vollständige Suppression von *IL12B* durch IL-10 gezeigt werden, was auf die Präsenz weiterer antiinflammatorischer Faktoren im Aszites hindeutet, die die Suppression bedingen.

Die Rolle von NF-κB in der Regulation von IL-12

Da *c*-REL als Hauptregulator von IL-12p40 beschrieben ist (Sanjabi et al. 2000) wurde die Funktionalität der Translokation dieses Faktors, als auch die Translokation von RELA nach Aszitesbehandlung untersucht. Die Aszitesbehandlung, parallel zur Stimulation und auch die Differenzierung in Aszites führte zu drastisch verminderten kernständigen REL und RELA Proteinkonzentrationen, welche durch Aszitesentzug teilweise wieder erhöht werden konnten. Aufgrund dieser Tatsache wurde die Stabilität der NF-κB Inhibitoren (IκBs) überprüft. Hierbei ist zu erwähnen, dass die NF-κB Antwort in zwei zeitliche Einheiten eingeteilt wird, zum einen kommt es zu einer sehr schnellen Aktivierung des Signalweges, welche als primäre Antwort gesehen wird und zum anderen gibt es eine sekundäre Antwort mit einer verzögerten Kinetik, die Zielgene

dieser Gruppe langsamer induziert. Zu diesen Genen zählt auch *IL12B*. Für diese verspätete Induktion der Zielgene ist vermutlich die Bindung der Transkriptionsfaktoren, die eine Chromatinveränderung bedingt, verantwortlich (S. Saccani, Pantano, and Natoli 2001), (Schultze 2017). Da IκBα, als Inhibitor des NF-κB Signalweges, vielen schnell induzierbaren Zielgenen zugeordnet wird, und für einen negativen Rückkopplungsmechanismus verantwortlich ist (Brown et al. 1993), lässt sich seine verstärkte Proteinsynthese zum Betrachtungszeitpunkt nach LPS und IFNγ Stimulation in unseren Versuchen erklären. Weiterhin lässt sich aus diesen Ergebnissen schließen, dass ein IκBα Abbau vermutlich nicht essentiell für die Induktion von *IL12B* ist, obwohl interessanterweise IL-10 zu einer Stabilisierung von IκBα und der somit verminderten Translokation von RELA führt (Rahim et al. 2005), (Shames et al. 1998). Eine Involvierung, bzw. nicht funktioneller IκB Abbau der zwei anderen zytoplasmatischen inhibitorischen Faktoren IκBβ und IκBε konnte in dieser Arbeit weitgehend ausgeschlossen werden, da der Abbau nach Aktivierung des Signalweges deutlich sichtbar und somit funktionell ist.

Allerdings kann eine Involvierung anderer, atypischer IκBs nicht ausgeschlossen werden. Nennenswert ist hier IκBζ, welches als Regulator der H3K4 Trimethylierung und als Induktor des transkriptionellen Präinitiationskomplexes nach Nukleosomumbau beschrieben wurde (Annemann et al. 2016) und durch Bindung an den *Il12b* Promoter dessen Aktivität reguliert (Kayama et al. 2008).

Trotz der sehr geringen kernständigen Konzentrationen von REL und RELA kam es lediglich in Aszites differenzierten aber nicht in Kurzzeit-Aszites-exponierten Zellen zu einer verminderten DNA Bindung an einen in dieser Arbeit neu identifizierten, dem Transkriptionsstart vorgelagerten, erweiterten Promotorbereich. An der annotierten TSS konnte keine NF-κB Bindung detektiert werden.

Auch am *CXCL10*-Lokus konnte eine der TSS vorgelagerte Bindungsstelle von REL und RELA identifiziert werden. Hier kam es zu keiner Aszites vermittelten Änderung in der Anreicherung der beiden Transkriptionsfaktoren. Dies bedeutet, dass eine verminderte DNA-Bindung nach Langzeitexposition des Aszites vermutlich genspezifisch ist. Möglicherweise fehlt ein Komplex-stabilisierender Bindungspartner oder es kommt zu einer Blockierung der Bindung durch einen Repressor. Auch könnten posttranslationale Modifikationen der Transkriptionsfaktoren für die Regulation bedeutend sein.

ChIP Sequenzierungen von *ex vivo* TAM ließen eine repressive Modifikation, H3K27me3 an einem Bereich ca. 20 kbp stromabwärts der annotierten TSS erkennen. In Aszites kultivierten Makrophagen konnte an diesem Bereich allerdings keine

Veränderung der Histonmodifikation im Vergleich zu Makrophagen in normalem Kulturmedium festgestellt werden.

Zusammengefasst bedeutet dies, dass die Induktion von *IL12B* zwar eine REL und/oder RELA DNA Bindung benötigt, (erkennbar auch an eigenen RNAi Daten von von *REL* und *RELA* und knockout Daten von Rel), die Suppression jedoch aufgrund der noch vorhandenen DNA Bindung der NF-κB Faktoren vermutlich noch durch andere Faktoren reguliert wird.

Potentielle Beteiligung weiterer Signalwege an der IL-12 Suppression

Da eine volle Induktion von IL-12 nur durch eine Kombination der TLR4 oder CD40L und IFNγ gesteuerten Signalwege erreicht wird (Liu et al. 2003), (Conzelmann et al. 2010) und eine STAT1 Defizienz zu einer Suppression des TLR Signaling führt, welche die Aktivierung STAT3 regulierter Zielgene fördert (H. S. Kim et al. 2015), könnte eine verminderte oder veränderte Funktion von STAT1 maßgeblich an der durch Aszites induzierten Suppression von IL-12 beteiligt sein.

Auch weitere Faktoren wie Prostaglandin E2 (van der Pouw Kraan 1995), (Mitsuhashi et al. 2004), Arachidonsäure (Zhang and Fritsche 2004), Adenosin (HASKO 2000) und die Phosphatidylserin vermittelte Phagozytose vermitteln einen antiinflammatorischen Status, der die Inhibition der Synthese von IL-12 mit sich zieht (S. Kim, Elkon, and Ma 2004), (Birge et al. 2016).

In Magen, Darm oder auch Leberkrebs konnte zum einen eine physikalische Interaktion von STAT3 und dem NF-κB-Signalweg festgestellt werden. Zum anderen konkurrieren die Transkriptionsfaktoren um die Bindung an Promotor und Enhancerbereiche. Des Weiteren wird durch NF-κB die Expression von STAT3 Inhibitoren induziert (Grivennikov and Karin 2010), (Hoentjen et al. 2005). Da STAT3 in Makrophagen im Ovarialkarzinom durch Phosphorylierung konstitutiv aktiv vorliegt (Saini et al. 2017) und auch STAT3 Zielgenprodukte wie IL-6 in hohen Konzentrationen im Aszites vorhanden sind (Reinartz et al. 2014), die im Mausmodell die Interleukin-12 Produktion über die Inhibition der Phosphorylierung von *c*-Rel supprimieren (E. J. Lee et al. 2016), liegt es nahe, dass dieser Signalweg, höchst wahrscheinlich in Kooperation mit NF-κB, einen großen Einfluss auf die protumorigenen Eigenschaften der TAM ausübt. Da der NF-κB Weg als alleiniger Hauptregulator der IL-12 Induktion ausgeschlossen werden kann, sollte in erweiterten Studien die Rolle anderer beteiligter Signalwege und deren Mediatoren auf die IL-12 Suppression hin überprüft werden um zukünftige therapeutische Maßnahmen für eine funktionelle zytokinvermittelte proinflammatorische Immunantwort zu generieren. Hierbei ist auf die hohe Diversität der

Makrophagen einzelner Spenderinnen zu achten, die auch in den hier dargestellten Experimenten häufig vorhanden war und von höchstem therapeutischem Interesse ist. Nur durch die genaue Charakterisierung der Zellen einzelner Spenderinnen kann eine individuelle Therapie mit bestmöglichen effektiven Heilungschancen generiert werden.

5 Literaturverzeichnis

Adhikary, T., D. T. Brandt, K. Kaddatz, J. Stockert, S. Naruhn, W. Meissner, F. Finkernagel, et al. 2013. “Inverse PPARβ/δ Agonists Suppress Oncogenic Signaling to the ANGPTL4 Gene and Inhibit Cancer Cell Invasion.” *Oncogene* 32 (44):5241–52. https://doi.org/10.1038/onc.2012.549.

Adhikary, Till, Kerstin Kaddatz, Florian Finkernagel, Anne Schönbauer, Wolfgang Meissner, Maren Scharfe, Michael Jarek, Helmut Blöcker, Sabine Müller-Brüsselbach, and Rolf Müller. 2011. “Genomewide Analyses Define Different Modes of Transcriptional Regulation by Peroxisome Proliferator-Activated Receptor-β/δ (PPAR β/δ).” *PLoS ONE* 6 (1). https://doi.org/10.1371/journal.pone.0016344.

Adhikary, Till, Annika Wortmann, Florian Finkernagel, Sonja Lieber, Andrea Nist, Thorsten Stiewe, Uwe Wagner, Sabine Müller-Brüsselbach, Silke Reinartz, and Rolf Müller. 2017. “Interferon Signaling in Ascites-Associated Macrophages Is Linked to a Favorable Clinical Outcome in a Subgroup of Ovarian Carcinoma Patients.” *BMC Genomics* 18 (1):243. https://doi.org/10.1186/s12864-017-3630-9.

Annemann, Michaela, Carlos Plaza-Sirvent, Marc Schuster, Konstantinos Katsoulis-Dimitriou, Stefanie Kliche, Burkhart Schraven, and Ingo Schmitz. 2016. “Atypical IκB Proteins in Immune Cell Differentiation and Function.” *Immunology Letters*. https://doi.org/10.1016/j.imlet.2016.01.006.

Ashall, Louise, Caroline a Horton, David E Nelson, Pawel Paszek, Claire V Harper, Kate Sillitoe, Sheila Ryan, et al. 2009. “Pulsatile Stimulation Determines Timing and Specificity of NF-kappaB-Dependent Transcription.” *Science (New York, N.Y.)* 324 (5924):242–46. https://doi.org/10.1126/science.1164860.

Aste-Amezaga, Miguel, Xiaojing Ma, Alexandrina Sartori, and Giorgio Trinchieri. 1998. “Molecular Mechanisms of the Induction of IL-12 and Its Inhibtion by IL-10.” *Journal of Immunology* 160 (12):5963–5944.

Baeuerle, P. A. 1994. “Function and Activation of NF-Kappa B in the Immune System.” *Annual Review of Immunology* 12 (1):141–79. https://doi.org/10.1146/annurev.immunol.12.1.141.

Bamias, A., M. L. Tsiatas, E. Kafantari, C. Liakou, A. Rodolakis, Z. Voulgaris, G. Vlahos, et al. 2007. “Significant Differences of Lymphocytes Isolated from Ascites of Patients with Ovarian Cancer Compared to Blood and Tumor Lymphocytes. Association of CD3+CD56+ Cells with Platinum Resistance.” *Gynecologic Oncology* 106 (1):75–81. https://doi.org/10.1016/j.ygyno.2007.02.029.

Becskei, Attila, and Michael J. Grusby. 2007. “Contribution of IL-12R Mediated Feedback Loop to Th1 Cell Differentiation.” *FEBS Letters* 581 (27):5199–5206. https://doi.org/10.1016/j.febslet.2007.10.007.

Bellora, Francesca, Roberta Castriconi, Alessandra Dondero, Anna Pessino, Alessio Nencioni, Giovanni Liggieri, Lorenzo Moretta, Alberto Mantovani, Alessandro Moretta, and Cristina Bottino. 2014. “TLR Activation of Tumor-Associated Macrophages from Ovarian Cancer Patients Triggers Cytolytic Activity of NK Cells.” *European Journal of Immunology* 44 (6):1814–22. https://doi.org/10.1002/eji.201344130.

Bettelli, Estelle, Yijun Carrier, Wenda Gao, Thomas Korn, Terry B. Strom, Mohamed Oukka, Howard L. Weiner, and Vijay K. Kuchroo. 2006. “Reciprocal Developmental Pathways for the Generation of Pathogenic Effector TH17 and Regulatory T Cells.” *Nature* 441 (7090):235–38. https://doi.org/10.1038/nature04753.

Beyer, Marc, and Joachim L. Schultze. 2006. “Regulatory T Cells in Cancer.” *Blood*. https://doi.org/10.1182/blood-2006-02-002774.

Birge, R. B., S. Boeltz, S. Kumar, J. Carlson, J. Wanderley, D. Calianese, M. Barcinski, et al. 2016. “Phosphatidylserine Is a Global Immunosuppressive Signal in Efferocytosis, Infectious Disease, and Cancer.” *Cell Death and Differentiation*. https://doi.org/10.1038/cdd.2016.11.

Biswas, S. K., and C. E. Lewis. 2010. “NF- B as a Central Regulator of Macrophage Function in Tumors.” *Journal of Leukocyte Biology* 88 (5):877–84. https://doi.org/10.1189/jlb.0310153.

Biswas, Subhra K., Lisa Gangi, Saki Paul, Tiziana Schioppa, Alessandra Saccani, Marina Sironi, Barbara Bottazzi, et al. 2006. “A Distinct and Unique Transcriptional Program Expressed by Tumor-Associated Macrophages (Defective NF-κB and Enhanced IRF-3/STAT1 Activation).” *Blood* 107 (5):2112–22. https://doi.org/10.1182/blood-2005-01-0428.

Bowtell, David D., Steffen Böhm, Ahmed A. Ahmed, Paul-Joseph Aspuria, Robert C. Bast, Valerie Beral, Jonathan S. Berek, et al. 2015. “Rethinking Ovarian Cancer II: Reducing Mortality from High-Grade Serous Ovarian Cancer.” *Nature Reviews Cancer* 15 (11):668–79. https://doi.org/10.1038/nrc4019.

Braissant, O, F Foufelle, C Scotto, M Dauça, and W Wahli. 1996. “Differential Expression of Peroxisome Proliferator-Activated Receptors (PPARs): Tissue Distribution of PPAR-Alpha, -Beta, and -Gamma in the Adult Rat.” *Endocrinology* 137 (1):354–66. https://doi.org/10.1210/endo.137.1.8536636.

Brown, K, S Park, T Kanno, G Franzoso, and U Siebenlist. 1993. “Mutual Regulation of the Transcriptional Activator NF-Kappa B and Its Inhibitor, I Kappa B-Alpha.” *Proceedings of the National Academy of Sciences of the United States of America* 90 (6):2532–36. https://doi.org/10.1073/pnas.90.6.2532.

Brunda, M J, L Luistro, R R Warrier, R B Wright, B R Hubbard, M Murphy, S F Wolf, and M K Gately. 1993. “Antitumor and Antimetastatic Activity of Interleukin 12 against Murine Tumors.” *The Journal of Experimental Medicine* 178 (4):1223–30. https://doi.org/10.1084/jem.178.4.1223.

Bustamante, Jacinta, Stéphanie Boisson-Dupuis, Laurent Abel, and Jean Laurent Casanova. 2014. “Mendelian Susceptibility to Mycobacterial Disease: Genetic, Immunological, and Clinical Features of Inborn Errors of IFN-γ Immunity.” *Seminars in Immunology*. https://doi.org/10.1016/j.smim.2014.09.008.

Buy, J N, A A Moss, M A Ghossain, C Sciot, L Malbec, D Vadrot, B J Paniel, and Y Decroix. 1988. “Peritoneal Implants from Ovarian Tumors: CT Findings.” *Radiology* 169 (3):691–94. https://doi.org/10.1148/radiology.169.3.3186993.

Carmody, Ruaidhrí J, Qingguo Ruan, Hsiou-Chi Liou, and Youhai H Chen. 2007. “Essential Roles of c-Rel in TLR-Induced IL-23 p19 Gene Expression in Dendritic Cells.” *Journal of Immunology (Baltimore, Md. : 1950)* 178 (1):186–91. https://doi.org/10.4049/jimmunol.178.1.186.

Cavallo, Federica, Carla De Giovanni, Patrizia Nanni, Guido Forni, and Pier Luigi Lollini. 2011. “2011: The Immune Hallmarks of Cancer.” In *Cancer Immunology, Immunotherapy*, 60:319–26. https://doi.org/10.1007/s00262-010-0968-0.

Chanput, Wasaporn, Jurriaan J. Mes, Huub F. J. Savelkoul, and Harry J. Wichers. 2013. “Characterization of Polarized THP-1 Macrophages and Polarizing Ability of LPS and Food Compounds.” *Food Funct.* 4 (2):266–76. https://doi.org/10.1039/C2FO30156C.

Chong, Han Chung, Ming Jie Tan, Virginie Philippe, Siew Hwey Tan, Chek Kun Tan, Chee Wai Ku, Yan Yih Goh, Walter Wahli, Liliane Michalik, and Nguan Soon Tan. 2009. “Regulation of Epithelial-Mesenchymal IL-1 Signaling by PPARβ/δ Is Essential for Skin Homeostasis and Wound Healing.” *Journal of Cell Biology* 184 (6):817–31. https://doi.org/10.1083/jcb.200809028.

Conzelmann, Michael, Andreas H. Wagner, Anke Hildebrandt, Elena Rodionova, Michael Hess, Annika Zota, Thomas Giese, et al. 2010. “IFN–γ Activated JAK1 Shifts CD40-Induced Cytokine Profiles in Human Antigen-Presenting Cells toward High IL-12p70 and Low IL-10 Production.” *Biochemical Pharmacology* 80 (12). Elsevier Inc.:2074–86. https://doi.org/10.1016/j.bcp.2010.07.040.

Cooper, Andrea M., and Shabaana A. Khader. 2007. “IL-12p40: An Inherently Agonistic Cytokine.” *Trends in Immunology*. https://doi.org/10.1016/j.it.2006.11.002.

Curiel, Tyler J., Pui Cheng, Peter Mottram, Xavier Alvarez, Lieve Moons, Melina Evdemon-Hogan, Shuang Wei, et al. 2004. “Dendritic Cell Subsets Differentially Regulate Angiogenesis in Human Ovarian Cancer.” *Cancer Research* 64 (16):5535–38. https://doi.org/10.1158/0008-5472.CAN-04-1272.

Curiel, Tyler J., George Coukos, Linhua Zou, Xavier Alvarez, Pui Cheng, Peter Mottram, Melina Evdemon-Hogan, et al. 2004. “Specific Recruitment of Regulatory T Cells in Ovarian Carcinoma Fosters Immune Privilege and Predicts Reduced Survival.” *Nature Medicine* 10 (9):942–49. https://doi.org/10.1038/nm1093.

Daynes, Raymond A., and Dallas C. Jones. 2002. “Emerging Roles of PPARs in Inflammation and Immunity.” *Nature Reviews Immunology*. https://doi.org/10.1038/nri912.

Delerive, P., P. Gervois, J. C. Fruchart, and B. Staels. 2000. “Induction of IκBα Expression as a Mechanism Contributing to the Anti-Inflammatory Activities of Peroxisome Proliferator-Activated Receptor-α Activators.” *Journal of Biological Chemistry* 275 (47):36703–7. https://doi.org/10.1074/jbc.M004045200.

Delerive, Philippe, Karolien De Bosscher, Sandrine Besnard, Wim Vanden Berghe, Jeffrey M. Peters, Frank J. Gonzalez, Jean Charles Fruchart, Alain Tedgui, Guy Haegeman, and Bart Staels. 1999. “Peroxisome Proliferator-Activated Receptor α Negatively Regulates the Vascular Inflammatory Gene Response by Negative Cross-Talk with Transcription Factors NF-κB and AP-1.” *Journal of Biological Chemistry* 274 (45):32048–54. https://doi.org/10.1074/jbc.274.45.32048.

Desvergne, B., and W. Wahli. 1999. “Peroxisome Proliferator-Activated Receptors: Nuclear Control of Metabolism.” *Endocrine Reviews*. https://doi.org/10.1210/er.20.5.649.

Duluc, Dorothée, Murielle Corvaisier, Simon Blanchard, Laurent Catala, Philippe Descamps, Erick Gamelin, Stéphane Ponsoda, Yves Delneste, Mohamed Hebbar, and Pascale Jeannin. 2009. “Interferon-γ Reverses the Immunosuppressive and Protumoral Properties and Prevents the Generation of Human Tumor-Associated Macrophages.” *International Journal of Cancer* 125 (2):367–73. https://doi.org/10.1002/ijc.24401.

Escher, P., O. Braissant, S. Basu-Modak, L. Michalik, W. Wahli, and B. Desvergne. 2001. “Rat PPARs: Quantitative Analysis in Adult Rat Tissues and Regulation in Fasting and Refeeding.” *Endocrinology* 142 (10):4195–4202. https://doi.org/10.1210/en.142.10.4195.

Faveeuw, C, S Fougeray, V Angeli, J Fontaine, G Chinetti, P Gosset, P Delerive, et al. 2000. “Peroxisome Proliferator-Activated Receptor Gamma Activators Inhibit Interleukin-12 Production in Murine Dendritic Cells.” *FEBS Letters* 486:261–66.

Feldman, G.B.a b, and R.C.a b Knapp. 1974. “Lymphatic Drainage of the Peritoneal Cavity and Its Significance in Ovarian Cancer.” *American Journal of Obstetrics and Gynecology* 119 (7):991–94. https://doi.org/10.1016/0002-9378(74)90021-0.

Ferriss, James S., James J. Java, Michael A. Bookman, Gini F. Fleming, Bradley J. Monk, Joan L. Walker, Howard D. Homesley, et al. 2015. “Ascites Predicts Treatment Benefit of Bevacizumab in Front-Line Therapy of Advanced Epithelial Ovarian, Fallopian Tube and Peritoneal Cancers: An NRG Oncology/GOG Study.” *Gynecologic Oncology* 139 (1):17–22. https://doi.org/10.1016/j.ygyno.2015.07.103.

Finkernagel, Florian, Silke Reinartz, Sonja Lieber, Till Adhikary, Annika Wortmann, Nathalie Hoffmann, Tim Bieringer, et al. 2016. “The Transcriptional Signature of Human Ovarian Carcinoma Macrophages Is Associated with Extracellular Matrix Reorganization.” *Oncotarget* 7 (46):75339–52. https://doi.org/10.18632/oncotarget.12180.

Forman, B M, J Chen, and R M Evans. 1997. “Hypolipidemic Drugs, Polyunsaturated Fatty Acids, and Eicosanoids Are Ligands for Peroxisome Proliferator-Activated Receptors Alpha and Delta.” *Proceedings of the National Academy of Sciences of the United States of America* 94 (9):4312–17. https://doi.org/10.1073/pnas.94.9.4312.

Forman, Barry M., Peter Tontonoz, Jasmine Chen, Regina P. Brun, Bruce M. Spiegelman, and Ronald M. Evans. 1995. “15-Deoxy-Δ12,14-Prostaglandin J2is a Ligand for the Adipocyte Determination Factor PPARγ.” *Cell* 83 (5):803–12. https://doi.org/10.1016/0092-8674(95)90193-0.

Giuntoli, Robert L., Tonya J. Webb, Alessia Zoso, Ophelia Rogers, Teresa P. Diaz-Montes, Robert E. Bristow, and Mathias Oelke. 2009. “Ovarian Cancer-Associated Ascites Demonstrates Altered Immune Environment: Implications for Antitumor Immunity.” *Anticancer Research* 29 (8):2875–84. https://doi.org/29/8/2875 [pii].

Gomez Perdiguero, Elisa, Kay Klapproth, Christian Schulz, Katrin Busch, Emanuele Azzoni, Lucile Crozet, Hannah Garner, et al. 2014. “Tissue-Resident Macrophages Originate from Yolk-Sac-Derived Erythro-Myeloid Progenitors.” *Nature* 518 (7540). Nature Publishing Group:547–51. https://doi.org/10.1038/nature13989.

Gordon, Ilyssa O., and Ralph S. Freedman. 2006. “Defective Antitumor Function of

Monocyte-Derived Macrophages from Epithelial Ovarian Cancer Patients." *Clinical Cancer Research* 12 (5):1515–24. https://doi.org/10.1158/1078-0432.CCR-05-2254.

Grivennikov, Sergei I., and Michael Karin. 2010. "Dangerous Liaisons: STAT3 and NF-κB Collaboration and Crosstalk in Cancer." *Cytokine and Growth Factor Reviews* 21 (1):11–19. https://doi.org/10.1016/j.cytogfr.2009.11.005.

Gross, Thomas J, Karol Kremens, Linda S Powers, Brandi Brink, Tina Knutson, Frederick E Domann, Robert A Philibert, Mohammed M Milhem, and Martha M Monick. 2014. "Epigenetic Silencing of the Human NOS2 Gene: Rethinking the Role of Nitric Oxide in Human Macrophage Inflammatory Responses." *J. Immunol.* https://doi.org/10.4049/jimmunol.1301758.

Grumont, R, H Hochrein, M O'Keeffe, R Gugasyan, C White, I Caminschi, W Cook, and S Gerondakis. 2001. "C-Rel Regulates Interleukin 12 p70 Expression in CD8(+) Dendritic Cells by Specifically Inducing p35 Gene Transcription." *The Journal of Experimental Medicine* 194 (8):1021–32. https://doi.org/10.1084/jem.194.8.1021.

Guiducci, Cristiana, Alain P. Vicari, Sabina Sangaletti, Giorgio Trinchieri, and Mario P. Colombo. 2005. "Redirecting in Vivo Elicited Tumor Infiltrating Macrophages and Dendritic Cells towards Tumor Rejection." *Cancer Research* 65 (8):3437–46. https://doi.org/10.1158/0008-5472.CAN-04-4262.

Hagemann, Thorsten, Toby Lawrence, Iain McNeish, Kellie A. Charles, Hagen Kulbe, Richard G. Thompson, Stephen C. Robinson, and Frances R. Balkwill. 2008. "'Re-Educating' Tumor-Associated Macrophages by Targeting NF-κB." *The Journal of Experimental Medicine* 205 (6):1261–68. https://doi.org/10.1084/jem.20080108.

Haicheur, N., B. Escudier, T. Dorval, S. Negrier, P. H M De Mulder, J. M. Dupuy, D. Novick, et al. 2000. "Cytokines and Soluble Cytokine Receptor Induction after IL-12 Administration in Cancer Patients." *Clinical and Experimental Immunology* 119 (1):28–37. https://doi.org/10.1046/j.1365-2249.2000.01112.x.

Hao, Ning Bo, Mu Han Lü, Ya Han Fan, Ya Ling Cao, Zhi Ren Zhang, and Shi Ming Yang. 2012. "Macrophages in Tumor Microenvironments and the Progression of Tumors." *Clinical and Developmental Immunology* 2012. https://doi.org/10.1155/2012/948098.

HASKO, G. 2000. "Adenosine Inhibits IL-12 and TNF-Alpha Production via Adenosine A2a Receptor-Dependent and Independent Mechanisms." *The FASEB Journal* 14 (13):2065–74. https://doi.org/10.1096/fj.99-0508com.

He, Weijing, Mei Qiang, Wuqiong Ma, Anthony J. Valente, Marlon P. Quinones, Wen Wang, Robert L. Reddick, et al. 2006. "Development of a Synthetic Promoter for

Macrophage Gene Therapy." *Human Gene Therapy* 17 (9):949–59. https://doi.org/10.1089/hum.2006.17.949.

Hoentjen, Frank, R Balfour Sartor, Michitaka Ozaki, and Christian Jobin. 2005. "STAT3 Regulates NF-kappaB Recruitment to the IL-12p40 Promoter in Dendritic Cells." *Blood* 105 (2):689–96. https://doi.org/10.1182/blood-2004-04-1309.

Hoesel, Bastian, and Johannes A Schmid. 2013. "The Complexity of NF-κB Signaling in Inflammation and Cancer." *Molecular Cancer* 12 (1). Molecular Cancer:86. https://doi.org/10.1186/1476-4598-12-86.

Hu, X, Sd Chakravarty, and Lb Ivashkiv. 2008. "Regulation of IFN and TLR Signaling During Macrophage Activation by Opposing Feedforward and Feedback Inhibition Mechanisms." *Immunological Reviews*, 41–56. https://doi.org/10.1111/j.1600-065X.2008.00707.x.Regulation.

Hu, Xiaoyu, Soumya D. Chakravarty, and Lionel B. Ivashkiv. 2008. "Regulation of Interferon and Toll-like Receptor Signaling during Macrophage Activation by Opposing Feedforward and Feedback Inhibition Mechanisms." *Immunological Reviews*. https://doi.org/10.1111/j.1600-065X.2008.00707.x.

Issemann, I, and S Green. 1990. "Activation of a Member of the Steroid Hormone Receptor Superfamily by Peroxisome Proliferators." *Nature* 347 (6294):645–50. https://doi.org/10.1038/347645a0.

Ito, S, and Parswa Ansari. 1999. "Interleukin-10 Inhibits Expression of Both Interferon– and Interferon γ–Induced Genes by Suppressing Tyrosine Phosphorylation of STAT1." *Blood* 93 (5):1456–63. https://doi.org/papers3://publication/uuid/E13FC7A1-0D03-4F24-969C-8391C8A400C3.

Jemal, A., R. Siegel, E. Ward, Y. Hao, J. Xu, and M. J. Thun. 2009. "Cancer Statistics, 2009." *CA: A Cancer Journal for Clinicians* 59 (4):225–49. https://doi.org/10.3322/caac.20006.

Kaddatz, Kerstin, Till Adhikary, Florian Finkernagel, Wolfgang Meissner, Sabine Müller-Brüsselbach, and Rolf Müller. 2010. "Transcriptional Profiling Identifies Functional Interactions of TGFβ and PPARβ/δ Signaling: Synergistic Induction of ANGPTL4 Transcription." *Journal of Biological Chemistry* 285 (38):29469–79. https://doi.org/10.1074/jbc.M110.142018.

Kanakasabai, Saravanan, Wanida Chearwae, Crystal C Walline, Wade Iams, Suzanne M Adams, and John J Bright. 2010. "Peroxisome Proliferator-Activated Receptor Delta Agonists Inhibit T Helper Type 1 (Th1) and Th17 Responses in Experimental Allergic Encephalomyelitis." *Immunology* 130 (4):572–88.

https://doi.org/10.1111/j.1365-2567.2010.03261.x.

Kang, Kihwa, Shannon M Reilly, Volkan Karabacak, Matthew R Gangl, Kelly Fitzgerald, Ben Hatano, and Chih-hao Lee. 2008a. “Adipocyte-Derived Th2 Cytokines and Myeloid PPARdelta Regulate Macrophage Polarization and Insulin Sensitivity.” *Cell Metabolism* 7 (6):485–95. https://doi.org/10.1016/j.cmet.2008.04.002.

Kang, Kihwa, Shannon M Reilly, Volkan Karabacak, Matthew R Gangl, Kelly Fitzgerald, Ben Hatano, and Chih-Hao Lee. 2008b. “Adipocyte-Derived Th2 Cytokines and Myeloid PPARdelta Regulate Macrophage Polarization and Insulin Sensitivity.” *Cell Metabolism* 7 (6):485–95. https://doi.org/10.1016/j.cmet.2008.04.002.

Kaplan, Daniel H, Vijay Shankaran, Anand S Dighe, Elisabeth Stockert, Michel Aguet, Lloyd J Old, and Robert D Schreiber. 1998. “Demonstration of an Interferon ⁄-Dependent Tumor Surveillance System in Immunocompetent Mice.” *Immunology* 95 (June):7556–61. https://doi.org/10.1073/pnas.95.13.7556.

Kayama, Hisako, Vladimir R. Ramirez-Carrozzi, Masahiro Yamamoto, Taketoshi Mizutani, Hirotaka Kuwata, Hideo Iba, Makoto Matsumoto, Kenya Honda, Stephen T. Smale, and Kiyoshi Takeda. 2008. “Class-Specific Regulation of pro-Inflammatory Genes by MyD88 Pathways and IκBζ.” *Journal of Biological Chemistry* 283 (18):12468–77. https://doi.org/10.1074/jbc.M709965200.

Kim, Hun Sik, Dong Chan Kim, Hong Mi Kim, Hyung Joon Kwon, Soon Jae Kwon, Suk Jo Kang, Sun Chang Kim, and Go Eun Choi. 2015. “STAT1 Deficiency Redirects IFN Signalling toward Suppression of TLR Response through a Feedback Activation of STAT3.” *Scientific Reports* 5 (August). Nature Publishing Group:1–15. https://doi.org/10.1038/srep13414.

Kim, Sunjung, Keith B. Elkon, and Xiaojing Ma. 2004. “Transcriptional Suppression of Interleukin-12 Gene Expression Following Phagocytosis of Apoptotic Cells.” *Immunity* 21 (5):643–53. https://doi.org/10.1016/j.immuni.2004.09.009.

Kobayashi, M, Lori Fitz, Mary Ryan, Rodney M Hewick, Steven C Clark, Susan Chan, Robert Loudon, Frederick Sherman, B Perussia, and G Trinchieri. 1989. “Identification and Purification of Natural Killer Cell Stimulatory Factor (NKSF), a Cytokine with Multiple Biologic Effects on Human Lymphocytes.” *The Journal of Experimental Medicine* 170 (3):827–45. https://doi.org/10.1084/jem.170.3.827.

Kortylewski, Marcin, Hong Xin, Maciej Kujawski, Heehyoung Lee, Yong Liu, Timothy Harris, Charles Drake, Drew Pardoll, and Hua Yu. 2009. “Regulation of the IL-23 and IL-12 Balance by Stat3 Signaling in the Tumor Microenvironment.” *Cancer Cell* 15 (2):114–23. https://doi.org/10.1016/j.ccr.2008.12.018.

Kostadinova, Radina, Walter Wahli, and Liliane Michalik. 2005. “PPARs in Diseases:

Control Mechanisms of Inflammation." *Current Medicinal Chemistry* 12 (25):2995–3009. https://doi.org/10.2174/092986705774462905.

Kusmartsev, S., and D. I. Gabrilovich. 2005. "STAT1 Signaling Regulates Tumor-Associated Macrophage-Mediated T Cell Deletion." *The Journal of Immunology* 174 (8):4880–91. https://doi.org/10.4049/jimmunol.174.8.4880.

Langowski, John L., Xueqing Zhang, Lingling Wu, Jeanine D. Mattson, Taiying Chen, Kathy Smith, Beth Basham, Terrill McClanahan, Robert A. Kastelein, and Martin Oft. 2006. "IL-23 Promotes Tumour Incidence and Growth." *Nature* 442 (7101):461–65. https://doi.org/10.1038/nature04808.

Lee, C.-H. 2003. "Transcriptional Repression of Atherogenic Inflammation: Modulation by PPAR ." *Science* 302 (5644):453–57. https://doi.org/10.1126/science.1087344.

Lee, Eun Jung, Seo Jin Lee, Ji Hye Kim, Kyoung Jin Kim, Seung Hyun Yang, Keun Yeong Jeong, and Jinsil Seong. 2016. "Radiation Inhibits Interleukin-12 Production via Inhibition of C-Rel through the Interleukin-6/signal Transducer and Activator of Transcription 3 Signaling Pathway in Dendritic Cells." *PLoS ONE* 11 (1). https://doi.org/10.1371/journal.pone.0146463.

Leffers, Ninke, Marloes J.M. Gooden, Renske A. De Jong, Baukje Nynke Hoogeboom, Klaske A. Ten Hoor, Harry Hollema, H. Marieke Boezen, Ate G.J. Van Der Zee, Toos Daemen, and Hans W. Nijman. 2009. "Prognostic Significance of Tumor-Infiltrating T-Lymphocytes in Primary and Metastatic Lesions of Advanced Stage Ovarian Cancer." *Cancer Immunology, Immunotherapy* 58 (3):449–59. https://doi.org/10.1007/s00262-008-0583-5.

Lengyel, Ernst. 2010. "Ovarian Cancer Development and Metastasis." *The American Journal of Pathology* 177 (3):1053–64. https://doi.org/10.2353/ajpath.2010.100105.

Liou, H C, and D Baltimore. 1993. "Regulation of the NF-Kappa B/rel Transcription Factor and I Kappa B Inhibitor System." *Current Opinion in Cell Biology* 5 (3):477–87. https://doi.org/10.1016/0955-0674(93)90014-H.

Liu, Jianguo, Shanjin Cao, Lisa M Herman, and Xiaojing Ma. 2003. "Differential Regulation of Interleukin (IL)-12 p35 and p40 Gene Expression and Interferon (IFN)-Gamma-Primed IL-12 Production by IFN Regulatory Factor 1." *The Journal of Experimental Medicine* 198 (8):1265–76. https://doi.org/10.1084/jem.20030026.

Mantovani, Alberto, and Massimo Locati. 2013. "Tumor-Associated Macrophages as a Paradigm of Macrophage Plasticity, Diversity, and Polarization Lessons and Open Questions." *Arteriosclerosis, Thrombosis, and Vascular Biology* 33 (7):1478–83. https://doi.org/10.1161/ATVBAHA.113.300168.

Mantovani, Alberto, Silvano Sozzani, Massimo Locati, Paola Allavena, and Antonio Sica. 2002. “Macrophage Polarization: Tumor-Associated Macrophages as a Paradigm for Polarized M2 Mononuclear Phagocytes.” *Trends in Immunology*. https://doi.org/10.1016/S1471-4906(02)02302-5.

Martinez, Fernando O., Laura Helming, and Siamon Gordon. 2009. “Alternative Activation of Macrophages: An Immunologic Functional Perspective.” *Annual Review of Immunology* 27 (1):451–83. https://doi.org/10.1146/annurev.immunol.021908.132532.

Matte, Isabelle, Denis Lane, Claude Laplante, Claudine Rancourt, and Alain Piché. 2012. “Profiling of Cytokines in Human Epithelial Ovarian Cancer Ascites.” *American Journal of Cancer Research* 2 (5):566–80.

Matulonis, Ursula A., Anil K. Sood, Lesley Fallowfield, Brooke E. Howitt, Jalid Sehouli, and Beth Y. Karlan. 2016. “Ovarian Cancer.” *Nature Reviews Disease Primers* 2:1–22. https://doi.org/10.1038/nrdp.2016.61.

McKenzie, Brent S., Robert A. Kastelein, and Daniel J. Cua. 2006. “Understanding the IL-23-IL-17 Immune Pathway.” *Trends in Immunology*. https://doi.org/10.1016/j.it.2005.10.003.

Mills, Charles D., and Klaus Ley. 2014. “M1 and M2 Macrophages: The Chicken and the Egg of Immunity.” *Journal of Innate Immunity* 6 (6):716–26. https://doi.org/10.1159/000364945.

Mills, G B, C May, M McGill, C M Roifman, and A Mellors. 1988. “A Putative New Growth Factor in Ascitic Fluid from Ovarian Cancer Patients: Identification, Characterization, and Mechanism of Action.” *Cancer Res* 48 (5):1066–71..

Mitsuhashi, Maki, Jianguo Liu, Shanjin Cao, Xiaoyan Shi, and Xiaojing Ma. 2004. “Regulation of Interleukin-12 Gene Expression and Its Anti-Tumor Activities by Prostaglandin E 2 Derived from Mammary Carcinomas Tration of Recombinant IL-12 Could Therapeutically.” *Journal of Leukocyte Biology* 76 (2):322–32. https://doi.org/10.1189/jlb.1203641.1.

Mukherjee, Abir, Jinhua Wu, Suzanne Barbour, and Xianjun Fang. 2012. “Lysophosphatidic Acid Activates Lipogenic Pathways and de Novo Lipid Synthesis in Ovarian Cancer Cells.” *Journal of Biological Chemistry* 287 (30):24990–0. https://doi.org/10.1074/jbc.M112.340083.

Müller, Rolf. 2017. “PPARβ/δ in Human Cancer.” *Biochimie* 136:90–99. https://doi.org/10.1016/j.biochi.2016.10.019.

Murray, Peter J., Judith E. Allen, Subhra K. Biswas, Edward A. Fisher, Derek W. Gilroy, Sergij Goerdt, Siamon Gordon, et al. 2014. “Macrophage Activation and

Polarization: Nomenclature and Experimental Guidelines." *Immunity* 41 (1):14–20. https://doi.org/10.1016/j.immuni.2014.06.008.

Naruhn, S, W Meissner, T Adhikary, K Kaddatz, T Klein, B Watzer, S Muller-Brusselbach, and R Muller. 2009. "15-Hydroxyeicosatetraenoic Acid (15-HETE) Is a Preferential PPARβ/δ Agonist." *Mol.Pharmacol.* https://doi.org/10.1124/mol.109.060541.

Naruhn, S, P M Toth, T Adhikary, K Kaddatz, V Pape, S Dorr, G Klebe, S Muller-Brusselbach, W Diederich, and R Muller. 2011. "High Affinity PPARβ/δ-Specific Ligands with Pure Antagonistic or Inverse Agonistic Properties." *Mol.Pharmacol.* 80 (5). https://doi.org/10.1124/mol.111.074039.

Network, Cancer Genome Atlas Research. 2011. "Integrated Genomic Analyses of Ovarian Carcinoma." *Nature* 474 (7353):609–15. https://doi.org/10.1038/nature10166.

Odegaard, Justin I., Roberto R. Ricardo-Gonzalez, Alex Red Eagle, Divya Vats, Christine R. Morel, Matthew H. Goforth, Vidya Subramanian, Lata Mukundan, Anthony W. Ferrante, and Ajay Chawla. 2008. "Alternative M2 Activation of Kupffer Cells by PPARdelta Ameliorates Obesity-Induced Insulin Resistance." *Cell Metabolism* 7 (6):496–507. https://doi.org/10.1016/j.cmet.2008.04.003.

Parkin, D M, F Bray, J Ferlay, and P Pisani. 2005. "Global Cancer Statistics, 2002." *CA Cancer J Clin* 55:74–108. https://doi.org/10.3322/caac.20107.Available.

Pascual, Gloria, Alexandra Avgustinova, Stefania Mejetta, Mercè Martín, Andrés Castellanos, Camille Stephan Otto Attolini, Antoni Berenguer, et al. 2017. "Targeting Metastasis-Initiating Cells through the Fatty Acid Receptor CD36." *Nature* 541 (7635):41–45. https://doi.org/10.1038/nature20791.

Peraza, Marjorie A., Andrew D. Burdick, Holly E. Marin, Frank J. Gonzalez, and Jeffrey M. Peters. 2006. "The Toxicology of Ligands for Peroxisome Proliferator-Activated Receptors (PPAR)." *Toxicological Sciences*. https://doi.org/10.1093/toxsci/kfj062.

Pignata, Sandro, Lucia Cannella, Davide Leopardo, Carmela Pisano, Giovanni Salvatore Bruni, and Gaetano Facchini. 2011. "Chemotherapy in Epithelial Ovarian Cancer." *Cancer Letters*. https://doi.org/10.1016/j.canlet.2011.01.026.

Piva, Roberto, Giuseppe Belardo, and M. Gabriella Santoro. 2006. "NF-κB: A Stress-Regulated Switch for Cell Survival." *Antioxidants & Redox Signaling* 8 (3–4):478–86. https://doi.org/10.1089/ars.2006.8.478.

Portielje, Johanna E.A., Cor H.J. Lamers, Wim H.J. Kruit, Alex Sparreboom, Reinder L.H. Bolhuis, Gerrit Stoter, Christoph Huber, and Jan W. Gratama. 2003. "Repeated Administrations of Interleukin (IL)-12 Are Associated with Persistently

Elevated Plasma Levels of IL-10 and Declining IFN-Γ, Tumor Necrosis Factor-A, IL-6, and IL-8 Responses." *Clinical Cancer Research* 9 (1):76–83. https://doi.org/10.1177/019262339902700112.

Pouw Kraan, T. C. van der. 1995. "Prostaglandin-E_2 Is a Potent Inhibitor of Human Interleukin 12 Production." *Journal of Experimental Medicine* 181 (2):775–79. https://doi.org/10.1084/jem.181.2.775.

Rahim, Sheikh Showkat, Nooruddin Khan, Chandra Sekhar Boddupalli, Seyed E. Hasnain, and Sangita Mukhopadhyay. 2005. "Interleukin-10 (IL-10) Mediated Suppression of IL-12 Production in RAW 264.7 Cells Involves c-Rel Transcription Factor." *Immunology* 114 (3):313–21. https://doi.org/10.1111/j.1365-2567.2005.02107.x.

Reinartz, Silke, Tim Schumann, Florian Finkernagel, Annika Wortmann, Julia M. Jansen, Wolfgang Meissner, Michael Krause, et al. 2014. "Mixed-Polarization Phenotype of Ascites-Associated Macrophages in Human Ovarian Carcinoma: Correlation of CD163 Expression, Cytokine Levels and Early Relapse." *International Journal of Cancer* 134 (1):32–42. https://doi.org/10.1002/ijc.28335.

Rival, Yves, Nathalie Benéteau, Thierry Taillandier, Mylène Pezet, Elisabeth Dupont-Passelaigue, Jean François Patoiseau, Didier Junquéro, Francis C. Colpaert, and André Delhon. 2002. "PPARalpha And PPARdelta Activators Inhibit Cytokine-Induced Nuclear Translocation of NF-κB and Expression of VCAM-1 in EAhy926 Endothelial Cells." *European Journal of Pharmacology* 435 (2–3):143–51. https://doi.org/10.1016/S0014-2999(01)01589-8.

Romanowska, Malgorzata, Louise Reilly, Colin N A Palmer, Mattias C U Gustafsson, and John Foerster. 2010. "Activation of PPARβ/δ Causes a Psoriasis-like Skin Disease in Vivo." *PLoS ONE* 5 (3). https://doi.org/10.1371/journal.pone.0009701.

Rosen, Evan D., and Bruce M. Spiegelman. 2001. "PPARγ: A Nuclear Regulator of Metabolism, Differentiation, and Cell Growth." *Journal of Biological Chemistry*. https://doi.org/10.1074/jbc.R100034200.

Saccani, Alessandra, Tiziana Schioppa, Chiara Porta, Subhra K. Biswas, Manuela Nebuloni, Luca Vago, Barbara Bottazzi, Mario P. Colombo, Alberto Mantovani, and Antonio Sica. 2006. "p50 Nuclear Factor-κB Overexpression in Tumor-Associated Macrophages Inhibits M1 Inflammatory Responses and Antitumor Resistance." *Cancer Research* 66 (23):11432–40. https://doi.org/10.1158/0008-5472.CAN-06-1867.

Saccani, Simona, Serafino Pantano, and Gioacchino Natoli. 2001. "Two Waves of Nuclear Factor Kb Recruitment to Target Promoters." *The Journal of Experimental*

Medicine 193 (12):1351–60. https://doi.org/10.1084/jem.193.12.1351.

Saini, U., S. Naidu, A. C. Elnaggar, H. K. Bid, J. J. Wallbillich, K. Bixel, C. Bolyard, et al. 2017. "Elevated STAT3 Expression in Ovarian Cancer Ascites Promotes Invasion and Metastasis: A Potential Therapeutic Target." *Oncogene* 36 (2):168–81. https://doi.org/10.1038/onc.2016.197.

Sanjabi, S., A. Hoffmann, H.-C. Liou, D. Baltimore, and S. T. Smale. 2000. "Selective Requirement for c-Rel during IL-12 P40 Gene Induction in Macrophages." *Proceedings of the National Academy of Sciences* 97 (23):12705–10. https://doi.org/10.1073/pnas.230436397.

Santin, A D, S Bellone, A Ravaggi, J Roman, C V Smith, S Pecorelli, M J Cannon, and G P Parham. 2001. "Increased Levels of Interleukin-10 and Transforming Growth Factor-Beta in the Plasma and Ascitic Fluid of Patients with Advanced Ovarian Cancer." *BJOG : An International Journal of Obstetrics and Gynaecology* 108 (8):804–8. http://www.ncbi.nlm.nih.gov/pubmed/11510703.

Santin, A D, P L Hermonat, A Ravaggi, M J Cannon, S Pecorelli, and G P Parham. 1999. "Secretion of Vascular Endothelial Growth Factor in Ovarian Cancer." *Eur.J.Gynaecol.Oncol.* 20 (0392–2936):177–81.

Schultze, J. L. 2017. "Chromatin Remodeling in Monocyte and Macrophage Activation." In *Advances in Protein Chemistry and Structural Biology*, 106:1–15. https://doi.org/10.1016/bs.apcsb.2016.09.001.

Segal, Benjamin M., Bonnie K. Dwyer, and Ethan M. Shevach. 1998. "An Interleukin (IL)-10/IL-12 Immunoregulatory Circuit Controls Susceptibility to Autoimmune Disease." *The Journal of Experimental Medicine* 187 (4):537–46. https://doi.org/10.1084/jem.187.4.537.

Sen, Ranjan, and David Baltimore. 1986. "Multiple Nuclear Factors Interact with the Immunoglobulin Enhancer Sequences." *Cell* 46 (5):705–16. https://doi.org/10.1016/0092-8674(86)90346-6.

Shames, B D, C H Selzman, D R Meldrum, E J Pulido, H A Barton, X Meng, A H Harken, and R C McIntyre. 1998. "Interleukin-10 Stabilizes Inhibitory kappaB-Alpha in Human Monocytes." *Shock (Augusta, Ga.)* 10 (6):389–94. https://doi.org/10.1097/00024382-199812000-00002.

Shen, Z, M Wu, P Elson, a W Kennedy, J Belinson, G Casey, and Y Xu. 2001. "Fatty Acid Composition of Lysophosphatidic Acid and Lysophosphatidylinositol in Plasma from Patients with Ovarian Cancer and Other Gynecological Diseases." *Gynecologic Oncology* 83 (1):25–30. https://doi.org/10.1006/gyno.2001.6357.

Sherer, D M, R Eliakim, and O Abulafia. 2000. "The Role of Angiogenesis in the

Accumulation of Peritoneal Fluid in Benign Conditions and the Development of Malignant Ascites in the Female." *Gynecol Obstet Invest* 50 (4):217–24. https://doi.org/10320 [pii]10320 [doi].

Sica, A., A. Saccani, B. Bottazzi, N. Polentarutti, A. Vecchi, J. V. Damme, and A. Mantovani. 2000. "Autocrine Production of IL-10 Mediates Defective IL-12 Production and NF- B Activation in Tumor-Associated Macrophages." *The Journal of Immunology* 164 (2):762–67. https://doi.org/10.4049/jimmunol.164.2.762.

Sica, Antonio, and Vincenzo Bronte. 2007. "Altered Macrophage Differentiation and Immune Dysfunction in Tumor Development." *Journal of Clinical Investigation*. https://doi.org/10.1172/JCI31422.

Sica, Antonio, and Alberto Mantovani. 2012. "Macrophage Plasticity and Polarization: In Vivo Veritas." *The Journal of Clinical Investigation* 122 (3). American Society for Clinical Investigation:787–95. https://doi.org/10.1172/JCI59643.

Solinas, G., G. Germano, A. Mantovani, and P. Allavena. 2009. "Tumor-Associated Macrophages (TAM) as Major Players of the Cancer-Related Inflammation." *Journal of Leukocyte Biology* 86 (5):1065–73. https://doi.org/10.1189/jlb.0609385.

Stockert, Josefine, Till Adhikary, Kerstin Kaddatz, Florian Finkernagel, Wolfgang Meissner, Sabine Müller-Brüsselbach, and Rolf Müller. 2011. "Reverse Crosstalk of TGFβ And PPARβ/δ Signaling Identified by Transcriptional Profiling." *Nucleic Acids Research* 39 (1):119–31. https://doi.org/10.1093/nar/gkq773.

Stockert, Josefine, Alexander Wolf, Kerstin Kaddatz, Evelyn Schnitzer, Florian Finkernagel, Wolfgang Meissner, Sabine Müller-Brüsselbach, Michael Kracht, and Rolf Müller. 2013. "Regulation of TAK1/TAB1-Mediated IL-1β Signaling by Cytoplasmic PPARβ/δ" *PLoS ONE* 8 (4). https://doi.org/10.1371/journal.pone.0063011.

Straus, Daniel S., and Christopher K. Glass. 2007. "Anti-Inflammatory Actions of PPAR Ligands: New Insights on Cellular and Molecular Mechanisms." *Trends in Immunology*. https://doi.org/10.1016/j.it.2007.09.003.

Straus, D S, G Pascual, M Li, J S Welch, M Ricote, C H Hsiang, L L Sengchanthalangsy, G Ghosh, and C K Glass. 2000. "15-Deoxy-Delta 12,14-Prostaglandin J2 Inhibits Multiple Steps in the NF-Kappa B Signaling Pathway." *Proceedings of the National Academy of Sciences of the United States of America* 97 (9):4844–49. https://doi.org/10.1073/pnas.97.9.4844.

Sznaidman, Marcos L., Curt D. Haffner, Patrick R. Maloney, Adam Fivush, Esther Chao, Donna Goreham, Michael L. Sierra, et al. 2003. "Novel Selective Small Molecule Agonists for Peroxisome Proliferator-Activated Receptor δ (PPARδ)—

synthesis and Biological Activity." *Bioorganic & Medicinal Chemistry Letters* 13 (9):1517–21. https://doi.org/10.1016/S0960-894X(03)00207-5.

Thanos, Dimitris, and Tom Maniatis. 1995. "NF-κB: A Lesson in Family Values." *Cell*. https://doi.org/10.1016/0092-8674(95)90506-5.

Toth, Philipp M., Sonja Lieber, Frithjof M. Scheer, Tim Schumann, Yvonne Schober, Wolfgang A. Nockher, Till Adhikary, Sabine Müller-Brüsselbach, Rolf Müller, and Wibke E. Diederich. 2016. "Design and Synthesis of Highly Active Peroxisome Proliferator-Activated Receptor (PPAR) B/δ Inverse Agonists with Prolonged Cellular Activity." *ChemMedChem* 11 (5):488–96. https://doi.org/10.1002/cmdc.201500594.

Trinchieri, Giorgio. 1995. "Interleukin-12: A Proinflammatory Cytokine with Immunoregulatory Functions That Bridge Innate Resistance and Antigen-Specific Adaptive Immunity." *Annual Review of Immunology* 13 (1):251–76. https://doi.org/10.1146/annurev.iy.13.040195.001343.

Vignali, Dario A A, and Vijay K. Kuchroo. 2012. "IL-12 Family Cytokines: Immunological Playmakers." *Nature Immunology*. https://doi.org/10.1038/ni.2366.

Wagner, Andreas H., Michael Conzelmann, Franziska Fitzer, Thomas Giese, Karsten Gülow, Christine S. Falk, Oliver H. Krämer, Sascha Dietrich, Markus Hecker, and Thomas Luft. 2015. "JAK1/STAT3 Activation Directly Inhibits IL-12 Production in Dendritic Cells by Preventing CDK9/P-TEFb Recruitment to the p35 Promoter." *Biochemical Pharmacology* 96:52–64. https://doi.org/10.1016/j.bcp.2015.04.019.

Wang, I M, C Contursi, a Masumi, X Ma, G Trinchieri, and K Ozato. 2000. "An IFN-Gamma-Inducible Transcription Factor, IFN Consensus Sequence Binding Protein (ICSBP), Stimulates IL-12 p40 Expression in Macrophages." *Journal of Immunology (Baltimore, Md. : 1950)* 165 (1):271–79. https://doi.org/ji_v165n1p271 [pii].

Westergaard, Majken, Jeanette Henningsen, Claus Johansen, Sofie Rasmussen, Morten Lyhne Svendsen, Uffe Birk Jensen, Henrik Daa Schrøder, et al. 2003. "Expression and Localization of Peroxisome Proliferator-Activated Receptors and Nuclear Factor κB in Normal and Lesional Psoriatic Skin." *Journal of Investigative Dermatology* 121 (5):1104–17. https://doi.org/10.1046/j.1523-1747.2003.12536.x.

Williams, Lynn M., Giuseppe Ricchetti, Usha Sarma, Timothy Smallie, and Brian M.J. Foxwell. 2004. "Interleukin-10 Suppression of Myeloid Cell Activation - A Continuing Puzzle." *Immunology* 113 (3):281–92. https://doi.org/10.1111/j.1365-2567.2004.01988.x.

Worzfeld, Thomas, Elke Pogge von Strandmann, Magdalena Huber, Till Adhikary, Uwe

Wagner, Silke Reinartz, and Rolf Müller. 2017. “The Unique Molecular and Cellular Microenvironment of Ovarian Cancer.” *Frontiers in Oncology* 7. https://doi.org/10.3389/fonc.2017.00024.

Xu, Jihong, and Paul D Drew. 2007. “Peroxisome Proliferator-Activated Receptor-Gamma Agonists Suppress the Production of IL-12 Family Cytokines by Activated Glia.” *Journal of Immunology (Baltimore, Md. : 1950)* 178 (3):1904–13. https://doi.org/178/3/1904 [pii].

Xu, Jihong, Michael K. Racke, and Paul D. Drew. 2007. “Peroxisome Proliferator-Activated Receptor-α Agonist Fenofibrate Regulates IL-12 Family Cytokine Expression in the CNS: Relevance to Multiple Sclerosis.” *Journal of Neurochemistry* 103 (5):1801–10. https://doi.org/10.1111/j.1471-4159.2007.04875.x.

Yu, Hua, and Richard Jove. 2004. “The STATs of Cancer--New Molecular Targets Come of Age.” *Nature Reviews. Cancer* 4 (2):97–105. https://doi.org/10.1038/nrc1275.

Zhang, Meijuan, and Kevin L Fritsche. 2004. “Fatty Acid-Mediated Inhibition of IL-12 Production by Murine Macrophages Is Independent of PPARgamma.” *British Journal of Nutrition* 91 (5):733–39. https://doi.org/10.1079/BJN20041096.

6 Anhang

6.1 Verzeichnis akademischer Lehrer

Meine akademischen Lehrer waren die Damen und Herren in

Saarbrücken/Homburg (Saar):

Bauer, Beck, Bernhardt, Breinig, Cavalié, Deicher, Faas, Flockerzi, Freichel, Grässer, Heinzle, Helms, Hoth, Huber, Kallenborn, Katzmaier, Kohring, Lancaster, Maurer, Meese, Meyerhans, Mohrmann, Montenarh, Mues, Müller, Oberwinkler, Paulsen, Phillip, Römisch, Rother, Schmitt, Sester, Smola, Veith, Walldorf, Walter, Wisser, Wollenberg

Marburg:

Adhikary, Bauer, Brendel, Buchholz, Burchert, Dodel, Eming, Exner, Garn, Hertl, Hoyer, Irle, Kinscherf, Moll, Müller-Brüsselbach, Müller, Ocker, Pfefferle, Pucetti, Reinartz, Rogosch, Schäfer, Schmidt, Stiewe, Wrocklage

Deregulation of PPARβ/δ target genes in tumor-associated macrophages by fatty acid ligands in the ovarian cancer microenvironment

Tim Schumann[1,*], Till Adhikary[1,*], Annika Wortmann[1,*], Florian Finkernagel[1], Sonja Lieber[1], Evelyn Schnitzer[1], Nathalie Legrand[1], Yvonne Schober[2], W. Andreas Nockher[2], Philipp M. Toth[3], Wibke E. Diederich[3], Andrea Nist[4], Thorsten Stiewe[4], Uwe Wagner[5], Silke Reinartz[5], Sabine Müller-Brüsselbach[1] and Rolf Müller[1]

[1] Institute of Molecular Biology and Tumor Research (IMT), Philipps University, Marburg, Germany

[2] Metabolomics Core Facility and Institute of Laboratory Medicine and Pathobiochemistry, Philipps University, Marburg, Germany

[3] Medicinal Chemistry Core Facility and Institute of Pharmaceutical Chemistry, Philipps University, Marburg, Germany

[4] Genomics Core Facility, Philipps University, Marburg, Germany

[5] Clinic for Gynecology, Gynecological Oncology and Gynecological Endocrinology, Center for Tumor Biology and Immunology (ZTI), Philipps University, Marburg, Germany

[*] These authors have contributed equally to this work

Correspondence to: *Rolf Müller*, ***email***: *rmueller@imt.uni-marburg.de*

Keywords: *PPARβ/δ, ANGPTL4, ovarian carcinoma, tumor-associated macrophages, linoleic acid*

Received: *December 23, 2014* ***Accepted***: *March 29, 2015* ***Published***: *April 15, 2015*

ABSTRACT

The nuclear receptor peroxisome proliferator-activated receptor β/δ (PPARβ/δ) is a lipid ligand-inducible transcription factor associated with macrophage polarization. However, its function in tumor-associated macrophages (TAMs) has not been investigated to date. Here, we report the PPARβ/δ-regulated transcriptome and cistrome for TAMs from ovarian carcinoma patients. Comparison with monocyte-derived macrophages shows that the vast majority of direct PPARβ/δ target genes are upregulated in TAMs and largely refractory to synthetic agonists, but repressible by inverse agonists. Besides genes with metabolic functions, these include cell type-selective genes associated with immune regulation and tumor progression, e.g., *LRP5, CD300A, MAP3K8 and ANGPTL4*. This deregulation is not due to increased expression of PPARβ/δ or its enhanced recruitment to target genes. Instead, lipidomic analysis of malignancy-associated ascites revealed high concentrations of polyunsaturated fatty acids, in particular linoleic acid, acting as potent PPARβ/δ agonists in macrophages. These fatty acid ligands accumulate in lipid droplets in TAMs, thereby providing a reservoir of PPARβ/δ ligands. These observations suggest that the deregulation of PPARβ/δ target genes by ligands of the tumor microenvironment contributes to the pro-tumorigenic polarization of ovarian carcinoma TAMs. This conclusion is supported by the association of high *ANGPTL4* expression with a shorter relapse-free survival in serous ovarian carcinoma.

INTRODUCTION

Macrophages of the tumor microenvironment play a pivotal role in promoting the growth, invasion, metastazation and therapy resistance of malignant tumors, as suggested by the correlation of disease progression with macrophage density in different types of human cancer and shown in mouse tumor models [1, 2]. Under the influence of chemokines, cytokines and growth factors secreted by tumor cells and other host-derived cells, monocytes are recruited from the circulation and differentiate into tumor-associated macrophages (TAMs) that are programmed

to promote tumor progression [3-5]. Macrophages react to their microenvironment with an extreme plasticity [6], resulting in highly diverse phenotypes, with pro-inflammatory "M1" and anti-inflammatory "M2" macrophages [4] as the extremes. Macrophages can also adopt mixed-polarization phenotypes with properties of both M1 and M2 cells [6], TAMs being a prominent example [4, 5, 7, 8].

Macrophage polarization is regulated by a plethora of signaling molecules and transcriptional regulators. These include the nuclear receptor proliferator-activated receptor β/δ (PPARβ/δ), a ligand-inducible transcription factor with established functions in intermediary metabolism and immune regulation [9, 10]. The latter has been documented in several reports addressing the role of PPARβ/δ in inflammatory responses of the skin [11, 12] and the M2-like polarization of macrophages in adipose tissue and liver [13, 14]. PPARβ/δ has also been implicated in tumorigenesis in a number of studies with conflicting results [15], which may be due to divergent functions of the receptor in tumor cells and tumor-associated host cells as well as differences in the experimental models used (mouse strains, synthetic ligands).

PPARβ/δ binds to PPAR response elements (PPREs) at its target genes as a heterodimer with a retinoid X receptor (RXR), which is activated only upon interaction with an agonistic ligand (canonical regulation) [15]. These include unsaturated fatty acids [16], prostaglandin I_2 (prostacyclin) [17], 15-hydroxyeicosatetraenoic acid (15-HETE) [18] and a range of synthetic ligands, originally developed in light of the association of PPARβ/δ with metabolic diseases [15]. Genome-wide analyses have identified PPRE-mediated repression as a major mechanism of transcriptional regulation by unliganded PPARβ/δ, and showed that an agonist-mediated switch induces a subset of these genes [19]. PPRE-mediated repression is enhanced by inverse agonists, such as ST247 [20], which establish a repressor complex that apparently is different from the unliganded receptor complex [21].

PPARβ/δ can also regulate genes by interacting with specific transcription factors both in a PPRE-dependent [22] and independent fashion [23]. For example, unliganded PPARβ/δ in murine macrophages sequesters BCL6, a transcriptional repressor of inflammatory NFκB-regulated genes [23]. PPARβ/δ also modulates NFκB signaling by other mechanisms, including its interaction with the p65 subunit of NFκB [24-27].

We have recently addressed the function of PPARβ/δ in normal human macrophages by determining the global PPARβ/δ-regulated signaling network in primary monocyte-derived macrophages [28]. Besides canonically regulated genes with metabolic functions, we also identified a number of target genes with immune regulatory functions. These are type-selective and subject to either canonical regulation, such as *CD1D, CD52, CD300A, LRP5, NLRC,* or indirect repression by agonists, mainly affecting NFκB and STAT target genes. Consistent with these findings, PPARβ/δ agonists triggered hallmarks of an anti-inflammatory phenotype. However, we also identified positive regulatory effects on specific immune modulatory modules, in particular a stimulation of T-cell activation. PPARβ/δ agonists thus induce a unique macrophage activation state with strong anti-inflammatory but also specific stimulatory components, suggesting a context-dependent function of PPARβ/δ in immune regulation.

To date, transcriptome data for human TAMs has not been reported. Furthermore, the gene regulatory function of PPARβ/δ in TAMs has not been analyzed. Ovarian cancer is an excellent model to study TAMs, since these cells can be isolated in large quantities from the malignancy-associated peritoneal ascites. These ascites-derived macrophages display a mixed-polarization phenotype expressing both M1 and M2 markers [8]. Consistent with this finding, interpatient polarization differences unrelated to the M1/M2 classification scheme showed a clear association with the clinical outcome [8]. To elucidate the mechanisms underlying the pro-tumorigenic polarization of TAMs in ovarian cancer and the role of PPARβ/δ in this context we determined the PPARβ/δ-regulated transcriptome and PPARβ/δ cistrome in ovarian carcinoma TAMs in comparison to normal human monocyte-derived macrophages (MDMs).

RESULTS

Ligand-induced cellular alterations in human MDMs

$CD14^+$ cells from human serous ovarian carcinoma ascites (TAMs) rapidly adhere to cell culture dishes and assume a macrophage-like morphology. We used this experimental system to investigate the affects of the synthetic PPARβ/δ agonist L165,041 on freshly isolated TAMs in short-term culture in comparison to normal monocyte-derived macrophages (MDMs). This comparison is conceptually relevant, since TAMs, including ascites-associated macrophages, are derived from blood monocytes [29-32]. Under the experimental conditions used TAMs showed a clearly enhanced expression of *CD163* and a very low level of *MMP9* mRNA relative to MDMs (Figure 1A), which is consistent with the polarization phenotype of TAMs *in vivo* [8]. We therefore conclude that our experimental system is suitable to investigate ligand-induced changes in TAMs compared to MDMs.

We have previously described that the synthetic PPARβ/δ agonist L165,041 induces a morphology in MDMs that resembles that of IL-4 treated macrophages [28] (Figure 1B and 1C). TAMs, on the other hand,

displayed an unchanged morphology upon L165,041 treatment (Figure 1D and 1E). This observation suggests that TAMs are largely unresponsive to exogenous PPARβ/δ ligands. In order to address the mechanistic basis of this observation we performed comprehensive genome-wide studies as described below.

Impaired ligand response and upregulation of PPARβ/δ target genes in cultured ovarian carcinoma TAMs

Ascites-derived adherent macrophages showed a clear accumulation of PPARβ/δ and RXR at the upstream enhancer of the established PPARβ/δ target gene *PDK4* [19, 33] *in vivo* (Figure 2A) with a strong enrichment of both factors (30-fold relative to IgG control for PPARβ/δ; 40-fold for RXR). This is similar to the enrichment in MDMs (30- and 43-fold, respectively), but much higher compared to monocytes (4- to 5-fold, respectively). These data are therefore consistent with the definition of ascites-derived $CD14^+$ cells as TAMs rather than ascites-associated monocytes and confirm their suitability for PPARβ/δ centered genome-wide studies.

Toward this end, MDMs in normal growth medium and freshly isolated TAMs in ascites were exposed to a synthetic PPARβ/δ agonist, inverse PPARβ agonists or solvent (DMSO) for 1 day and analyzed by RNA-Seq (Table S2). The specificity of these ligands for PPARβ/δ is illustrated in Figure S1. Only a small number of genes (n = 30) were found to be induced by the agonist L165,041 in TAMs (logFC≥1; FPKM≥0.3) compared to MDMs (n = 102) with a small intersection (n = 7; Figure 2B, top; Figure 2C; Table S3). On the other hand, the number of genes downregulated by the inverse agonists ST247 or PT-S264 was considerably greater in TAMs (n = 50) relative to MDMs (n = 18) with a minor overlap (n = 8; Figure 2B, bottom; Table S3). These findings would be consistent with the presence of high concentrations of PPARβ/δ agonists in TAMs relative to MDMs.

The observation that the majority of PPARβ/δ target genes were refractory to synthetic agonists was confirmed by RT-qPCR for *PDK4 and ANGPTL4* (Figure 2D). Both genes were induced by L165,041 in MDMs >50-fold (average; blue symbols), whereas induction in TAMs cultured in ascites (orange symbols) was <10-fold (*PDK4*) or undetectable (*ANGPTL4*). When TAMs were cultured in R10 for 24 h instead of ascites, *PDK4* induction was only slightly higher (grey symbols). These findings indicate that the loss of ligand regulation in TAMs is not dependent on the continuous presence of ascites, pointing to a relatively stable alteration affecting the regulation of PPARβ/δ target genes.

We have previously identified canonical PPARβ/δ

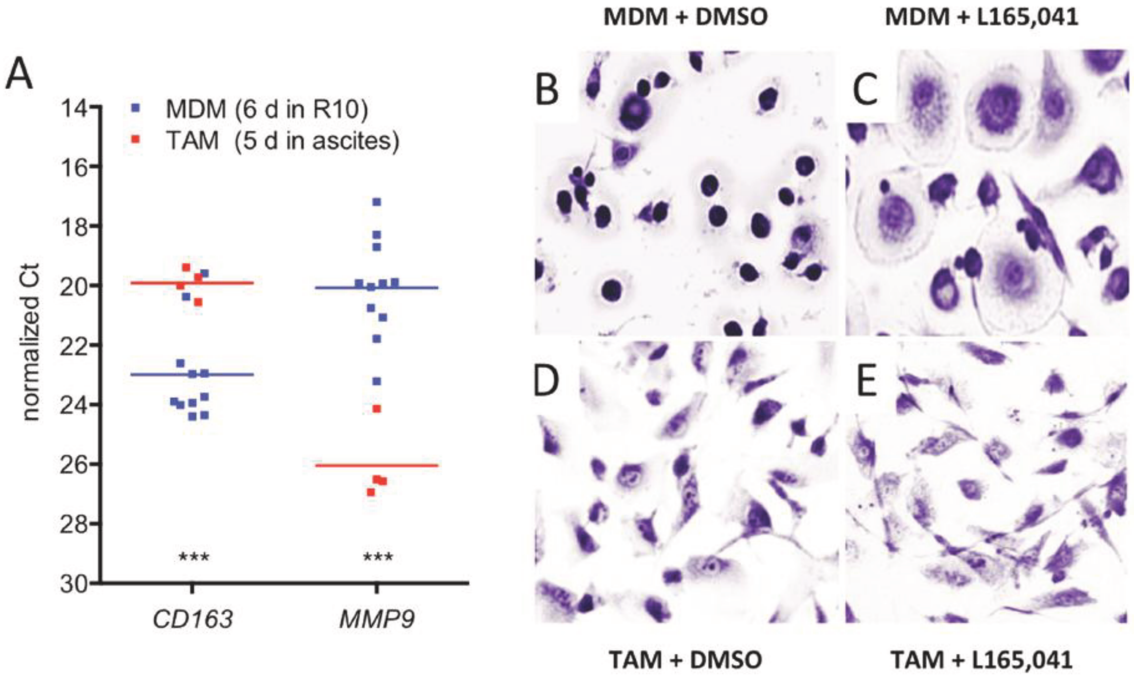

Figure 1: Effects of PPARβ/δ ligands on the morphology of human MDMs and ovarian carcinoma TAMs. A. Expression of the macrophage polarization marker genes *CD163* and *MMP9* in cultured TAMs and MDMs. The data were obtained by RT-qPCR analysis of TAMs (red data points; n = 4) and MDMs (blue: n = 11) from different donors. Horizontal lines show the medians; asterisks indicate statistical significance. **B, C.** Giemsa staining of human MDMs differentiated in XV0 medium for 8 days in the presence of the PPARβ/δ agonist L165,041 or solvent (DMSO). **D, E.** TAMs treated with agonist or DMSO as in panel B and C.

target genes in human MDMs that are agonist-induced and occupied by PPARβ/δ-RXR complexes [28]. In combination with the additional RNA-Seq data of the present study, a total of 195 ligand-regulated target genes were identified, defined as "upregulated by agonist versus inverse agonist", 95 of which were associated with PPARβ/δ enrichment sites (Figure 2E; Table S3, columns "L" and "K"). Delineation of the PPARβ/δ cistrome for 3 different patient samples in the present study (Suppl. Table S4) showed that at least 45 of these genomic loci were also occupied by PPARβ/δ in TAMs (Figure 2E; Table S3, column "J"), including those genes showing an altered ligand regulation in TAMs, exemplified by *PDK4, CPT1A, SLC25A20, CD52* and *PHACTR1* (Figure 2F).

Deregulation of PPARβ/δ target genes in ovarian carcinoma TAMs *in vivo*

We next compared the expression and ligand regulation of PPARβ/δ target genes in ascites-associated macrophages from ten different patients (Table S5) with the set of 195 ligand-regulated target genes in MDMs identified by RNA-Seq analysis of cells from 5 healthy donors (see above; Table S3). Intriguingly, a large fraction of these PPARβ/δ target genes (dark blue dots; n = 54)

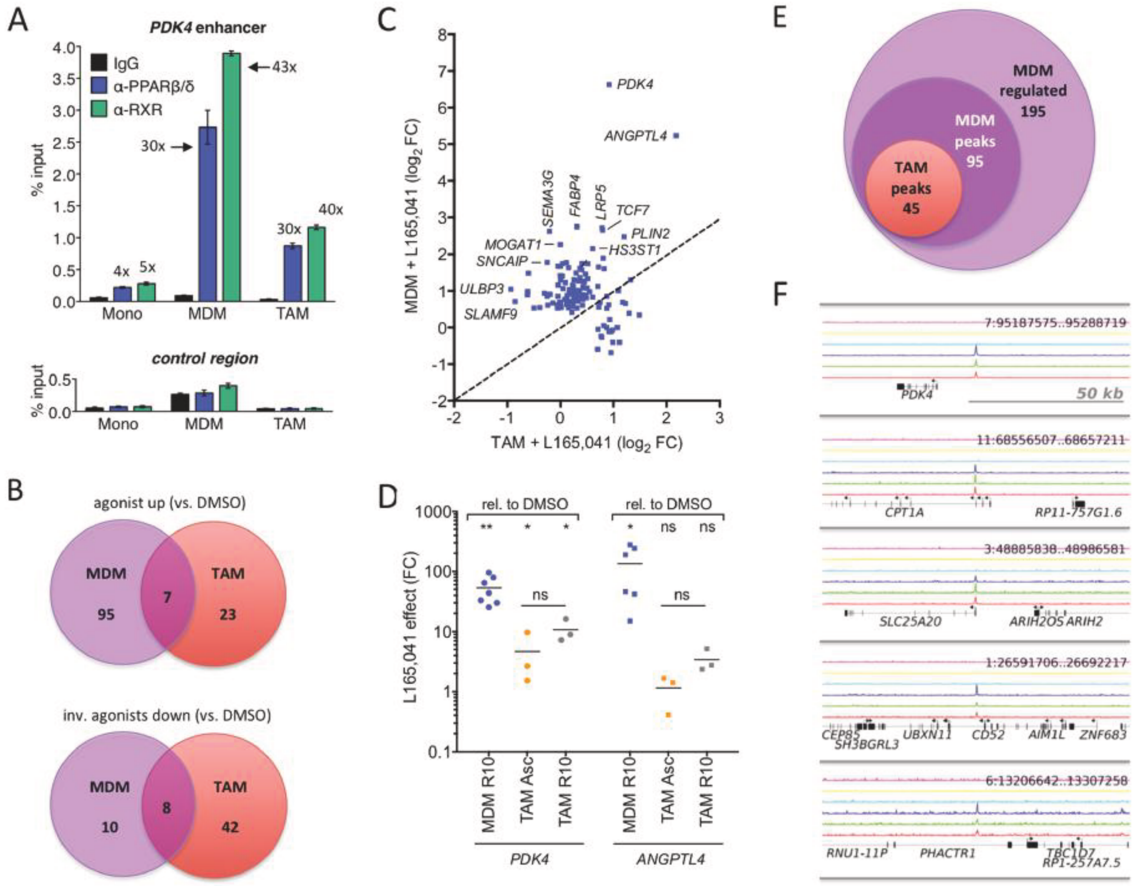

Figure 2: Deregulation of PPARβ/δ target genes in cultured ovarian carcinoma TAMs. A. PPARβ/δ and RXR enrichment at the *PDK4* enhancer and an irrelevant control region in human monocytes, MDMs and TAMs (ChIP-qPCR; sample size: 4). **B.** Venn diagrams of RNA-Seq data showing overlaps of ligand-regulated high-confidence direct target genes in MDMs grown in R10 medium or purified TAMs cultured in ascites for 1 day in the presence of agonist (L165,041), inverse agonist (ST247or PT-S264) or solvent (DMSO). **C.** Ligand response of PPARβ/δ target genes in TAMs versus MDMs. Data represents the $\log_2$ fold change (L165,041 relative to DMS0) calculated from RNA-Seq data. The diagonal line indicates equal regulation in both cell types. **D.** Expression and ligand response of *PDK4* and *ANGPTL4* by L165,041 in MDMs in R10 (n = 7) and TAMs (n = 3) cultured in either ascites or R10 medium. Cells were cultured in the presence of ligand or DMSO for 24 h and analyzed by RT-qPCR. Data are expressed as fold regulation (FC) relative to DMSO-treated cells. **E.** Overlap of genes regulated in MDMs (agonist versus inverse agonist), genomic regions with PPARβ/δ binding sites in MDMs and PPARβ/δ enrichment sites in TAMs (ChIP-Seq). **F.** PPARβ/δ enrichment (ChIP-Seq) at the *PDK4, CPT1A, SLC25A20, CD52* and *PHACTR1* loci for 3 different TAM samples (bottom 3 lines: dark blue, green, red). The top 3 lanes (magenta, yellow, light blue) represent the corresponding control IgG runs.

Table 1: PPARβ/δ target genes upregulated[1] in ovarian cancer TAMs.

Gene	Description	agonist MDM (FC)[2]	PPARβ/δ peak[3]	refractory in TAM[4]
ACADVL	acyl-CoA dehydrogenase, very long chain	3.3	+	+
ACSS3	acyl-CoA synthetase short-chain family member 3	2.3	-	+
AMOTL1	angiomotin like 1	1.9	-	+
ANGPTL4	angiopoietin-like 4	37.8	+	+
ANKRD1	ankyrin repeat domain 1 (cardiac muscle)	1.8	-	-
C19orf59	chromosome 19 open reading frame 59	6.7	+	+
C1orf162	chromosome 1 open reading frame 162	2.2	+	+
C1QC	complement component 1, q subcomponent, C chain	1.5	-	-
CABLES1	Cdk5 and Abl enzyme substrate 1	3.2	-	+
CACNB1	calcium channel, voltage-dependent, beta 1 subunit	2.4	+	+
CD300A	CD300a molecule	1.5	+	-
CLDND2	claudin domain containing 2	2.2	+	+
CPT1A	carnitine palmitoyltransferase 1A (liver)	3.4	+	+
CXorf21	chromosome X open reading frame 21	1.8	+	+
DLG4	discs, large homolog 4 (Drosophila)	1.6	+	+
FAM3B	family with sequence similarity 3, member B	2.7	-	+
FCGR3A	Fc fragment of IgG, low affinity IIIa, receptor (CD16a)	1.5	+	-
FCGRT	Fc fragment of IgG, receptor, transporter, alpha	1.5	+	-
FOS	FBJ murine osteosarcoma viral oncogene homolog	1.1	+	-
GPA33	glycoprotein A33 (transmembrane)	1.8	-	+
HMOX1	heme oxygenase (decycling) 1	1.3	+	-
HP	haptoglobin	2.2	-	-
HPR	haptoglobin-related protein	2.6	-	-
HS3ST1	heparan sulfate (glucosamine) 3-O-sulfotransferase 1	4.4	-	+
IL27	interleukin 27	1.2	-	-
IMPA2	inositol(myo)-1(or 4)-monophosphatase 2	2.6	+	+
INF2	inverted formin, FH2 and WH2 domain containing	1.5	-	+
KBTBD11	kelch repeat and BTB (POZ) domain containing 11	1.3	-	-
KLF11	Kruppel-like factor 11	1.4	-	-
KRT4	keratin 4	1.9	-	+
LRP5	low density lipoprotein receptor-related protein 5	6.6	+	+
MACC1	metastasis associated in colon cancer 1	1.8	+	-
MAP3K8	mitogen-activated protein kinase kinase kinase 8	1.5	-	+
MEGF9	multiple EGF-like-domains 9	1.5	+	-
MS4A14	membrane-spanning 4-domains, subfam. A, member 14	1.6	-	+
MS4A7	membrane-spanning 4-domains, subfamily A, member 7	1.6	-	-

PCOLCE2	procollagen C-endopeptidase enhancer 2	1.9	-	-
PDE1B	phosphodiesterase 1B, calmodulin-dependent	2.2	-	-
PDK4	pyruvate dehydrogenase kinase 4	99.0	+	+
PHACTR1	phosphatase and actin regulator 1	3.1	+	+
PLIN2	perilipin 2	5.5	+	+
PPP1R15B	protein phosphatase 1, regulatory subunit 15B	1.6	+	-
RBP7	retinol binding protein 7, cellular	1.8	-	+
RCN3	reticulocalbin 3, EF-hand calcium binding domain	2.6	+	+
RETN	resistin	1.3	+	+
S100Z	S100 calcium binding protein Z	3.1	+	-
SIPA1L2	signal-induced proliferation-associated 1 like 2	2.1	+	+
ST14	suppression of tumorigenicity 14 (colon carcinoma)	2.4	+	+
TCF7	transcription factor 7 (T-cell specific, HMG-box)	6.3	+	+
TMEM150B	transmembrane protein 150B	1.2	+	-
TMEM37	transmembrane protein 37	1.7	+	+
TRIM14	tripartite motif containing 14	1.6	-	+
TSKS	testis-specific serine kinase substrate	0.8	+	-
VSIG10L	V-set and immunoglobulin domain containing 10 like	1.4	+	-

[1] LogFC TAMs in vivo vs MDMs > 0.7 (Figures 4A and 4B; Tables S3, S5)
[2] Ratio FPKM L165,041 / FPKM DMSO in MDMs (Figure 2B; Table S2)
[3] Peak in MDMs or TAMs: ChIP-Seq data (Figures 2E ad 2F; Table S4; Adhikary et al., 2015)
[4] Refractory to synthetic agonist in TAMs (Figure 3C; Table S3); <2.0-fold (Fig. 2D, 4A, 4C; Table S2)

were upregulated ($log_2FC \geq 0.7$) in freshly isolated TAMs relative to MDMs (Figure 3A). Approximately half of the genes upregulated in cultured TAMs (21/40) overlapped with the genes upregulated *in vivo* (Figure 3B; Table S3), thus validating the results obtained *in vitro*. Most of the genes upregulated in TAMs were also refractory to regulation by a synthetic agonist ($n = 32$; Figure 3C; Table S3), suggesting a link between upregulation and loss of ligand regulation. A summary of these data is shown in Table 1.

Comparison of the expression levels of three PPARβ/δ target genes, *PDK4, ANGPTL4* and *CPT1A* in TAMs from 12 patients and MDMs from 12 healthy donors confirmed this result (Figure 3D). As shown for *PDK4*, deregulation of gene expression in TAMs correlated with increased protein levels, which, in contrast to MDMs, were largely insensitive to ligand stimulation (Figure 3E).

Interestingly, we also found a number of PPARβ/δ target genes downregulated in TAMs relative to MDMs, for example *FABP4* and *ABCG2* (Figure 3A; cyan data points). Ovarian cancer is known to consist of a plethora of signaling mediators, including cytokines [8] and lipids (see data below). It is therefore likely that a subset of target genes is downregulated by repressive signaling pathways triggered by specific components of the ovarian cancer microenvironment, thereby preventing their potential stimulation analogous to the PPARβ/δ target genes discussed in the preceding paragraph.

The deregulation of *ANGPTL4* is of particular interest, since its secreted product has been associated with cancer cell invasion and metastasis and is present in substantial amounts in the malignancy-associated ascites of most serous ovarian carcinoma patients (Figure 3F). We therefore tested the Cancer Genome Atlas (TCGA) cohort of 506 high grade serous ovarian cancer patients [34] for a potential link of *ANGPTL4* expression to the clinical outcome of the disease. As depicted by the Kaplan-Meier plot in Figure 3G, *ANGPTL4* levels showed a significant inverse association with relapse-free survival (RFS) [$p = 0.0154$; hazard ratio = 1.38 (1.06-1.79); median RFS: 15.63 versus 19.8 months].

Annotation of all PPARβ/δ target genes constitutively upregulated in TAMs by Ingenuity Pathway Analysis (IPA) identified metabolism (glucose, lipid), inflammation, cell migration and survival as top functions (Figure 4A). As expected, the PPAR ligands (benzafibrate, EPA, rosiglitazone, pirinixic acid) were found among the top upstream regulators (Figure 4B). The presence of the pro-inflammatory mediator LPS in this list is consistent with the results obtained by the functional annotation analysis (inflammation).

Deregulation of PPARβ/δ target genes by soluble mediators in malignancy-associated ascites

The data in Figure 2 suggests that the unaltered occupancy of direct target genes by PPARβ/δ-RXR in conjunction with a TAM-specific mechanism activating these chromatin-bound complexes is responsible for their deregulation in TAMs. One explanation for this deregulation could be the presence of ascites-associated activators of PPARβ/δ. We addressed this question by testing the effect of cell-free ascites samples on the regulation of PPARβ/δ target genes in MDMs. Figure 5A shows a clear upregulation of the target genes *PDK4, CPT1A, ANGPTL4, LRP5 and CD300A* by two different ascites samples, which in several cases reached the level of L165,041 induction (Figure 5B; blue dots). Furthermore, induction of all 5 genes by L165,041 was severely diminished in the presence of ascites (Figure 5B; orange dots).

Therefore, we sought to investigate whether deregulation of target genes by ascites might be attributable to the activation of PPARβ/δ, and thus dependent on PPARβ/δ binding sites (PPREs) in these genes. It has previously been shown that an upstream enhancer with three contiguous PPREs mediates induction of *PDK4* by PPARβ/δ ligands [19]. A luciferase construct with a genomic 1.5 kb fragment encompassing this enhancer showed a dramatic upregulation by three

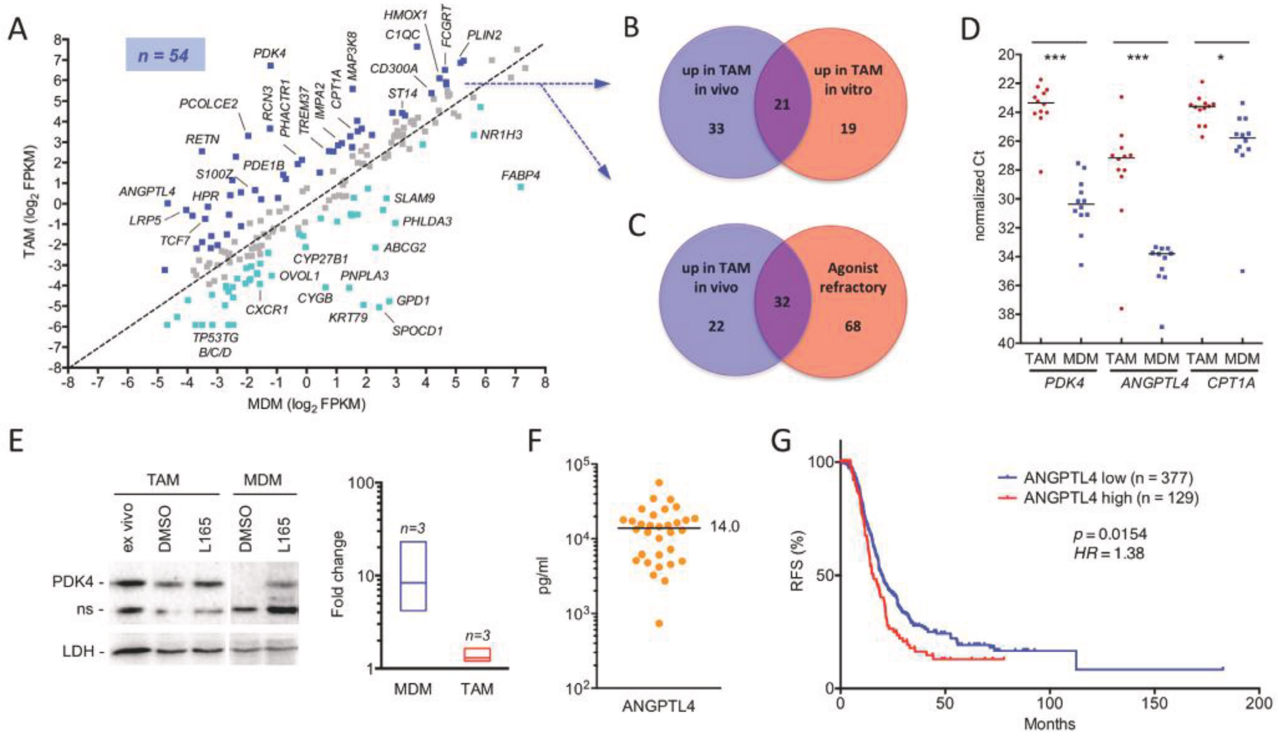

Figure 3: Deregulation of PPARβ/δ target genes in ovarian carcinoma TAMs *in vivo*. A. Expression of PPARβ/δ target genes (median FPKM values) in freshly isolated TAMs (median of 10 samples) versus MDMs (5 samples). The diagonal line indicates equal levels in both cell types. Blue dots: upregulation in TAMs ≥2-fold; cyan dots: downregulation ≥2-fold in TAMs; grey dots: no change. **B.** Overlap of PPARβ/δ target genes upregulated in freshly isolated TAMs versus MDMs (blue dots in A) and in cultured TAMs (experimental setup as in Figure 2). **C.** Overlap of PPARβ/δ target genes upregulated in TAMs versus MDMs (blue dots in A) and target genes refractory to synthetic agonists in TAMs (data from Figure 2B). **D.** RT-qPCR analysis of *PDK4, ANGPTL4* and *CPT1A* mRNA expression levels in freshly isolated TAMs and MDMs from ovarian cancer patients ($n = 12$) and healthy donors ($n = 12$), respectively. Horizontal bars indicate the median. Statistical significance was tested between the respective TAM and MDM groups. **E.** Immunoblot analysis of PDK4 protein induction by PPARβ/δ agonist in MDMs and TAMs. The figure shows representative immunoblots (including PPARβ/δ and LDH as the loading control) for both cell types and a quantitative evaluation of biological replicates with TAMs from 3 different patients and MDMs from 3 donors. Cells were exposed to ligands for 1 d in R10 medium; TAMs were also analyzed directly after isolation ("*ex vivo*"). Signal intensities were quantified and standardized to LDH. The diagram on the right depicts the induction by L165,041 (fold change) in TAMs and MDMs *in vitro*; boxes show the ranges of inducibility and the median for each group of samples. Induction values for MDMs represent estimations due to the extremely low basal level of PDK4 in MDMs. The α-PDK4 antibody was validated as shown in Figure S2. n.s., non-specific band. **F.** Concentrations of ANGPTL4 protein in the ascites of serous ovarian carcinoma patients ($n = 32$) determined by ELISA. The horizontal line indicated the median. **G.** Meier-Kaplan plot showing a correlation of high *ANGPTL4* expression with the relapse-free survival of high grade serous ovarian carcinoma patients of the TCGA cohort ($n = 377$ in *ANGPTL4* high group; $n = 129$ *ANGPTL4* low) [62].

different ascites samples (Figure 5C). These effects were clearly PPRE-dependent, since the mutation of 1, 2 or 3 sites gradually abrogated the induction of luciferase activity by ascites (Figure 5C).

We found that PPARβ/δ target genes are inducible by ascites in murine bone marrow-derived macrophages (BMDMs), similar to human MDMs. We were therefore able to show that the observed target gene deregulation was dependent on functional PPARβ/δ. Ascites upregulated the *Pdk4* and *Angptl4* genes and abrogated their induction by L165,041 in wild-type BMDMs, whereas no significant ascites effect was detected on *PDK4* in cells with disrupted *Ppard* alleles (Figure 5D). Likewise, the ascites-mediated induction of *ANGPTL4* was either absent (Asc69) or strongly reduced (Asc78) in *Ppard* null cells. These observations indicate that PPARβ/δ is responsible for the deregulation of PPARβ/δ target genes by ascites, even though a minor contribution by other PPAR subtypes cannot be unequivocally ruled out. *ANGPTL4* is induced by a plethora of signaling pathways [35], which presumably explains the residual induction by Asc78 in Ppard null cells.

Endogenous agonists present in ovarian carcinoma ascites deregulate PPARβ/δ target genes in MDMs

The results described above suggest that ovarian cancer associated ascites might contain high levels of endogenous PPARβ/δ agonists. Since all known PPARβ/δ agonists are fatty acids or fatty acid derivatives, we performed a systematic lipidomic analysis of 97 molecules in 38 different ascites samples by LC-MS/MS (Suppl. Table S6). This analysis revealed consistently very high concentrations of several polyunsaturated fatty acids (PUFAs) known as PPARβ/δ agonists [16], with the highest levels observed with linoleic acid (LA) (Figure 6A). The median concentration for LA was ~50 μg/ml (~180 μM), which is far above the described IC_{50} of 0.75 μM for PPARβ/δ binding [16]. This also applies to arachidonic acid (AA) and docosahexaenoic acid (DHA) with median ascites concentrations around 10 μg/ml (Figure 6A).

Addition of AA, LA or DHA to MDM cultures at a concentration of 20 μM for 24 h resulted in a strong induction of the *PDK4* gene, while eicosapentaenoic acid (EPA) and α-linolenic acid (ALA) had only very modest effects (Figure 6B). *PDK4* induction by LA was dose-dependent and rapid with a nearly 10-fold induction

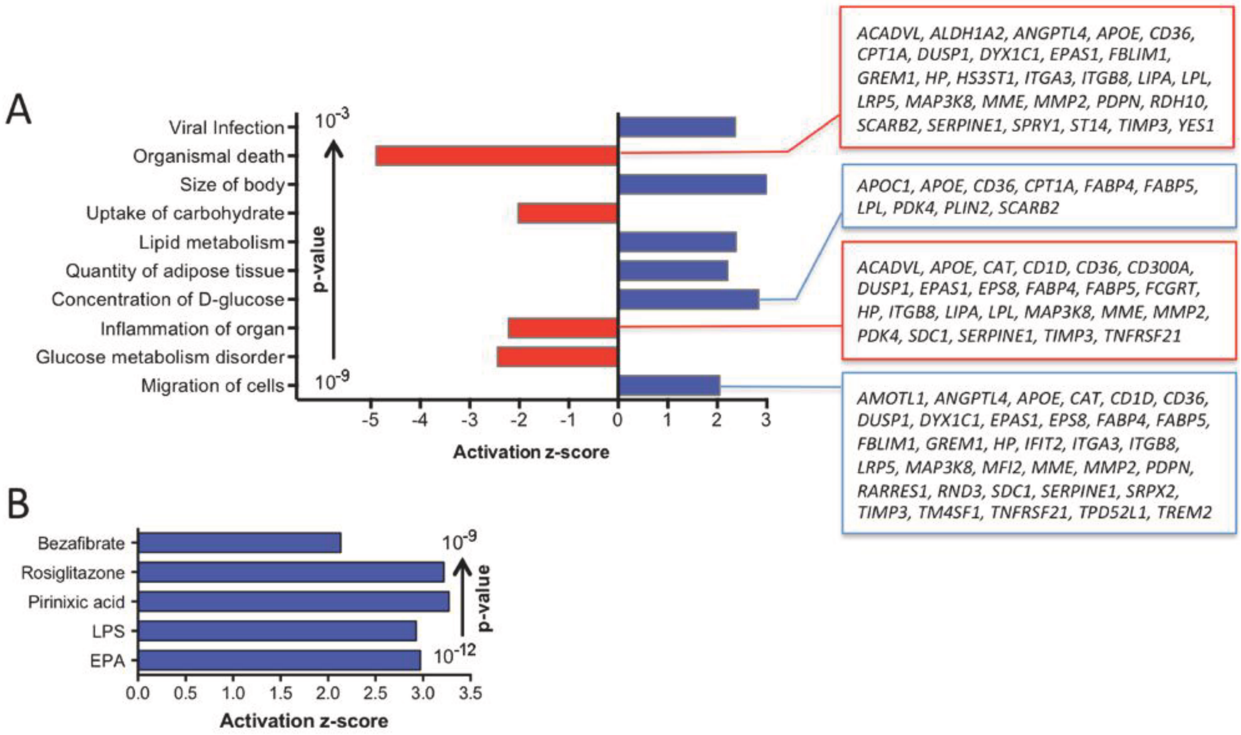

Figure 4: Pathway analyses of PPARβ/δ target genes constitutively upregulated in TAMs. A. IPA *Diseases and Functions Annotation* (functionally different clusters with lowest p-values and highest z-scores). Gene names are shown for the clusters with the largest number of genes. **B.** IPA *Upstream Regulator Analysis* (5 top regulators by p-value; z-score >2).

already after 3 h (Figure 6C). Similar results were obtained with the conjugated LAs 9(Z),11(E)LA and 10(Z),12(E) LA (Figure 6C). LA also potently induced other direct PPARβ/δ target genes, and this induction was close, or even equal, to activation by L165,041, as shown for *PDK4, CPT1A, PLIN2, SLC25A20, ANGPTL4, LRP5 and CD300A* in Figure 6D.

A number of PPARβ/δ target genes deregulated by ovarian cancer ascites have functions in oncogenesis and immune regulation. It was therefore of great interest to investigate whether their overexpression could be reverted by inverse PPARβ/δ agonists in spite of the high concentrations of agonists in ascites. As shown in Figure 6E, treatment of MDMs cultured in ascites with increasing concentrations of PT-S264 for 24 h led to progressively lower levels of *PDK4* mRNA expression. At the highest tested concentration (20 μM), expression was reduced to less than 5%. Likewise, *CPT1A, SLC25A20, LRP5* and *ANGPTL4* mRNA expression was reduced to basal levels by PT-S264, with *LRP5* and *ANGPTL4* being strongly repressed already at concentrations of 1 μM. These results clearly indicate that inverse agonists are suitable to counteract the deregulation of PPARβ/δ target genes in ovarian carcinoma TAMs.

We also found two other endogenous PPARβ/δ agonists, 15-HETE [18] and 6-keto-prostglandin $F_{1\alpha}$ (6-kPGF$_{1\alpha}$), the stable degradation product of prostacyclin [17, 36] in all ascites samples (Figure 6F). Both, 6-kPGF$_{1\alpha}$ and 15-HETE were found at median levels of ~10 ng/ml (~30 nM), which corresponds to approximately 3% of the IC_{50} concentrations required for PPARβ/δ activation [18, 36]. Both metabolites are therefore unlikely to play a role in the deregulation of PPARβ/δ target genes in TAMs.

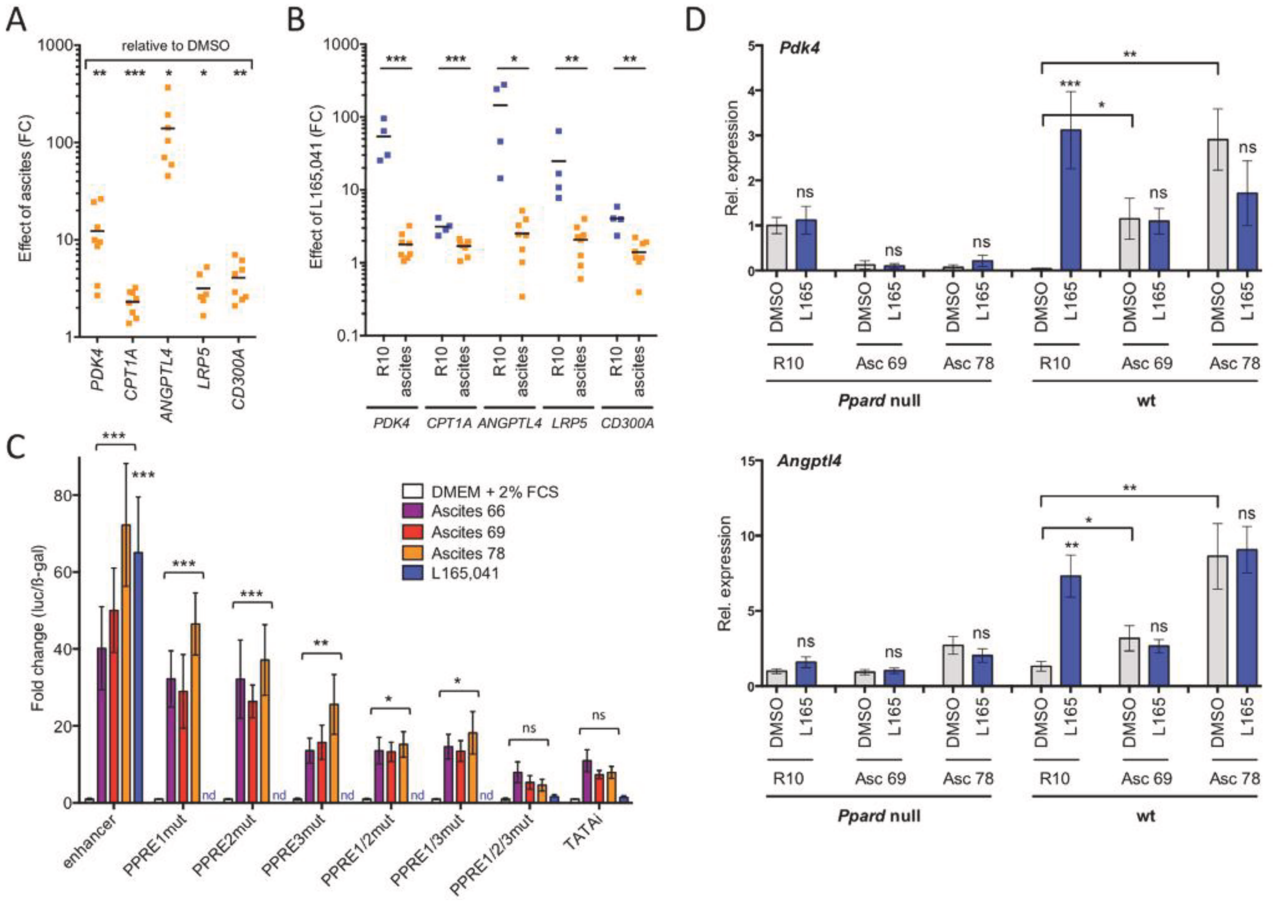

Figure 5: Ascites deregulates PPARβ/δ target genes in normal macrophages and in a PPARβ/δ-dependent fashion. **A.** Upregulation of PPARβ/δ target genes by ascites in MDMs (n = 8; 4 different MDM samples; 2 different ascites samples). RT-qPCR data are expressed as fold change (FC) relative to MDMs R10 medium. **B.** Regulation of target genes by L165,041 in MDMs (n = 4) in R10 or ascites (2 different samples). Data indicate FC relative to DMSO-treated cells. **C.** PPRE-dependent induction of a *PDK4* enhancer-luciferase construct in transiently transfected HEY cells (n = 3). Constructs were mutated in either 1, 2 or all 3 PPREs, as indicated. Data were normalized to β-galactosidase activity from a co-transfected CMV-β-gal expression vector. **D.** Response of the direct PPARβ/δ target genes *Pdk4* and *Angptl4* to two different ascites samples and L165,041 in bone marrow-derived macrophages from wild-type and *Ppard* null mice (sample size: 3 each). Statistical significance was tested for induction by ascites relative to DMSO-treated cells in C and D (asterisks/ns above square brackets) and for induction by L165,041 or in D (asterisks/ns above blue bars).

Fatty acid accumulation in lipid droplets correlates with transcriptional deregulation

The data in Figure 2D showed that ligand regulation in TAMs can only be partially restored by culturing the cells in normal cell culture medium. Since macrophages have a propensity to accumulate intracellular lipids, which is enhanced by PPARβ/δ [37], we tested this for ovarian carcinoma TAMs. As shown by staining with the fluorescent dye Nile Red, ascites-derived TAMs harbor a huge amount of lipid droplets, which remains basically unchanged upon culturing these cells in normal growth medium for 4 days (Figure 7A, 7B). The stability of lipid droplets correlated with a compromised ligand regulation of the PPARβ/δ target gene *PDK4* (Figure 7C). Consistent with this finding, MDMs rapidly accumulate lipid droplets when exposed to LA at a high level found in ascites, which persisted upon withdrawal of the fatty acids (Figure 7D, 7E), concomitantly with an impaired inducibility by synthetic ligands (Figure 7F). It is therefore likely that internalization of PUFAs from the tumor microenvironment generates a reservoir of agonists contributing to a stable upregulation of PPARβ/δ target genes.

DISCUSSION

PPARβ/δ regulates a large group of genes with functions in intermediary metabolism, inflammation and tumor progression, which are coordinately upregulated in TAMs by PUFA ligands present at high concentrations in the ascites of ovarian cancer patients (Table 1). Functional annotation analyses showed that these genes are not only associated with cell type-independent roles in energy production, fatty acid oxidation and lipid storage, but also figure in inflammation, cell migration and cell survival. Upregulation of several of these genes in TAMs is compatible with the pro-tumorigenic role of TAMs and may serve not only to skew TAM polarization but may

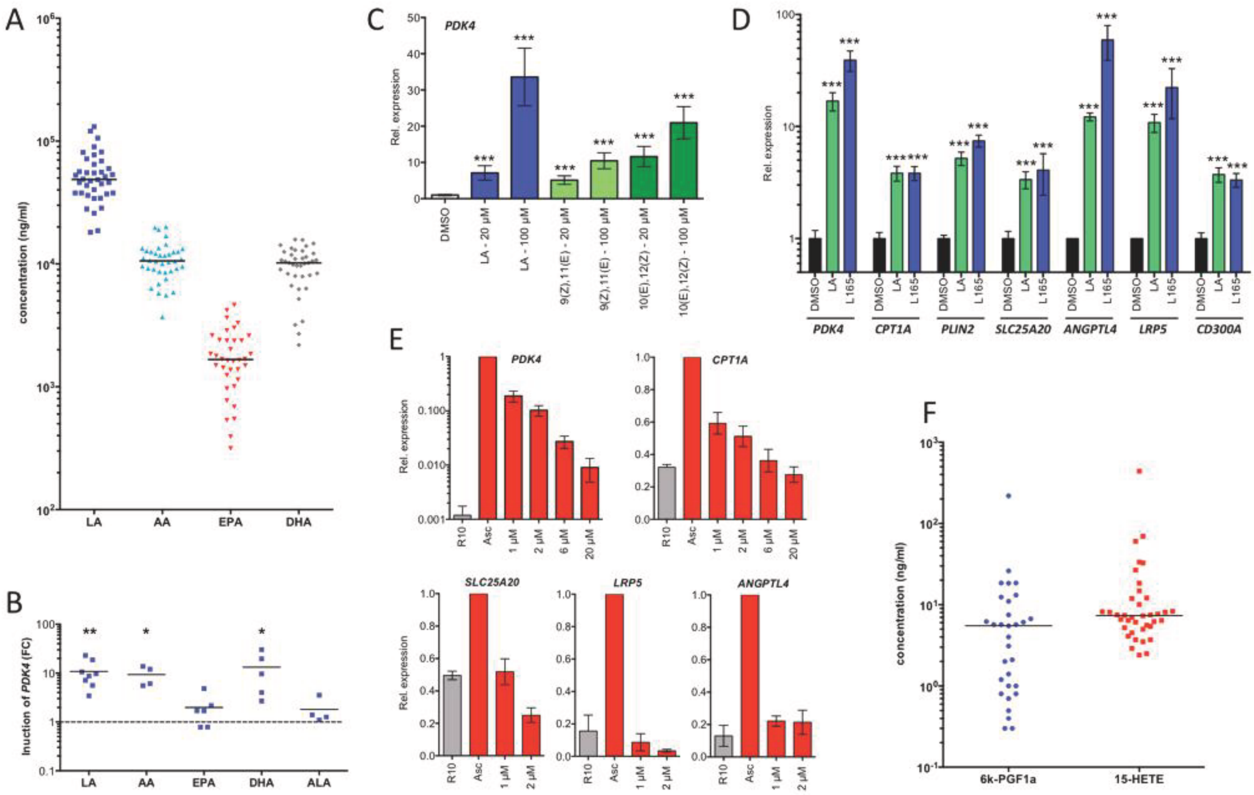

Figure 6: PPARβ/δ ligands are present in ascites at high concentrations and induce PPARβ/δ target genes. A. LC-MS/MS analysis of polyunsaturated fatty acids (PUFAs) in ascites from ovarian carcinoma patients (n = 38). **B.** Induction of *PDK4* in MDMs after 24 h exposure to different PUFAs in different donors (n = 4-8). Each data point represents a biological replicate. **C.** Rapid induction (3 h stimulus) of *PDK4* by LA and conjugated 9(Z),11(E)-LA and 10(Z),12(E)-LA in MDMs (triplicates). **D.** Induction of PPARβ/δ target genes in MDMs after 24 h exposure to linoleic acid (LA) in comparison to L165,041 (triplicates). **E.** Repression of PPARβ/δ target genes in MDMs (n = 3) cultured in ascites for 48 h by different concentrations of PT-S264 added during for the last 24 h of the experiment. Values were normalized to 1 for cells in ascites. **F.** LC-MS analysis of 15-HETE and the stable prostacyclin derivative 6k-PGF1α in the same samples as in A. Horizontal bars show the medians in panels A and B. Values represent averages of triplicate measurements ± standard deviation in all panels. Significance was tested relative to control cells.

also directly promote tumor progression, for instance via the secretion of soluble mediators, such as ANGPTL4. We therefore propose that the deregulation of PPARβ/δ target genes by mediators of the tumor environment acts in conjunction with other signaling mechanisms to effect the pro-tumorigenic conversion of host-derived monocytic cells.

Fatty acid PPARβ/δ ligands in ascites

Several PUFAs known to act as PPARβ/δ agonists were found in all ascites samples tested at levels exceeding the concentrations required for maximal PPARβ/δ activation, in particular LA, but also arachidonic acid and docosahexaenoic acid [16]. High levels of lipoprotein complexes in ovarian cancer ascites have been described in a previous study, but their fatty acid composition was not determined [38]. Another report suggests the mobilization of LA from omentum in ovarian cancer patients [39], consistent with the very high levels of this fatty acid in the malignancy-associated ascites found in the present study. Several studies also indicate that fatty acids are relevant to the biology and clinical outcome of ovarian cancer. Thus, the increased expression of the fatty acid synthase gene (*FAS*) predicts shorter survival [40], dietary fat intake and altered lipid metabolism are linked to ovarian cancer risk [41] and in a mouse model tumor growth and invasion are fueled by direct transfer of lipids from omental adipocytes to ovarian cancer with a key role for fatty acid-binding protein 4 [42].

Blood plasma also contains high concentrations of PUFAs [43], yet PPARβ/δ target genes are expressed at low levels in blood monocytes, which is presumably

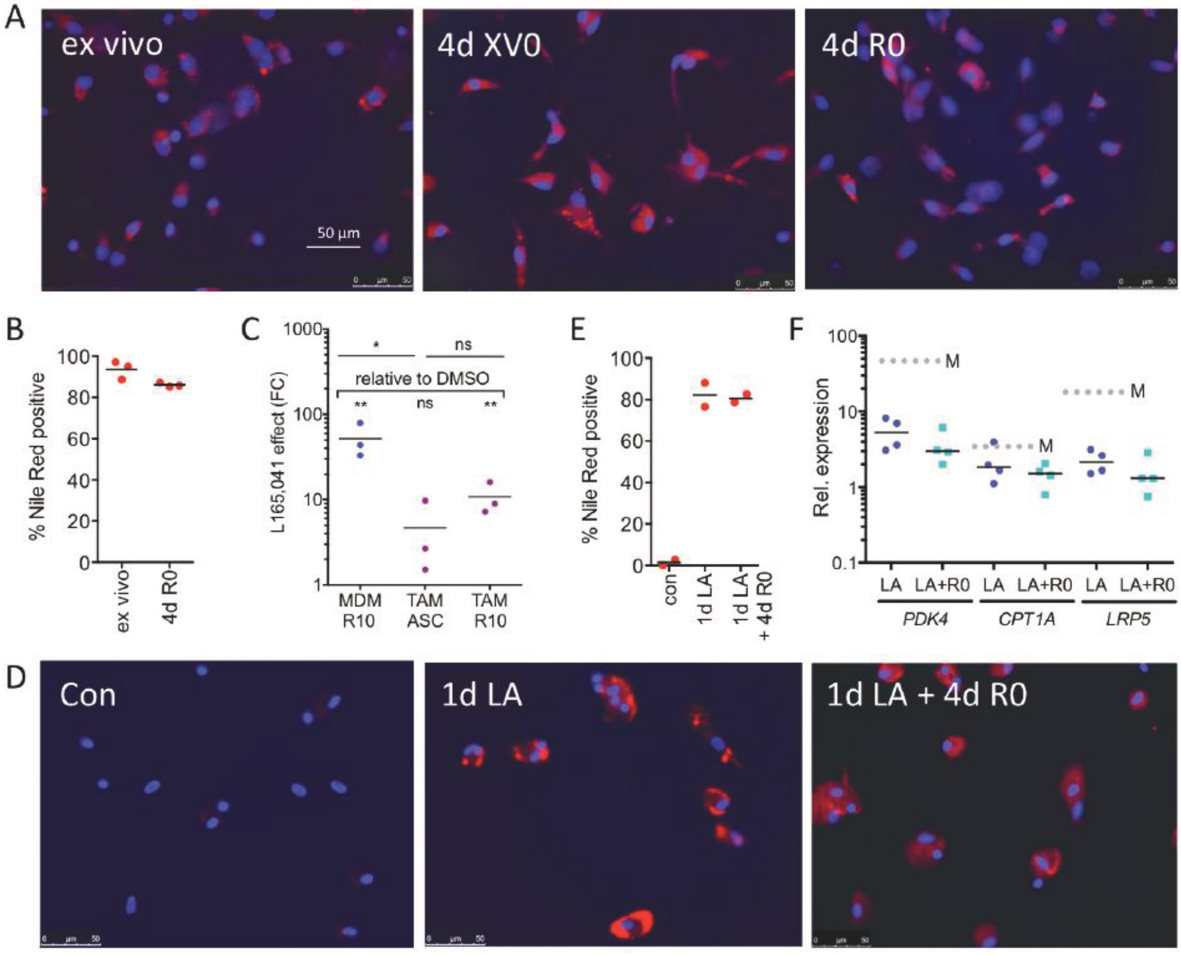

Figure 7: Association of the stable accumulation of lipid droplets in TAMs with the deregulation of the PPARβ/δ target gene *PDK4*. **A.** Staining of primary TAMs with Nile Red 0 h (*ex vivo*) and 4 d after plating in serum-free XV0 or R0 medium. **B.** Quantification of Nile Red stained TAMs ($n = 3$) treated as in A. **C.** L165,041 induction of *PDK4* in MDMs ($n = 3$) and in TAMs ($n = 3$) cultured for 4d in ascites or R10 medium. **D.** Staining of MDMs with Nile Red before (d0) and after a 24-hour exposure to LA (d1), followed by a 4d fatty acid withdrawal in serum-free R0 medium (d1+4). **E.** Quantification of Nile Red stained MDMs ($n = 2$) before and after LA exposure as in **D**. **F.** L165,041 induction of PPARβ/δ target genes in MDMs ($n = 4$) pretreated with LA for 1 d, followed by a 4d serum-free R0 medium lacking fatty acids.

due to the low level of PPARβ/δ expression in monocytes (Figure 2A and [28]), at least in part. TAMs represent a special situation in that these cells express PPARβ/δ at readily detectable levels and at the same time are exposed to high levels of ligands in the tumor microenvironment. Our findings also suggest that PPARβ/δ may serve as a marker to distinguish monocytes from macrophages, and also support the conclusion that ascites-associated $CD14^+$ cells are macrophages rather than monocytes.

Deregulated PPARβ/δ target genes in TAMs

The target gene *ANGPTL4* [44, 45] is of particular interest in the context of the present study, since it not only figures in lipid metabolism as a regulator of lipoprotein lipase, but also plays an apparently essential role in tumor progression [46]. Thus, ANGPTL4 secreted by tumor cells in response to TGF-β and released into the circulation increases the permeability of lung capillaries and facilitates the extravasation of disseminated breast cancer cells in a mouse model [35]. Furthermore, *ANGPTL4* increases cancer cell invasion [21] and is part of gene expression signatures associated with distant metastasis in human cancer patients [35, 47]. ANGPTL4 also inhibits anoikis, which is essential for the survival of circulating tumor cells [48]. Consistent with these observations, several oncogenic signaling pathways converge on the *ANGPTL4* gene, including TGFβ [21, 35, 45] and AP1 [45].

Deregulated PPARβ/δ target genes with potential roles in macrophage regulation are *CD300A* and *FOS*. CD300A is a membrane glycoprotein with anti-inflammatory functions. For example, deletion of the *Cd300a* gene in mice has been shown to result in pro-inflammatory activation of peritoneal macrophages [49], suggesting that its upregulation in TAMs has an immune suppressive effect. On the other hand, FOS has been strongly associated with the pro-inflammatory activation of macrophages [50]. These observations are compatible with a role of deregulated PPARβ/δ target genes in mediating the mixed-polarization phenotype of TAMs [4, 5, 7, 8].

Several other novel PPARβ/δ target genes upregulated in TAMs potentially play a role in promoting macrophage migration. i.e., *PHACTR1* (phosphatase and actin regulator 1), *MACC1* and *ST14*. PHACTR1 plays a role in the G-actin mediated control of actomyosin assembly [51], MACC1 is a transcriptional activator of *MET* (HGF receptor) and acts as a key regulator of cell motility [52], and ST14/epithin is a protease transcriptionally induced in macrophages by pro-inflammatory pathways to mediate transendothelial migration [53].

Another PPARβ/δ target gene upregulated in TAMs is *LRP5*. Its product LRP5 acts as a Frizzled co-receptor and activator of Wnt signaling [54]. In macrophages, LRP5 is involved in the innate inflammatory reaction to lipid infiltration by activating the Wnt pathway and promoting lipid uptake, leading to the formation of foam cells [55]. It is possible that the deregulation of LRP5 in TAMs contributes to the intracellular accumulation of fatty acids in lipid droplets observed in the present study.

Finally, the dramatic upregulation of *PDK4* probably affect energy metabolism in TAMs such that glucose catabolism is shifted towards glycolysis and lactate production (Warburg effect) [56]. This would render TAMs largely independent from the availability of oxygen, thus endowing the cells with the ability to cope with the hypoxic conditions frequently encountered in the tumor microenvironment.

Our data also show that a large number of target genes that are deregulated by ovarian cancer ascites are repressed by inverse PPARβ/δ agonists, with PT-S264 being able to suppress these genes below the basal level observed in the absence of ascites. Since several of these genes have functions in disease-associated processes as discussed above, inverse PPARβ/δ agonists may represent invaluable experimental tools to interfere with the tumor-promoting effects of the ovarian cancer microenvironment.

Expression of indirect PPARβ/δ target genes in TAMs

A large group of PPARβ/δ target genes in macrophages is repressed by PPARβ/δ agonists independent of direct DNA contacts (see Introduction). These genes are mostly associated with pro-inflammatory functions exerted by macrophages. In TAMs these inverse target genes are also frequently deregulated and refractory to synthetic ligands. However, the underlying mechanisms are complex, as indicated by the extreme variability of expression levels, ligand inducibility and ascites effects observed for different genes as well as individual patients (see Suppl. Figures S3 and S4 for examples). It is likely that the inverse target genes are highly prone to such variations, since they are regulated by multiple signaling pathways that are triggered by numerous cytokines whose concentrations are highly divergent among patients. It is obvious that these variabilities contribute to the observed heterogeneity, in many cases presumably without a significant contribution of PPARβ/δ itself. To understand the mechanistic basis of the altered transcriptome of inverse PPARβ/δ target genes in TAMs it will be necessary to perform in-depth analyses of transcription factor occupancy and epigenetic modifications at individual genes and relate this data to specific pathways and mediators.

MATERIALS AND METHODS

Ligands

L165,041 was purchased from Biozol. ST247 was synthesized as described [20, 57]. The inverse PPARβ/δ agonist PT-S264 is an optimized derivative of ST247 with improved plasma stability (Toth et al., manuscript submitted). Synthetic ligands were used at a concentration of 1 μM in all experiments unless indicated otherwise. Cells were treated for 24 h unless indicated otherwise. PUFAs were obtained from Biomol.

Mice

Ppard null and wt mice were generated by crossing floxed *Ppard* mice [58] and Sox2-Cre mice [59] as described [60]. Sox2-Cre mice were obtained from Jackson Laboratory (Bar Harbor, Maine), the floxed *Ppard* mouse strain was kindly provided by Dr. R. Evans (Salk Institute, La Jolla, CA). For genotyping the following primers were used: *Ppard* intron 3 (forward: GGC TGG GTC ACA AGA GCT ATT GTC TC), *Ppard* exon 4 (forward: GGC GTG GGG ATT TGC CTG CTT CA); *Ppard* intron 4 (reverse: GAG CCG CCT CTC GCC ATC CTT TCA G; fragment sizes: *Ppard* wt: 360 bp; *Ppard* floxed: 400 bp; *Ppard* ko: 240 bp; *Cre* (forward: CCT GGA AAA TGC TTC TGT CCG; reverse: CAG GGT GTT ATA AGC AAT CCC); fragment size: 390 bp.

Patient samples

Peripheral blood mononuclear cells (PBMCs) were obtained from healthy adult volunteers. Ascites was collected from untreated high-grade serous ovarian carcinoma patients undergoing surgery at the University Hospital Marburg. Informed consent was obtained from all patients according to the protocols approved by the institutional ethics committee.

Isolation of $CD14^+$ cells

Mononuclear cells were isolated from ascites and peripheral blood by Lymphocyte Separation Medium 1077 (PromoCell) density gradient centrifugation and purified by magnetic cell sorting (MACS) using CD14 microbeads (Miltenyi Biotech) or adherence selection on cell culture dishes for 30 min. For ChIP experiments, TAMs were purified by adherence selection. The purity of $CD14^+$ cells was > 90%. Purified TAMs and MDMs were analyzed by FACS, lysed in PeqGold (Peqlab) for RNA preparation or cultured as described below.

Cell culture and cytokine treatment of TAMs and MDMs

$CD14^+$ monocytes and TAMs were cultured either in RPMI1640 with 10% fetal bovine serum (FCS; R10 medium), serum-free RPMI1640 (R0 medium) or in serum-free macrophage X-VIVO 10 medium (XV0 medium) (Biozym Scientific). Monocyte-derived macrophages (MDMs) were differentiated from $CD14^+$ monocytes of healthy volunteers for 5-7 d at $1x10^6$ cells/ml. HEY ovarian cancer cells (ATCC) were maintained in DMEM plus 10% FCS.

Lipidomic analysis

Ascites samples (1 ml) were spiked with 100 μl deuterated internal standard and extracted using solid reverse phase extraction columns (Strata-X 33, Phenomenex). Fatty acids derivatives were eluted into 1.0 ml of methanol, lyophilized and resuspended in 100 ml of water/acetonitrile/formic acid (70:30:0.02, v/v/v; solvent A) and analyzed by LC-MS/MS on an Agilent 1290 separation system. Samples were separated on a Synergi reverse-phase C18 column (2.1×250 mm; Phenomenex) using a gradient as follows: flow rate =0.3 μl/min, 1 min (acetonitrile/isopropyl alcohol, 50:50, v/v; solvent B), 3 min (25% solvent B), 11 min (45% solvent B), 13 min (60% solvent B), 18 min (75% solvent B), 18.5 min (90% solvent B), 20 min (90% solvent B), 21 min (0% solvent). The separation system was coupled to an electrospray interface of a QTrap 5500 mass spectrometer (AB Sciex). Compounds were detected in scheduled multiple reaction monitoring mode. For quantification a 12-point calibration curve for each analyte was used. Data analysis was performed using Analyst (v1.6.1) and MultiQuant (v2.1.1) (AB Sciex).

Immunoblotting

Immunoblots were performed following standard protocols using the following antibodies: α-PPARβ/δ (sc-74517; Santa Cruz, Heidelberg, Germany), α-PDK4 (ab110336; Abcam, Cambridge, United Kingdom), α-LDH (sc-33781; Santa Cruz, Heidelberg, Germany), α-rabbit IgG HRP-linked AB and α-mouse IgG HRP-linked AB (cs7074, cs7076; Cell Signaling, NEB, Frankfurt, Germany). ChemiDoc MP system and Image Lab software version 5 (Bio-Rad, München, Germany) were used for detection and quantification.

Quantification of secreted ANGPTL4 protein

ANGPTL4 levels in ascites from ovarian cancer patients were determined by ELISA (Aviscera Bioscience,

Santa Clara, CA), according to the instructions of the manufacturer. The antibody used in this kit recognizes the bioactive C-terminal processing product (cANGPTL4).

Nile Red staining

Cells were stained for 10 minutes at 37 °C with 500 nM Nile Red (Biomol, Hamburg, Germany) in PBS and visualized using a Leica DM5000 B microscope. Nuclei were stained using Vecta Shield with DAPI (Biozol, Eching, Germany). For quantification the percentage of Nile Red positive cells was determined by counting 20 faces per donor or patient per treatment.

Luciferase reporter assay

The *PDK4* upstream enhancer region was cloned into pGL3-TATAi [61] via *Kpn*I sites using the following primers:

5'-AAAGGTACCAAATGCTGAGTTTGGGCAAC and 5'-AAAGGTACCAGCCTTGTGAGCAACCAAAG. PPREs were mutated with the following primers 5' -CAGGCTAAGTTGGTGTATGGTCAGTCCCACACC, 5'-GAAGTTTAGTAGGTGTACGGTCACTGCTGCCGA and5'-AGAGCTCACTAGGGGTATGGTCGGGGAGAC CAAG, and their respective reverse complement primers. HEY1 cells were transfected with the indicated reporter vector and pEF6/V5-His-TOPO/*lacZ* (Life Technologies) as described [18] and incubated overnight in DMEM with 2% FCS. On the next day, cells were washed with PBS and received either fresh medium with or without 1 μM L165,041 or ascites for 24 h. Lysates were prepared and measured according to the manufacturer's instructions (Beetle Juice Big and β-Gal Juice PLUS Kit for normalization; pjk GmbH) with an Orion L luminometer (Berthold).

RT-qPCR and RNA-Seq

cDNA isolation and qPCR analyses were performed as described [20]. L27 was used for normalization. Primer sequences are listed in Suppl. Table S1. RNA-Seq was carried out as described elsewhere [28]. Sequencing data were deposited at EBI ArrayExpress (accession number TAM data: E-MTAB-3167; MDM data: E-MTAB-3114 and E-MTAB-3398). Data were quantile normalized using all RNA-Seq datasets. Gene model data were retrieved from Ensembl revision 74.

Bioinformatic analysis of RNA-Seq data

We sequenced 10 TAMs samples from 10 patients directly after harvesting ("*in vivo*"), one additional TAM sample was used for ligand response experiments in autologous ascites ("*in vitro*"; L165,041, ST247 and DMSO). In addition to previously described MDM ligand response experiments from two donors [28] in R10 and X0 medium (L165,041, ST247, PT-S264, DMSO), we performed three additional sets from three donors in R10 (L165,041, PT-S264 and DMSO control). ST247 was used at a concentrations of 300 nM, all others at 1 μM.

Genes were considered for differential expression analyses only if they had an FPKM of at least 0.3 and a minimum of 50 tags in at least one sample. LogFC values for ligand experiments were calculated pairwise for individual donors. For ligand regulation in MDMs (Figure 2B) a logFC of at least 0.7 in 4 out of 5 replicates was required. Figure 2C shows median pairwise logFC data. Regulated target genes in MDMs (n = 195; Figures 2E and 3A) were defined as genes showing regulation in at least one of the following comparisons: agonist *vs* DMSO control (up regulated), inverse agonist *vs* DMSO control (down regulated) or agonist *vs* inverse agonist (up regulated). Figure 3A shows median FPKM values of 10 TAM samples and 5 MDM DMSO control samples. In Figure 3B and 3C, "up in TAM *in vivo*" is a subset of the canonical target genes that showed a 2-fold (1 logFC unit) difference between TAMs and MDMs. Table S5 was filtered based on t-tests between 10 TAM *in vitro* samples and 5 MDM DMSO samples (FDR/Benjamini-Hochberg ≤0.05). The set "up in TAM *in vitro*" is similarly defined as canonical target genes that (i) were upregulated (0.7 logFC) in TAM/DMSO compared to the two previously reported MDM/DMSO samples, and (ii) showed an at least 0.5 units higher FPKM value in the TAM sample compared to both MDM samples. Agonist refractory genes (Figure 3C) are agonist inducible genes in MDMs that showed no such regulation (same logFC threshold) or less than 50% induction (fold change) by L165,041 in TAMs relative to MDMs.

ChIP-PCR and ChIP-Seq

ChIP was performed and evaluated as described using the following antibodies: IgG pool, I5006 (Sigma Aldrich); α-PPARβ/δ, sc-7197; α-RXR, sc-774 (Santa Cruz, Heidelberg, Germany). ChIP-Seq, mapping of ChIP-Seq reads and peak calling were carried out as described [28].

Bioinformatic analysis of ChIP-Seq data

ChIP-Seq peaks were filtered for at least 30 deduplicated tags and a fold change (FC) over IgG of ≥2 (normalized total read counts). Regions were considered bound by PPARβ/δ in TAMs if they enrichment sites were observed in at least two out of three TAM samples sequenced. PPARβ/δ binding in MDMs has been described elsewhere [28]. For Figure 2E, PPARβ/δ-occupied genes

were identified as genes with a transcription start site close to, or within 50 kb of, an enrichment site. All genomic sequence and gene annotation data was retrieved from Ensembl revision 74.

Functional annotations and pathway analyses

Functional annotations and pathway analyses were performed using the Ingenuity Pathway Analysis (IPA) application and knowledge database (Qiagen Redwood City, CA, USA). Results were sorted according to p-value of overlap (minimum 0.001) and activation z-scores (≤-2.0 or ≥+2.0) Sequencing data were deposited at EBI ArrayExpress (accession number E-MTAB-3166).

Statistical analysis of experimental data

Data are presented as the average of replicates (n = 3 unless indicated otherwise) with error bars indicating standard deviations and horizontal lines in dot plots representing averages. Comparative data were statistically analyzed by Student's t-test (two-sided, equal variance) and results expressed as follows: ns, not significant ($p \geq 0.05$); *$p < 0.05$, **$p < 0.01$ or ***$p < 0.001$.

Survival-associated gene expression analysis

Associations between gene expression and relapse-free survival of ovarian cancer patients were analyzed using the web based tool "KM Plotter" (http://kmplot.com/analysis/index.php?p=service&cancer=ovar) [62] with the following settings: 'auto select best cutoff', stage: 2+3+4, histology: serous, dataset: TCGA; other settings: default). Logrank Mantel-Cox test (p-values), logrank Hazard Ratio (HR) and median survival times were calculated using the GraphPad Prism software.

ACKNOWLEDGMENTS

We are grateful to Dr. Robert Geffers (Helmholtz-Zentrum für Infektionsforschung, Braunschweig, Germany) for valuable discussions on ChIP-seq library synthesis and to Margitta Alt, Traute Plaum and Achim Allmeroth for expert technical assistance.

GRANT SUPPORT

This research was supported by research grants from the Deutsche Forschungsgemeinschaft to RM (MU601/13), the Wilhelm-Sander-Stiftung to SMB, SR and UW, the Stiftung P.E. Kempkes and the Universitätsklinikum Giessen-Marburg (UKGM Forschungsförderung) to TA, SR and UW.

CONFLICTS OF INTEREST

All authors have nothing to disclose.

Abbreviations

AA, arachidonic acid; ALA; α-linolenic acid; ANGPTL4: angiopoietin-like 4; ChIP, chromatin immune precipitation; BMDM: marrow-derived macrophage; ChIP-Seq, ChIP sequencing; D10, DMEM with 10% FCS; DHA, docosahexaenoic acid; EPA, eicosapentaenoic acid; FCS, fetal calf serum; 15-HETE, 15-hydroxyeicosatetraenoic acid; IPA: Ingenuity Pathway Analysis; 6-kPGF$_{1\alpha}$: 6-keto-prostglandin F$_{1\alpha}$; LA: linoleic acid; MDM, monocyte-derived macrophage; NFκB: nuclear factor κB; PDK4, pyruvate dehydrogenase 4; PPAR, peroxisome proliferator-activated receptor; PPARβ/δ, proliferator-activated receptor β/δ ; PPRE, PPAR response element; PUFA, polyunsaturated fatty acid; RNA-Seq, RNA sequencing; RT-qPCR, reverse transcriptase quantitative PCR; RXR, retinoid X receptor; TAM: tumor-associated macrophage; XV0: X-VIVO 10 medium without serum.

REFERENCES

1. Condeelis J and Pollard JW. Macrophages: obligate partners for tumor cell migration, invasion, and metastasis. Cell. 2006; 124:263-266.
2. Hagemann T, Biswas SK, Lawrence T, Sica A and Lewis CE. Regulation of macrophage function in tumors: the multifaceted role of NF-kappaB. Blood. 2009; 113:3139-3146.
3. Pollard JW. Tumour-educated macrophages promote tumour progression and metastasis. Nat Rev Cancer. 2004; 4:71-78.
4. Sica A and Mantovani A. Macrophage plasticity and polarization: *in vivo* veritas. J Clin Invest. 2012; 122:787-795.
5. Gabrilovich DI, Ostrand-Rosenberg S and Bronte V. Coordinated regulation of myeloid cells by tumours. Nat Rev Immunol. 2012; 12:253-268.
6. Xue J, Schmidt SV, Sander J, Draffehn A, Krebs W, Quester I, De Nardo D, Gohel TD, Emde M, Schmidleithner L, Ganesan H, Nino-Castro A, Mallmann MR, Labzin L, Theis H, Kraut M, et al. Transcriptome-based network analysis reveals a spectrum model of human macrophage activation. Immunity. 2014; 40:274-288.
7. Qian BZ and Pollard JW. Macrophage diversity enhances tumor progression and metastasis. Cell. 2010; 141:39-51.
8. Reinartz S, Schumann T, Finkernagel F, Wortmann A, Jansen JM, Meissner W, Krause M, Schworer AM, Wagner U, Muller-Brusselbach S and Muller R. Mixed-polarization phenotype of ascites-associated macrophages in human

ovarian carcinoma: Correlation of CD163 expression, cytokine levels and early relapse. Int J Cancer. 2014; 134:32-42.

9. Kostadinova R, Wahli W and Michalik L. PPARs in diseases: control mechanisms of inflammation. Curr Med Chem. 2005; 12:2995-3009.
10. Wahli W and Michalik L. PPARs at the crossroads of lipid signaling and inflammation. Trends Endocrinol Metab. 2012; 23:351-363.
11. Peters JM, Lee SS, Li W, Ward JM, Gavrilova O, Everett C, Reitman ML, Hudson LD and Gonzalez FJ. Growth, adipose, brain, and skin alterations resulting from targeted disruption of the mouse peroxisome proliferator-activated receptor beta(delta). Mol Cell Biol. 2000; 20:5119-5128.
12. Chong HC, Tan MJ, Philippe V, Tan SH, Tan CK, Ku CW, Goh YY, Wahli W, Michalik L and Tan NS. Regulation of epithelial-mesenchymal IL-1 signaling by PPARbeta/delta is essential for skin homeostasis and wound healing. J Cell Biol. 2009; 184:817-831.
13. Kang K, Reilly SM, Karabacak V, Gangl MR, Fitzgerald K, Hatano B and Lee CH. Adipocyte-derived Th2 cytokines and myeloid PPARdelta regulate macrophage polarization and insulin sensitivity. Cell Metab. 2008; 7:485-495.
14. Odegaard JI, Ricardo-Gonzalez RR, Red Eagle A, Vats D, Morel CR, Goforth MH, Subramanian V, Mukundan L, Ferrante AW and Chawla A. Alternative M2 activation of Kupffer cells by PPARdelta ameliorates obesity-induced insulin resistance. Cell Metab. 2008; 7:496-507.
15. Peters JM, Shah YM and Gonzalez FJ. The role of peroxisome proliferator-activated receptors in carcinogenesis and chemoprevention. Nat Rev Cancer. 2012; 12:181-195.
16. Xu HE, Lambert MH, Montana VG, Parks DJ, Blanchard SG, Brown PJ, Sternbach DD, Lehmann JM, Wisely GB, Willson TM, Kliewer SA and Milburn MV. Molecular recognition of fatty acids by peroxisome proliferator-activated receptors. Mol Cell. 1999; 3:397-403.
17. Lim H, Gupta RA, Ma WG, Paria BC, Moller DE, Morrow JD, DuBois RN, Trzaskos JM and Dey SK. Cyclo-oxygenase-2-derived prostacyclin mediates embryo implantation in the mouse via PPARdelta. Genes Dev. 1999; 13:1561-1574.
18. Naruhn S, Meissner W, Adhikary T, Kaddatz K, Klein T, Watzer B, Müller-Brüsselbach S and Müller R. 15-hydroxyeicosatetraenoic acid is a preferential peroxisome proliferator-activated receptor β/δ agonist. Mol Pharmacol. 2010; 77:171-184.
19. Adhikary T, Kaddatz K, Finkernagel F, Schönbauer A, Meissner W, Scharfe M, Jarek M, Blöcker H, Müller-Brüsselbach S and Müller R. Genomewide analyses define different modes of transcriptional regulation by peroxisome proliferator-activated receptor-beta/delta (PPARbeta/delta). PLoS One. 2011; 6:e16344.
20. Naruhn S, Toth PM, Adhikary T, Kaddatz K, Pape V, Dörr S, Klebe G, Müller-Brüsselbach S, Diederich WE and Müller R. High-affinity peroxisome proliferator-activated receptor beta/delta-specific ligands with pure antagonistic or inverse agonistic properties. Mol Pharmacol. 2011; 80:828-838.
21. Adhikary T, Brandt DT, Kaddatz K, Stockert J, Naruhn S, Meissner W, Finkernagel F, Obert J, Lieber S, Scharfe M, Jarek M, Toth PM, Scheer F, Diederich WE, Reinartz S, Grosse R, et al. Inverse PPARbeta/delta agonists suppress oncogenic signaling to the ANGPTL4 gene and inhibit cancer cell invasion. Oncogene. 2013; 32:5241-5252.
22. Oishi Y, Manabe I, Tobe K, Ohsugi M, Kubota T, Fujiu K, Maemura K, Kubota N, Kadowaki T and Nagai R. SUMOylation of Kruppel-like transcription factor 5 acts as a molecular switch in transcriptional programs of lipid metabolism involving PPAR-delta. Nat Med. 2008; 14:656-666.
23. Lee CH, Chawla A, Urbiztondo N, Liao D, Boisvert WA, Evans RM and Curtiss LK. Transcriptional repression of atherogenic inflammation: modulation by PPARdelta. Science. 2003; 302:453-457.
24. Planavila A, Rodriguez-Calvo R, Jove M, Michalik L, Wahli W, Laguna JC and Vazquez-Carrera M. Peroxisome proliferator-activated receptor beta/delta activation inhibits hypertrophy in neonatal rat cardiomyocytes. Cardiovasc Res. 2005; 65:832-841.
25. Westergaard M, Henningsen J, Johansen C, Rasmussen S, Svendsen ML, Jensen UB, Schroder HD, Staels B, Iversen L, Bolund L, Kragballe K and Kristiansen K. Expression and localization of peroxisome proliferator-activated receptors and nuclear factor kappaB in normal and lesional psoriatic skin. J Invest Dermatol. 2003; 121:1104-1117.
26. Ding G, Cheng L, Qin Q, Frontin S and Yang Q. PPARdelta modulates lipopolysaccharide-induced TNFalpha inflammation signaling in cultured cardiomyocytes. J Mol Cell Cardiol. 2006; 40:821-828.
27. Stockert J, Wolf A, Kaddatz K, Schnitzer E, Finkernagel F, Meissner W, Müller-Brüsselbach S, Kracht M and Müller R. Regulation of TAK1/TAB1-Mediated IL-1beta Signaling by Cytoplasmic PPARbeta/delta. PLoS One. 2013; 8:e63011.
28. Adhikary T, Wortmann A, Schumann T, Finkernagel F, Lieber S, Roth K, Toth PM, Diederich WE, Nist A, Stiewe T, Kleinesudeik L, Reinartz S, Müller-Brüsselbach S and Müller R. The transcriptional PPARβ/δ network in human macrophages defines a unique agonist-induced activation state. Nucl Acids Res. 2015:in press.
29. Yamashiro S, Takeya M, Nishi T, Kuratsu J, Yoshimura T, Ushio Y and Takahashi K. Tumor-derived monocyte chemoattractant protein-1 induces intratumoral infiltration of monocyte-derived macrophage subpopulation in transplanted rat tumors. Am J Pathol. 1994; 145:856-867.
30. Silzle T, Kreutz M, Dobler MA, Brockhoff G, Knuechel R and Kunz-Schughart LA. Tumor-associated fibroblasts recruit blood monocytes into tumor tissue. Eur J Immunol.

2003; 33:1311-1320.

31. Murdoch C, Giannoudis A and Lewis CE. Mechanisms regulating the recruitment of macrophages into hypoxic areas of tumors and other ischemic tissues. Blood. 2004; 104:2224-2234.
32. Ahmed N and Stenvers KL. Getting to Know Ovarian Cancer Ascites: Opportunities for Targeted Therapy-Based Translational Research. Front Oncol. 2013; 3:256.
33. Degenhardt T, Saramaki A, Malinen M, Rieck M, Vaisanen S, Huotari A, Herzig KH, Müller R and Carlberg C. Three Members of the Human Pyruvate Dehydrogenase Kinase Gene Family Are Direct Targets of the Peroxisome Proliferator-activated Receptor β/δ. J Mol Biol. 2007.
34. Network TCGAR. Integrated genomic analyses of ovarian carcinoma. Nature. 2011; 474:609-615.
35. Padua D, Zhang XH, Wang Q, Nadal C, Gerald WL, Gomis RR and Massague J. TGFbeta primes breast tumors for lung metastasis seeding through angiopoietin-like 4. Cell. 2008; 133:66-77.
36. Gupta RA, Tan J, Krause WF, Geraci MW, Willson TM, Dey SK and DuBois RN. Prostacyclin-mediated activation of peroxisome proliferator-activated receptor delta in colorectal cancer. Proc Natl Acad Sci U S A. 2000; 97:13275-13280.
37. Vosper H, Patel L, Graham TL, Khoudoli GA, Hill A, Macphee CH, Pinto I, Smith SA, Suckling KE, Wolf CR and Palmer CN. The peroxisome proliferator-activated receptor delta promotes lipid accumulation in human macrophages. J Biol Chem. 2001; 276:44258-44265.
38. Caselmann WH and Jungst D. Isolation and characterization of a cellular protein-lipid complex from ascites fluid caused by various neoplasms. Cancer Res. 1986; 46:1547-1552.
39. Yam D, Ben-Hur H, Dgani R, Fink A, Shani A and Berry EM. Subcutaneous, omentum and tumor fatty acid composition, and serum insulin status in patients with benign or cancerous ovarian or endometrial tumors. Do tumors preferentially utilize polyunsaturated fatty acids? Cancer Lett. 1997; 111:179-185.
40. Gansler TS, Hardman W, 3rd, Hunt DA, Schaffel S and Hennigar RA. Increased expression of fatty acid synthase (OA-519) in ovarian neoplasms predicts shorter survival. Hum Pathol. 1997; 28:686-692.
41. Tania M, Khan MA and Song Y. Association of lipid metabolism with ovarian cancer. Curr Oncol. 2010; 17:6-11.
42. Nieman KM, Kenny HA, Penicka CV, Ladanyi A, Buell-Gutbrod R, Zillhardt MR, Romero IL, Carey MS, Mills GB, Hotamisligil GS, Yamada SD, Peter ME, Gwin K and Lengyel E. Adipocytes promote ovarian cancer metastasis and provide energy for rapid tumor growth. Nat Med. 2011; 17:1498-1503.
43. Fraser DA, Thoen J, Rustan AC, Forre O and Kjeldsen-Kragh J. Changes in plasma free fatty acid concentrations in rheumatoid arthritis patients during fasting and their effects upon T-lymphocyte proliferation. Rheumatology (Oxford). 1999; 38:948-952.
44. Mandard S, Zandbergen F, van Straten E, Wahli W, Kuipers F, Muller M and Kersten S. The fasting-induced adipose factor/angiopoietin-like protein 4 is physically associated with lipoproteins and governs plasma lipid levels and adiposity. J Biol Chem. 2006; 281:934-944.
45. Kaddatz K, Adhikary T, Finkernagel F, Meissner W, Müller-Brüsselbach S and Müller R. Transcriptional profiling identifies functional interactions of TGFβ and PPARβ/δ signaling: synergistic induction of ANGPTL4 transcription. J Biol Chem. 2010; 285:29469-29479.
46. Zhu P, Goh YY, Chin HF, Kersten S and Tan NS. Angiopoietin-like 4: a decade of research. Biosci Rep. 2012; 32:211-219.
47. Hu Z, Fan C, Livasy C, He X, Oh DS, Ewend MG, Carey LA, Subramanian S, West R, Ikpatt F, Olopade OI, van de Rijn M and Perou CM. A compact VEGF signature associated with distant metastases and poor outcomes. BMC Med. 2009; 7:9.
48. Zhu P, Tan MJ, Huang RL, Tan CK, Chong HC, Pal M, Lam CR, Boukamp P, Pan JY, Tan SH, Kersten S, Li HY, Ding JL and Tan NS. Angiopoietin-like 4 Protein Elevates the Prosurvival Intracellular O(2)(-):H(2)O(2) Ratio and Confers Anoikis Resistance to Tumors. Cancer Cell. 2011; 19:401-415.
49. Tanaka T, Tahara-Hanaoka S, Nabekura T, Ikeda K, Jiang S, Tsutsumi S, Inagaki T, Magoori K, Higurashi T, Takahashi H, Tachibana K, Tsurutani Y, Raza S, Anai M, Minami T, Wada Y, et al. PPARbeta/delta activation of CD300a controls intestinal immunity. Sci Rep. 2014; 4:5412.
50. Higuchi Y, Setoguchi M, Yoshida S, Akizuki S and Yamamoto S. Enhancement of c-fos expression is associated with activated macrophages. Oncogene. 1988; 2:515-521.
51. Wiezlak M, Diring J, Abella J, Mouilleron S, Way M, McDonald NQ and Treisman R. G-actin regulates the shuttling and PP1 binding of the RPEL protein Phactr1 to control actomyosin assembly. J Cell Sci. 2012; 125:5860-5872.
52. Zhang Y, Wang Z, Chen M, Peng L, Wang X, Ma Q, Ma F and Jiang B. MicroRNA-143 targets MACC1 to inhibit cell invasion and migration in colorectal cancer. Mol Cancer. 2012; 11:23.
53. Lee D, Lee HS, Yang SJ, Jeong H, Kim DY, Lee SD, Oh JW, Park D and Kim MG. PRSS14/Epithin is induced in macrophages by the IFN-gamma/JAK/STAT pathway and mediates transendothelial migration. Biochem Biophys Res Commun. 2011; 405:644-650.
54. Tamai K, Semenov M, Kato Y, Spokony R, Liu C, Katsuyama Y, Hess F, Saint-Jeannet JP and He X. LDL-receptor-related proteins in Wnt signal transduction. Nature. 2000; 407:530-535.

55. Borrell-Pages M, Romero JC, Juan-Babot O and Badimon L. Wnt pathway activation, cell migration, and lipid uptake is regulated by low-density lipoprotein receptor-related protein 5 in human macrophages. Eur Heart J. 2011; 32:2841-2850.

56. Grassian AR, Metallo CM, Coloff JL, Stephanopoulos G and Brugge JS. Erk regulation of pyruvate dehydrogenase flux through PDK4 modulates cell proliferation. Genes Dev. 2011; 25:1716-1733.

57. Toth PM, Naruhn S, Pape VF, Dörr SM, Klebe G, Müller R and Diederich WE. Development of Improved PPARbeta/delta Inhibitors. ChemMedChem. 2012; 7:159-170.

58. Barak Y, Liao D, He W, Ong ES, Nelson MC, Olefsky JM, Boland R and Evans RM. Effects of peroxisome proliferator-activated receptor delta on placentation, adiposity, and colorectal cancer. Proc Natl Acad Sci U S A. 2002; 99:303-308.

59. Hayashi S, Lewis P, Pevny L and McMahon AP. Efficient gene modulation in mouse epiblast using a Sox2Cre transgenic mouse strain. Mech Dev. 2002; 119 Suppl 1:S97-S101.

60. Scholtysek C, Katzenbeisser J, Fu H, Uderhardt S, Ipseiz N, Stoll C, Zaiss MM, Stock M, Donhauser L, Bohm C, Kleyer A, Hess A, Engelke K, David JP, Djouad F, Tuckermann JP, et al. PPARbeta/delta governs Wnt signaling and bone turnover. Nat Med. 2013:19.

61. Jérôme V and Müller R. Tissue-specific, cell cycle-regulated chimeric transcription factors for the targeting of gene expression to tumor cells. Hum Gene Ther. 1998; 9:2653-2659.

62. Gyorffy B, Lanczky A and Szallasi Z. Implementing an online tool for genome-wide validation of survival-associated biomarkers in ovarian-cancer using microarray data from 1287 patients. Endocr Relat Cancer. 2012; 19:197-208.

Published online 30 April 2015

Nucleic Acids Research, 2015, Vol. 43, No. 10 ***5033–5051***
doi: 10.1093/nar/gkv331

The transcriptional PPARβ/δ network in human macrophages defines a unique agonist-induced activation state

Till Adhikary[1,†], Annika Wortmann[1,†], Tim Schumann[1,†], Florian Finkernagel[1,†], Sonja Lieber[1], Katrin Roth[2], Philipp M. Toth[3], Wibke E. Diederich[3], Andrea Nist[4], Thorsten Stiewe[4], Lara Kleinesudeik[5], Silke Reinartz[5], Sabine Müller-Brüsselbach[1] and Rolf Müller[1,*]

[1]Institute of Molecular Biology and Tumor Research (IMT), Center for Tumor Biology and Immunology (ZTI), Philipps University, 35043 Marburg, Germany, [2]Cellular Imaging Core Facility, Philipps University, Center for Tumor Biology and Immunology (ZTI), 35043 Marburg, Germany, [3]Medicinal Chemistry Core Facility and Institute of Pharmaceutical Chemistry, Center for Tumor Biology and Immunology (ZTI), Philipps University, 35043 Marburg, Germany, [4]Genomics Core Facility, Center for Tumor Biology and Immunology (ZTI), Philipps University, 35043 Marburg, Germany and [5]Clinic for Gynecology, Gynecological Oncology and Gynecological Endocrinology, Center for Tumor Biology and Immunology (ZTI), Philipps University, 35043 Marburg, Germany

Received December 18, 2014; Revised March 28, 2015; Accepted April 01, 2015

ABSTRACT

Peroxisome proliferator-activated receptor β/δ (PPARβ/δ) is a lipid ligand-inducible transcription factor with established metabolic functions, whereas its anti-inflammatory function is poorly understood. To address this issue, we determined the global PPARβ/δ-regulated signaling network in human monocyte-derived macrophages. Besides cell type-independent, canonical target genes with metabolic and immune regulatory functions we identified a large number of inflammation-associated NFκB and STAT1 target genes that are repressed by agonists. Accordingly, PPARβ/δ agonists inhibited the expression of multiple pro-inflammatory mediators and induced an anti-inflammatory, IL-4-like morphological phenotype. Surprisingly, bioinformatic analyses also identified immune stimulatory effects. Consistent with this prediction, PPARβ/δ agonists enhanced macrophage survival under hypoxic stress and stimulated CD8$^+$ T cell activation, concomitantly with the repression of immune suppressive target genes and their encoded products CD274 (PD-1 ligand), CD32B (inhibitory Fcγ receptor IIB) and indoleamine 2,3-dioxygenase 1 (IDO-1), as well as a diminished release of the immune suppressive IDO-1 metabolite kynurenine. Comparison with published data revealed a significant overlap of the PPARβ/δ transcriptome with coexpression modules characteristic of both anti-inflammatory and pro-inflammatory cytokines. Our findings indicate that PPARβ/δ agonists induce a unique macrophage activation state with strong anti-inflammatory but also specific immune stimulatory components, pointing to a context-dependent function of PPARβ/δ in immune regulation.

INTRODUCTION

Macrophages display an enormous degree of plasticity and react to their microenvironment by profoundly different phenotypes, with classically activated, pro-inflammatory macrophages [e.g. by tumor necrosis factor-α (TNFα) or interleukin-1β (IL-1β)] and anti-inflammatory macrophages [e.g. by interleukin 4 or 10 (IL-4 or IL-10)] as the extremes, originally designated as M1 and M2 macrophages (1). However, the macrophage phenotype is highly dynamic, depending on the precise environmental cues (2). Consequently, a spectrum of defined activation/polarization states has recently been proposed (3). A protein involved in the regulation of macrophage activation and polarization is the nuclear receptor peroxisome proliferator-activated receptor β/δ (PPARβ/δ). PPARβ/δ is a ligand-inducible transcription factor with established functions in intermediary metabolism and a less well-defined anti-inflammatory role in immune regu-

*To whom correspondence should be addressed. Tel: +49 6421 2866236; Fax: +49 6421 2868923; Email: rmueller@imt.uni-marburg.de
†These authors contributed equally to the paper as first authors.

lation (4–7). Thus, PPARβ/δ deficiency exacerbated the inflammatory response to topical O-tetradecanoylphorbol-13-acetate in mice (8). Furthermore, PPARβ/δ dampened the inflammatory response in a human model of dermal wound healing by stimulating the secretion of IL-1 receptor antagonist in dermal fibroblasts (9). Anti-inflammatory effects of PPARβ/δ agonists have also been observed in mouse models of intestinal inflammation (10) and experimental allergic encephalomyelitis, the latter involving an inhibition of interferon γ (IFNγ) and IL-17 production by Th1 and Th17 cells (11). An anti-inflammatory function of PPARβ/δ in macrophages has been demonstrated in two studies reporting that M2 polarization of murine macrophages in adipose tissue and liver is dependent on the induction of PPARβ/δ expression by IL-4 or IL-13 (12,13). The precise mechanism of anti-inflammatory macrophage polarization by PPARβ/δ remains, however, unclear. Moreover, inconsistent with a purely anti-inflammatory function, PPARβ/δ is overexpressed in human psoriasis (14) and ligand activation induces a proinflammatory psoriasis-like response in a mouse model (15,16), even though the molecular mechanisms underlying the latter observation and its relevance for the human system remain unclear.

PPARβ/δ regulates its direct target genes through binding to PPAR response elements (PPREs) as a heterodimer with a retinoid X receptor (RXR) (17). Genome-wide analyses have identified PPRE-mediated repression as a major mechanism of transcriptional regulation in the absence of a PPARβ/δ agonist and showed that an agonist-mediated switch induces a subset of these genes (18). PPRE-mediated repression is enhanced by inverse agonists, which establish a repressor complex that apparently is different from the unliganded receptor complex (19). Besides this canonical mechanism, agonist-bound PPARβ/δ can also repress genes by interacting with specific transcription factors without establishing direct DNA contact. For example, PPARβ/δ interacts with the p65 subunit of the nuclear factor kappa B (NFκB) dimer in different cell types (14,20,21), PPARβ/δ ligands decrease NFκB activity via crosstalk with other signaling pathways, including ERK in adipocytes (22) and BCL-6 in macrophages (23). BCL-6 is a transcriptional repressor of inflammatory genes, many of which are targets of NFκB (24). Deletion of *Ppard* or application of a PPARβ/δ ligand abolishes the sequestration of BCL-6 by PPARβ/δ, resulting in the repression of BCL-6 target genes (23).

PPARβ/δ serves as a receptor for a broad range of natural agonists with function in inflammatory processes, including unsaturated fatty acids (25) and 15-hydroxyeicosatetraenoic acid (15-HETE) (26). The function of prostaglandin I_2 (prostacyclin) as a PPARβ/δ agonist is controversial (27,28), which might be due to its extreme instability at pH values below 7.8 (29), making the microenvironment an essential determinant in this context. Owing to the association of PPARβ/δ with major human diseases a number of PPARβ/δ-specific agonists have been developed, several of which are well characterized and have been used in numerous preclinical studies (30,31). Furthermore, several synthetic inhibitory ligands for PPARβ/δ have been described over the past years. These include the PPARβ/δ-specific GSK0660 (32) and its improved derivative ST247 (33,34). These ligands inhibit the basal expression of PPARβ/δ target genes by enhancing the recruitment of transcriptional corepressors, classifying them as inverse agonists (33).

To date, genome-wide studies addressing the transcriptional PPARβ/δ signaling network in primary macrophages have not been performed. Recently published transcriptome data for myeloid leukemia THP-1 cells, induced to differentiation toward macrophage-like cells by phorbol ester exposure, do not reflect the situation in normal primary macrophages (35). However, such studies are urgently required to understand the multi-faceted role of PPARβ/δ in immune regulation. In the present study, we applied next-generation sequencing technologies to determine the PPARβ/δ-regulated transcriptome and the PPARβ/δ-RXR cistrome in human monocyte-derived macrophages (MDMs) with the goal to establish the PPARβ/δ-controlled regulatory network in these cells.

MATERIALS AND METHODS

Ligands

L165,041 was purchased from Biozol (Eching, Germany) and GW501516 from Axxora (Lörrach, Germany). ST247 was synthesized as described (33,34). The inverse PPARβ/δ agonist PT-S264 is a novel derivative of ST247 with improved plasma stability (Toth, P.M. *et al.*, submitted for publication). Ligands were used at a concentration of 1 μM in all experiments.

Cell culture

MDA-MB-231 cells were purchased from Caliper Life Science (MDA-MB-231-luc2). WPMY-1 cells were obtained from the ATCC. Cells were maintained in Dulbecco's modified Eagle's medium supplemented with 10% fetal bovine serum, 100 U/ml penicillin and 100 μg/ml streptomycin in a humidified incubator at 37°C and 5% CO_2.

Isolation of $CD14^+$ cells

Peripheral blood mononuclear cells were obtained from healthy adult volunteers for MDM stimulation. Mononuclear cells were isolated by Lymphocyte Separation Medium 1077 density gradient centrifugation (PromoCell GmbH, D-69126 Heidelberg, Germany) and further purified by adherent cell positive selection.

Cell culture and cytokine treatment of MDMs

$CD14^+$ monocytes were cultured either in RPMI1640 with 10% fetal calf serum (FCS) (R10 medium) or in serum-free macrophage X-VIVO 10 medium (Biozym Scientific GmbH, Hessisch Oldendorf, Germany; subsequently referred to as XV0 medium). MDMs were differentiated from $CD14^+$ monocytes of healthy volunteers for 5–7 days at 1×10^6 cells/ml. In some experiments MDMs were treated with 20 ng/ml IL-4 (Biozol, Eching, Germany), 100 ng/ml (lipopolysaccharide (LPS); *Escherichia coli* 0111:b4 L4391; Sigma Aldrich, Steinheim, Germany) or 10 ng/ml IFNγ (Biomol, Hamburg, Germany) during differentiation for

5–7 days. Isolation of murine bone marrow cells (BMCs), differentiation to macrophages (BMDMs) by granulocyte-macrophage colony stimulating factor (GM-CSF) and ligand treatment were carried out as described (36).

Propidium iodide uptake under hypoxia

MDMs were treated with ligands as indicated and kept under 1% oxygen starting directly after isolation of monocytes. Propidium iodide (Sigma Aldrich, Steinheim, Germany) was added to a 1 ml cell suspension containing 1–2 × 10^6 MDMs to yield a final concentration of 1 μg/ml. Cells were kept at ambient temperature in the dark for 1 h followed by fluorescence-activated cell sorting (FACS) analysis using an FACS Canto cytometer and BD FACSDiva software (BD Biosciences, Heidelberg, Germany).

Phagocytosis assay

Phagocytosis assay was performed with d6 MDMs using 0.5 mg/ml fluorescein isothiocyanate (FITC) dextran (Sigma Aldrich, Steinheim, Germany). Cells were kept under standard culture conditions for 1 h. Negative control cells were incubated for 1 h at 4°C. Following the incubation, cells were washed three times and analyzed by FACS.

FACS phenotyping

Cells were pretreated and stained for macrophage markers as previously described (37). In addition, FITC-labeled anti-human CD86 (Miltenyi Biotech, Bergisch Gladbach, Germany), FITC-labeled anti-CD32A (Clone IV.3, Stemcell Technologies, Cologne, Germany) and allophycocyanin (APC)-labeled anti-CD274 (BD Biosciences) were used. Intracellular staining of permeabilized cells with anti-CD32B (Clone C2C3, Genetex, Irvine, CA, USA) and FITC-labeled secondary antibody (eBioscience, Frankfurt a.M., Germany) was performed as published (37). Isotype control antibodies were purchased from BD Biosciences, Miltenyi Biotech and eBioscience. Cells were analyzed using an FACS Canto cytometer and BD FACSDiva software (BD Biosciences). Results were calculated as mean fluorescence intensities.

T cell activation

For antigen-specific T cell activation, autologous $CD14^+$ monocytes from buffy coats of healthy donors were differentiated to MDMs in the presence of different stimuli for 5–7 days and used as antigen-presenting cells for antigen-specific T cell activation. Eighty thousand MDMs per 96 well culture plate were loaded with 1 μg/ml cytomegalovirus, Epstein-Barr virus, influenza virus and tetanus toxoid (CEFT) peptide pool of 27 peptides (jpt Peptide Technologies, Berlin, Germany) for 24 h (37°C, 5% CO_2). After washing with phosphate buffered saline, peptide-pulsed MDMs were cocultured with 4 × 10^5 autologous lymphocytes ($CD14^-$ fraction after MACS selection of buffy coats) at a 5:1 ratio of lymphocytes to MDMs in XV0 medium. MDMs pulsed with dimethylsulfoxide (DMSO; 0.2% final concentration) were used as unstimulated controls for antigen-specific T cell activation. For polyclonal T cell stimulation, 4 × 10^5 lymphocytes were incubated in 96 well culture plates coated with mouse anti-human CD3 mAb (500 ng/well; clone OKT3, Biolegend, San Diego, CA, USA) in the absence of autologous MDMs. Experimental controls included non-stimulated lymphocytes cultured without anti-CD3 mAb. Polyclonal and peptide-specific T cell stimulation were performed at 37°C and 5% CO_2 for a total of 18 h with 5 μg/ml Brefeldin A (Sigma Aldrich, Steinheim, Germany) for the last 16 h. Activated lymphocytes were harvested and stained with surface markers anti-human CD8 APC (Miltenyi Biotec, Bergisch Gladbach, Germany). After permeabilization (BD Cytofix/Cytoperm Kit, BD Bioscience, Heidelberg, Germany) anti-human IFNγ FITC (eBioscience, Frankfurt a.M., Germany) was added according to the manufacturer's instructions. Frequencies of activated T cells were measured by flow cytometry (FACS Canto, BD Bioscience, Heidelberg, Germany) and expressed as IFNγ+/CD8+ cells after subtracting background staining of corresponding non-stimulated controls.

Immunoblotting

Immunoblots were performed according to standard protocols using the following antibodies: α-PPARβ/δ (sc-74517; Santa Cruz, Heidelberg, Germany); α-IDO-1 (MAB10009; Millipore, Darmstadt, Germany), α-LDH (sc-33781; Santa Cruz, Heidelberg, Germany), α-rabbit IgG HRP-linked AB and α-mouse IgG HRP-linked AB (cs7074, cs7076; Cell Signaling, NEB, Frankfurt, Germany). Imaging and quantification was done using the ChemiDoc MP system and Image Lab software version 5 (Bio-Rad, München, Germany).

Kynurenine assay

Kynurenine was measured according to a published procedure (38). Supernatant of MDM cultures (360 μl) was incubated with 180 μl of 30% trichloroacetic acid (TCA) for 30 min at 50°C. After centrifugation at 3000 × g for 10 min, the supernatant was collected, mixed with an equal volume of freshly prepared Ehrlich Reagent (2% p-dimethylaminobenzaldehyde in glacial acetic acid) and incubated for 12–30 min at ambient temperature. The absorbance was measured at 492 nm and compared to a calibration curve obtained with L-kynurenine (Santa Cruz, Heidelberg, Germany).

Reverse transcription quantitative polymerase chain reaction (RT-qPCR)

cDNA isolation and qPCR analyses were performed as described (33). L27 was used for normalization. Primer sequences are listed in Supplementary Table S1.

RNA sequencing

RNA was extracted with TRIfast (Peqlab, Erlangen, Germany) according to the manufacturer's instructions. Genomic DNA was removed by incubation with RNase-free DNase (Macherey-Nagel, Düren, Germany) for 15 min at

room temperature. After column-based purification (Qiagen Minelute, Hilden Germany), 0.1–0.5 μg of DNA-depleted RNA was used for library preparation according to the manufacturer's instructions (ScriptSeq Complete Gold Kit, Human/Mouse/Rat-Low Input, Epicentre, Madison, WI, USA) utilizing Qiagen Minelute columns and Beckman Coulter Agencourt AMpure XP beads. Samples were sequenced on an Illumina HiSeq 1500.

Chromatin immunoprecipitation (ChIP) sequencing

ChIP was performed and evaluated as described (18,19) using the following antibodies: IgG pool, I5006 (Sigma-Aldrich, Steinheim, Germany); α-PPARβ/δ, sc-7197; α-RXR, sc-774 (Santa Cruz, Heidelberg, Germany). For precipitation, a mixture of Dynabeads Protein A (10002D) and Dynabeads Protein G (10004D; both from Life Technologies, Carlsbad, CA, USA) was blocked with 1 g/l bovine serum albumin overnight, and 50 μl was used per immunoprecipitation (IP). DNA was purified using Qiagen Minelute columns. Preceding the PE washing step, the membranes were washed twice with pure methanol in order to remove contaminating DNA-binding lipids that inhibit subsequent low-temperature enzymatic modification steps, which we found to be present in samples from primary macrophages. Libraries were synthesized from 1–2 ng of genomic DNA using the MicroPlex kit (Diagenode, Seraing, Belgium). Samples were sequenced on an Illumina Hi-Seq 1500 (Illumina, San Diego, CA, USA).

Mapping of ChIP sequencing reads and peak calling

ChIP sequencing (ChIP-Seq) mapping and peak calling was performed as described (18,19) except that (i) Subread (version 1.4.3-p1) (39) was used for alignment, (ii) reads were filtered to a maximum of five mismatches and five repetitions of each read start site (deduplication) and (iii) updated versions of Ensembl (v74) and MACS (1.4.0rc2 20110214) were employed. The number of usable reads was 46 299 322 (PPARβ/δ), 39 483 674 (RXR) and 42 750 342 (IgG control). Peaks were filtered for at least 15 deduplicated tags, a fold change (FC) over IgG of ≥2 (normalized total read counts) and at most 60 deduplicated IgG tags. Venn diagrams for peak overlaps were calculated by building the interval union and testing each resulting interval for overlaps with the initial peak sets. Genes were associated with peaks based on the closest transcription start site (TSS) from the peak summit and all TSSs within 50 kb of the summit (internal TSSs were considered). A peak could thus be assigned to multiple genes.

RNA sequencing analysis

RNA sequencing (RNA-Seq) data were aligned to Ensembl v74 using STAR (version STAR_2.3.1z13_r470) (40). Gene read counts were established as read count within merged exons of protein coding transcripts (for genes with a protein gene product) or within merged exons of all transcripts (for non-coding genes). FPKM (fragments per kb per million) were calculated based on the total gene read counts and length of merged exons. Raw read counts were quantile normalized within each comparison and logFC values were calculated (after adding 1/60 to the normalized FPKM values to avoid undefined values). Genes were considered regulated if they had a logFC of at least 0.7 (∼1.62-fold), a minimum FPKM of 0.3 in any condition and at least 50 raw reads.

Comparisons with published ChIP-Seq data

For comparison of the PPAR bound gene sets, signal transducer and activator of transcription 1 (STAT1) data were retrieved from (41) and gene IDs updated to Ensembl v74. STAT3 data were retrieved from Supplementary Table S1 in (42), updated to Ensembl v74 and translated from mouse to human via Ensembl Compara. NFκB bound regions (24) were retrieved from Gene Expression Omnibus (GSM61116, GSM61117, union), lifted from mm9 to mm10 using UCSCs liftOver utility and associated with the mouse gene with the closest transcription start site (internal TSSs were considered). Translation to human genes was again by Ensembl Compara. BCL6 bound sites from the same publication (24) (GSE16723, top level data file) were treated identically. P300 associated genes were extracted from (43) (Supplementary Table S1), assigned to mouse stable IDs using the 'Official Gene Symbol' column and Ensembl v64, updated to Ensembl v74 and translated to human genes via Ensembl Compara.

Comparisons with published stimulus-specific MDM transcriptomes

Raw microarray data (3) (GSE46903, 'GSE46903_non-normalized.txt.gz') quantile normalized using the lumi Bioconductor package annotated using Supplementary Table S1B in (3) were used to calculate logFC values versus basal (M0) condition based on expression values averages within each condition. Only GM-CSF stimulated macrophage samples were analyzed. WGCNA output (49 modules; Supplementary Table S2B in (3)) was translated to Ensembl stable gene IDs using Illumina Human-HT-12_v3 annotation ('HumanHT-12_V3_0_R3_11283641_A'). Translation was preferentially based on Entrez IDs with gene symbols as a fall back. Overlaps between modules and L165,041 regulated genes were assessed by Fisher's exact test. For Figure 8, a directional score for overlapping genes was calculated as follows: the number of genes regulated in the same direction by L165,041 and a given stimulus minus the number of genes regulated in the opposite direction. Only genes showing an at least 1.5-fold induction by the respective stimulus [3] and 1.62-fold by L165,041 (Supplementary Table S2) were included.

Comparison with published genomic PPARβ/δ data for other cell types

For comparisons based on peaks, original sequencing data (18,19) were reanalyzed as described in section 'Mapping of ChIP-Seq reads and peak calling'. Microarray based transcription assay results were retrieved from supplementary tables of the aforementioned publications and their gene stable IDs updated to the Ensembl revision used. In comparisons depicting both RNA-Seq and microarray data,

genes were filtered to those occurring on both microarray chip types used (Agilent-028004 and Agilent-014850).

Databases

All genomic sequence and gene annotation data were retrieved from Ensembl release 74, genome assembly hg19. Our full analysis scripts and computational pipeline are available upon request.

Statistical analysis of experimental data

Data are presented as the average of biological replicates ($n \geq 3$; precise numbers for each experiment indicated in the figure legends) ± standard deviations (error bars). Comparative data were statistically analyzed by Student's *t*-test (two-sided, equal variance) using GraphPad Prism 6.0. Results were expressed as follows: $*P < 0.05$, $**P < 0.01$ and $***P < 0.001$. When appropriate, correction for multiple hypothesis testing was done by Benjamini–Hochberg adjustment, as indicated.

Functional annotations, networks and pathway analyses

RNA-Seq data were analyzed using the Ingenuity Pathway Analysis (IPA) application and knowledge database (Qiagen Redwood City, CA, USA). The functions 'Upstream Regulators, Diseases and Bio Functions and Networks' were applied using the default settings. Results were sorted according to *P*-value of overlap (minimum 10^{-5}) and activation z-scores (≤ -2.0 or $\geq +2.0$ required).

RESULTS

Induction of PPARβ/δ during differentiation of human monocytes to MDMs

First, we sought to identify an experimental system suitable for studying the PPARβ/δ cistrome and ligand-regulated transcriptome. Human monocytes were differentiated to MDMs in RPMI1640 with 10% FCS medium (R10) and characterized with respect to PPARβ/δ expression and activity. RT-qPCR analysis showed increasing PPARD mRNA levels after initiation of cultures reaching a maximum around day 5 (Figure 1A), which was paralleled by a strong increase in PPARβ/δ protein expression (Figure 1B and Supplementary Figure S1) and ligand inducibility of the well-established target gene *PDK4* (Figure 1C), both reaching maximum levels around day 6. Chromatin-bound PPARβ/δ and RXR were detected by ChIP at the PPAR-responsive *PDK4* enhancer already on day 0 (monocytes; Figure 1D), which explains the ligand responsiveness of the *PDK4* gene at early time points (Figure 1C). Re-ChIP analyses showed that PPARβ/δ and RXR formed complexes on the PDK4 enhancer, as expected (Supplementary Figure S2). The induction of PPARβ/δ expression and activity during differentiation was paralleled by an increased surface expression of the macrophage markers CD32, CD63, CD86, CD206 and HLA-DR and an induction of intracellular CD68 (Supplementary Figure S3). MDMs thus appear to be suitable for investigating effects of PPARβ/δ ligands on macrophage activation and/or polarization, in particular since plastic adherence partially activates monocytes and macrophages (44–48), including increased STAT1 and NFκB signaling (49,50), thus allowing for a potential modulation by agonists or inverse agonists in either direction. We therefore chose day-6 MDMs for the subsequent studies.

The transcriptome of PPARβ/δ ligand-regulated genes in human MDMs

We used this experimental system to identify ligand-responsive genes as well as PPARβ/δ and RXR binding sites in macrophages by deep sequencing technologies. RNA-Seq data obtained with MDMs cultured either in R10 or serum-free synthetic X-VIVO 10 medium (XV0) revealed a total of 285 protein-coding genes upregulated by PPARβ/δ agonist L165,041 and 246 genes downregulated by the inverse agonists ST247 or PT-S264; logFC ≥ 0.7; FPKM ≥ 0.3), 29.6% of the latter ($n = 73$) overlapping with the agonist-induced gene set (Figure 2A; Supplementary Table S2). Our RNA-Seq also identified a large fraction of genes repressed by the agonist L165,041 ($n = 388$) and upregulated by the inverse agonist ST247 ($n = 174$), with 40 genes (10.3%) overlapping (Figure 2B; Supplementary Table S2). Diseases and functions annotation of the L165,041-induced gene set showed a strong association with the inhibition of cell death of immune cells and suppression of immune cell functions, including migration, inflammatory response, activation, homing, adhesion, chemotaxis and phagocytosis (Figure 2C; Supplementary Table S3). The gene set representing inflammation clearly overlapped with cell survival, migration/movement, adhesion and recruitment/infiltration/ chemotaxis (Figure 2D), suggesting that these to a large extent represent genes with functions in immune regulation. Interestingly, 'Inflammation of intestine' and 'Colitis' showed a positive activation z-score (Figure 2C), providing a first hint that the response to L165,041 may not be strictly anti-inflammatory. Likewise, lipid metabolism ('Concentration of acylglycerol') was upregulated, consistent with the known metabolic role of PPARβ/δ. Finally, analysis of the known upstream regulators of these genes (signaling molecules and transcription factors) identified two groups: canonically regulated (L165,041-induced) genes known to be activated by PPAR agonists (pirixinic acid, fibrates, glitazones) were upregulated by L165,041, while genes induced by pro-inflammatory signaling via LPS, TNFα, IFNγ, IL-1β, STAT3 or TLR4 were downregulated (inverse target genes).

To rule out the possibility that inverse regulation may be due to PPARβ/δ-independent off-target mechanisms we analyzed the regulation of target genes in bone marrow-derived macrophages (BMDMs) from wild-type and *Ppard* null mice. As shown in Figure 2F, *Ccl24, Tnfsf15* and *Serpinb2* were repressed upon agonist treatment specifically in wild-type cells. Two other genes found to be repressed by agonists in human MDMs were not regulated *(Ccl8)* or not expressed *(Enpp2)* in murine BMDMs, while the canonical target *genes Pdk4* and *Angptl4* showed the expected PPARβ/δ-dependent induction. These observations confirm the PPARβ/δ dependence of agonist-mediated regulation, but also point to cell type (BMDM versus MDM)

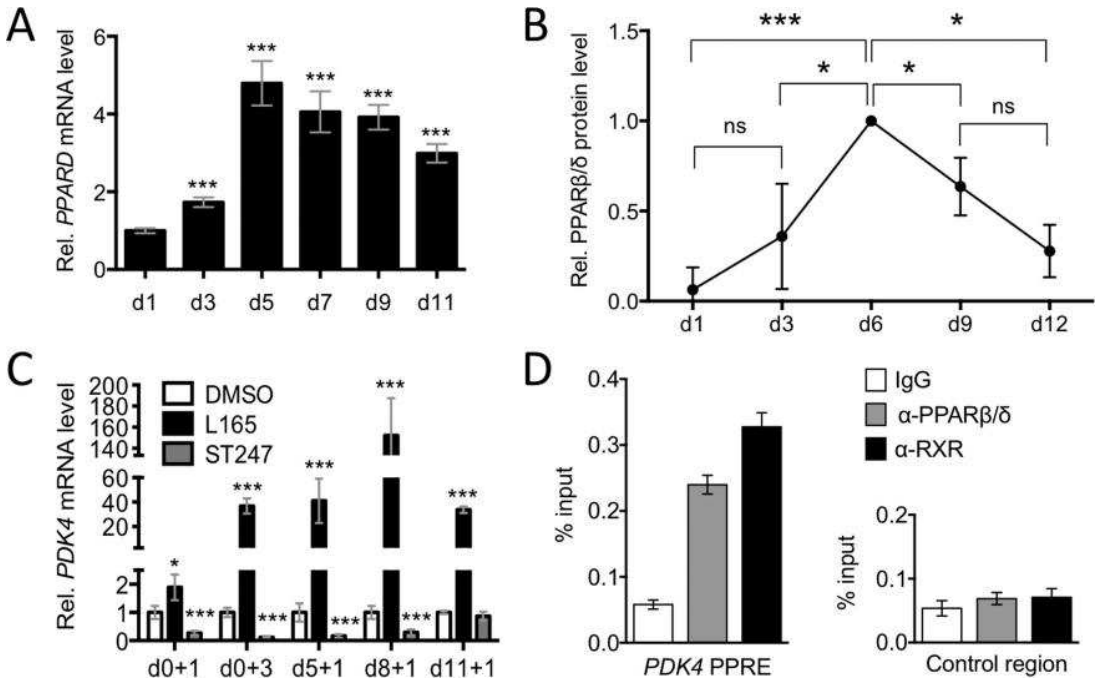

Figure 1. PPARβ/δ expression and activity in differentiating human MDMs. Human monocytes were differentiated in R10 medium for 11 days and analyzed at the indicated times after initiation of differentiation. (**A**) Expression of *PPARD* mRNA measured by RT-qPCR relative d1 (sample size = 3). (**B**) Quantitation of immunoblot analyses of PPARβ/δ protein expression in differentiating MDMs from four different donors relative to LDH (loading control). The individual blots are shown in Supplementary Figure S1. Values were normalized to 1.0 on d6 (maximum expression). (**C**) Ligand-mediated induction relative to DMSO of *PDK4* determined by RT-qPCR. Cells (sample size = 3) were exposed to L165,041 for 1 or 3 days (+1 or +3) at the indicated d (d0, d5, d8, d11). (**D**) PPARβ/δ and RXR enrichment at the *PDK4* enhancer at −12 kb from the transcription start site and an irrelevant control region (Con) in human monocytes (ChIP analysis; sample size = 6). Statistical significance was tested relative to d0 (panel (A)) or DMSO (panel (C)).

and/or species-specific differences in the regulation of inverse PPARβ/δ target genes.

To gain further insight into the diverse functions and regulatory mechanisms suggested by the data in Figure 1 we separately analyzed canonically regulated and inverse target genes as described in the following.

Canonical PPARβ/δ target genes in MDMs

ChIP-Seq analyses identified 1175 enrichment sites for PPARβ/δ associated with 3798 genes located within a distance of 50 kb, and 27 255 RXR enrichment sites associated with 32 720 genes (Figure 3A and B; Supplementary Tables S4 and S5). The majority of overlapping binding sites occurred at transcription start sites (within 1250 bp, 29.1%), within introns (31.6%) or upstream locations (5000 bp, 5.7%) (Figure 3C). A large fraction of the L165,041-induced genes ($n = 132$; 46.3%) showed clear enrichment of PPARβ/δ *in vivo*, and most of these sites ($n = 130$; 98.5%) were co-occupied by RXR (Figure 3A and B). Another fraction of L165,041-induced genes were occupied by RXR, but enrichment for PPARβ/δ at the same genomic region was less clear or not visible ($n = 139$; 48.8%; Figure 3A). These include the strongly regulated (Supplementary Figure S4) and established (51) canonical PPARβ/δ target gene *ANGPTL4*, which shows readily detectable ChIP-Seq peaks in other cell types under identical assay conditions (18,19). This may be due to cell type-specific PPARβ/δ transcription complexes in macrophages that limit accessibility to the antibody. We therefore assume that the presence of RXR on PPREs of L165,041-induced genes indicates canonical PPARβ/δ regulation. This is supported by the results of the upstream regulator analysis of L165,041-induced genes, which identified PPAR ligands and the PPAR coactivator PPARGC1A as the top regulators (nine out of 10; Figure 3D).

Diseases and functions annotation of the canonical target genes showed the strongest positive correlation (by *P*-value) with lipid metabolism (Figure 3E). The identified genes include established PPAR target genes with functions in lipid metabolism, such as *ACADVL, ACAA2, ANGPTL4, CAT, CPT1A, FABP4, ECH1, PDK4, SLC25A20* and *PLIN2*, but also novel target genes, such as *ETFB, ETFDH* and *ISCA1,* the products of which play important roles in electron transfer and iron-sulfur cluster assembly, respectively. Other sets of canonical target genes were either positively associated with cell movement or negatively correlated with systemic autoimmune syndrome (Figure 3E). Consistent with this finding, the canonical target gene set encompasses a number of genes with functions in immune regulation, e.g. *CD1D, CD36, CD52, CD300A, LRP5, NLRC4* and *PHACTR1* (Table 1 and Figure 3B). Several of these examples were validated by RT-qPCR with MDMs from three to seven independent donors (Supplementary Figure S4).

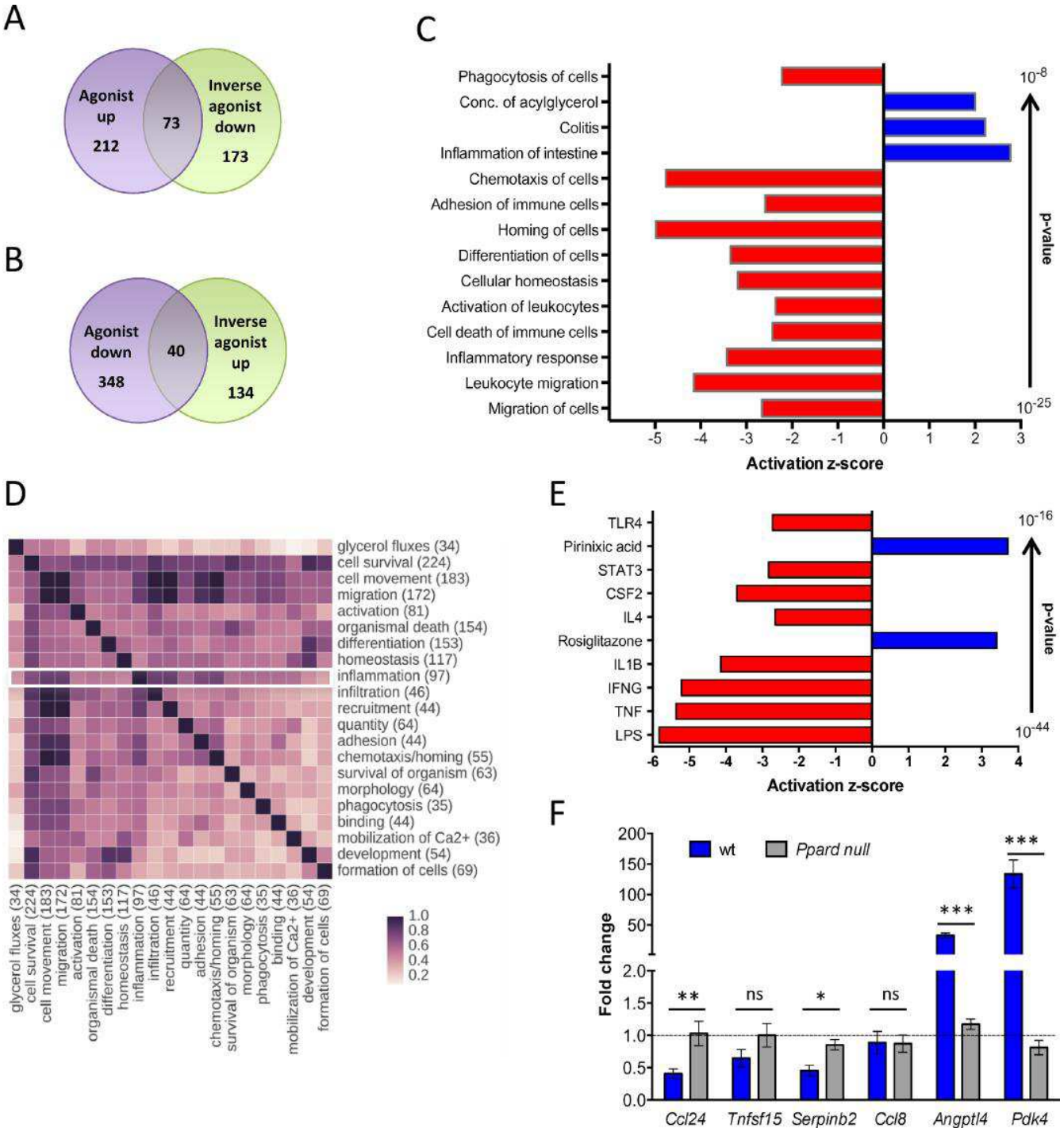

Figure 2. Genome-wide identification of PPARβ/δ target genes in macrophages. (**A**) Overlap of genes induced by L165,041 and repressed by ST247 or PT-S264 in MDMs cultured for 6 days followed by treatment with DMSO or ligands for 24 h. Data are derived from two independent experiments using either R10 (L165,041, ST247) or XV0 (L165,041, PT-S264) medium. Genes with a logFC > 0.7 in one culture condition, a logFC > 0 in both media, an FPKM ≥ 0.3 and a raw tag count of at least 50 were scored as positive. (**B**) Overlap of genes repressed by L165,041 and activated by ST247 in MDMs (conditions as in (A)). (**C**) IPA 'Diseases and Functions Annotation' of L165,041-regulated genes (examples of functionally different clusters with low *P*-values and high z-scores). (**D**) Overlap of L165,041-regulated genes linked to different functions (according to IPA 'Diseases and Functions Annotation'; all clusters with $n > 30$ genes). (**E**) IPA 'Upstream Regulator Analysis' of L165,041-regulated genes (top regulators by *P*-value). (**F**) RT-qPCR analysis of target gene regulation by the PPARβ/δ agonist GW501516 in BMDMs from wild-type and *Ppard* null mice differentiated for 6 days in the presence of GM-CSF (sample size: 3 each). The data show the fold change (mean of triplicates) in response to the ligand relative to solvent treated wild-type and *Ppard* null control cells.

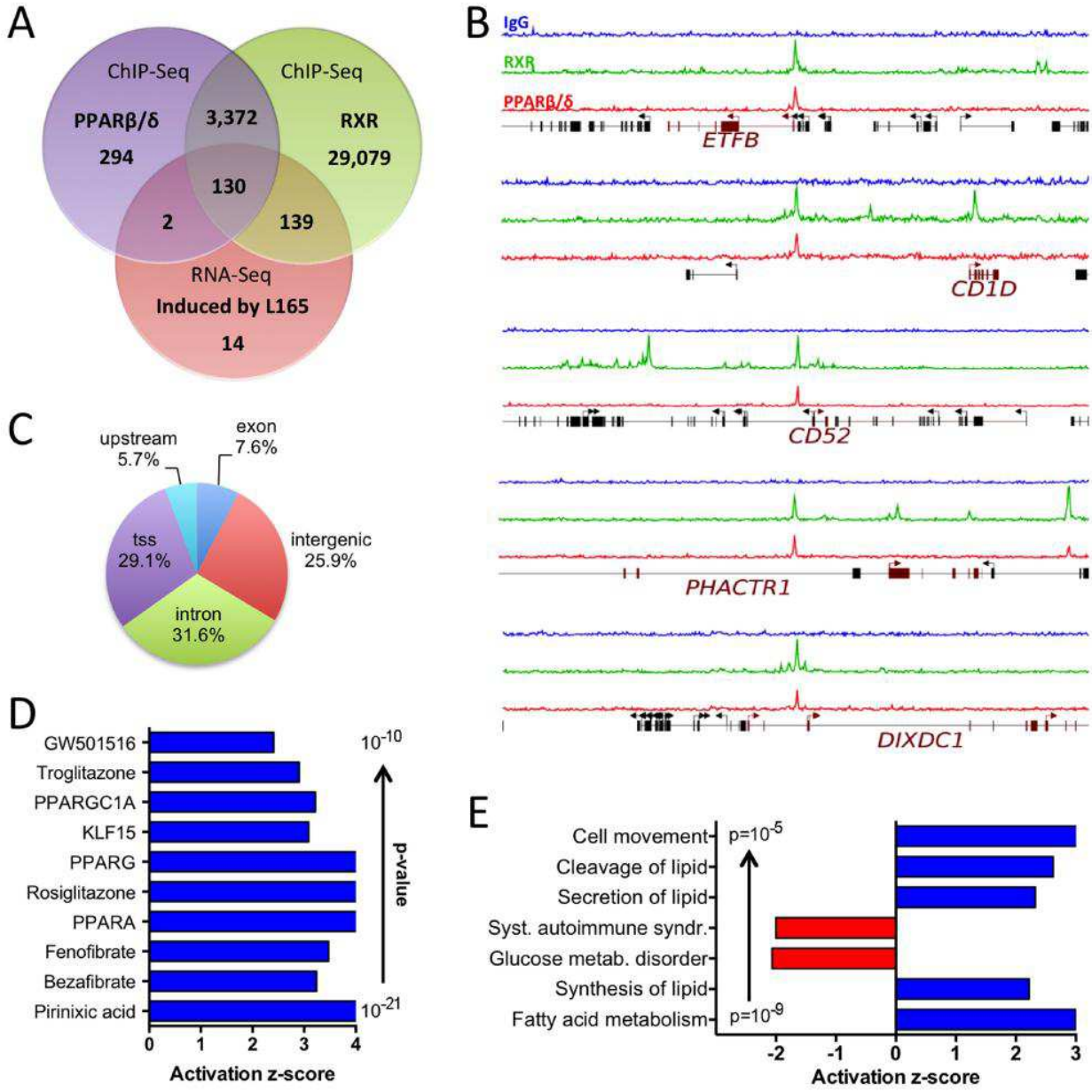

Figure 3. Genome-wide identification of agonist-induced direct PPARβ/δ target genes in MDMs. (**A**) Overlap of genes associated with PPARβ/δ and RXR binding sites in MDMs (ChIP-Seq; peaks filtered and associated with genes as described in the Materials and Methods section) and L165,041-induced genes (RNA-Seq). (**B**) Examples of RXR (green) and PPARβ/δ (red) enrichment peaks at novel canonical target genes (ChIP-Seq data). Blue: control IgG. (**C**) Locations of PPARβ/δ sites identified by ChIP-Seq. tss: within 1250 bp of a transcription start site; upstream: within 5 kb upstream of a transcription start site. (**D**) IPA 'Upstream Regulator Analysis' of L165,041-induced genes (top regulators by *P*-value). (**E**) IPA 'Diseases and Functions Annotation' of L165,041-induced genes in MDMs.

Inverse PPARβ/δ target genes in MDMs

As described above, our RNA-Seq also identified a large fraction of genes repressed by the agonist L165,041, which we subsequently refer to as 'inverse target genes'. As shown in Figure 4A, less than 9% of these genes (34 out of 385) harbored a PPARβ/δ-RXR binding site, which almost uniformly showed low enrichment compared to canonical, agonist-induced PPARβ/δ genes (Figure 4B). This could be due to their regulation by a non-canonical mechanism involving indirect chromatin recruitment, but these genomic regions could also be fortuitous non-functional enrichment sites.

Upstream regulator analysis of the inverse target gene set identified exclusively cytokine signaling pathways (12 out of 12) as top regulators (Figure 4C). In agreement with this finding, published binding sites detected by ChIP-Seq for IFNγ-induced STAT1 (41), LPS-induced NFκB-p65 (24), BCL-6 (24) or LPS-induced P300 (43) were found in a sub-

Table 1. Canonical and inverse PPARβ/δ target genes with immune regulatory functions in MDMs (examples)

Canonical target genes	
CD1D	CD1D molecule
CD36	CD36 molecule (thrombospondin receptor)
CD52	CD52 molecule
CD300A	CD300a molecule
CD300LB	CD300 molecule-like family member b
DIXDC1	DIX domain containing 1
LRP5	Low density lipoprotein receptor-related protein 5
MME	Membrane metallo-endopeptidase
NLRC4	NLR family, CARD domain containing 4
PHACTR1	Phosphatase and actin regulator 1
S100Z	S100 calcium binding protein Z
SCARB2	Scavenger receptor class B, member 2
SLAMF9	SLAM family member 9
ST14	Suppression of tumorigenicity 14
Inverse target genes	
ARG2	Arginase 2
BCL3	B-Cell CLL/Lymphoma 3
CASP5	Caspase 5, apoptosis-related cysteine peptidase
CCL13	Chemokine (C-C motif) ligand 13
CCL24	Chemokine (C-C motif) ligand 24
CCL8	Chemokine (C-C motif) ligand 8
CD1A	CD1a molecule
CD1B	CD1b molecule
CD1E	CD1e molecule
CD300E	CD300e molecule
CXCL1	Chemokine (C-X-C motif) ligand 1
CXCL10	Chemokine (C-X-C motif) ligand 10
CXCL11	Chemokine (C-X-C motif) ligand 11
CXCL6	Chemokine (C-X-C motif) ligand 6
CXCL9	Chemokine (C-X-C motif) ligand 9
FCGR2B	Fc fragment of IgG, low affinity IIb, receptor (CD32B)
IDO1	Indoleamine 2,3-dioxygenase 1
IDO2	Indoleamine 2,3-dioxygenase 2
IL10	Interleukin 10
IL8	Interleukin 8
NLRP12	NLR family, pyrin domain containing 12
TLR3	Toll-like receptor
TNF	Tumor necrosis factor α

stantial fraction of the inverse PPARβ/δ target genes (Figure 4D), with BCL-6 and LPS-induced P300 presumably indicative of NFκB recruitment. These associations suggest that NFκB plays an essential role in the regulation of inverse target genes by PPARβ/δ agonists. RNA-Seq analyses also identified *BCL3* as an inverse target gene (Supplementary Table S2). Since BCL-3 can activate transcription via nuclear NFκB complexes (52), its repression by L165,041 potentially contributes to the inhibition of NFκB target genes.

Proteasome inhibitors block the function of NFκB by different mechanisms, including a blockade of IκB degradation or an inhibition of NFκB precursor processing (53). Consistent with the predicted role of NFκB in the regulation of inverse PPARβ/δ target genes, we found that the 'bona fide' (24) NFκB target genes *APOBEC3A, BCL3, CCL24, FCGR2B, IL10, S100A8* and *S100A9* were strongly downregulated by the proteasome inhibitor MG132. The only exception was *IL8*, which was strongly induced by MG132, indicating a different mechanism of regulation, consistent with published observations (54). A role of NFκB in the agonist-mediated regulation of inverse target genes is supported by our observation that MG132 diminished the magnitude of repression of several of these genes to a statistically not significant level in all cases but *APOBEC3A* and *BCL3*. However, repression by L165,041 was not completely abrogated, pointing to the involvement of other signaling pathways.

In contrast to the canonically regulated genes, the inverse target genes are mostly associated with functions in immune regulation as indicated by the diseases and functions annotation in Figure 4F. Strong negative correlations were found for leukocyte migration/movement/homing, proliferation and cell death, indicating an anti-inflammatory and pro-survival agonist effect via inverse target genes. However, positive associations with pro-inflammatory functions were also observed ('Inflammation of organ' and 'Colitis').

The inverse target genes include cytokines, chemokines and enzymes involved in immune regulation (Table 1). Most of these genes are pro-inflammatory (e.g. *IL8*), but a small number of immunosuppressive genes are also found among the inverse target genes (e.g. *IDO1*), consistent with the results of the diseases and functions annotation analysis above.

Functional networks derived from genomic data

In view of the above findings, several functional networks centered on NFκB (or its upstream regulator TNFα) or biological functions relevant to immune regulation were

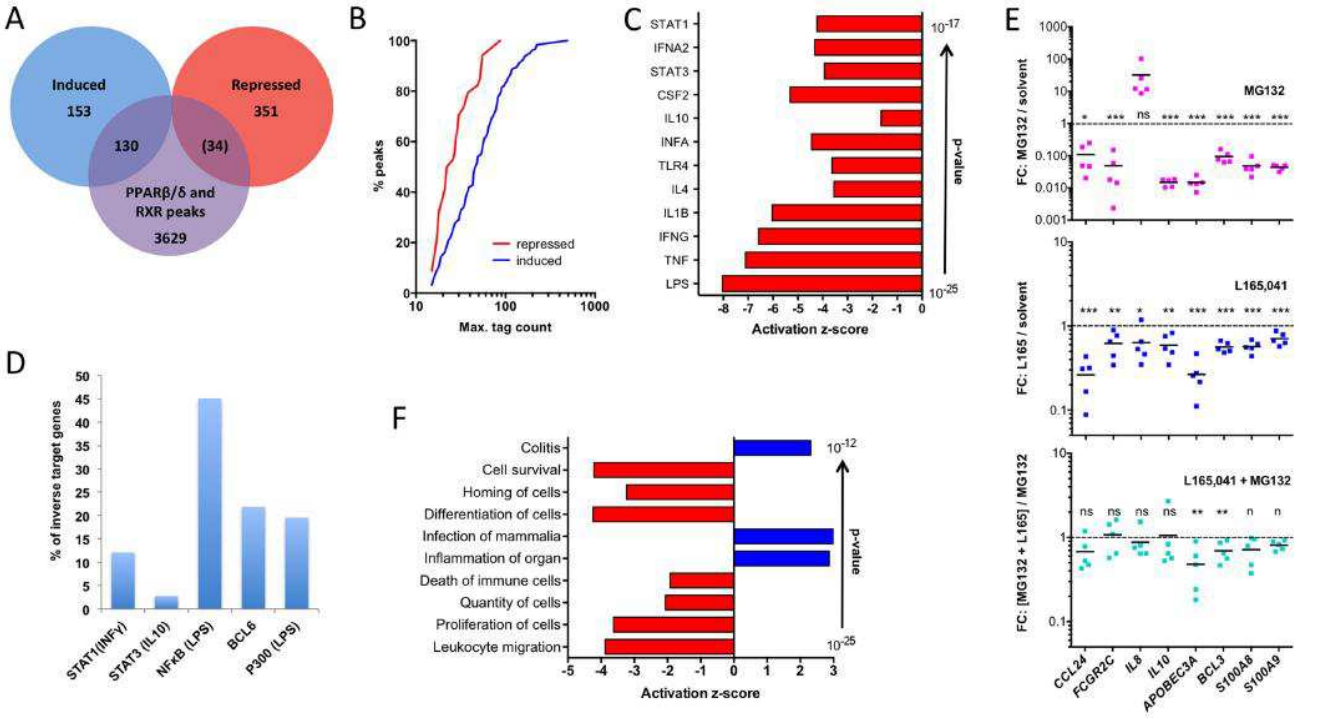

Figure 4. Genome-wide identification of agonist-repressed (inverse) PPARβ/δ target genes. (**A**) Overlap of genes associated with PPARβ/δ and RXR binding sites in MDMs with L165,041-regulated genes. Number in parentheses indicates low enrichment sites. (**B**) Cumulative read distribution for all PPARβ/δ binding sites separated into agonist induced and agonist repressed genes. Plotted is the percentage of reads with *n* or fewer reads in PPARβ/δ ChIP-Seq analyses. (**C**) IPA 'Upstream Regulator Analysis' of L165,041-repressed genes (top regulators by *P*-value). (**D**) Percentage of inverse PPARβ/δ target genes in MDMs (this study) with published binding sites (ChIP-Seq) for STAT1 (INFγ induced) (41), STAT3 (IL-10 induced) (42), NFκB-p65 (24), BCL-6 (24) (43) or P300 (LPS-induced). (**E**) Effect (fold change) of MG132 (10 μM), L165,041 or a combination of both compounds on inverse target genes with 'bona fide' NFκB binding sites (24-h treatment) in MDMs from five donors. *T*-tests of the corresponding groups in the two L165,041 panels against each other showed a statistical significance for *CCL24* ($P < 0.05$). (**F**) IPA 'Diseases and Functions Annotation' of L165,041-repressed genes in MDMs.

studied in further detail. It is obvious from the pathways depicted in Figure 5 that numerous L165,041-regulated genes impact on various aspects of inflammation and/or immune modulation. Anti-inflammatory, agonist-mediated mechanisms include inhibition of the NALP1 inflammasome through modulation of caspase 5 and multiple members of the NOD-like receptor (NLR) family (Figure 5A), reduced TLR signaling (Figure 5B) and diminished NFκB activation (Figure 5A).

In contrast, repression of indoleamine 2,3-dioxygenase 1 (encoded by *IDO1;* Figure 5B), which catabolizes tryptophan to kynurenine, would be predicted to be immune stimulatory, since both tryptophan depletion and kynurenine production have been linked to T cell suppression (55). Moreover, *CD274*, which codes for the transmembrane glycoprotein PD-L1 (PD-1 ligand; B7-H1) and suppresses T cell proliferation (56), is repressed by PPARβ/δ agonists (Figure 5B). L165,041 also impinges on the regulation of macrophage activity by immunoglobulin binding to Fc receptors (Figure 5C). In this context, repression of the inhibitory *FCGR2B* gene encoding CD32B is of particular interest and points to another immune stimulatory action of PPARβ/δ agonists.

In addition, different pathways of antigen presentation are modulated by PPARβ/δ agonists. These include both MHCI and MHCII (HLA-DR, HLA-B27) complexes and MHC-like CD1 proteins involved in the presentation of different lipid antigens (57). These are modulated either directly by PPARβ/δ ligands, by ligand-regulated members of the leukocyte immunoglobulin-like receptor (LIR) family and/or by NFκB (Figure 5A and D). As the genes involved are either canonically or inversely regulated by ligands, and their encoded proteins include both inhibitory and stimulatory molecules, the immune modulatory effect of L165,041 on antigen presentation is likely to be context-dependent.

These predictions clearly point to a specific phenotype triggered by PPARβ/δ agonists that includes both positive and negative effects on immune regulation, consistent with the conclusions drawn from the functional annotation analyses above (Figures 2–4).

Ligand-induced anti-inflammatory alterations in human MDMs

To elucidate the phenotypic alterations induced by PPARβ/δ agonists in MDMs we first analyzed potential morphological alterations triggered by the PPARβ/δ agonists during the 6-day differentiation period of MDMs. For comparison, LPS with or without IFNγ (inducing M1 polarization) or IL-4 (triggering M2 polarization) were added to separate cultures. Figure 6A–E shows a clear

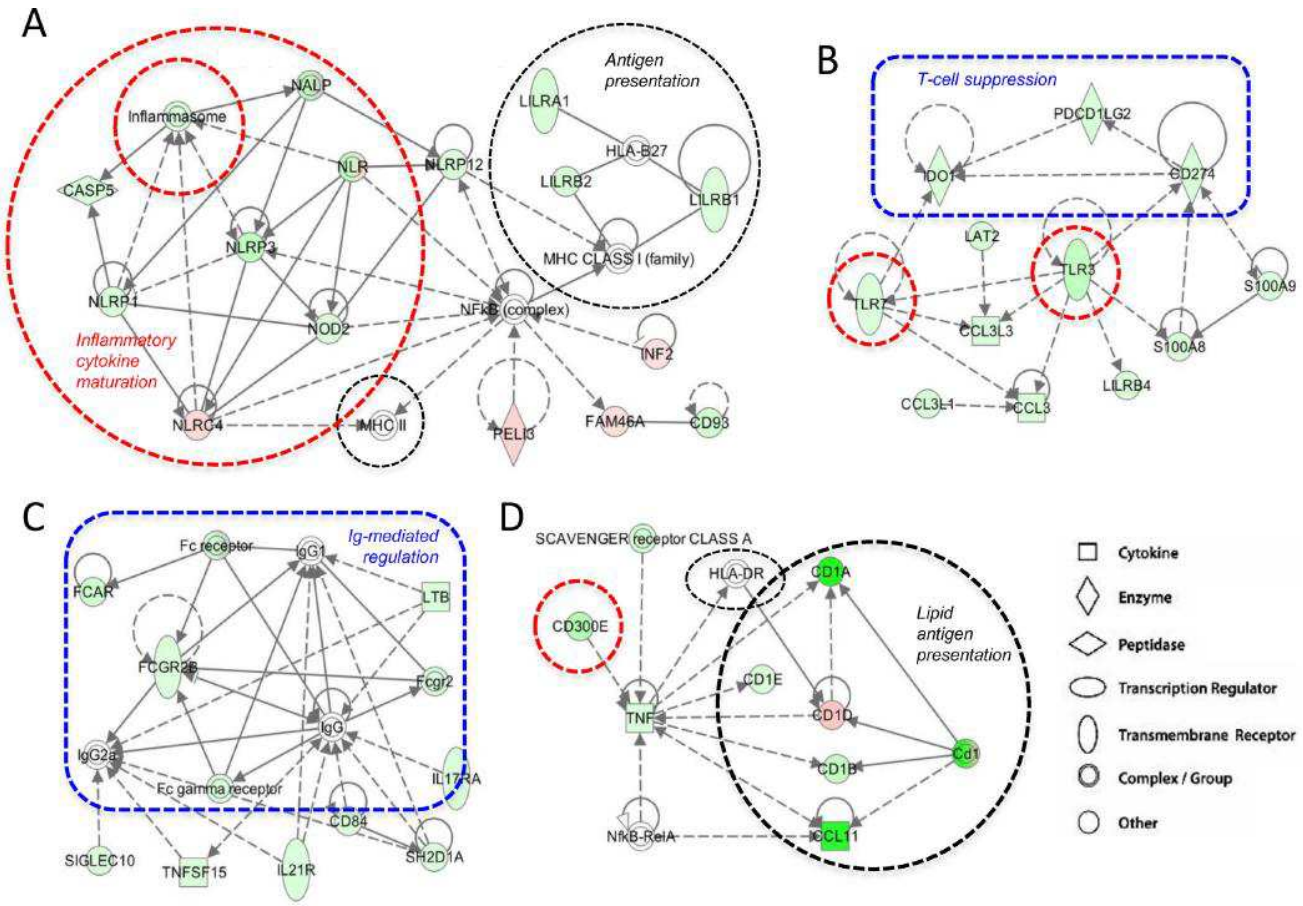

Figure 5. Effects of L165,041 on immune regulatory modules. The scheme displays functional modules derived from the IPA 'Functional Network Analysis' (Supplementary Table S6; modules 2, 3, 4 and 10). Pink symbols: genes upregulated by L165,041; green symbols: genes downregulated by L165,041. Dashed lines: indirect effects or interactions. Encircled areas indicate functional units with pro-inflammatory (red), anti-inflammatory (blue) or context-dependent (black) functions.

morphological resemblance between L165,041 (agonist) and IL-4 treated cultures, while PT-S264 (inverse agonist) induced a morphology reminiscent of M1 cells. Very similar results were obtained irrespective of the culture medium (R10 in Figure 6; XV0 medium in Supplementary Figure S5).

These morphological alterations are in agreement with the observed downregulation of pro-inflammatory genes by L165,041, exemplified by *IL8* and *CCL24* (Figure 4E), which was confirmed for GW501516 (Supplementary Figure S6). Consistent with this conclusion we also found that L165,041 inhibited phagocytosis. As shown in Figure 6F, L165,041 significantly decreased the macropinocytotic/phagocytotic activity for FITC-dextran upon PPARβ/δ activation in six independent experiments, as determined by the diminished uptake of fluorescent FITC-dextran by MDMs.

Ligand-induced immune stimulatory alterations in human MDMs

The functional networks in Figure 5 also predicted an increased T cell activation by agonist-treated MDMs as antigen-presenting cells. We tested this hypothesis by measuring intracellular IFNγ in $CD8^+$ T cells after coculture with MDMs exposed to an antigen peptide mix (CEFT). Figure 7A shows that L165,041 pretreatment of MDMs (during the 6-day differentiation period) led to a clear increase in the fraction of $IFN\gamma^+CD8^+$ cells with samples from five out of six donors.

The product of the inverse PPARβ/δ target gene *IDO1*, which suppresses T cell activation via the production of kynurenine (55), may be involved in this effect. As shown in Figure 7, the agonist-mediated transcriptional repression of *IDO1* (Figure 7B) was paralleled by a decreased protein level (Figure 7C; Supplementary Figure S7) and a clearly diminished release of kynurenine into the supernatant of MDM cultures (Figure 7D). Importantly, the level of kynurenine produced under these conditions was sufficient to significantly inhibit polyclonal (CD3 antibody-mediated) T cell activation (Figure 7E).

Another potentially important player in this scenario is the *CD274* gene. Figure 7F shows that the inverse regulation of *CD274* resulted in a reduced surface expression of its encoded product, the PD-1 ligand, a key regulator of an inhibitory T cell checkpoint (56). The agonist-mediated in-

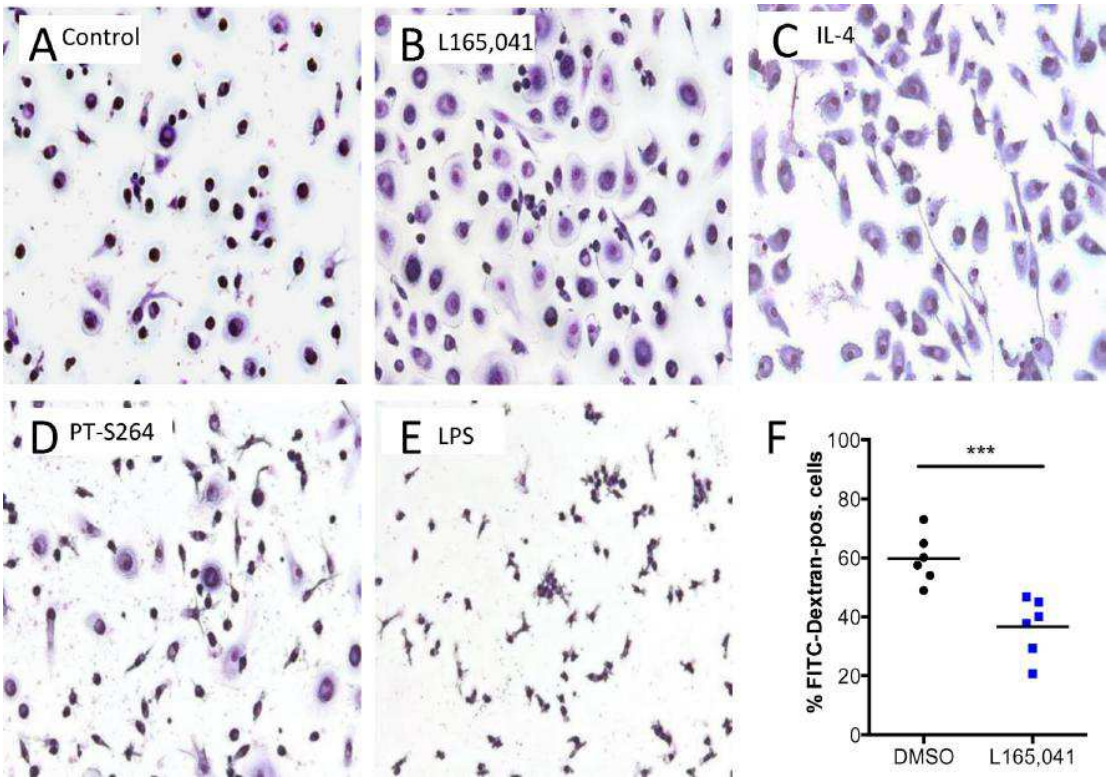

Figure 6. Inhibitory effects of PPARβ/δ ligands on human MDMs. Human monocytes were differentiated in XV0 medium for 6 days in the presence of the indicated additives. Cells were stained with Giemsa dye after treatment with (**A**) DMSO (solvent control), (**B**) L165,041 (agonist), (**C**) IL-4 ('M2' macrophages), (**D**) PT-S264 (inverse agonist) and (**E**) LPS ('M1' macrophages). (**F**) Effect of L165,041 on FITC-dextran uptake (FACS analysis) by MDMs. Data of six biological replicates with cells from four different donors are shown.

hibition of kynurenine production may thus cooperate with downregulation of PD-1 ligand expression to stimulate T cell activation.

Our bioinformatic analyses also pointed to immune stimulatory effects via the agonist-mediated repression of the *FCGR2B* gene. *FCGR2B* codes for CD32B, a low affinity Fcγ receptor that inhibits the phagocytosis of opsonized antigens (58). In contrast to *FCGR2B, FCGR2A* was only weakly repressed by L165,041 and not significantly affected by the inverse agonists ST247 (Figure 7G). *FCGR2B* repression led to downregulation of CD32B protein as determined by flow cytometry (Figure 7H). *FCGR2B* thus represents a PPARβ/δ target gene potentially mediating an agonist-triggered immune stimulatory event.

The functional annotation and networks analysis (Figure 2C; Supplementary Table S3) also predicted an inhibition of cell death of immune cells by L165,041 (Figure 2C), which could be relevant under the stressful conditions of inflammation. We therefore tested this prediction in the context of hypoxia and found a clear pro-survival effect of L165,041, while PT-S264 exacerbated hypoxia-induced cell death, as indicated by the fraction of healthy cells and cell debris in Supplementary Figure S8A. A similar effect was seen in MMT-based viability assays of the adherent cell fraction (Supplementary Figure S8B). Propidium iodide uptake assays showed a time-dependent pro-survival effect of both PPARβ/δ agonists tested (L165,041, GW501516) peaking on day 4 (Figure 7I). As MDMs do not proliferate under the culture conditions used here, a ligand effect on proliferation could not contribute to these observations.

Finally, time-lapse video microscopy revealed a slight, but statistically significant inhibitory effect of L165,041 on the motility of MDMs (Supplementary Figure S9), as predicted by the functional annotation analysis in Figure 2C.

Comparison of the PPARβ/δ agonist-induced transcriptome with defined MDM activation states

A recent study (3) defined a spectrum of macrophage activation/polarization states extending the M1/M2-model based on microarray data derived from MDMs exposed to an array of different stimuli (28 plus baseline). In an attempt to define the PPARβ/δ agonist-induced MDM phenotype more precisely we compared the L165,041-induced transcriptome to the 143 comparable microarray data sets provided by the quoted study (3), as outlined in Figure 8A. Toward this end, we first identified overlaps between the PPARβ/δ target gene set and the 49 modules representing coregulated gene sets as defined by Xue *et al.* (3). Five modules yielding P-value <0.001 by hypergeometric test were identified and further analyzed (modules 8, 15, 16, 21 and 43; Figure 8B). For each gene in the overlap between a module and the L165,041 regulated set, we determined the direction of regulation by L165,041 (as in Supplementary Table S2) and the 28 non-baseline stimuli. The heatmap in

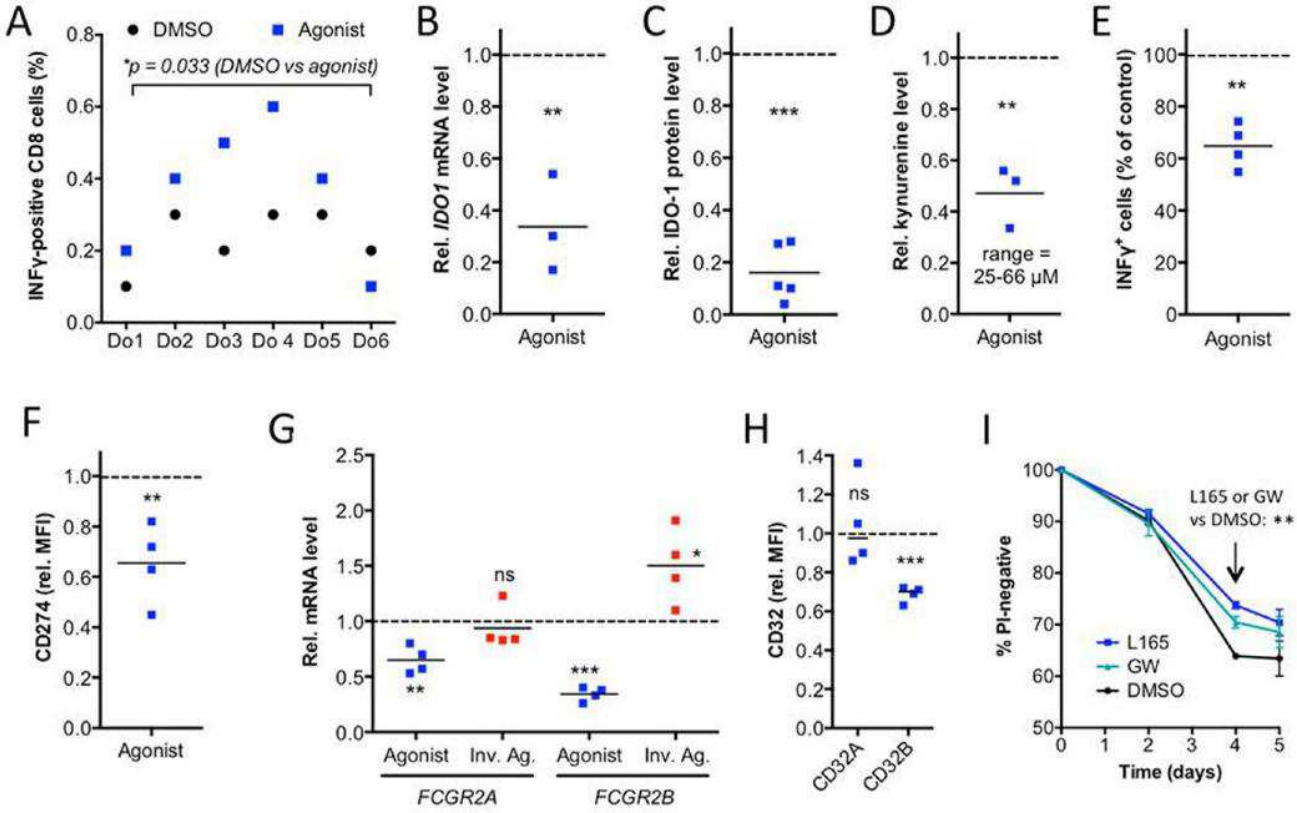

Figure 7. PPARβ/δ ligand-induced immune stimulatory alterations in human MDMs. (**A**) Effects of L165,041 on T cell activation by the recall antigen peptide mix CEFT. MDMs from six different donors differentiated in the presence of agonist or DMSO (solvent control) were analyzed for their ability to stimulate CEFT-peptide induced INFγ production by co-cultured autologous T cells. The fraction of $CD8^+IFN\gamma^+$ cells was determined by FACS. The experiment was performed with six independent donors (Do1–Do6) showing a CEFT-directed response. (**B**) RT-qPCR analysis of *IDO1* by L165,041 (24 h) in MDMs from three donors relative to DMSO control. Each dot represents the average of technical triplicates. (**C**) Quantitation of immunoblot analyses of IDO-1 protein expression in L165,041-treated (24 h) MDMs from five different donors relative to DMSO control. Blots are shown in Supplementary Figure S7. (**D**) Kynurenine production by MDMs from three different donors treated with L165,041 for 24 h relative to DMSO control. (**E**) Effect of L165,041 on polyclonal T cell activation relative to DMSO control (four different donors). (**F**) FACS analysis of CD274 expression on MDMs treated with L165,041 or solvent (DMSO) during differentiation (four different donors). (**G**) RT-qPCR analysis of *FCGR2A* and *FCGR2B* expression on MDMs treated with L165,041 or ST247 during differentiation relative to DMSO control (four donors as in (F)). (**H**) FACS analysis of CD32A and CD32B, conditions as in (F). (**I**) Effect of PPARβ/δ ligands on the time course of hypoxia-induced cell death. MDMs were cultured in XV0 medium at <1% oxygen for up to 5 days in the presence or absence of L165,041 or GW501516 and analyzed for propidium (PI) uptake by flow cytometry. Data represent the mean of three biological replicates with cells from different donors. Horizontal lines in panels (B–H) and error bars in panel (I) indicate the average.

Figure 8B represents gene subsets regulated in the same or opposite direction in red and blue, respectively. It is evident that for most stimulation conditions the five module-specific subsets show divergent directions of regulation. For instance, the classical inducers of alternative macrophage polarization (M2), IL-4 and IL-13, regulate genes in modules 15 and 43 in the same direction as L165,041, but in the opposite direction in module 16. Pro-inflammatory stimuli, like TNFα, IFNγ and LPS (stimulation conditions 10, 19–29), predominantly yield opposite patterns (modules 8 and 16), but also show a weak coordinate regulation within modules 15 and 43, consistent with a predominantly, but not exclusive anti-inflammatory effect exerted by L165,041. On the other hand, lipid-triggered (conditions 14–18) and agonist-induced patterns are similar in modules 15, 21 and 43. These data are in good agreement with our conclusion that PPARβ/δ induces a unique activation phenotype with components of anti-inflammatory, pro-inflammatory and fatty acid-mediated activation states.

Common and cell type-specific PPARβ/δ target genes

Finally, we compared the PPARβ/δ cistrome and the ligand-responsive transcriptome with those obtained with the human myofibroblastic cell line WPMY-1 (18) and the human breast cancer cell line MDA-MB-231 (19). The Venn diagrams in Figure 9A indicate a clear overlap of genes with PPARβ/δ binding sites in all three cell types ($n = 129$; Supplementary Table S7). Diseases and functions annotation revealed a statistically highly significant overlap with energy production and lipid metabolism ($P = 4.3 \times 10^{-9}$). In contrast, there was no inverse target gene common to all three cell types (Figure 9B). Our genomic studies in conjunction with the RT-qPCR analyses thus led to three conclusions: (i) a subgroup of canonical target genes are common target genes, including those with functions in intermediary metabolism (Figure 9A); (ii) another subgroup of canonical target genes are cell type-specific, such as *CD52* and *LRP5*, which are ligand-responsive only in MDMs (Supple-

mentary Figure S4 and Supplementary Table S2) compared to WPMY-1 and MDA-MB-231 cells (Figure 9C); and (iii) inverse target genes, such as *IDO1* and *IL8,* are not regulated in WPMY1 and MDA-MB-231 cells (Figure 9C) as opposed to the clear ligand regulation in MDMs (Figures 4E and 7B; Supplementary Table S2).

DISCUSSION

Our data show that PPARβ/δ target genes in normal macrophages (MDMs) fall into two major classes. The first class represents canonical genes with PPARβ/δ–RXR binding sites (PPREs), induced by agonists and repressed by inverse agonists. The second class is composed of genes lacking direct PPARβ/δ contact sites that are repressed by agonists, which we have termed inverse regulation. Importantly, inverse regulation was also seen in murine BMDMs for several target genes, and was impaired in cells with disrupted *Ppard* alleles, unequivocally demonstrating the dependence of non-canonical, ligand-mediated repression on functional PPARβ/δ. Clear evidence for the high selectivity of one of the ligands (GW501516) used in our study is also provided by published microarray data (36) obtained with differentiating murine BMCs, as depicted in the evaluation in Supplementary Figure S10.

Canonical and inverse target genes

A considerable fraction of canonical PPARβ/δ target genes have roles in lipid metabolism shared with other cell types. These include the known PPAR target genes with functions in fatty acid oxidation (*ACADVL, ACAA2, CAT, CPT1A, ECH1, PDK4, SLC25A20)* or other aspects of lipid metabolism (*ANGPTL4, FABP4, PLIN2*), but also genes not previously described as PPARβ/δ targets, such as *ETFDH* and *ISCA1*. Another large fraction of direct PPARβ/δ target genes are associated with non-metabolic functions, in particular immune regulation, such as *CD300A, CD52, LRP5, NLRC4* and *PHACTR1*, and most of these genes are cell type-selective with respect to agonist-mediated regulation.

In contrast, inverse target genes are almost exclusively regulated by PPARβ/δ ligands in a cell type-specific fashion, at least for the three cell types analyzed, i.e. macrophages, myofibroblastic cells and breast cancer cells. Consistent with this finding, a large fraction of these genes are associated with pro-inflammatory functions exerted by macrophages, including immune cell activation, migration, chemotaxis and cellular survival, exemplified by a number of cytokine and chemokine genes (e.g. *IL8, CCL24*). However, several inverse target genes have immune suppressive rather than pro-inflammatory functions, for example *IDO1*, *CD274* (PD-1L) and *CD32B*, which play essential roles in the inhibition of T cell activation. This data strongly suggested that the response to PPARβ/δ agonists is mainly anti-inflammatory, but also has immune stimulatory components.

Bioinformatic analyses showed that many of the inverse target genes are controlled by NFκB and STAT1 signaling pathways. This finding is consistent with the reported upregulation of inflammatory signaling through these pathways in adherent monocytic cells (49,50), which apparently is attenuated by PPARβ/δ agonists. PPARβ/δ has been reported to impinge on NFκB signaling by physically and/or functionally interacting with p65 in endothelial cells, cardiomyocytes, smooth muscle cells and keratinocytes (14,20,59,60) or though ERK1/2 signaling in adipocytes (22). However, in most cases the precise underlying mechanisms are not entirely clear. In mouse macrophages, a cell type selective mechanism involving the transcriptional repressor BCL-6 has been identified (23). BCL-6 is a repressor of NFκB target genes, which is sequestered by PPARβ/δ in the absence of PPARβ/δ agonists.

Our own data are consistent with the conclusion that PPARβ/δ agonists repress a subset of NFκB-regulated genes in macrophages, based on the observation that MG132 diminished the L165,041 effect on several NFκB target genes previously identified by ChIP-Seq in mouse macrophages (24). This effect of MG132 is presumably due to the inhibition of IκB degradation or a blockade of proteasome-dependent processing of p105 to p50 (53). Both effects would lead to the loss of regulation by NFκB and agonist-mediated regulation, as observed in our experiments, independent of a potential role of BCL-6 and/or other signaling pathways impinging on NFκB regulation. Obviously, proteasome inhibitors also target numerous other signaling pathways and transcription factors that might contribute to the observed effect, as exemplified by *IL8*, which has been suggested to be induced by proteasome inhibitors via reactive oxygen-mediated AP-1 activation (54).

The involvement of PPARβ/δ in modulating STAT activity is even less understood with all published evidence restricted to STAT3 (61–64). The identification of strongly regulated inverse target genes in the present study paves the way for addressing these open questions using individual genes as experimental models and for elucidating the mechanisms underlying the crosstalk between PPARβ/δ and pro-inflammatory signaling cascades.

Effects of PPARβ/δ agonists on inflammatory pathways

'Functional Annotation and Networks Analysis' indicated that inflammatory signaling is targeted by PPARβ/δ agonists at two different levels. First, several genes encoding pro-inflammatory cytokines (e.g. *IL8, IFNG*) and chemokines (e.g. *CCL3/MIP1A, CCL8/MCP2, CCL11/eotaxin, CCL13/MCP4*) are downregulated as inverse target genes with predicted anti-inflammatory effects. In addition, a few anti-inflammatory cytokine genes (e.g. *IL10, IL13*) are similarly affected, suggesting that agonist effects on immune cells are not exclusively inhibitory. Second, our RNA-Seq analyses identified several key components of NALP inflammasomes as novel PPARβ/δ targets (Figure 5C). These include the canonical target gene *NLR4C* and the inverse target genes *NLRP1*, *NLRP3* and *CASP5*. NLR family proteins act as a sensor of pathogenic signals and promotes inflammasome assembly, leading to caspase-1 activation and inflammatory cytokine (IL-1β, IL-18) production (65). *NLR4C* encoded CARD12 is activated by microbial proteinaceous ligands, while

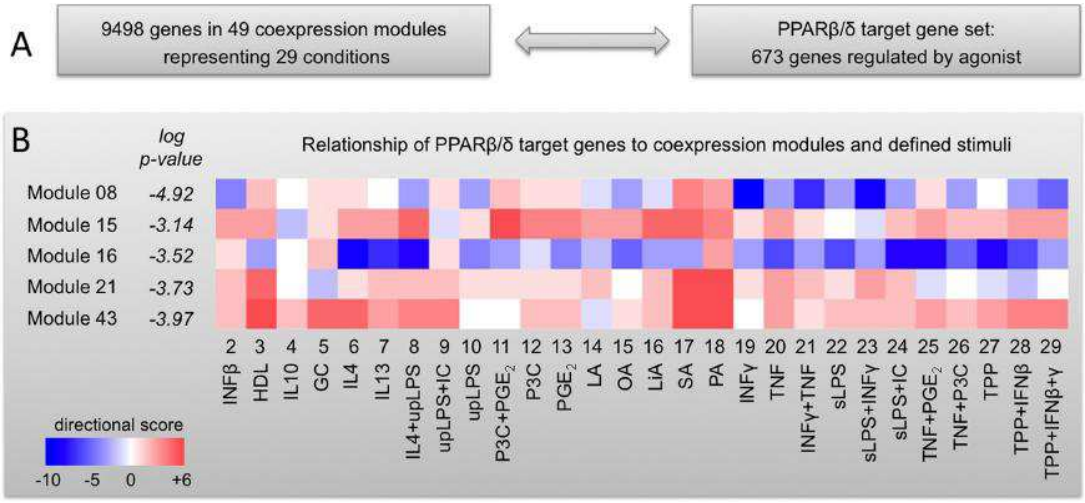

Figure 8. Comparison of the PPARβ/δ transcriptome with a spectrum of defined MDM activation states. (**A**) Scheme outlining the basis for the comparative analyses. (**B**) Relationship of PPARβ/δ target genes to expression data obtained with 29 different stimuli grouped into 49 coexpression modules (3). Overlaps between PPARβ/δ target genes and each module were determined by hypergeometric test. Modules yielding *P*-values <0.001 (modules 8, 15, 16, 21 and 43) were further analyzed by determining for each gene the direction of regulation by L165,041 (Supplementary Table S2) compared to all 29 stimuli (3). Results are displayed for each subset of genes (defined by specific stimulation conditions within individual modules) as a heatmap. The color code is based on a directional score reflecting the number of genes regulated in the same direction (red) or in opposite directions (blue; for details see the Materials and Methods section). GC, glucocorticoid; HDL, high density lipoprotein; IC, immune complexes; LA, lauric acid; LiA, linoleic acid; OA, oleic acid; P3C, Pam3CysSerLys4; PA, palmitic acid; SA, stearic acid; sLPS, standard lipopolysaccharide; TPP, TNFα+PGE_2+P3C; upLPS, ultrapure lipopolysaccharide.

NLRP1 recognizes muramyl dipeptide and diverse stimuli (e.g. crystalline material, peptide aggregates, bacterial toxins) can trigger NLRP3 activation (65). Non-canonical inflammasome activation by Gram-negative bacteria can involve the additional recruitment of caspase 5, encoded by another inverse PPARβ/δ target gene. Taken together, these findings indicate that PPARβ/δ agonists can have pro- and anti-inflammatory effects on specific inflammasome functions and suggest that the precise outcome is stimulus-dependent.

Our data confirm and extend a previous study identifying *CD300A* as a PPARβ/δ target gene in macrophage-like cells derived from the human leukemia cell line THP-1 (35). In mice, disruption of the *Cd300a* gene resulted in pro-inflammatory activation of peritoneal macrophages, identifying CD300a-mediated inhibitory signaling in macrophages as a critical regulator of intestinal immune homeostasis (35). *CD300E*, coding for an activating CD300 subtype, is repressed by L165,041 (Figure 5D) simultaneously with the induction of the inhibitory *CD300A* gene, consistent with an immunosuppressive agonist function via regulation of CD300 family members.

We also identified *PHACTR1* as a novel canonical PPARβ/δ target gene. This gene encodes phosphatase and actin regulator 1, which is involved in the G-actin mediated control of actomyosin assembly (66) and may thus play a role in modulating macrophage migration and phagocytosis. However, the agonist-mediated induction of *PHACTR1* appears to be inconsistent with the observed inhibition of phagocytosis/macropinocytosis of FITC-dextran, suggesting that other genes contribute to this effect. An example is *DIXDC1*, another canonical PPARβ/δ target gene implicated in cell migration by modulating the WNT and PI_3K signaling pathways (67,68).

Immune stimulatory effects of PPARβ/δ agonists

As shown by our functional studies, PPARβ/δ agonists stimulate CD8+ T cell activation. Based on our bioinformatic analyses at least two mechanisms may be involved in this effect, i.e. the IDO-1 mediated catabolism of tryptophan and synthesis of PD-1 ligand (CD274). The inhibitory effect of agonists on *CD274* and *IDO1* transcription resulted in a decreased expression of both proteins and synthesis of the IDO-1 product kynurenine. The latter is a known suppressor of T cell activation (55), which we confirmed for the concentrations achieved in our experimental system. Repression of *CD274* by PPARβ/δ agonist has previously also been described for human myofibroblastic cells (69), emphasizing the potential relevance of this regulatory effect of PPARβ/δ. *CD274*/PD-L1 engagement of the PD-1 receptor on T cells activates a key checkpoint restraining T cell activation (56), which constitutes a key component of immune suppression in the tumor microenvironment. We also found several genes with functions in antigen presentation to be modulated by PPARβ/δ agonists. Whether these changes play a role in the observed stimulation of T cell activation remains to be investigated.

Pro-survival effects of PPARβ/δ agonists

Another clear biological effect of PPARβ/δ agonists is the suppression of macrophage cell death under hypoxia, which is frequently associated with inflammation (70) and imposes environmental stress on the resident inflammatory

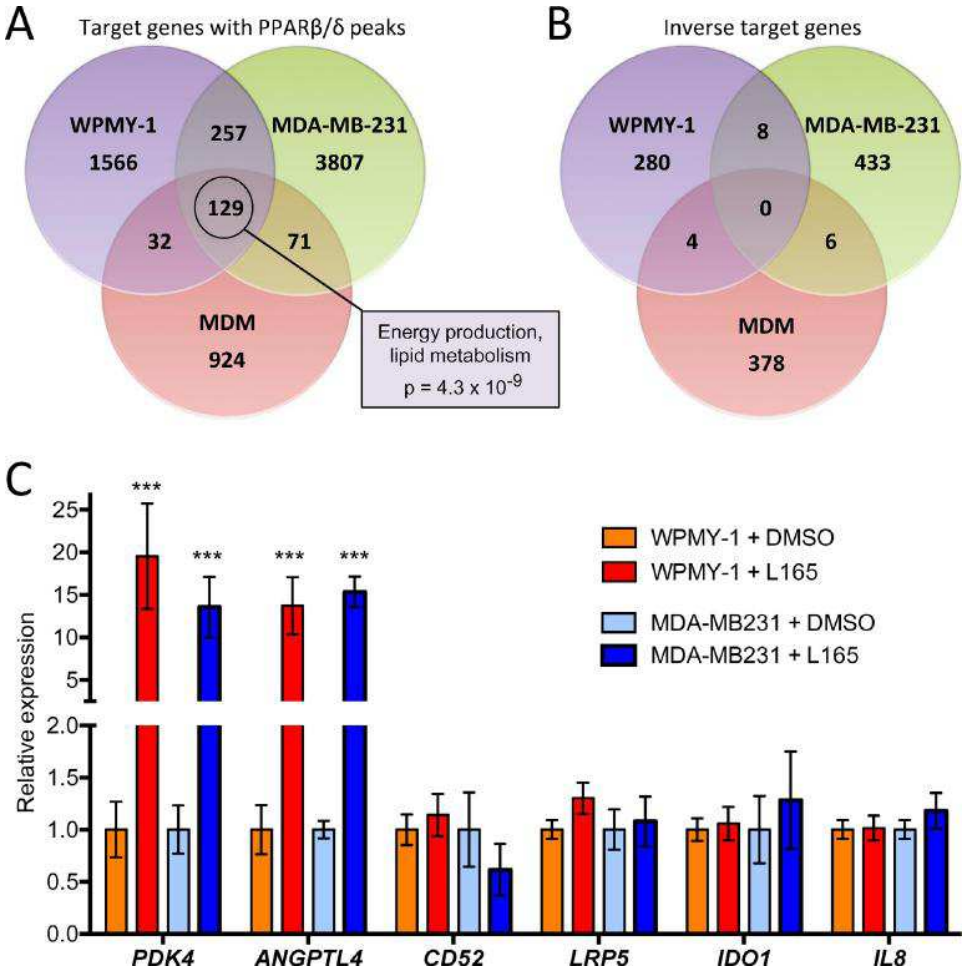

Figure 9. Identification of common and cell type-specific PPARβ/δ target genes. **(A)** Overlap of PPARβ/δ binding sites in WPMY-1 myofibroblast-like cells, MDA-MB-231 breast cancer cells and MDMs. Common target genes (n = 129) were analyzed by IPA *Diseases and Functions Annotation*. The box shows the top term by p-value of overlap. **(B)** Overlap of agonist-repressed genes. **(C)** RT-qPCR validation of common and macrophage-specific PPARβ/δ target genes in WPMY-1 and MDA-MB-231 cells. Values were normalized to 1 for untreated cells (solvent only) individually for each gene and cell line. Statistical significance was tested relative to DMSO-treated cells.

cells. This biological effect of PPARβ/δ agonists is mirrored by the observed changes in gene expression. Thus, several transcription factor genes with death promoting functions (e.g. *ID3* and *MYC*) are downregulated by agonists, while genes with pro-survival effects are upregulated (e.g. *EGR3* and *VDR*). Our functional annotation analyses also showed a strong overlap of PPARβ/δ target genes associated with the inhibition of inflammation and cell survival, suggesting a functional link. This group indeed harbors a number of inverse target genes with both pro-inflammatory and death-promoting functions, for example the cytokines TNFα and IL-1β. In these cases, the downregulation of the same genes by PPARβ/δ agonist may thus contribute to both an attenuation of the inflammatory response and a promotion of cell survival.

A specific macrophage activation state induced by PPARβ/δ agonists

The bioinformatic analyses and biological data described above clearly indicate that PPARβ/δ agonists have a predominantly, but not exclusively, anti-inflammatory effect on MDMs. A recent study (3) reporting the transcriptomes for MDMs exposed to 28 different stimuli provided a resource to characterize the phenotype of agonist-stimulated MDMs in further detail. The authors used these data to define 49 modules of coregulated genes and determined the extent to which each of these modules was associated with the different stimulation conditions, resulting in the development of a spectrum model of macrophage activation. Comparison of these modules with the transcriptomes of L165,041-stimulated cells unraveled highly significant overlaps with activation states triggered by IL-4/IL13, TNFα/INFγ and fatty acids. These observations clearly confirm the hypothesis that PPARβ/δ induces a unique activation phenotype with components of anti-inflammatory, immune stimulatory and lipid-triggered activation states.

CONCLUSIONS

Numerous literature reports have documented an anti-inflammatory effect of PPARβ/δ agonists with few dis-

crepant findings. However, the molecular mechanisms underlying the regulation of immune cells by PPARβ/δ are only partially understood. In the present study, we have determined the PPARβ/δ transcriptome and PPARβ/δ-RXR cistrome in human MDMs to establish the global PPARβ/δ-regulated signaling network in human macrophages. This study showed that genes with immune regulatory functions are regulated by PPARβ/δ agonists in a macrophage-selective fashion by at least two mechanisms: (i) canonical regulation, analogous to ubiquitous PPARβ/δ target genes with metabolic functions, which involves transcriptional induction by agonists and direct DNA contacts of PPARβ/δ-RXR heterodimers, and (ii) repression by agonists (inverse regulation) in the absence of PPARβ/δ DNA binding. The latter mechanism affects to a large extent NFκB and STAT1 target genes, resulting in the inhibition of multiple pro-inflammatory mediators in line with the known anti-inflammatory effect of PPARβ/δ activation. However, consistent with the results of different bioinformatic approaches, we also identified specific immune stimulatory effects exerted by PPARβ/δ agonists. Besides a pro-survival effect on macrophages and inhibition of CD32B surface expression, the most prominent example in this context is the stimulation of T cell activation. The latter is presumably linked to the repression of the *CD274* and *IDO1* genes, resulting in a diminished surface expression of PD-1 ligand and a decreased production of the immune suppressive kynurenine. Consistent with these observations, the PPARβ/δ agonist-regulated transcriptome shows a significant overlap with coexpression modules triggered by either the anti-inflammatory IL-4 and IL-13 cytokines or the pro-inflammatory mediators TNFα and IFNγ. These findings clearly indicate that PPARβ/δ agonists induce a novel and unique macrophage activation state with strong anti-inflammatory but also specific immune stimulatory components. Collectively, these findings suggest that contrary to the prevailing opinion PPARβ/δ exerts context-dependent rather than merely inhibitory functions in immune regulation.

It is obviously of great interest to analyze the effects of PPARβ/δ ligands on macrophages in the context of other immune cells *in vivo*. However, the identification of a mouse model suitable to recapitulate the global role of PPARβ/δ in the human immune system is associated with problems that cannot easily be solved, if at all. Thus, as suggested by our own data obtained with murine BMCs, murine BMDMs and human MDMs, the effect of PPARβ/δ ligands on the transcriptome of myeloid cells appears to be influenced by their differentiation and/or activation state, and perhaps also by species-specific effects. This suggests that data obtained with human MDMs may not be easily transferable to a mouse model. Testing the relevance of our findings in a physiological setting therefore remains a major challenge of future studies.

ACCESSION NUMBERS

RNA-Seq and ChIP-Seq data sets have been deposited at EBI ArrayExpress under accession numbers E-MTAB-3114 and E-MTAB-3113, respectively.

SUPPLEMENTARY DATA

Supplementary Data are available at NAR Online.

ACKNOWLEDGEMENTS

We are grateful to Dr Robert Geffers (Helmholtz-Zentrum für Infektionsforschung, Braunschweig, Germany) for valuable discussions on ChIP-Seq library synthesis. We thank Margitta Alt, Traute Plaum and Achim Allmeroth for expert technical assistance.

FUNDING

The Deutsche Forschungsgemeinschaft [MU601/13 to R.M.]; the Wilhelm-Sander-Stiftung [to S.M.B. and S.R.]; the Universitätsklinikum Giessen-Marburg [to T.A. and S.R.].
Conflict of interest statement. None declared.

REFERENCES

1. Sica,A. and Mantovani,A. (2012) Macrophage plasticity and polarization: in vivo veritas. *J. Clin. Invest.*, **122**, 787–795.
2. Martinez,F.O. and Gordon,S. (2014) The M1 and M2 paradigm of macrophage activation: time for reassessment. *F1000Prime Rep.*, **6**, 13.
3. Xue,J., Schmidt,S.V., Sander,J., Draffehn,A., Krebs,W., Quester,I., De Nardo,D., Gohel,T.D., Emde,M., Schmidleithner,L. *et al.* (2014) Transcriptome-based network analysis reveals a spectrum model of human macrophage activation. *Immunity*, **40**, 274–288.
4. Kostadinova,R., Wahli,W. and Michalik,L. (2005) PPARs in diseases: control mechanisms of inflammation. *Curr. Med. Chem.*, **12**, 2995–3009.
5. Yang,Y., Lovett-Racke,A.E. and Racke,M.K. (2010) Regulation of immune responses and autoimmune encephalomyelitis by PPARs. *PPAR Res.*, **2010**, 104705.
6. Wahli,W. and Michalik,L. (2012) PPARs at the crossroads of lipid signaling and inflammation. *Trends Endocrinol. Metab.*, **23**, 351–363.
7. Michalik,L. and Wahli,W. (2008) PPARs mediate lipid signaling in inflammation and cancer. *PPAR Res.*, **2008**, 134059.
8. Peters,J.M., Lee,S.S., Li,W., Ward,J.M., Gavrilova,O., Everett,C., Reitman,M.L., Hudson,L.D. and Gonzalez,F.J. (2000) Growth, adipose, brain, and skin alterations resulting from targeted disruption of the mouse peroxisome proliferator-activated receptor beta(delta). *Mol. Cell. Biol.*, **20**, 5119–5128.
9. Chong,H.C., Tan,M.J., Philippe,V., Tan,S.H., Tan,C.K., Ku,C.W., Goh,Y.Y., Wahli,W., Michalik,L. and Tan,N.S. (2009) Regulation of epithelial-mesenchymal IL-1 signaling by PPARbeta/delta is essential for skin homeostasis and wound healing. *J. Cell Biol.*, **184**, 817–831.
10. Bassaganya-Riera,J., DiGuardo,M., Climent,M., Vives,C., Carbo,A., Jouni,Z.E., Einerhand,A.W., O'Shea,M. and Hontecillas,R. (2011) Activation of PPARgamma and delta by dietary punicic acid ameliorates intestinal inflammation in mice. *Br. J. Nutr.*, **106**, 878–886.
11. Kanakasabai,S., Chearwae,W., Walline,C.C., Iams,W., Adams,S.M. and Bright,J.J. (2010) Peroxisome proliferator-activated receptor delta agonists inhibit T helper type 1 (Th1) and Th17 responses in experimental allergic encephalomyelitis. *Immunology*, **130**, 572–588.
12. Kang,K., Reilly,S.M., Karabacak,V., Gangl,M.R., Fitzgerald,K., Hatano,B. and Lee,C.H. (2008) Adipocyte-derived Th2 cytokines and myeloid PPARdelta regulate macrophage polarization and insulin sensitivity. *Cell Metab.*, **7**, 485–495.
13. Odegaard,J.I., Ricardo-Gonzalez,R.R., Red Eagle,A., Vats,D., Morel,C.R., Goforth,M.H., Subramanian,V., Mukundan,L., Ferrante,A.W. and Chawla,A. (2008) Alternative M2 activation of Kupffer cells by PPARdelta ameliorates obesity-induced insulin resistance. *Cell Metab.*, **7**, 496–507.
14. Westergaard,M., Henningsen,J., Johansen,C., Rasmussen,S., Svendsen,M.L., Jensen,U.B., Schroder,H.D., Staels,B., Iversen,L., Bolund,L. *et al.* (2003) Expression and localization of peroxisome

proliferator-activated receptors and nuclear factor kappaB in normal and lesional psoriatic skin. *J. Invest. Dermatol.*, **121**, 1104–1117.
15. Romanowska,M., Reilly,L., Palmer,C.N., Gustafsson,M.C. and Foerster,J. (2010) Activation of PPARbeta/delta causes a psoriasis-like skin disease in vivo. *PLoS One*, **5**, e9701.
16. Hack,K., Reilly,L., Palmer,C., Read,K.D., Norval,S., Kime,R., Booth,K. and Foerster,J. (2012) Skin-targeted inhibition of PPAR beta/delta by selective antagonists to treat PPAR beta/delta - mediated psoriasis-like skin sisease in vivo. *PLoS One*, **7**, e37097.
17. Peters,J.M., Shah,Y.M. and Gonzalez,F.J. (2012) The role of peroxisome proliferator-activated receptors in carcinogenesis and chemoprevention. *Nat. Rev. Cancer*, **12**, 181–195.
18. Adhikary,T., Kaddatz,K., Finkernagel,F., Schönbauer,A., Meissner,W., Scharfe,M., Jarek,M., Blöcker,H., Müller-Brüsselbach,S. and Müller,R. (2011) Genomewide analyses define different modes of transcriptional regulation by peroxisome proliferator-activated receptor-beta/delta (PPARbeta/delta). *PLoS One*, **6**, e16344.
19. Adhikary,T., Brandt,D.T., Kaddatz,K., Stockert,J., Naruhn,S., Meissner,W., Finkernagel,F., Obert,J., Lieber,S., Scharfe,M. *et al.* (2013) Inverse PPARbeta/delta agonists suppress oncogenic signaling to the ANGPTL4 gene and inhibit cancer cell invasion. *Oncogene*, **32**, 5241–5252.
20. Planavila,A., Rodriguez-Calvo,R., Jove,M., Michalik,L., Wahli,W., Laguna,J.C. and Vazquez-Carrera,M. (2005) Peroxisome proliferator-activated receptor beta/delta activation inhibits hypertrophy in neonatal rat cardiomyocytes. *Cardiovasc. Res.*, **65**, 832–841.
21. Stockert,J., Wolf,A., Kaddatz,K., Schnitzer,E., Finkernagel,F., Meissner,W., Müller-Brüsselbach,S., Kracht,M. and Müller,R. (2013) Regulation of TAK1/TAB1-mediated IL-1beta signaling by cytoplasmic PPARbeta/delta. *PLoS One*, **8**, e63011.
22. Rodriguez-Calvo,R., Serrano,L., Coll,T., Moullan,N., Sanchez,R.M., Merlos,M., Palomer,X., Laguna,J.C., Michalik,L., Wahli,W. *et al.* (2008) Activation of peroxisome proliferator-activated receptor beta/delta inhibits lipopolysaccharide-induced cytokine production in adipocytes by lowering nuclear factor-kappaB activity via extracellular signal-related kinase 1/2. *Diabetes*, **57**, 2149–2157.
23. Lee,C.H., Chawla,A., Urbiztondo,N., Liao,D., Boisvert,W.A., Evans,R.M. and Curtiss,L.K. (2003) Transcriptional repression of atherogenic inflammation: modulation by PPARdelta. *Science*, **302**, 453–457.
24. Barish,G.D., Yu,R.T., Karunasiri,M., Ocampo,C.B., Dixon,J., Benner,C., Dent,A.L., Tangirala,R.K. and Evans,R.M. (2010) Bcl-6 and NF-kappaB cistromes mediate opposing regulation of the innate immune response. *Genes Dev.*, **24**, 2760–2765.
25. Xu,H.E., Lambert,M.H., Montana,V.G., Parks,D.J., Blanchard,S.G., Brown,P.J., Sternbach,D.D., Lehmann,J.M., Wisely,G.B., Willson,T.M. *et al.* (1999) Molecular recognition of fatty acids by peroxisome proliferator-activated receptors. *Mol. Cell*, **3**, 397–403.
26. Naruhn,S., Meissner,W., Adhikary,T., Kaddatz,K., Klein,T., Watzer,B., Müller-Brüsselbach,S. and Müller,R. (2010) 15-hydroxyeicosatetraenoic acid is a preferential peroxisome proliferator-activated receptor β/δ agonist. *Mol. Pharmacol.*, **77**, 171–184.
27. Lim,H., Gupta,R.A., Ma,W.G., Paria,B.C., Moller,D.E., Morrow,J.D., DuBois,R.N., Trzaskos,J.M. and Dey,S.K. (1999) Cyclo-oxygenase-2-derived prostacyclin mediates embryo implantation in the mouse via PPARdelta. *Genes Dev.*, **13**, 1561–1574.
28. Fauti,T., Müller-Brüsselbach,S., Kreutzer,M., Rieck,M., Meissner,W., Rapp,U., Schweer,H., Kömhoff,M. and Müller,R. (2006) Induction of PPARbeta and prostacyclin (PGI2) synthesis by Raf signaling: failure of PGI2 to activate PPARbeta. *FEBS J.*, **273**, 170–179.
29. Rao,G.H., Reddy,K.R., Hagert,K. and White,J.G. (1980) Influence of pH on the prostacyclin (PGI2) mediated inhibition of platelet function. *Prostaglandins Med.*, **4**, 263–273.
30. Billin,A.N. (2008) PPAR-beta/delta agonists for Type 2 diabetes and dyslipidemia: an adopted orphan still looking for a home. *Expert Opin. Investig. Drugs*, **17**, 1465–1471.
31. Peraza,M.A., Burdick,A.D., Marin,H.E., Gonzalez,F.J. and Peters,J.M. (2006) The toxicology of ligands for peroxisome proliferator-activated receptors (PPAR). *Toxicol. Sci.*, **90**, 269–295.
32. Shearer,B.G., Steger,D.J., Way,J.M., Stanley,T.B., Lobe,D.C., Grillot,D.A., Iannone,M.A., Lazar,M.A., Willson,T.M. and Billin,A.N. (2008) Identification and characterization of a selective peroxisome proliferator-activated receptor beta/delta (NR1C2) antagonist. *Mol. Endocrinol.*, **22**, 523–529.
33. Naruhn,S., Toth,P.M., Adhikary,T., Kaddatz,K., Pape,V., Dörr,S., Klebe,G., Müller-Brüsselbach,S., Diederich,W.E. and Müller,R. (2011) High-affinity peroxisome proliferator-activated receptor beta/delta-specific ligands with pure antagonistic or inverse agonistic properties. *Mol. Pharmacol.*, **80**, 828–838.
34. Toth,P.M., Naruhn,S., Pape,V.F., Dörr,S.M., Klebe,G., Müller,R. and Diederich,W.E. (2012) Development of improved PPARbeta/delta inhibitors. *ChemMedChem*, **7**, 159–170.
35. Tanaka,T., Tahara-Hanaoka,S., Nabekura,T., Ikeda,K., Jiang,S., Tsutsumi,S., Inagaki,T., Magoori,K., Higurashi,T., Takahashi,H. *et al.* (2014) PPARbeta/delta activation of CD300a controls intestinal immunity. *Sci. Rep.*, **4**, 5412.
36. Lieber,S., Scheer,F., Finkernagel,F., Meissner,W., Giehl,G., Brendel,C., Diederich,W.E., Muller-Brusselbach,S. and Muller,R. (2015) The inverse agonist DG172 triggers a PPARbeta/delta-independent myeloid lineage shift and promotes GM-CSF/IL-4-induced dendritic cell differentiation. *Mol. Pharmacol.*, **87**, 162–173.
37. Reinartz,S., Schumann,T., Finkernagel,F., Wortmann,A., Jansen,J.M., Meissner,W., Krause,M., Schworer,A.M., Wagner,U., Muller-Brusselbach,S. *et al.* (2014) Mixed-polarization phenotype of ascites-associated macrophages in human ovarian carcinoma: Correlation of CD163 expression, cytokine levels and early relapse. *Int. J. Cancer*, **134**, 32–42.
38. Braun,D., Longman,R.S. and Albert,M.L. (2005) A two-step induction of indoleamine 2,3 dioxygenase (IDO) activity during dendritic-cell maturation. *Blood*, **106**, 2375–2381.
39. Liao,Y., Smyth,G.K. and Shi,W. (2013) The Subread aligner: fast, accurate and scalable read mapping by seed-and-vote. *Nucleic Acids Res.*, **41**, e108.
40. Dobin,A., Davis,C.A., Schlesinger,F., Drenkow,J., Zaleski,C., Jha,S., Batut,P., Chaisson,M. and Gingeras,T.R. (2013) STAR: ultrafast universal RNA-seq aligner. *Bioinformatics*, **29**, 15–21.
41. Satoh,J. and Tabunoki,H. (2013) A comprehensive profile of ChIP-Seq-based STAT1 target genes suggests the complexity of STAT1-mediated gene regulatory mechanisms. *Gene Regul. Syst. Bio.*, **7**, 41–56.
42. Hutchins,A.P., Poulain,S. and Miranda-Saavedra,D. (2012) Genome-wide analysis of STAT3 binding in vivo predicts effectors of the anti-inflammatory response in macrophages. *Blood*, **119**, e110–e119.
43. Ghisletti,S., Barozzi,I., Mietton,F., Polletti,S., De Santa,F., Venturini,E., Gregory,L., Lonie,L., Chew,A., Wei,C.L. *et al.* (2010) Identification and characterization of enhancers controlling the inflammatory gene expression program in macrophages. *Immunity*, **32**, 317–328.
44. Haskill,S., Johnson,C., Eierman,D., Becker,S. and Warren,K. (1988) Adherence induces selective mRNA expression of monocyte mediators and proto-oncogenes. *J. Immunol.*, **140**, 1690–1694.
45. Sporn,S.A., Eierman,D.F., Johnson,C.E., Morris,J., Martin,G., Ladner,M. and Haskill,S. (1990) Monocyte adherence results in selective induction of novel genes sharing homology with mediators of inflammation and tissue repair. *J. Immunol.*, **144**, 4434–4441.
46. Kelley,J.L., Rozek,M.M., Suenram,C.A. and Schwartz,C.J. (1987) Activation of human blood monocytes by adherence to tissue culture plastic surfaces. *Exp. Mol. Pathol.*, **46**, 266–278.
47. Fuhlbrigge,R.C., Chaplin,D.D., Kiely,J.M. and Unanue,E.R. (1987) Regulation of interleukin 1 gene expression by adherence and lipopolysaccharide. *J. Immunol.*, **138**, 3799–3802.
48. Eierman,D.F., Johnson,C.E. and Haskill,J.S. (1989) Human monocyte inflammatory mediator gene expression is selectively regulated by adherence substrates. *J. Immunol.*, **142**, 1970–1976.
49. Coccia,E.M., Del Russo,N., Stellacci,E., Testa,U., Marziali,G. and Battistini,A. (1999) STAT1 activation during monocyte to macrophage maturation: role of adhesion molecules. *Int. Immunol.*, **11**, 1075–1083.
50. Rosales,C. and Juliano,R. (1996) Integrin signaling to NF-kappa B in monocytic leukemia cells is blocked by activated oncogenes. *Cancer Res.*, **56**, 2302–2305.

51. Mandard,S., Zandbergen,F., Tan,N.S., Escher,P., Patsouris,D., Koenig,W., Kleemann,R., Bakker,A., Veenman,F., Wahli,W. *et al.* (2004) The direct peroxisome proliferator-activated receptor target fasting-induced adipose factor (FIAF/PGAR/ANGPTL4) is present in blood plasma as a truncated protein that is increased by fenofibrate treatment. *J. Biol. Chem.*, **279**, 34411–34420.
52. Bours,V., Franzoso,G., Azarenko,V., Park,S., Kanno,T., Brown,K. and Siebenlist,U. (1993) The oncoprotein Bcl-3 directly transactivates through kappa B motifs via association with DNA-binding p50B homodimers. *Cell*, **72**, 729–739.
53. Palombella,V.J., Rando,O.J., Goldberg,A.L. and Maniatis,T. (1994) The ubiquitin-proteasome pathway is required for processing the NF-kappa B1 precursor protein and the activation of NF-kappa B. *Cell*, **78**, 773–785.
54. Wu,H.M., Wen,H.C. and Lin,W.W. (2002) Proteasome inhibitors stimulate interleukin-8 expression via Ras and apoptosis signal-regulating kinase-dependent extracellular signal-related kinase and c-Jun N-terminal kinase activation. *Am. J. Respir. Cell Mol. Biol.*, **27**, 234–243.
55. Munn,D.H. and Mellor,A.L. (2013) Indoleamine 2,3 dioxygenase and metabolic control of immune responses. *Trends Immunol.*, **34**, 137–143.
56. Francisco,L.M., Sage,P.T. and Sharpe,A.H. (2010) The PD-1 pathway in tolerance and autoimmunity. *Immunol. Rev.*, **236**, 219–242.
57. Silk,J.D., Salio,M., Brown,J., Jones,E.Y. and Cerundolo,V. (2008) Structural and functional aspects of lipid binding by CD1 molecules. *Annu. Rev. Cell Dev. Biol.*, **24**, 369–395.
58. Guilliams,M., Bruhns,P., Saeys,Y., Hammad,H. and Lambrecht,B.N. (2014) The function of Fcgamma receptors in dendritic cells and macrophages. *Nat. Rev. Immunol.*, **14**, 94–108.
59. Rival,Y., Beneteau,N., Taillandier,T., Pezet,M., Dupont-Passelaigue,E., Patoiseau,J.F., Junquero,D., Colpaert,F.C. and Delhon,A. (2002) PPARalpha and PPARdelta activators inhibit cytokine-induced nuclear translocation of NF-kappaB and expression of VCAM-1 in EAhy926 endothelial cells. *Eur. J. Pharmacol.*, **435**, 143–151.
60. Ding,G., Cheng,L., Qin,Q., Frontin,S. and Yang,Q. (2006) PPARdelta modulates lipopolysaccharide-induced TNFalpha inflammation signaling in cultured cardiomyocytes. *J. Mol. Cell. Cardiol.*, **40**, 821–828.
61. Wang,L.H., Yang,X.Y., Zhang,X., Huang,J., Hou,J., Li,J., Xiong,H., Mihalic,K., Zhu,H., Xiao,W. *et al.* (2004) Transcriptional inactivation of STAT3 by PPARgamma suppresses IL-6-responsive multiple myeloma cells. *Immunity*, **20**, 205–218.
62. Kino,T., Rice,K.C. and Chrousos,G.P. (2007) The PPARdelta agonist GW501516 suppresses interleukin-6-mediated hepatocyte acute phase reaction via STAT3 inhibition. *Eur. J. Clin. Invest.*, **37**, 425–433.
63. Serrano-Marco,L., Barroso,E., El Kochairi,I., Palomer,X., Michalik,L., Wahli,W. and Vazquez-Carrera,M. (2011) The peroxisome proliferator-activated receptor (PPAR) beta/delta agonist GW501516 inhibits IL-6-induced signal transducer and activator of transcription 3 (STAT3) activation and insulin resistance in human liver cells. *Diabetologia*, **55**, 743–751.
64. Serrano-Marco,L., Rodriguez-Calvo,R., El Kochairi,I., Palomer,X., Michalik,L., Wahli,W. and Vazquez-Carrera,M. (2011) Activation of peroxisome proliferator-activated receptor-beta/-delta (PPAR-beta/-delta) ameliorates insulin signaling and reduces SOCS3 levels by inhibiting STAT3 in interleukin-6-stimulated adipocytes. *Diabetes*, **60**, 1990–1999.
65. Latz,E., Xiao,T.S. and Stutz,A. (2013) Activation and regulation of the inflammasomes. *Nat. Rev. Immunol.*, **13**, 397–411.
66. Wiezlak,M., Diring,J., Abella,J., Mouilleron,S., Way,M., McDonald,N.Q. and Treisman,R. (2012) G-actin regulates the shuttling and PP1 binding of the RPEL protein Phactr1 to control actomyosin assembly. *J. Cell Sci.*, **125**, 5860–5872.
67. Singh,K.K., Ge,X., Mao,Y., Drane,L., Meletis,K., Samuels,B.A. and Tsai,L.H. (2010) Dixdc1 is a critical regulator of DISC1 and embryonic cortical development. *Neuron*, **67**, 33–48.
68. Xu,Z., Liu,D., Fan,C., Luan,L., Zhang,X. and Wang,E. (2014) DIXDC1 increases the invasion and migration ability of non-small-cell lung cancer cells via the PI3K-AKT/AP-1 pathway. *Mol. Carcinog.*, **53**, 917–925.
69. Stockert,J., Adhikary,T., Kaddatz,K., Finkernagel,F., Meissner,W., Müller-Brüsselbach,S. and Müller,R. (2011) Reverse crosstalk of TGFβ and PPARβ/δ signaling identified by transcriptional profiling. *Nucleic Acids Res.*, **39**, 119–131.
70. Eltzschig,H.K. and Carmeliet,P. (2011) Hypoxia and inflammation. *N. Engl. J. Med.*, **364**, 656–665.

Supplementary Figures

The transcriptional PPARβ/δ network in human macrophages defines a unique agonist-induced activation state

Till Adhikary[1] , Annika Wortmann[1] , Tim Schumann[1] , Florian Finkernagel[1], Sonja Lieber[1], Katrin Roth[2], Philipp M. Toth[3], Wibke E. Diederich[3], Andrea Nist[4], Thorsten Stiewe[4], Lara Kleinesudeik[5], Silke Reinartz[5], Sabine Müller-Brüsselbach[1] and Rolf Müller[1]*

[1] Institute of Molecular Biology and Tumor Research (IMT), [2] Cellular Imaging Core Facility, [3] Institute of Pharmaceutical Chemistry, [4] Genomics Core Facility, [5] Clinic for Gynecology, Gynecological Oncology and Gynecological Endocrinology; Center for Tumor Biology and Immunology (ZTI), Philipps University, 35043 Marburg, Germany

The first 4 authors should be regarded as joint First Authors

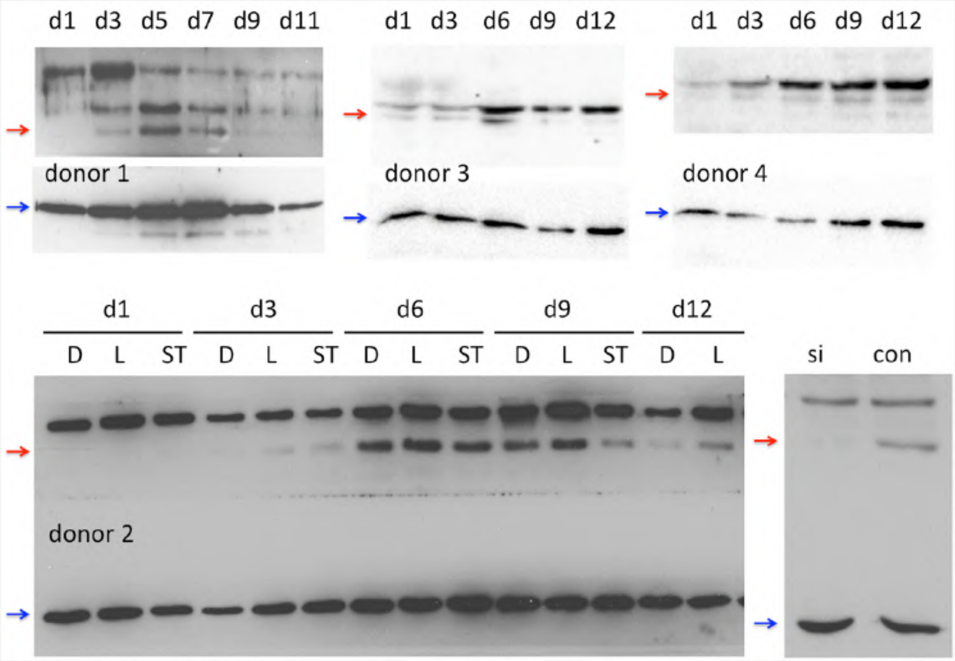

Figure S1 – Immunoblot analysis of PPARβ/δ expression during MDM differentiation. The blot shows the data for cells from four different donors used for the quantification in Figure 1B. Red arrows: PPARβ/δ bands, identified by siRNA-mediated knockdown (bottom right blot). Blue arrows: lactate dehydrogenase (LDH; loading control). PPARβ/δ bands were quantified (ChemiDoc MP) and adjusted to LDH band intensities(Figure 1B). The immunoblot of donor 2 MDMs shows that the agonist L165,041 (L) and the inverse agonist ST247 (ST) have no effect on PPARβ/δ protein expression.

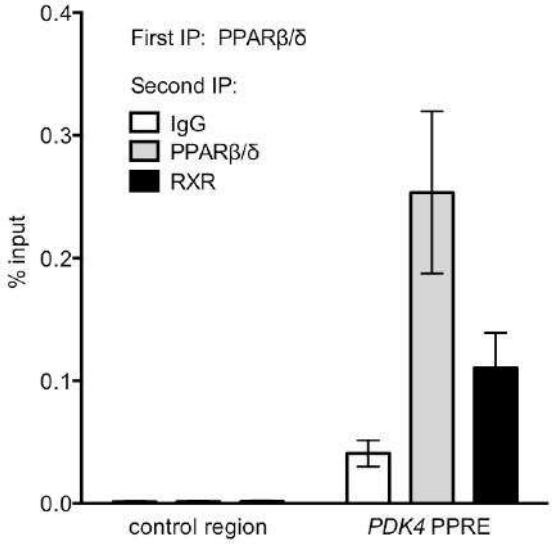

Figure S2 – Re-ChIP analysis of PPARβ/δ-RXR complexes at the *PDK4* enhancer in MDMs. After differentiation for 7 days, MDMs (sample size = 5) were fixed with formaldehyde, and sequential ChIP (ChIP re-ChIP) was carried out with sc-7197 anti-PPARβ/δ (Santa Cruz), sc-553 anti-RXR (Santa Cruz) or rabbit IgG I5006 (Sigma-Aldrich). For re-ChIP, chromatin complexes were eluted with 50 µl of 1X TE containing 2% SDS, 15 mM DTT and protease inhibitors for 30 min at at 37 °C with agitation. After centrifugation, the supernatant was diluted 30X with dilution buffer (50 mM Tris pH 8.0, 200 mM NaCl, 5 mM EDTA, 0.5% NP40). The second round of IPs was carried out as described in the Methods section. DNA was analyzed by qPCR with primers for the *PDK4* upstream enhancer and an irrelevant control region as in Figure 1D. The control primers had the following sequences: AAGGGATTTCCCCAGCAG (forward); GAAATAGCAGGGACCTCGTG (reverse).

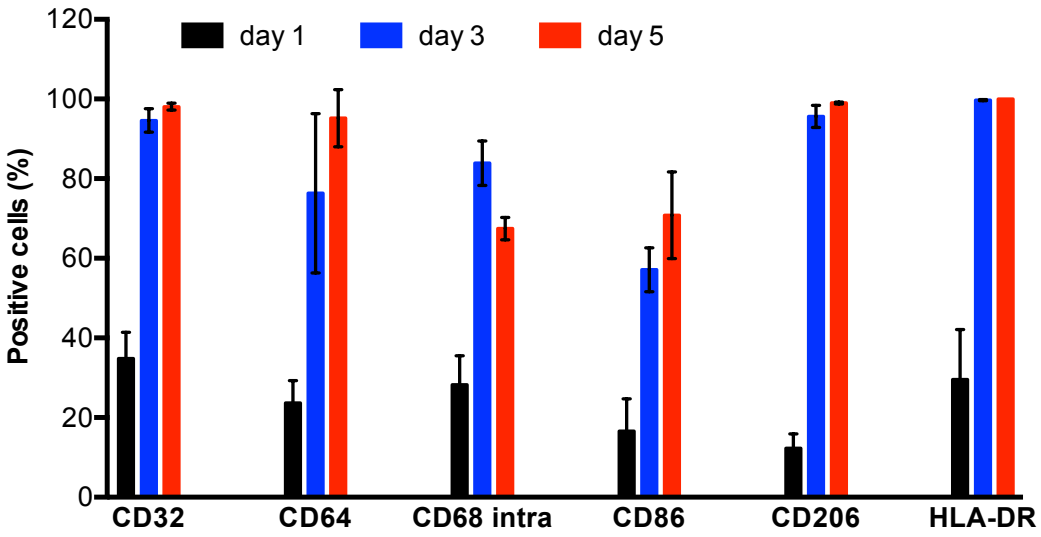

Figure S3 – Expression of the macrophage surface markers CD32, CD64, CD86, CD206 and HLA-DR and intracellular CD68 on differentiating MDMs (biological replicates with cells from 3 different donors; experimental setup as in Figure 1). Staining and FACS analysis were performed as described in Materials and Methods.

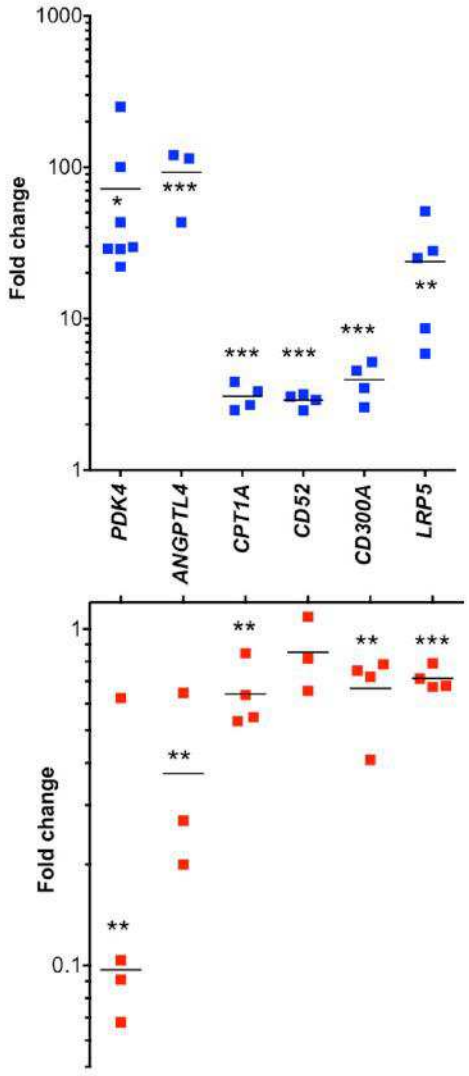

Figure S4 – RT-qPCR analysis of target gene regulation by L165,041 (agonist; blue dots) and ST247 (inverse agonist; red dots). Each dot represents a biological replicate with cells from a different donor (n = 4-9). Horizontal lines indicate the median. *P<0.05; **P<0.01; ***P<0.001 by t-test relative to DMSO-treated cells

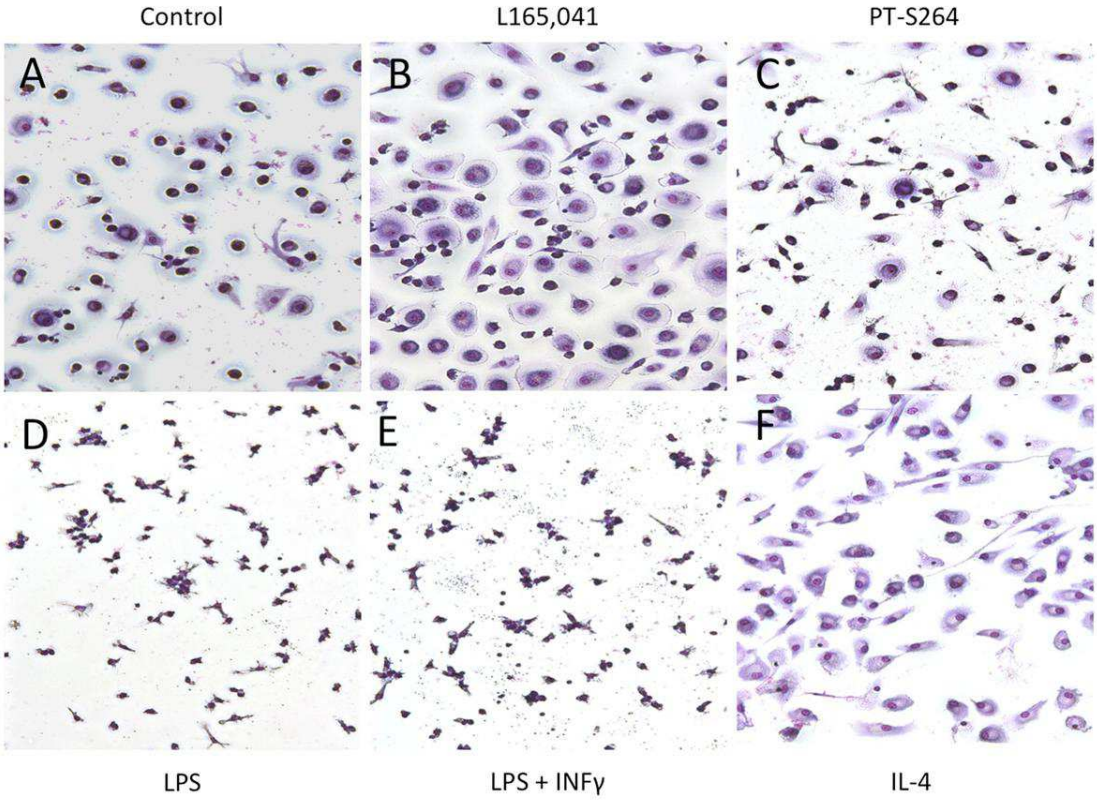

Figure S5 – Effects of PPARβ/δ ligands on the morphology of human MDMs. Human monocytes were differentiated in R10 medium for 6 d in the presence of the indicated additives. Cells were stained with Giemsa dye after treatment with **(A)** DMSO (solvent control), **(B)** L165,041 (agonist), **(C)** PT-S264 (inverse agonist), **(D**) LPS ("M1" macrophages), **(E)** ILPS+FNγ ("M1" macrophages) and **(F)** IL-4 ("M2" macrophages).

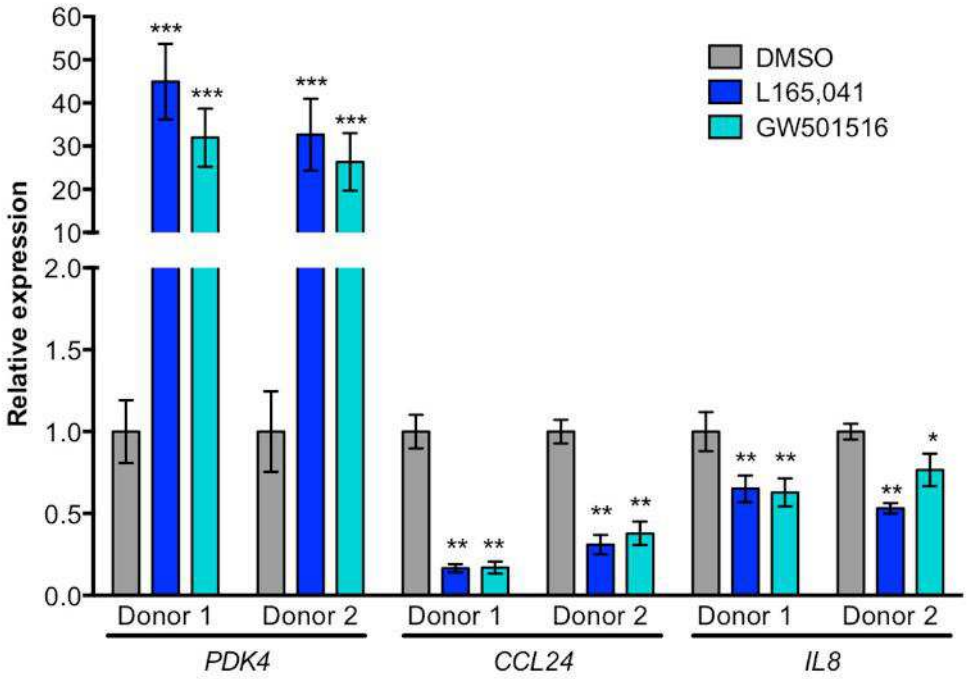

Figure S6 – RT-qPCR analysis of target gene regulation by GW501516 in MDMs compared to L165,041. The data represent 3 experiments performed with cells from two different donors; error bars show the standard deviation. *P<0.05; **P<0.01; ***P<0.001 by t-test relative to DMSO-treated cells.

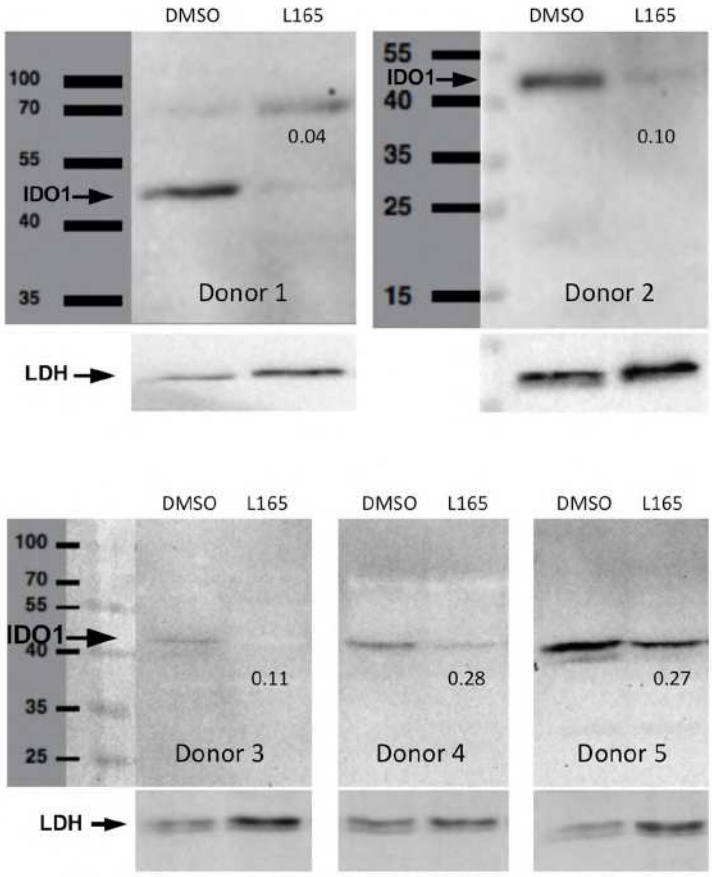

Figure S7 – Immunoblot analysis of IDO-1 expression in MDMs treated with DMSO or L165,041. The blot shows the data for cell from five different donors (as in Figure 7C). L165: L165,041, LDH: lactate dehydrogenase (loading control). IDO-1 bands were quantified (ChemiDoc MP) and adjusted to LDH band intensities. Expression values (relative to DMSO) are shown below the IDO-1 bands.

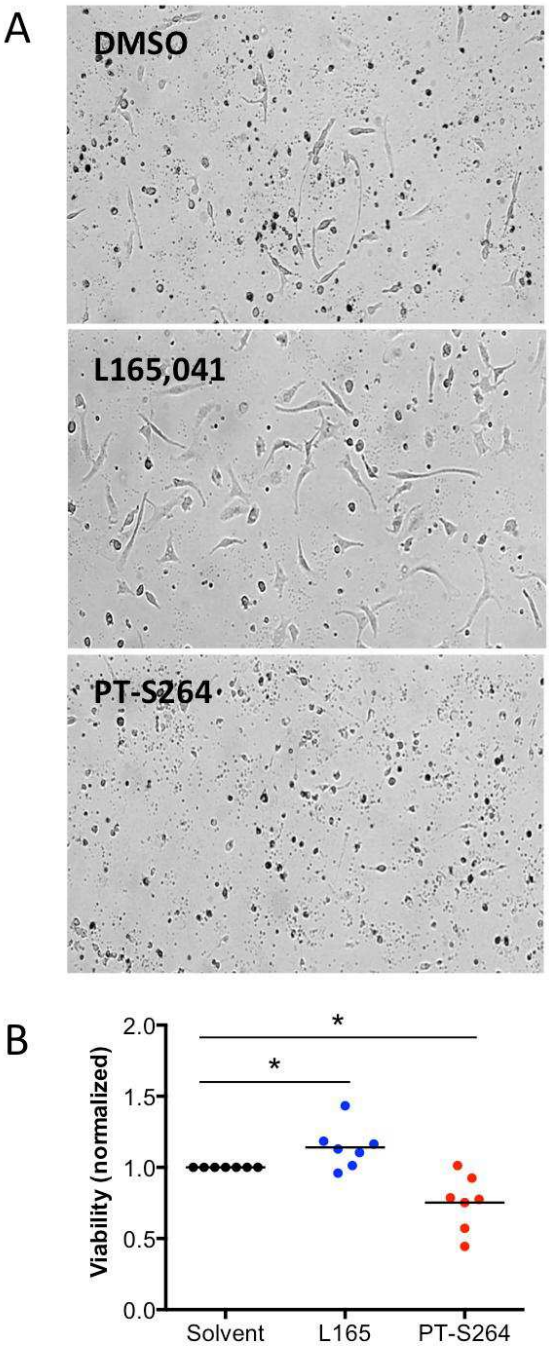

Figure S8 – Survival of MDMs exposed to hypoxia and L165,041 or PT-S264 for 4 d. (A) Photomicrographs of MDMs subjected to hypoxia for 2 days beginning on day 7 of differentiation in the presence of the indicated ligands or solvent. (B) Viability of adherent cells was determined by MTT assay with MDM from 7 different donors as follows: After the incubation period, cells were treated with 1.2 mM MTT (3-(4,5-dimethylthiazol-2-yl)-2,5-diphenyltetrazolium bromide; Sigma Aldrich) for four hours at 37 °C followed by a three-hour lysis in 0.005 mM HCl and 5% SDS (final concentration) at the same temperature. Measurements were performed with a SpectraMax 340 (MWGbiotech) at 570 nm.

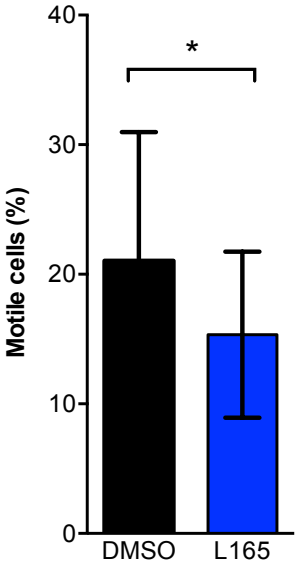

Figure S9 – Quantification of the MDM motility by time-lapse video microscopy. Cells on day 6 of differentiation (R0 medium) were treated with DMSO or 1 µM L165,041 for 2 h and images were captured by life cell video microscopy for 30 min at the same conditions as in regular cell culture incubator (37 °C, 5% CO_2). Recording was carried out with an Axiovert microscope (Zeiss) equipped with a 10x differential interference contrast (DIC) objecticve and a CO_2 incubator. Images were captured every 5 min. Cells were tracked with the Image J / Fiji Plugin "Particle Tracker 2D/3D" with a chosen radius of 11, a cutoff of 0,0 a percentile between 1-2, a link range of 5, a displacement of 60 and Brownian dynamics (Sbalzarini and Koumoutsakos, 2005). The data shown are derived from 5 independent experiments, tracking 910 cells in total. Statistical significance was determined by paired t test.

Reference

Sbalzarini, I.F. and Koumoutsakos, P. (2005) Feature point tracking and trajectory analysis for video imaging in cell biology. *J Struct Biol*, **151**, 182-195.

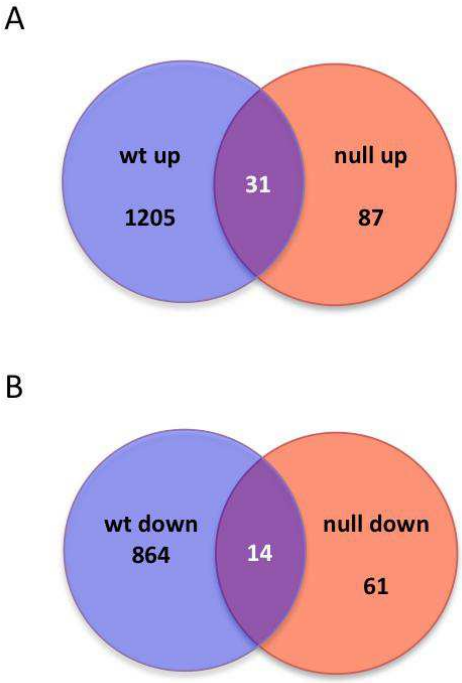

Figure S10 – Specificity of GW501516. Mouse bone marrow cells from wt and *Ppard* null mice were cultured for 2 days in GM-CSF, yielding a mixed population of granulocytes and immature monocytic cells at different stages of differentiation, as described in ref. 36. These cells were treated for 1 day with 1 μM GW501516 or solvent (DMSO) in the presence of GM-CSF. RNA was analyzed by microarrays as published (36). The Venn diagrams show the number of genes induced (A) or down-regulated (B) by the ligand in either wt (blue) or null (red) mice (fold change >1.5).

frontiers in Immunology

ORIGINAL RESEARCH
published: 27 June 2018
doi: 10.3389/fimmu.2018.01425

Chromatin Binding of *c*-REL and p65 Is Not Limiting for Macrophage *IL12B* Transcription During Immediate Suppression by Ovarian Carcinoma Ascites

*Annika Unger[1], Florian Finkernagel[1], Nathalie Hoffmann[2], Felix Neuhaus[1], Barbara Joos[1], Andrea Nist[3], Thorsten Stiewe[3], Alexander Visekruna[4], Uwe Wagner[5], Silke Reinartz[6], Sabine Müller-Brüsselbach[1], Rolf Müller[1] and Till Adhikary[1]**

[1] Institute for Molecular Biology and Tumor Research (IMT), Center for Tumor Biology and Immunobiology (ZTI), Philipps University of Marburg, Marburg, Germany, [2] Experimental Tumor Research Group, Center for Tumor Biology and Immunobiology (ZTI), Philipps University of Marburg, Marburg, Germany, [3] Genomics Core Facility, ZTI, Philipps University of Marburg, Marburg, Germany, [4] Institute for Medical Microbiology and Hygiene, Biomedical Research Center (BMFZ), Philipps University of Marburg, Marburg, Germany, [5] Clinic for Gynecology, Gynecological Oncology and Gynecological Endocrinology, Philipps University of Marburg, Marburg, Germany, [6] Clinic for Gynecology, Gynecological Oncology and Gynecological Endocrinology, ZTI, Philipps University of Marburg, Marburg, Germany

OPEN ACCESS

Edited by:
Uday Kishore, Brunel University London, United Kingdom

Reviewed by:
Kushagra Bansal, Harvard Medical School, United States
Junji Xing, Houston Methodist Research Institute, United States
Taruna Madan, National Institute for Research in Reproductive Health (ICMR), India

***Correspondence:**
Till Adhikary
adhikary@imt.uni-marburg.de

Specialty section:
This article was submitted to Molecular Innate Immunity, a section of the journal Frontiers in Immunology

Received: *23 December 2017*
Accepted: *08 June 2018*
Published: *27 June 2018*

Citation:
Unger A, Finkernagel F, Hoffmann N, Neuhaus F, Joos B, Nist A, Stiewe T, Visekruna A, Wagner U, Reinartz S, Müller-Brüsselbach S, Müller R and Adhikary T (2018) Chromatin Binding of c-REL and p65 Is Not Limiting for Macrophage IL12B Transcription During Immediate Suppression by Ovarian Carcinoma Ascites. Front. Immunol. 9:1425. doi: 10.3389/fimmu.2018.01425

Tumors frequently exploit homeostatic mechanisms that suppress expression of IL-12, a central mediator of inflammatory and anti-tumor responses. The p40 subunit of the IL-12 heterodimer, encoded by *IL12B*, is limiting for these functions. Ovarian carcinoma patients frequently produce ascites which exerts immunosuppression by means of soluble factors. The NFκB pathway is necessary for transcription of *IL12B*, which is not expressed in macrophages freshly isolated from ascites. This raises the possibility that ascites prevents *IL12B* expression by perturbing NFκB binding to chromatin. Here, we show that ascites-mediated suppression of *IL12B* induction by LPS plus IFNγ in primary human macrophages is rapid, and that suppression can be reversible after ascites withdrawal. Nuclear translocation of the NFκB transcription factors *c*-REL and p65 was strongly reduced by ascites. Surprisingly, however, their binding to the *IL12B* locus and to *CXCL10*, a second NFκB target gene, was unaltered, and the induction of *CXCL10* transcription was not suppressed by ascites. These findings indicate that, despite its reduced nuclear translocation, NFκB function is not generally impaired by ascites, suggesting that ascites-borne signals target additional pathways to suppress *IL12B* induction. Consistent with these data, IL-10, a clinically relevant constituent of ascites and negative regulator of NFκB translocation, only partially recapitulated *IL12B* suppression by ascites. Finally, restoration of a defective IL-12 response by appropriate culture conditions was observed only in macrophages from a subset of donors, which may have important implications for the understanding of patient-specific immune responses.

Keywords: IL12B, NFκB, REL, p65, ascites, ovarian carcinoma, macrophages, immunosuppression

1. INTRODUCTION

Solid tumors are frequently accompanied by large numbers of tumor-associated macrophages (TAMs), and their abundance is correlated with poor prognosis in several tumor types (1, 2). Advanced ovarian carcinoma (OC) often coincides with considerable accumulation of a malignant peritoneal effusion termed ascites which harbors large numbers of floating stromal and tumor cells. Its immunosuppressive properties are at least in part conferred by soluble mediators (3, 4). Like their counterparts from other tumor entities, TAMs isolated from OC ascites display an anti-inflammatory phenotype including high expression of the hemoglobin scavenger receptor CD163 (5). In follow-up studies, we found that the transcriptomes of ovarian carcinoma TAMs and those of peritoneal macrophages from non-tumor patients are very similar with the exception of a set of genes involved in extracellular matrix reorganization (6), which is a hallmark of wound healing and tumorigenesis. The expression of this gene set is correlated with poor survival (6, 7). On the other hand, elevated expression of an interferon (IFN)-inducible gene set in TAMs is correlated with improved survival (7). A recent meta-analysis of TAM studies in OC patients (8) reflects the findings that CD163 expression correlates with worse prognosis, while pro-inflammatory macrophage polarization is positively associated with survival.

The ability of human macrophages to produce nitric oxide has been debated extensively (9–14). Apparently, their cytotoxic activity is rather exerted indirectly *via* secretion of cytokines, especially interleukin-12 (IL-12), which activates cytotoxic functions of T and NK cells (15–19). IL-10 is an immunosuppressive cytokine present in large amounts in OC ascites (20), and there is a strong negative correlation of its level with patient survival (5, 21). In the ovarian tumor microenvironment, *IL10* is expressed predominantly by TAMs (3, 21, 22). A critical function of IL-10 is to repress transcription of *IL12B* (23, 24), which encodes for the p40 subunit of IL-12 and IL-23 that is limiting for heterodimer formation. Antigen-presenting cells are the main producers of IL-12p40 (25). On the other hand, IL-12 represses *IL10* transcription. This reciprocal blockade, "the IL-10–IL-12 circuit" (26), is enforced by positive feedback of IL-10 and IL-12 production, respectively (27). Mechanisms involved in these positive feedback loops are interdependent upregulations of IL-10 and CD163 (28–30) or, *vice versa*, instigation of IFNγ production by T and NK cells upon exposure to IL-12 (31–33); in turn, IFNγ enables production of IL-12 by monocytic cells. Indeed, it was shown that IFNγ is capable of relieving suppression of IL-12 production by OC ascites (7, 34) and is, therefore, required for the pro-inflammatory feedback loop. Taken together, switching between IL-10 and IL-12 production can toggle between the anti-inflammatory, immunosuppressive Th2 state, and pro-inflammatory, tumoricidal Th1 activation (23). The large number of immunosuppressive TAMs relative to other hematopoietic cells in OC ascites provides them with a decisive, pro-tumorigenic role in the microenvironment which at least in part depends on efficient suppression of *IL12B* transcription (4).

IL12B transcription is induced cooperatively by STAT1 and the NFκB pathway (27). Stimuli that activate each of these have antitumorigenic effects *in vivo* (7, 35). A critical role for the IFNγ pathway in *IL12B* expression is highlighted by mutations that cause autosomal Mendelian susceptibility to mycobacterial disease (MSMD). These were reported to occur in seven genes: *IL12B*, *IL12RB1*, *IFNGR1*, *IFNGR2*, *IRF8*, *ISG15*, and *STAT1* (36–38). IFNγ, if present during macrophage differentiation in OC ascites *in vitro*, can override suppression of IL-12 production (7, 34). Therefore, gene regulation by IFNγ and STAT1 is generally functional in macrophages exposed to ascites. Moreover, pretreatment of macrophages with IFNγ can prime them for stimulus-dependent IL-12 production (39), indicating that an IFNγ-mediated effect can limit the amplitude of the response.

The NFκB transcription factor *c*-REL (from now on abbreviated as REL), which is predominantly expressed in hematopoietic cells (40, 41), is crucial for *IL12B* expression (42, 43). The requirement for NFκB is underscored by the finding that mutations in *NEMO/IKKG* which disrupt induction of *IL12B via* CD40-IKKγ cause X-linked MSMD (37). Concomitant with diminished nuclear localization of p65, enhanced expression of p50 was observed in murine TAMs. Nuclear p50 may form heterodimers that contribute to *Il12b* suppression, and in TAMs lacking p50, *Il12b* inducibility was restored (44). IL-10 was shown to impinge on NFκB-dependent signaling by preventing nuclear translocation of p65 in human (45, 46) and rat macrophages (47) and of Rel in a mouse macrophage cell line (43). In summary, the pro-tumorigenic and anti-inflammatory effect of ascites may depend on restrainment of NFκB function, and IL-10 may be required for this effect.

We speculated that ascites disables translocation and chromatin binding of NFκB effector transcription factors and, in consequence, induction of *IL12B* transcription. To test this hypothesis, the impact of ascites on the induction of *IL12B* by the NFκB transcriptional activators REL and p65 was investigated. Our data show that cell-free OC ascites suppresses *IL12B* expression by primary human macrophages upon stimulation with LPS and IFNγ *in vitro via* a reversible mechanism. Both REL and p65 translocation to the nucleus was strongly impaired by exposure to ascites. However, induction of *CXCL10* mRNA by LPS and IFNγ was unaffected in the presence of ascites. High-throughput sequencing approaches after enrichment of several chromatin marks were used to map putative regulatory regions of the REL target genes *IL12B* and *CXCL10*. In the presence of ascites, REL and p65 were recruited to the *IL12B* and *CXCL10* loci, indicating that their reduced nuclear levels are still sufficient for chromatin

Abbreviations: APC, antigen-presenting cell; BMDM, bone marrow-derived macrophage; CD, cluster of differentiation; C/EBP, CCAAT/enhancer binding protein; ChIP, chromatin immunoprecipitation; ENCODE, encyclopedia of DNA elements; GEO, gene expression omnibus; IFN, interferon; IKK, IκB kinase; IL, interleukin; IκB, inhibitor of κ light chain enhancer of activated B cells; JAK, Janus kinase; LPS, lipopolysaccharide; MDM, monocyte-derived macrophage; MFI, mean fluorescence intensity; MIRA, methylated CpG island recovery assay; MSMD, Mendelian susceptibility to mycobacterial disease; NFκB, nuclear factor κ light chain enhancer of activated B cells; NK, natural killer; OC, ovarian carcinoma; PBMC, peripheral blood mononuclear cell; pMDM, monocyte-derived macrophage from a patient; REL, reticuloendotheliosis; RPL27, ribosomal protein 27, large subunit; RPMI, Roswell Park Memorial Institute; RRID, research resource identifier; STAT, signal transducer and activator of transcription; TAM, tumor-associated macrophage; Th, T helper; TSS, transcription start site.

binding. Furthermore, IL-10 contributes to but is not sufficient for full suppression of *IL12B* expression by macrophages *in vitro*. These data implicate an additional suppressive mechanism, mediated by ascites-borne soluble factors, which acts upstream of *IL12B* transcription.

2. MATERIALS AND METHODS

2.1. Ascites Collection and Isolation of TAMs From Ovarian Cancer Ascites

Ascites was collected from untreated high-grade serous ovarian carcinoma patients undergoing first-line surgery at the University Hospital Marburg. Informed consent was obtained from all patients according to the protocols approved by the institutional ethics committee. Mononuclear cells were isolated from ascites by Lymphocyte Separation Medium (Capricorn, no. LSM-A) density gradient centrifugation and subsequent enrichment by adherent cell positive selection in autologous ascites. Tumor-associated macrophages were directly harvested for chromatin immunoprecipitation, directly lysed for RNA isolation or cultivated in R5 medium (RPMI 1640 (Life Technologies, no. 61870044) with 5% (v/v) human AB serum (human serum type AB (male), (Sigma no. H4522)), and 1 mM sodium pyruvate (Sigma, no. S8636)) or in 100% cell-free autologous ascites for 1–2 days with or without recombinant 50 ng/ml IFNγ (from *E. coli*; Biomol, no. 51564) as indicated.

2.2. Isolation and Culture of Monocyte-Derived Macrophages

Buffy coats from healthy adult volunteers were kindly provided by the Center for Transfusion Medicine and Hemotherapy at the University Hospital Giessen and Marburg. Mononuclear cells were isolated from peripheral blood mononuclear cells from female healthy donors. Ficoll density gradient centrifugation was performed with Lymphocyte Separation Medium (Capricorn), and the cells were further purified by adherent cell positive selection of healthy donor monocytes. Monocyte-derived macrophages (MDMs) were generated from monocytes (6–12 days differentiation period) from healthy donors by cultivation in RPMI 1640 (Life Technologies, no. 61870044) with 5% (v/v) human AB serum (human serum type AB (male), Sigma no. H4522) and 1 mM sodium pyruvate (Sigma, no. S8636) (R5 medium) or in cell-free ascites from ovarian cancer patients, as indicated.

2.3. Cytokine Treatment

MDMs were stimulated with 100 ng/ml LPS (*E. coli* 0111:b4 L4391; Sigma) and 20 ng/ml recombinant human IFNγ (from *E. coli*; Biomol, no. 51564) or 20 ng/ml recombinant human IL-10 from HEK293 cells (Biomol, no. 97490) as indicated.

2.4. RNA Isolation and RT-qPCR

Total RNA from TAMs was extracted with TRIfast (Peqlab, no. 30-2020) or from MDMs with the NucleoSpin RNA kit (Macherey&Nagel, no. 740955) according to the manufacturer's instructions. Complementary DNA synthesis was carried out with the iScript cDNA Synthesis Kit (Bio-Rad, no. 170-8891SP) according to the manufacturer's instructions with 250–500 ng of purified RNA per sample. Quantitative PCR analyses were performed in three technical replicates per sample using ABsolute SYBR Green master mix (Thermo Scientific, no. AB-1158B) in Mx3000p and Mx3005 thermocyclers (Stratagene). The ribosomal protein 27, large subunit (*RPL27*) transcript was chosen for normalization after testing three housekeeping genes selected from our RNA-seq datasets with eight different TAM samples. RT-qPCR was carried out using the following primers: *RPL27*, AAAGCTGTCATCGTGAAGAAC and GCTGTCACTTTGCGGGGGTAG; *IL12B*, GCGAGGT TCTAAGCCATTCG and ACTCCTTGTTGTCCCCTCTG; *CXCL10*, AAGCAGTTAGCAAGGAAAGGTC and GACATA TACTCCATGTAGGGAAGTGA. Raw data were evaluated with the Cy0 method (48) or the MxPro 4.01 software from Stratagene for Ct value calculation as indicated.

2.5. IL-12p40 ELISA

Concentrations of p40 in cell-free supernatants of cultured cells were determined in three technical replicates per sample using an ELISA kit from Biolegend (no. 430706) according to the instructions of the manufacturer.

2.6. Flow Cytometry Analysis of Macrophages

MDMs were stained with APC-labeled α-CD206 (BioLegend Cat #321110 RRID:AB_571885) and PE-labeled α-CD163 (eBioscience no. 12-1639-42) as described previously (5). Isotype control antibodies were from BD Biosciences, Miltenyi Biotech, and eBioscience. Cells were analyzed by flow cytometry using a FACS Canto II cytometer and FACSDiva software (BD Bioscience), and results were calculated as percentage of positive cells and mean fluorescence intensities (MFI).

2.7. Subcellular Fractionation

Subcellular protein fractionation was performed after washing cells twice with ice cold PBS (Sigma). Cell pellets were subsequently lysed in hypotonic cytosol extraction buffer L1 (5 mM PIPES pH 8.0, 85 mM KCl, 0.5% (v/v) NP40, protease inhibitor mix (Sigma, no. P8340) 1:1,000) for 20–40 min on ice. Lysates were collected and centrifuged for 5 min at 2,000×*g*, 4 °C. Cytosolic extract (CE) supernatants were collected, and nuclear pellets were washed once in L1 and subsequently lysed in RIPA buffer (10 mM Tris–HCl pH 7.5, 150 mM NaCl, 1% NP40 (v/v), 1% sodium deoxycholate (w/v), 1 mM EDTA), 1:1,000 protease inhibitor Mix (Sigma), 25 U/ml benzonase (Merck Millipore, no. 70746) for generation of nuclear extracts (NE) in a ratio of 5:1 of cytosol to nuclear extract.

2.8. Immunoblotting and Protein Quantification

Immunoblots were performed according to standard protocols using the following antibodies: α-*c*-REL polyclonal antibody (Cell Signaling Technology Cat #4727 RRID:AB_2178843); α-p65/RELA monoclonal antibody (Cell Signaling Technology Cat #8242 also 8242P, 8242S RRID:AB_10859369); α-LDH polyclonal antibody (Santa Cruz Biotechnology Cat

#sc-33781 RRID:AB_2134947); α-acetyl-histone H3 polyclonal antibody (Millipore Cat #06-599 RRID:AB_2115283); α-β-actin (AC-15) monoclonal antibody (Sigma-Aldrich Cat #A5441 RRID:AB_476744); α-rabbit IgG, HRP-linked (Cell Signaling Technology Cat #7074 also 7074S, 7074V, 7074P2 RRID:AB_2099233), and α-mouse IgG, HRP-linked (Cell Signaling Technology Cat #7076 also 7076S, 7076V, and 7076P2 RRID:AB_330924). Imaging and quantification was done using the ChemiDoc MP chemoluminescence imaging system and Image Lab software version 5 (Bio-Rad).

2.9. RNA Interference

Small interfering RNA transfection was performed according to the manufacturer's protocol using the TransIT-X2 reagent from Mirus (no. 6000) or the Viromer GREEN reagent (Lipocalyx, no. 230055). The following equimolar mixtures of three siRNA oligonucleotides each from Sigma were used for transfection of macrophages: *REL* SASI-Hs01-00064620, SASI-Hs01-00064621, SASI-Hs01-00064622. Set of four Upgrade ON-TARGETplus from Dharmacon was used for *RELA* (LU-003533-00-0002), containing four siRNA oligonucleotides. MISSION siRNA Universal Negative Control #2 from Sigma was used as a control siRNA (si-ctrl). Cells were harvested 48 h after transfection.

2.10. Generation of Murine Bone Marrow-Derived Macrophages, *Il12b* Quantitative RT-PCR, and Il-12p40 ELISA

BMDMs were generated by cultivation of 2×10^6 bone marrow cells/well derived from wild-type and $Rel^{-/-}$ mice in RPMI 1640 medium supplemented with 10% heat-inactivated FCS and 10 ng/ml macrophage colony-stimulating factor (PeproTech) in six-well plates. After one week of cell culture, purity was tested by FACS staining for CD11b. Subsequently, BMDMs were stimulated with either LPS alone (100 ng/ml) or with LPS (100 ng/ml) in combination with recombinant IFNγ (10 ng/ml). 24 h after stimulation of BMDMs, supernatants from cell cultures were harvested. Murine Il-12p40 was measured with an ELISA kit (BD Biosciences, no. 555165) according to the manufacturer's protocol. Total RNA was extracted from BMDM-derived cell pellets using the High Pure RNA Isolation Kit (Roche, no. 11828665001). cDNA was synthesized using the RevertAid First Strand cDNA Synthesis Kit (Thermo Scientific, no. K1621). Gene expression was analyzed with a 7500 Fast Real-Time PCR System (Applied Biosystems). The gene expression of *Hprt1* was measured as an internal control. The following primer sets were used: *Hprt1*, CTGGTGAAAAGGACCTCTCG and TGAAGTAC TCATTATAGTCAAGGGCA; *Il12b*, ATGTGTCCTCAGAAG CTAACCATC and CGTGTCACAGGTGAGGTTCACT.

2.11. Chromatin Immunoprecipitation and MIRA

After adherence selection in Greiner tissue culture flasks (no. 660175) in autologous ascites, TAMs were washed with PBS twice. MDMs were differentiated as indicated. Fixation was performed with 1% formaldehyde in PBS for 10 min at room temperature followed by quenching with 125 mM glycin for 5 min. Cells were washed with ice-cold PBS twice and harvested using a cell scraper. The pellet was lysed in hypotonic buffer L1 (5 mM PIPES pH 8.0, 85 mM KCl, 0.5% (v/v) NP40) with protease inhibitor mix (Sigma, no. P8340, 1:1,000) for 20–40 min on ice. Nuclei were resuspended in ChIP RIPA buffer (10 mM Tris–HCl pH 7.5, 150 mM NaCl, 1% NP40 (v/v), 1% sodium deoxycholate (w/v), 1 mM EDTA) supplemented with 1:1,000 protease inhibitor mix (Sigma), incubated on ice for 10–20 min and sheared with a Branson S250D Sonifier (Branson Ultrasonics) using a microtip in 1 ml aliquots in 15 ml conical tubes. 52 pulses of 1 s, 4 s pause, 20% amplitude were applied with cooling of the sample in an ice–ethanol mixture or in a 15 ml tube cooler (Active Motif, no. 53077). A 15 min 20,000×*g* supernatant was precleared with 10 µg of IgG coupled to 100 µl of blocked sepharose slurry (see below) for 45 min at 4 °C with agitation. IP was carried out with 300 µl of precleared chromatin, equivalent to $3–8 \times 10^6$ cells. For MIRA, an aliquot of the sample was reverted as described below, purified on a Qiagen PCR purification column (no. 28106), and 250 ng of DNA were used according to the manufacturer's instructions (Methylcollector Ultra, Active Motif, no. 55005). ChIP was performed and evaluated as described using 4 µg per sample of the following antibodies: IgG pool, (Sigma-Aldrich Cat #I5006 RRID:AB_1163659) or normal rabbit IgG (Cell Signaling Technology Cat #2729S RRID:AB_1031062); α-*c*-REL (Santa Cruz Biotechnology Cat #sc-70 RRID:AB_2178727 and Santa Cruz Biotechnology Cat #sc-71 RRID:AB_2253705, 1:1 mixture); α-p65/RELA (Diagenode Cat #C15310256 RRID:AB_2721009); α-p65/RELA (Cell Signaling Technology Cat #8242 also 8242P, 8242S RRID:AB_10859369); α-H3K27me3 (Diagenode Cat #pAb-069-050 also ENCAB000ARJ RRID:AB_2616049); α-H3K4me3 (Diagenode Cat #pAb-003-050 also ENCAB000BKU, C15410003-50, C15410003-10 RRID:AB_2616052); α-H3K27ac (Diagenode, Diagenode, Cat #C15410174, RRID:AB_2716835); α-H3K4me1 (Diagenode Cat #pAb-037-050, RRID:AB_2561054); α-H3K9me3 (Diagenode Cat #pAb-056-050, RRID:AB_2616051); α-H3K36me3 (Abcam Cat #ab9050, RRID:AB_306966); α-C/EBPβ (Santa Cruz Biotechnology Cat #sc-150, RRID:AB_2260363). For precipitation, a mixture of protein A and protein G sepharose (GE Healthcare life sciences, no. 1752800 and no. 1706180) was washed twice with ChIP RIPA buffer and blocked with 1 g/l BSA and 0.4 g/l sonicated salmon sperm DNA (Life Technologies no. 15632011) overnight. 50 µl of blocked bead slurry (1:1 volume ratio with liquid phase) were used per IP. Samples were washed once in buffer I (20 mM Tris pH 8.1; 150 mM NaCl; 1% (v/v) Triton X-100; 0.1% (w/v) SDS; 2 mM EDTA), once in buffer II (20 mM Tris pH 8.1; 500 mM NaCl; 1% (v/v) Triton X-100; 0.1% (w/v) SDS; 2 mM EDTA), twice in buffer III (10 mM Tris pH 8.1; 250 mM LiCl; 1% (v/v) NP40; 1% (w/v) sodium deoxycholate; 1 mM EDTA) on ice, and twice in Qiagen buffer EB (no. 19086) at room temperature. Immune complexes were eluted twice with 100 mM $NaHCO_3$ and 1% SDS (w/v) under agitation. Eluates were incubated overnight at 65 °C after adding 10 µg of RNase A and 20 µg of proteinase K in the presence of 180 mM NaCl, 35 mM Tris–HCl pH 6.8, and 9 mM EDTA. An input sample representing 1% of the chromatin used per IP was reverted in parallel. Samples were purified using the Qiagen PCR purification kit according to the manufacturer's instructions, except that DNA-binding lipids were removed by washing the matrix twice with pure methanol as described (49) previous to the final washing step with the buffer included in the kit. ChIP-qPCR was performed in three technical replicates per sample with the ABsolute SYBR

Green master mix (Thermo Scientific, no. AB-1158B) in Mx3000p and Mx3005 thermocyclers (Stratagene) using the following primers: *IL12B* −1,200 bp CCATCCCTGCTCTCGACCT and GAAATCTGCGCCCGCCTAAA; *IL12B* TSS, AGTGCTTA CCTTGCTCTGGG and TACCAGCAACAGCAGCAGAA; *IL12B* +20 kbp, ACGCCGCCCTAGAAGAAG and TCCC TTTCACCTTCTCTGGA; *CXCL10* −5,000 bp, AGCTGGTG CAGAATATGCCTT and CACTGTGAGCTCGGGGAATC; *CXCL10* TSS, GAAGTCCCATGTTGCAGACTC and AACAGT TCATGTTTTGGAAAGTGA. Data were evaluated using the MxPro 4.01 software from Stratagene for Ct value calculation. Relative recoveries were determined as percentage of input using a ΔCt method (50).

2.12. Library Preparation and High-Throughput Sequencing

Libraries were synthesized from 1–2 ng of genomic DNA using the MicroPlex kit (Diagenode, no. C05010011) according to the manufacturer's instructions. Samples were sequenced on an Illumina Hi-Seq 1000 (single-ended, 50 bp).

2.13. Statistical Tests

Paired *t*-tests were used to calculate *p*-values.

2.14. Bioinformatics and Data Deposition

Mapping of ChIP-Seq reads and peak calling were carried out as described (49). Peaks were filtered for at least 30 deduplicated tags and a fold change (FC) over IgG of ≥2 (normalized total read counts). All genomic sequence and gene annotation data were retrieved from Ensembl revision 74. ChIP-seq data were deposited at ArrayExpress (no. E-MTAB-6297).

3. RESULTS

3.1. Suppression of *IL12B* in Monocytic Cells From Ovarian Carcinoma Patients Is Mediated by Soluble Factors From Ascites

We initially assessed whether the inability of TAMs to produce IL-12p40 is reversible in our experimental setups. *Ex vivo* TAMs were in autologous ascites or in normal medium (RPMI 1640 supplemented with 5% adult human serum, "R5") for 1 day or 2 days and stimulated with LPS and IFNγ 24 h prior to harvesting. *IL12B* expression was induced on both mRNA (**Figure 1A**; RT-qPCR) and protein levels (**Figure 1B**; α-p40 ELISA) in cells from four out of eight patients cultivated in ascites. After cultivation in autologous ascites for 2 days, the transcript and the protein were inducible to a lesser extent; LPS and IFNγ were added to the cultures 24 h prior to harvesting. The presence of IFNγ for the whole time of cultivation in 2 days samples led to increased induction. We conclude that suppression of *IL12B* in TAMs happens primarily at the transcriptional level, and suppression can be counteracted by IFNγ, as it was shown by others (34). Furthermore, we found that expression was inducible without IFNγ pretreatment in some samples (**Figure 1**). It is important to note that we added IFNγ in parallel with LPS to non-pretreated cultures, while the aforementioned study used LPS as a single stimulus after pretreatment with IFNγ (34). Apparently either a subpopulation of the cells from these patients is responsive to LPS and IFNγ *ex vivo*, or the autologous ascites samples are less capable of *IL12B* suppression. Strikingly, TAMs cultivated in normal medium in the absence of IFNγ were able to induce *IL12* transcription to similar levels as TAMs cultivated in ascites in the presence of IFNγ (**Figure 1A**). Cultivation in normal medium led to detectable transcripts in all donors analyzed ($N = 8$), while cultivation in the presence of IFNγ had this effect only in five out of eight donors. Taken together, this suggests that ascites-mediated suppression of *IL12B* induction is reversible, and this may depend on differences between ascites samples as well as cells from individual donors. Presumably due to biological heterogeneity, differences between the induced and non-induced conditions regarding p40 protein levels were not statistically significant when analyzing supernatants from TAMs cultivated in ascites (**Figure 1B**).

IL12B expression data from TAMs cultivated in normal medium or in ascites supplemented with IFNγ suggest that these cells are generally capable of inducing this transcript. Its induction in the presence of ascites could be due to an effect on monocytic cells that were freshly recruited to the tumor microenvironment and thus not yet strongly affected by ascites, or the effect of ascites on *IL12B* could be of a reversible nature. We, therefore, conducted the following experiments in MDMs differentiated from healthy donor monocytes *in vitro* in normal medium (R5) or in ascites as described previously (7)—this culture system allows for controlled differentiation as well as short-term treatment of cell populations that are less heterogeneous than TAM isolates. High levels of IL-12p40 can be produced by MDMs, and this is suppressed by ascites but overcome in the presence of IFNγ (7, 34). Priming of MDMs differentiated in R5 with IFNγ prior to stimulation with LPS and IFNγ did not potentiate IL-12p40 production (Figure S1 in Supplementary Material), indicating that our culture conditions do not limit expression of p40 in this regard.

3.2. Suppression of *IL12B* Can Be Reversible Upon Ascites Withdrawal

When MDM differentiation was carried out in normal medium for 6 days and followed by exposure to ascites for 1 day (short-term exposure, which was applied simultaneously with LPS and IFNγ), *IL12B* (**Figure 2A**, $N = 5$), and IL-12p40 (**Figure 2B**, $N = 8$) induction was efficiently suppressed. The effect was reverted in all MDM samples on RNA level by ascites withdrawal for 1 day after short-term exposure (**Figure 2A**), which was statistically significant; however, cells from most donors produced little or no p40, while others produced considerable levels (3/8; **Figure 2B**). This further point to a highly variable effect due to heterogeneity between biological samples, which could be due to the use of different ascites samples, different healthy donors, or both.

To clarify whether long-term exposure to ascites has lasting effects on the capacity of MDMs to express *IL12B*, monocytes from three healthy donors were differentiated either in R5 or in each of five different cell-free ascites samples from OC patients for 12 days (long-term exposure) in order to mimick the cellular state after differentiation in the ovarian tumor microenvironment. *IL12B* induction by LPS and IFNγ was markedly reduced

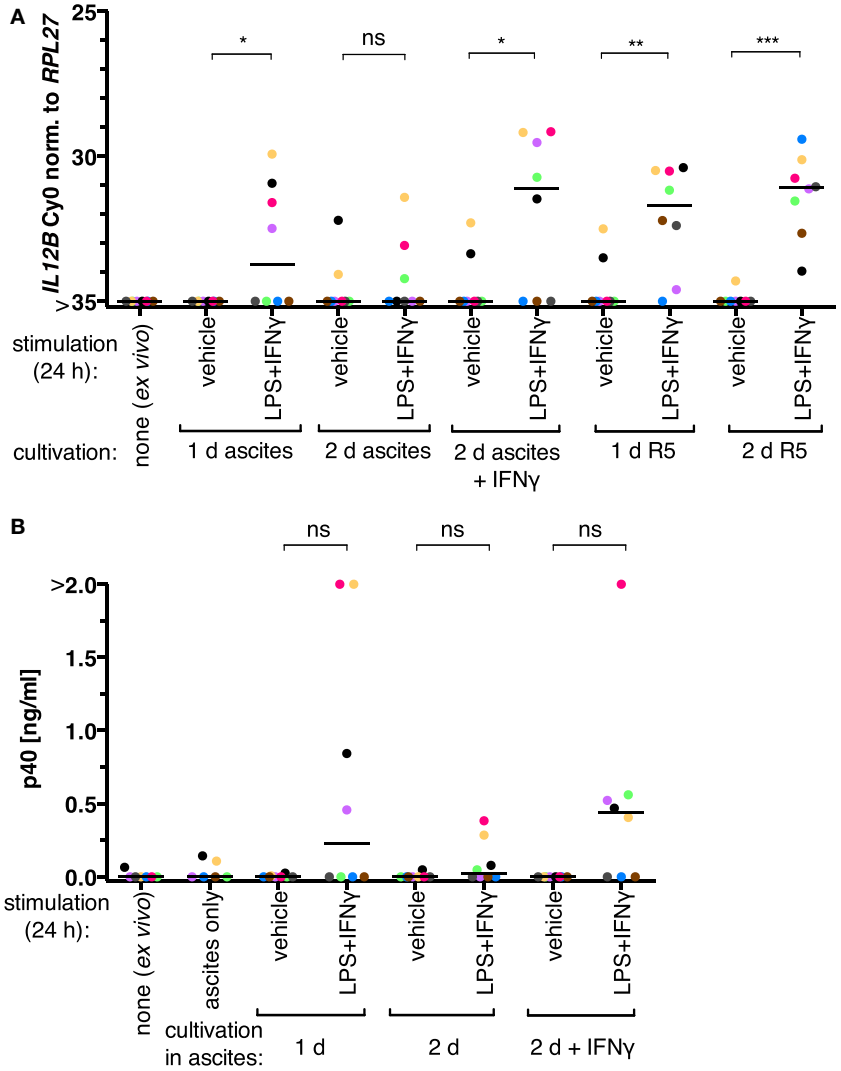

FIGURE 1 | IL-12 production by tumor-associated macrophages from ovarian carcinoma patients is suppressed by ascites *in vitro*. **(A)** *Ex vivo* TAMs ($N = 8$) were cultivated in autologous ascites in the presence or in the absence of IFNγ or in normal medium (R5) as indicated, and non-cultivated *ex vivo* TAMs served as an additional control. LPS and IFNγ or their respective solvents (vehicle) were added to the culture supernatants for 24 h prior to harvesting, and *IL12B* expression was measured by RT-qPCR. **(B)** Secreted IL-12p40 from these TAMs was measured by ELISA ($N \geq 6$). Cell-free autologous ascites was used as additional control. Each dot denotes a biological replicate. Median values are indicated by horizontal bars. Colors encode individual patients, and colors are consistent between panels within this figure. Statistical significances were calculated with paired *t*-tests. $^{*}P < 0.05$; $^{**}P < 0.01$; $^{***}P < 0.001$; ns, not significant.

in ascites-differentiated MDMs vs. MDMs differentiated in R5 medium on both mRNA (**Figure 2C**) and protein levels (**Figure 2D**). Although, suppression was not complete in some cultures, and this depended on both the donor cells and the ascites samples. MDMs differentiated in ascites for 6 days clearly induced *IL12B* expression after ascites withdrawal for 6 days (**Figures 2C,D**), albeit to lower levels than MDMs cultivated in normal medium for 12 days. Importantly, this happened in MDM cultures from all three donors in combinations with different ascites samples; p40 was detected in all but two combinations of donor cells with ascites samples. Induction after ascites withdrawal was elevated, but the effect did not reach statistical significance except for one comparison (**Figure 2D**, upper right panel). This can be attributed to the limiting number of samples analyzed and, importantly, to biological variation. Some ascites samples exerted suppressive effects that resulted in no or lesser reversibility, and MDMs from individual donors were susceptible to suppression by different ascites samples in a differential manner. We conclude that suppression of *IL12B* expression by OC ascites is reversible by ascites withdrawal in principle. On RNA level, reversal was more effective after short-term exposure. Since suppression was functional when ascites was added simultaneously with LPS and IFNγ, these data suggest that a suppressive mechanism acts immediately at the level of transcription and can affect MDMs which were differentiated in the absence of ascites (**Figure 2A**). Additional suppressive mechanisms apparently act posttranscriptionally (**Figure 2B**).

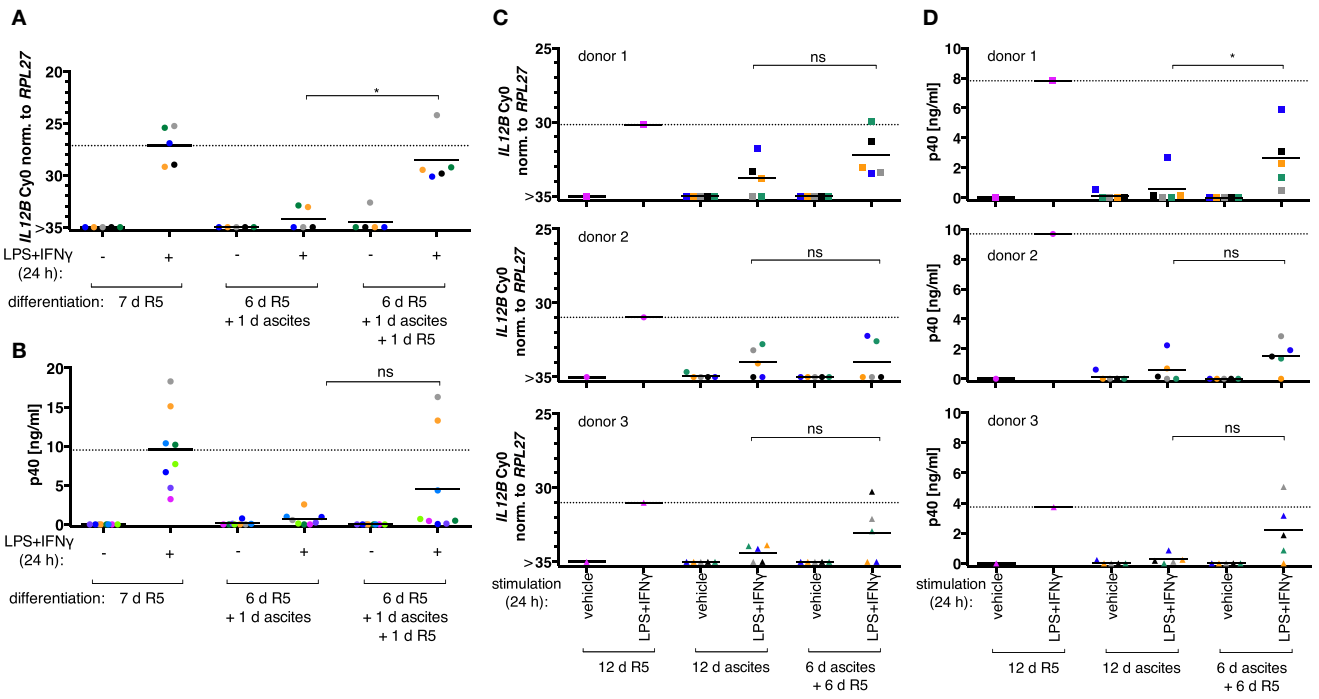

FIGURE 2 | Ascites-mediated suppression of *IL12B* in monocyte-derived macrophages is reversible upon ascites withdrawal. *IL12B* expression induced by LPS and IFNγ in MDMs (differentiated as indicated) was measured by RT-qPCR **(A,C)** or in culture supernatants by ELISA **(B,D)**. Cells were stimulated for 24 h prior to harvesting, or the respective solvents (vehicle) were added, respectively. **(A,B)** Each dot denotes a biological replicate (healthy donor; $N \geq 5$) randomly combined with different ascites samples encoded by color. **(C,D)** Colors encode ascites samples from five different patients; shapes encode different healthy donors ($N = 3$). Median values are indicated by horizontal bars. Statistical significances were calculated with paired *t*-tests. $^*P < 0.05$; ns, not significant.

The observation that *IL12B* suppression by ascites is rapid and reversible suggests that at least some of the mechanisms involved do not elicit a stable macrophage polarization state. In order to systematically characterize the state of MDMs upon suppression of *IL12B* expression by ascites *in vitro*, monocytes were differentiated in normal medium, in ascites in the presence of recombinant IFNγ, or in normal medium for 6 days followed by ascites for 1 day (short-term exposure). Under these conditions, we found that ascites leads to increased expression of the markers CD163 and CD206, indicating alternative polarization (Figure S3 in Supplementary Material). Upon cultivation in ascites in the presence of IFNγ, induction of these markers was partially reversed, concomitant with a restoration of *IL12B* inducibility. It can, therefore, not be excluded that an altered macrophage differentiation state might contribute to the blockade of *IL12B* transcription in TAMs. This notion would be consistent with the observed stable *IL12B* suppression by a prolonged exposure of MDMs to ascites.

3.3. Ascites Reversibly Suppresses Nuclear Translocation of REL and p65

Since suppression of *IL12B* induction by ascites is immediate and acts on the level of transcription, an obvious assumption is that NFκB function is compromised due to high levels of IL-10 in ascites. Nuclear translocation of REL was detected after both 1 and 2.5 h of stimulation with LPS and IFNγ in our MDM culture system in cells differentiated in normal medium (Figure S2B in Supplementary Material), and the latter time point coincided with measurable synthesis of *IL12B* mRNA (Figure S2A in Supplementary Material). This is in line with the regulation of "second wave" NFκB target genes such as *IL12B* (51). For subsequent analyses, LPS and IFNγ were added to the culture supernatants 2.5 h prior to harvesting.

According to our mass spectrometry data, REL, p65, and p50 are the main NFκB transcription factors expressed in TAMs (52). Nuclear translocation of the transcriptional activators REL and p65 was assessed by subcellular fractionation of MDMs after short-term (24 h) or long-term exposure to ascites (differentiation for 6 days or more). Representative immunoblots are shown in Figures S4B,C in Supplementary Material. Long-term exposure abrogated measurable REL translocation in six out of nine donors (**Figure 3A**) and translocation of p65 in all three donors analyzed (**Figure 3C**). Short-term exposure was less effective; detectable REL translocation was lost in two out of six donors (**Figure 3B**) and that of p65 in one out of three (**Figure 3D**). Although, exposure to ascites strongly reduced nuclear translocation in cells from all donors. Strikingly, ascites withdrawal for 1 day reinstalled nuclear localization of both REL (**Figure 3B**) and p65 (**Figure 3D**) in MDMs exposed to ascites for 24 h, which, however, did not reach the same levels as those of MDMs not exposed to ascites. In cells from the same donors used for short-term exposure experiments, reinstallation happened only in two out of three donors for REL (**Figure 3A**) and in one out of three donors for p65 (**Figure 3C**) after long-term exposure and 6 days of ascites withdrawal. Taken

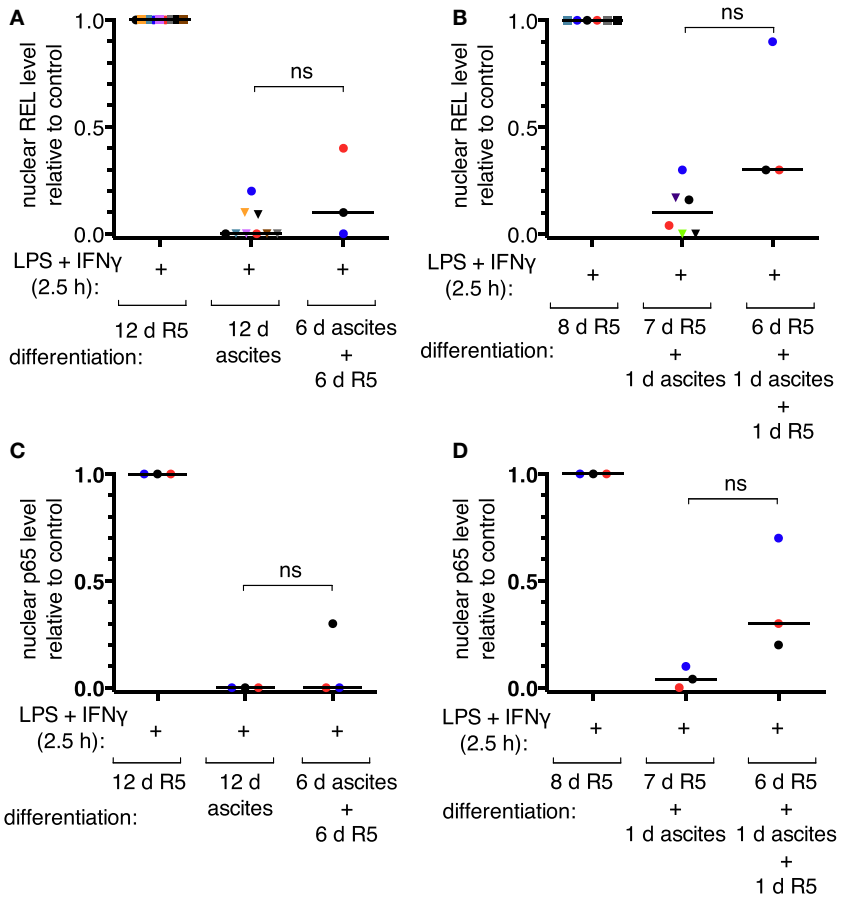

FIGURE 3 | Ascites impairs inducible nuclear translocation of REL and p65 in monocyte-derived macrophages. MDMs were differentiated in R5 medium or in ascites and cultivated consecutively as indicated. Cells were incubated with LPS and IFNγ for 2.5 h or their respective solvents (vehicle), harvested, and subcellular fractionation was performed. After immunoblotting, chemoluminescence was measured, nuclear levels of REL were calculated relative to the R5 control population after long-term ascites exposure with ($N = 9$) or without ($N = 3$) ascites withdrawal **(A)** or after short-term exposure **(B)**, respectively ($N = 6$ or $N = 3$ as plotted). Nuclear p65 levels were analyzed in a subset of the same samples ($N = 3$) accordingly **(C,D)**. Each color denotes a biological replicate (combination of healthy donor and randomly chosen ascites sample). Dots mark samples which were probed for both REL and p65 nuclear translocation. The code is consistent between panels within this figure. Median values are indicated by horizontal bars. Statistical significances were calculated with paired *t*-tests; ns, not significant ($P > 0.05$).

together, this demonstrates that impairment of REL and p65 nuclear translocation by ascites is rapid, and the effect can be reversible upon ascites withdrawal.

Nuclear localization of the NFκB transcriptional activators is controlled by IκB proteins, and their involvement in IL-10-mediated impairment of NFκB function is well documented (46, 53). We, therefore, measured the levels of IκBα, Iκβα, and IκBε proteins after stimulation of MDMs with LPS and IFNγ (Figures S5A–C in Supplementary Material; representative immunoblots are shown in Figure S4A in Supplementary Material) and found that, despite nuclear localization of REL, cellular IκBα levels were increased upon stimulation in all cell populations analyzed (Figure S5A in Supplementary Material). The levels of IκBβ and IκBε were strongly decreased upon stimulation under all conditions (Figures S5B,C in Supplementary Material). This is in line with the described positive feedback mechanism of IκBα after its initial rapid degradation, which subsequently leads to enhanced protein levels (53). Inducible Iκβα degradation was more pronounced in cells differentiated in ascites (Figure S5B in Supplementary Material). In conclusion, we did not observe a correlation between the levels of IκB proteins and the diminished capacity of *IL12B* transcription in MDMs exposed to ascites relative to non-exposed cells.

3.4. Induction of *CXCL10* Expression Is Not Prevented in the Presence of Ascites

Because nuclear translocation of REL and p65 is diminished in the presence of ascites, we speculated that transcription of target genes other than *IL12B* may be affected. *CXCL10*/*IP10* is a *bona fide* REL (54–56) and p65 target gene (57) which, however, is expressed in TAMs (7). A subset of cDNA samples shown in **Figure 2** was used to test ascites-mediated effects on the induction of *CXCL10* expression. We found that the levels of this highly inducible transcript—$\Delta Cy0 \geq 10$ in most sample combinations, which is equivalent to >1,000-fold induction—were weakly reduced after

short-term exposure, reaching statistical significance, and significantly elevated after short-term exposure and ascites withdrawal (Figure S6A in Supplementary Material). However, mean *CXCL10* levels (calculated for a total of six samples from three individual donors) were unaffected in MDMs stimulated with LPS and IFNγ after long-term exposure and ascites withdrawal (Figure S6B in Supplementary Material). *CXCL10* expression was uniformly high upon induction after both short-term and long-term exposure to ascites (Figures S6A,B in Supplementary Material). In some MDM populations, transcript levels were inducible to even higher levels compared to the control sample after long-term exposure (Figure S6B in Supplementary Material). In summary, this argues against a direct effect of ascites on *CXCL10* transcription. Therefore, our data do not show that mRNA synthesis of *CXCL10* is prevented in the presence of ascites. This argues against a general ascites-dependent perturbation of the function of REL and p65 provided that *CXCL10* is a direct target gene.

3.5. Chromatin Marks and Regulatory Elements at the *IL12B* Locus

Since translocation of REL and p65 is impaired in the presence of ascites, and *IL12B* mRNA induction is prevented, while that of *CXCL10* is not, an obvious hypothesis is that these transcripts are subject to gene-specific regulation. In order to address ascites-mediated effects on NFκB target genes, which are possibly locus-specific, we sought to map histone modifications and regulatory elements at these REL and p65 target genes in primary macrophages in an unbiased approach. To this end, ChIP-seq was performed in *ex vivo* OC TAMs with antibodies against the histone modification marks H3K4me1 (histone H3 lysine 4 monomethylation), H3K4me3, H3K9me3, H3K27me3, H3K27ac (H3K27 acetylation), H3K36me3, as well as the transcription factor C/EBPβ. Genome browser snapshots of the *IL12B* locus (**Figure 4A**) indicate that H3K4me1, which marks enhancer sequences, was detected at four sequence stretches within 25 kbp from either end of the coding region. These stretches are distinguished by the following features: (I) C/EBPβ binds to a region 11 kbp upstream of the *IL12B* transcription start site (TSS); (II) a region 7 kbp upstream of the TSS is decorated with H3K27ac, which marks active positive regulatory elements; (III) a local enrichment of H3K4me3 is localized 1,200 bp upstream of but not at the TSS itself, where this mark is usually found at active and poised genes (58); (IV) a region 4,500 bp downstream of the gene (20 kbp downstream of the TSS) harbors H3K27me3-modified nucleosomes, indicative of the Polycomb repressive complex 2 (58).

All four designated regions harbor highly conserved sequences, and none of them carry the heterochromatin mark H3K9me3. Consistent with minute or absent expression of *IL12B* transcripts in *ex vivo* OC TAMs (7), the coding region is devoid of the transcription elongation marker H3K36me3. Poorly annotated transcripts originate from regions III and IV. These long non-coding RNAs generally correlate with regulatory roles of the respective DNA sequences (59). Region II possibly is in spatial proximity to region I, since a minor but noticeable enrichment was caused by the C/EBPβ antibody at this site, which could be due to indirect crosslinking. We assume that regions I and II do not mediate repression due to the presence of the activating H3K27ac mark at region II and the absence of repressive marks at both regions.

The unusual configuration of the H3K4me3 mark appearing at a −1,200 bp upstream site (region III) but not at the TSS seems to be a hitherto undescribed characteristic of a set of cytokine-encoding genes: in our dataset, we observed similar distances at, for instance, *CXCL10/IP10* (−5,000 bp) and *IL2* (−2,000 bp), which both are REL target genes (42, 54–56, 60). Genome browser snapshots of both loci are shown in Figures S9A,B in Supplementary Material. *CXCL10* is expressed in OC TAMs as well as in peritoneal macrophages from tumor-free patients (6, 7), while *IL2* is not a transcribed gene in macrophages and hence is devoid of active marks but apparently harbors H3K4me3- and H3K4me1-modified nucleosomes within 2,000 bp of its TSS. We excluded the possibility that these H3K4me3 upstream shifts relative to the TSSs are due to mapping artifacts; moreover, these observations were confirmed in published datasets such as those from ENCODE (ChIP-seq tracks for H3K4me3; GSM1003536 and GSM945225 for monocytes; and GSM788075 for PBMCs) and an early ChIP-seq study in the Jurkat human T cell line (61).

Strikingly, a weak enrichment of region IV was also caused by the H3K4me3 antibody, which strongly enriches region III. Reciprocally, reads from the α-H3K27me3 ChIP, which are most prominent at region IV, are more densely spaced in an extended stretch, which encompasses region III and the TSS of *IL12B*, relative to the coding region. Taken together, region IV may be in proximity to region III in OC TAMs, since each region's more prominent of these two histone marks is, to a lesser extent, mirrored at the other region, presumably due to indirect crosslinking. The presence of both H3K4me3 and H3K27me3 at the same locus is reminiscent of the bivalent state which allows for stable repression and comparably fast induction of expression that was first described for developmental genes (58); however, bivalent genes carry the marks at or close to their TSSs.

To investigate whether cytosine methylation is involved in repression of *IL12B* in TAMs, we used MIRA (methylated CpG island recovery assay)-seq (62). CpG island methylation was not detected at the promoter region of *IL12B*, while robust signals originated at the penultimate exon and a region 9 kbp upstream of the TSS (**Figure 4A**). Importantly, the promoter as well as conserved sequences upstream (region I) and downstream of the coding region, 20 kbp from the TSS (region IV), harbor CpG islands according to DBCAT analysis (63), but were not enriched by MIRA. The human Jurkat T cell line and other cell lines analyzed show an enrichment of methylated CpG sequences at the promoter and region IV according to ENCODE datasets (with GEO accession numbers; Jurkat: GSM999367, HeLa-S3: GSM999337, H1: GSM999379, HepG2: GSM999338, HL-60: GSM999386, GM12878: GSM999376, K562: GSM999341, HUVEC: GSM999364, Ovcar-3: GSM999393). This potentially means that methylation of region IV and the promoter regulates cell-type specific expression of *IL12B*.

In summary, the next-generation sequencing analyses led to the hypothesis that suppression of *IL12B* in TAMs is mediated by an H3K27me3-dependent mechanism and involves the promoter/−1,200 bp region and a putative silencer element

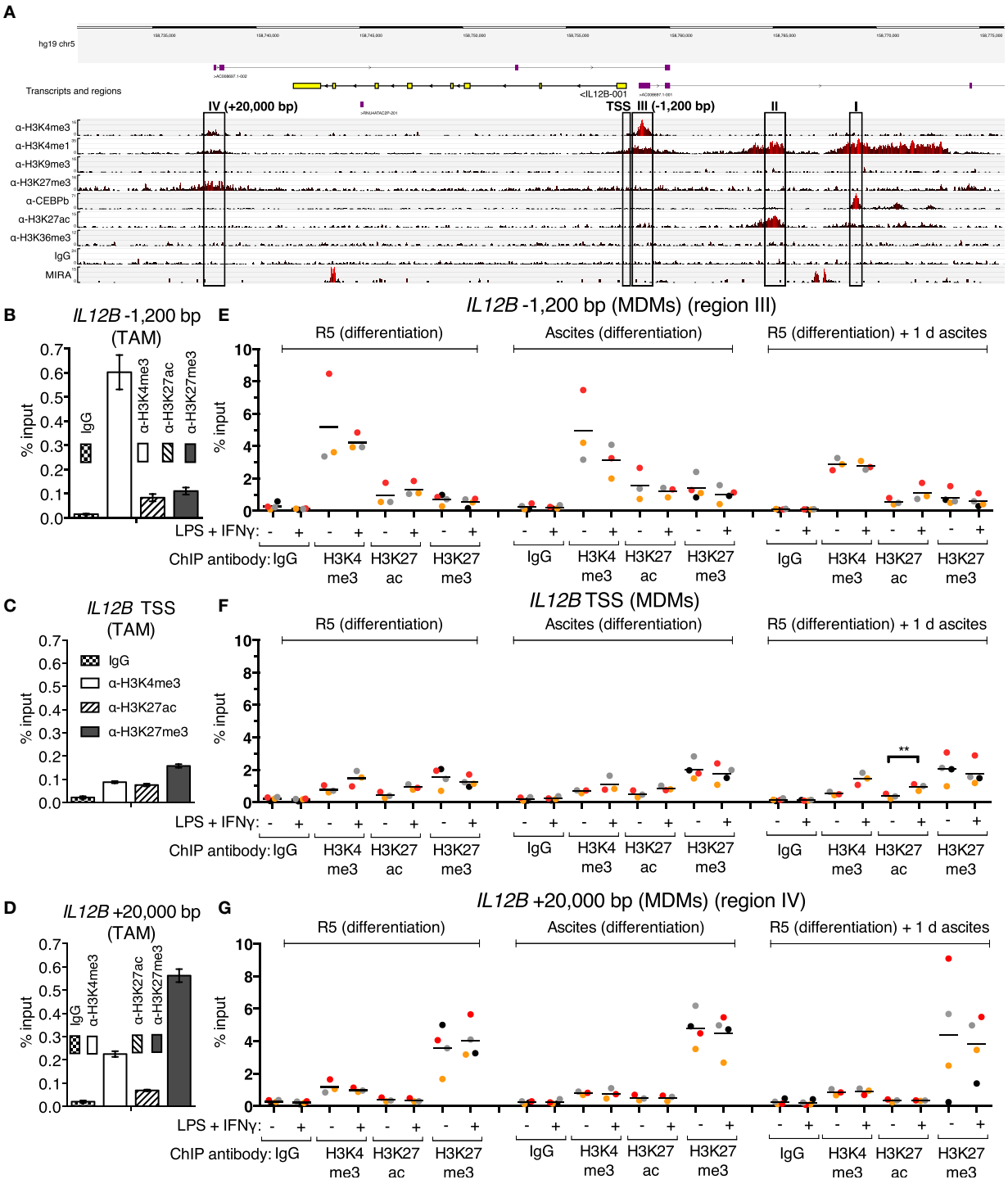

FIGURE 4 | Chromatin marks at the *IL12B* locus. **(A)** A genome browser snapshot, including ChIP-seq tracks for α-H3K4me3, α-H3K4me1, α-H3K9me3, α-H3K27me3, α-C/EBPβ, α-H3K27ac, α-H3K36me3, IgG (unspecific polyclonal rabbit IgG pool) chromatin immunoprecipitations, and MIRA from a TAM sample freshly isolated from ovarian carcinoma ascites. Regions of interest are highlighted by rectangles. **(B–D)** ChIP-qPCR analyses of the indicated histone marks in an independent TAM sample at the indicated genomic locations amplified by specific primers are indicated. The error bars denote SDs from technical PCR replicates. **(E–G)** ChIP-qPCR analyses of the indicated histone marks in MDMs from three different pooled donor populations ($N = 3$; $N = 4$ for IgG and α-H3K27me3 samples) differentiated in normal medium, in ascites, or in normal medium followed by ascites for 1 day. Cells were stimulated with or without LPS and IFNγ (+) or their respective solvents (–) 2.5 h prior to harvesting. Genomic regions were amplified by specific primers are indicated. Each dot denotes a biological replicate; for each replicate, MDMs from six donors were pooled after harvesting of the cells for each experiment. Median values are indicated by horizontal bars. Colors encode ascites samples from individual patients, and colors are consistent between panels within this figure, **Figure 5** and Figure S9 in Supplementary Material. Statistical significances were calculated with paired *t*-tests. $^{**}P < 0.01$; all other analyses did not show significance ($P > 0.05$).

20 kbp downstream of the TSS. For further analyses, we focused on elements that harbor repressive marks (regions III: −1,200 bp and IV: +20 kbp) as well as the TSS. The observed enrichment of H3K4me3 and H3K27me3 at these elements was confirmed by ChIP-qPCR in a different TAM sample (**Figures 4B–D**).

Using ChIP-qPCR, analysis of the chromatin marks H3K4me3, H3K27ac, and H3K27me3 was performed in MDMs differentiated in normal medium, in ascites, or in normal medium followed by exposure to ascites for one day in order to measure possible changes upon short-term and long-term suppression (**Figures 4E–G**). Cells were stimulated with LPS and IFNγ 2.5 h prior to fixation; at this time point, REL and p65 were detected in the nucleus (**Figure 3**; Figure S2B in Supplementary Material), and *IL12B* transcripts were detectable shortly thereafter (Figure S2A in Supplementary Material). The observed relative levels of the analyzed histone modifications generally mirrored the observations made in TAMs (**Figures 4B–D**), with absolute recoveries in MDMs being higher due to lower cell numbers that were obtained from MDM cultures in comparison to TAMs from large volumes of ascites. H3 lysine 4 trimethylation levels did not change consistently; at the TSS, levels were low but uniformly increased upon stimulation with LPS and IFNγ. At the *IL12B* TSS, the H3 lysine 27 acetylation signal increased consistently (**Figure 4F**) upon stimulation, and this was statistically significant in the short-term ascites-exposed population. Mean H3K27me3 signals at the TSS of *IL12B* were slightly elevated in MDMs exposed to ascites. The difference did not reach statistical significance. Upon stimulation, α-H3K27me3 signals were slightly diminished at the *IL12B* TSS (**Figure 4F**). This might reflect a decreased interaction between the TSS and the downstream putative silencer element at +20,000 bp, where robust enrichment of H3K27me3 was detected (**Figure 4G**). In summary, it seems plausible that the region IV downstream site and the TSS/−1,200 bp regions are in spatial proximity to each other, and H3K27me3 at the TSS might possibly be elevated after exposure to ascites. However, we cannot rule out that H3K27me3-dependent mechanisms are dispensable for suppression of *IL12B* due to the observation that enrichments by α-H3K27me3 at the TSS was only mildly elevated in MDMs exposed to ascites relative to the control population. The identified putative regulatory elements at the *IL12B* and *CXCL10* loci are candidate regions for assessing binding of transcription factors that regulate *IL12B* expression.

3.6. Inducible REL and p65 Binding to Chromatin Is Not Impaired in MDMs Exposed to Ascites

REL and p65 binding was measured (**Figures 5A–C**) in the same samples as in **Figures 4E–G** (identical data for IgG samples are shown). An enrichment with antibodies against each transcription factor was induced in the control population after stimulation at *IL12B* −1,200 bp (**Figure 5A**). Surprisingly, in the short-term ascites exposed population, REL and p65 were recruited to a similar extent at the −1,200 bp site of *IL12B*, while long-term exposure to ascites led to reduced but measurable recruitment. No recruitment was observed at the TSS and at +20,000 bp (**Figures 5B,C**). This indicates that chromatin binding of the NFκB transcriptional activators is functional in the presence of ascites despite their strongly impaired translocation (**Figure 3**). Notably, at the *CXCL10* locus, where REL and p65 recruitment was detected at both the TSS (**Figure 5D**) and an upstream element (**Figure 5E**), recruitment was enhanced by short-term ascites exposure but was unchanged after long-term exposure. These data show that, unexpectedly, nuclear REL and p65 levels are not measurably limiting for their binding to chromatin in MDMs exposed to ascites.

3.7. The Role of REL in the Induction of *IL12B* Expression

In order to clarify whether RNAi-mediated depletion of REL and p65 affects expression of *IL12B*, we employed knockdown approaches using siRNA in MDMs differentiated in normal medium. Functionality of the siRNA oligonucleotides was validated on protein level (Figure S8 in Supplementary Material). However, we were unable to achieve high knockdown efficiencies in primary macrophages, resulting in apparent protein levels of 60% relative to the control population or less. Knockdown of REL resulted in slightly diminished induction of IL-12p40 (Figure S7 in Supplementary Material). In a murine *Rel* knockout model, induction was largely dependent on Rel (42). However, the effects we observed after RNA interference are mild, which we attribute to incomplete depletion of the target proteins and to the effect that transfection with control siRNA also led to a strong reduction of p40 expression in most experiments. We could not find an efficient transfection reagent that did not elicit this effect, even in the absence of siRNA oligonucleotides (data not shown). In one of the MDM populations analyzed, *IL12B* expression was affected neither by REL knockdown nor by p65 knockdown (blue dots, Figure S7 in Supplementary Material) despite a measurable reduction of their protein levels, and in another sample, induction was increased after knockdown of p65 (black dots, Figure S7 in Supplementary Material). This prompted us to use a different experimental system in which Rel is genetically deleted. When we stimulated murine *Rel* knockout bone marrow-derived MDMs (BMDMs) with LPS and IFNγ, induction of *Il12b* (**Figure 6A**) as well as p40 (**Figure 6B**) was reduced to about 20% of the levels generated by wild-type cells, as it was similarly shown by others previously. These data suggest that REL is important but not necessary for *IL12B* induction. Indeed, it was observed previously by others that Rel-deficient murine antigen-presenting cells can produce IL-12p40 to a highly varying extent depending on the tissue they were isolated from Ref. (64). The function of REL is conceivably supplemented by and partially redundant with that of p65, as it was noted before (42, 65). The mild effects we observed after siRNA-mediated partial depletion are in line with the notion that levels of REL and p65 are not limiting for target gene induction in MDMs.

3.8. IL-10 Is Not Sufficient to Suppress *Il12b* Expression

The inability of MDMs to synthesize IL-12p40 after exposure to ascites could be explained by the negative effect of IL-10 on the translocation of REL and p65 (45–47) as well as its indirect actions *via* the induction of STAT3 target genes (23, 24, 66–68). However, treatment of MDMs (differentiated in normal medium)

with recombinant IL-10 from human cells in parallel with LPS and IFNγ did not recapitulate full suppression of IL-12p40 production (**Figure 7B**) and was unable to shut off *IL12B* transcription (**Figure 7A**) in cells from all but one donor. Importantly, the effects of partial suppression were highly significant on both mRNA (**Figure 7A**) and protein levels (**Figure 7B**), indicating

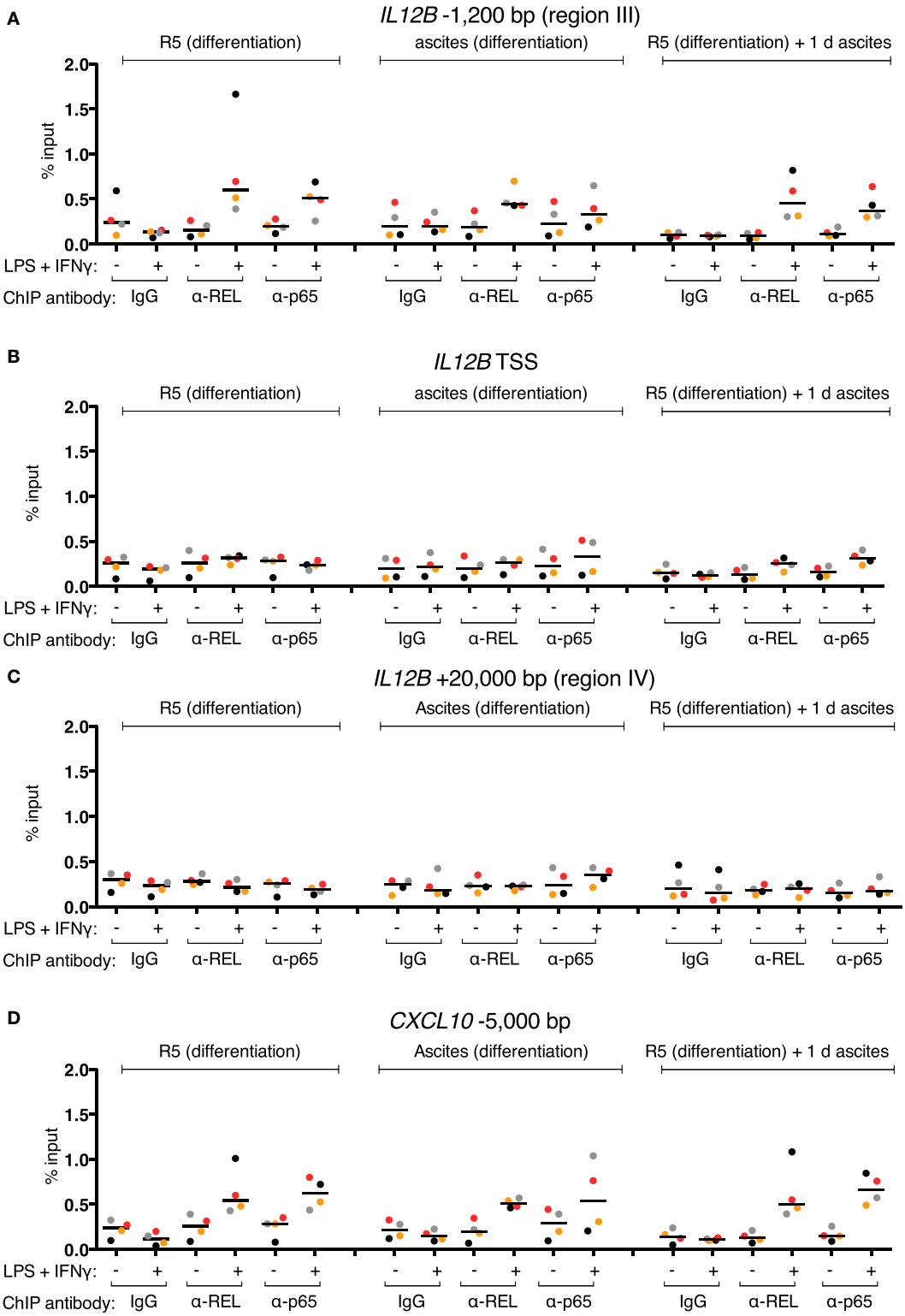

FIGURE 5 | Continued

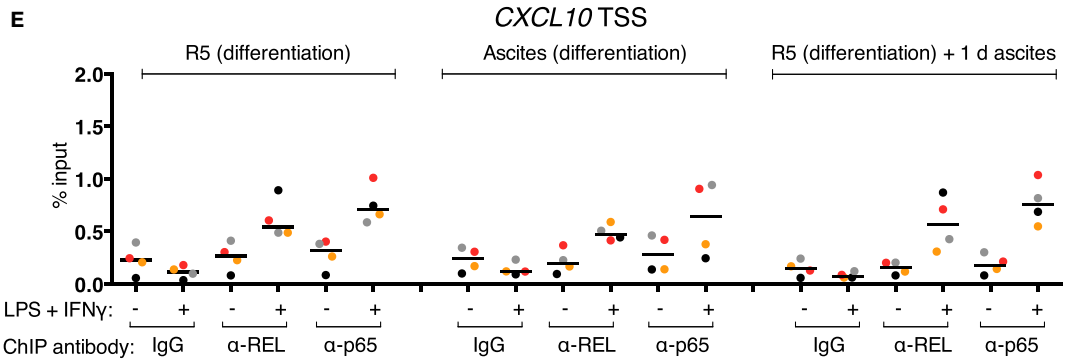

FIGURE 5 | Inducible REL and p65 binding at the *IL12B* and *CXCL10* loci in MDMs. **(A–E)** ChIP-qPCR analyses of REL and p65 binding in chromatin preparations from MDMs differentiated in normal medium, in ascites, or in normal medium followed by ascites for 1 day were conducted. Cells were stimulated with or without LPS and IFNγ (+) or their respective solvents (–) 2.5 h prior to harvesting. Genomic regions were amplified by specific primers are indicated. The same samples were used as in **Figure 4** ($N = 4$). Each dot denotes a biological replicate; for each replicate, MDMs from six donors were pooled after harvesting of the cells. Median values are indicated by horizontal bars. Colors encode ascites samples from individual patients, and colors are consistent between panels within this figure, **Figure 4** and Figure S9 in Supplementary Material.

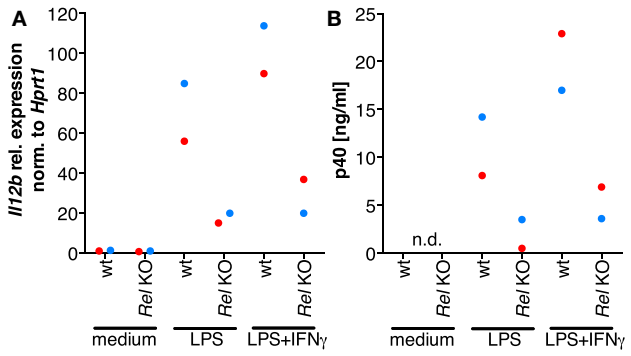

FIGURE 6 | The role of Rel in the induction of *Il12b* expression. Murine *Rel* knockout BMDMs or wild-type BMDMs ($N = 2$ each) were differentiated *in vitro* and stimulated with LPS or LPS and IFNγ for 24 h. Cells were used for RT-qPCR analysis of *Il12b* **(A)**, and Il-12p40 was measured in supernatants by ELISA **(B)**; n.d., not detected.

that the recombinant IL-10 was functional. MDMs from some individual donors were affected more than others, demonstrating that the amplitude of suppression is donor-dependent to a large extent. We conclude that other ascites-borne factors are necessary for full suppression of *IL12B*.

4. DISCUSSION

Our data suggest that (1) suppression of *IL12B* transcription by ovarian carcinoma ascites acts immediately and on differentiated macrophages, and it is reversible upon ascites withdrawal; (2) although ascites impinges on REL and p65 nuclear translocation, binding of these factors to chromatin is not diminished; and (3) IL-10 can only partially recapitulate suppression. This implicates that soluble factors in ascites may act combinatorially to achieve rapid, gene-specific suppression of *IL12B* transcription.

4.1. Reversibility and Immediacy of Ascites-Mediated *IL12B* Suppression

Immediately after ascites exposure, *IL12B* transcription was largely abrogated in MDMs simultaneously stimulated with LPS and IFNγ (**Figure 2A**). *IL12B* mRNA inducibility was partially restored in cells from all donors after ascites withdrawal. These data indicate that, while suppression is rapid, its effects are not permanent in cells exposed to ascites for 24 h. Additional post-transcriptional mechanisms negatively affecting p40 synthesis are likely (**Figure 2B**). Importantly, some MDM cultures retain the ability to secrete measurable amounts of p40 in the presence of ascites, and this apparently depends on both the donor and the ascites used. Ascites withdrawal further attenuates suppression (**Figures 2A–D**).

In line with reversibility of *IL12B* suppression, the transcript was detected in most *ex vivo* TAM samples in the absence of ascites (**Figure 1A**). *IL12B* expression reached levels similar to those in TAMs cultivated in ascites in the presence of IFNγ. Furthermore, exposure to ascites does not immediately induce macrophage M2 marker expression in MDMs (Figure S3 in Supplementary Material), an observation which is compatible with a model of transient suppression by ascites.

As mentioned before, our data indicate that biological variation is high among both donor cells and ascites samples, which agrees with our finding that, on transcriptome level, TAMs from OC patients can be clustered into two groups which differ in the expression levels of interferon-responsive genes. Higher expression of these genes is positively correlated with patient survival (7). From a therapeutical perspective, it might be beneficial to determine genetic predispositions and environmental factors involved in ascites-mediated suppression of *IL12B*.

4.2. Restrainment of NFκB by Ascites Is Not Complete

Ascites-exposed MDMs show strongly reduced REL and p65 nuclear translocation (**Figure 3**), yet chromatin binding of

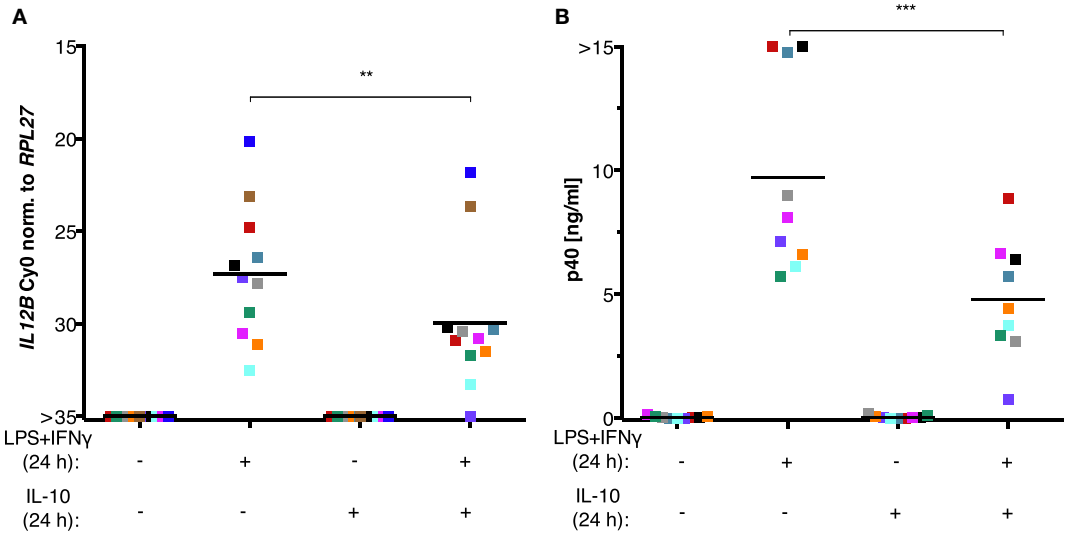

FIGURE 7 | IL-10 is not sufficient to suppress *IL12B* induction in MDMs. MDMs were differentiated in R5 medium for 6–7 days and stimulated with LPS and IFNγ, with recombinant IL-10 from human cells, or both for 24 h. **(A)** *IL12B* expression was measured by RT-qPCR ($N = 11$). **(B)** IL-12p40 in culture supernatants ($N = 9$) was measured by ELISA. Each square denotes a biological replicate (individual healthy donor). Colors encode individual healthy donors, and colors are consistent between panels within this figure. Median values are indicated by horizontal bars. Statistical significances were calculated with paired *t*-tests. $^{**}P < 0.01$; $^{***}P < 0.001$.

these factors is functional (**Figure 5**). Additionally, after short-term ascites exposure, REL and p65 translocation was not fully impaired in most samples (**Figures 3B,D**). In conclusion, nuclear REL and p65 levels after stimulus-dependent translocation are sufficient for saturation of their binding sites at the *IL12B* and *CXCL10* loci regardless of ascites-mediated reduction of nuclear translocation. Consistent with this, siRNA-mediated partial depletion of REL or p65 did not significantly influence *IL12B* induction (**Figure 6A**). However, it cannot be excluded that reduced binding of REL proteins to sites with lower affinity than at the *IL12B* and *CXCL10* loci has an indirect impact on *IL12B* transcription, e.g., by affecting the expression of a gene-specific coactivator.

Interestingly, IL-10 was reported to selectively inhibit expression of a subset of LPS-inducible genes in murine macrophages in the absence of endogenous IL-10, and *Il12b* was among the most strongly downregulated transcripts (69). Gene-specific mechanisms offer a conclusive explanation why other NFκB targets such as *CXCL10* are not suppressed by ascites (Figure S6 in Supplementary Material). Unaltered occupancy of REL and p65 at both the *IL12B* and *CXCL10* loci in the presence of ascites (**Figure 5**) strongly suggests that these gene-specific mechanisms do not affect NFκB chromatin binding. Induction of *CXCL10* expression depends on IFNγ, its receptor and STAT1 (70, 71), and also on NFκB (72). These factors are likewise required for *IL12B* expression. Induction of *IL12B* by LPS and IFNγ is not functional in MDMs exposed to ascites (**Figure 2**), while induction of *CXCL10* is (Figure S6 in Supplementary Material). *CXCL10* is expressed in *ex vivo* TAMs, while *IL12B* is not (7). The two genes are presumably not regulated by differential NFκB and STAT1 recruitment to chromatin in the presence of ascites. Gene-specific posttranslational modifications of transcription factors, availability of coactivators, regulation of DNA looping involving the region IV putative silencer element, or a repressor which does not affect the marks we used to characterize the chromatin state of *IL12B* may be involved in suppression.

4.3. The Role of IL-10 in *IL12B* Suppression

A plethora of studies ascribe a major role to IL-10 in the maintenance of homeostasis, including the prevention of IL-12 production *via* multiple mechanisms (23, 24, 39, 43, 45–47, 67, 68, 73). Our observation that IL-10 does not fully recapitulate ascites-mediated suppression of *IL12B in vitro* in cultures from most donors suggests that additional suppressive factors might be lacking. In addition to IL-10, prostaglandin E2 (73), phosphatidylserine (74), adenosine (75, 76), lysophosphatidic acid (33), polyunsaturated fatty acids (77), and α-fetoprotein (78, 79) were described to downregulate IL-12 production. Potential targets of soluble factors could be upstream signaling components, transcription factors, or cofactors.

In murine alveolar macrophages, the E3 ubiquitin ligase Trim29 was found to negatively regulate the host response after bacterial infection. Trim29, which is exclusively expressed in alveolar macrophages, can induce degradation of the Ikk regulatory subunit (80). This highlights a paradigm for tissue-specific regulation of the pro-inflammatory response. Analogously, the expression of a regulator impinging on IKK function could conceivably be modulated by soluble factors from ascites. A corepressor which suppresses *Il12b* expression in murine macrophages is Smrt (81). The study elucidates that the closely related proteins Ncor and Smrt can differentially repress sets of target genes. *Il12b* was repressed by Smrt exclusively, and Smrt could be displaced from

the locus by IFNγ treatment. It is conceivable that ascites-borne soluble factors stablize SMRT or another gene-specific corepressor at the *IL12B* locus, since the expression of *CXCL10* is not suppressed by ascites. Transcription factors described to repress *IL12B* expression such as Nfil3 in mice (24) or *c*-MAF (82) might contribute to the establishment of a locus-specific repressive complex.

Intriguingly, the levels of IL-10 as well as those of arachidonic acid in ascites are negatively correlated with patient survival according to our previous studies, and IL-10 and arachidonic acid levels are synergistically correlated with poor prognosis (21). This suggests that IL-10 alone is not sufficient to exert its full pro-tumorigenic effect *in vivo*. We postulate that other factors are required in addition to IL-10 for the suppression of a pro-inflammatory, anti-tumorigenic macrophage phenotype that includes expression of IL-12p40. Imbalances of this postulated interplay which are integrated into deregulated *IL12B* expression might be involved not only in tumorigenesis but could also contribute to diseases with an autoimmune component (26, 27). Future studies will investigate putative combinatorial suppressive mechanisms using a panel of purified factors.

DATA AVAILABILITY

The ChIP-seq datasets generated for this study can be found in the ArrayExpress repository at https://www.ebi.ac.uk/arrayexpress/experiments/E-MTAB-6297.

ETHICS STATEMENT

All patient samples were obtained in accordance with the recommendations of the Ethics Commission of the Department of Medicine, Philipps University of Marburg with written informed consent from all subjects. All subjects gave written informed consent in accordance with the Declaration of Helsinki. The protocol was approved by the Ethics Commission of the Department of Medicine, Philipps University of Marburg.

AUTHOR CONTRIBUTIONS

AU performed most experiments. FF applied all bioinformatical methods. TA performed TAM ChIPs, MIRA assays, and ChIP-seq library preparation. NH performed *IL12B* induction kinetics analysis. BJ and FN performed ELISA experiments. AN performed high-throughput sequencing. UW contributed clinical samples. SR prepared TAM samples. AV performed all experiments with murine cells. AU, FF, AV, SR, SM-B, RM, and TA conceived and designed the experiments. All authors analyzed data. RM and TA supervised the study. TA wrote the manuscript. AU, SM-B, and RM made major contributions to the writing of the manuscript.

ACKNOWLEDGMENTS

We thank Bernhard Wilke, Klaus Weber, Alexandra Schneider, Angelika Filmer, Margitta Alt, Achim Allmeroth, and Traute Plaum for expert technical support. This work was published as part of the doctoral thesis work of Annika Unger (née Wortmann) (83).

FUNDING

The study was supported by grants from the Universiätsklinikum Marburg und Giessen (01/2015 to TA and UW), from the DFG (RE 1590/1-1 to SR and MU 601/17-1 to RM), and from the Wilhelm-Sander-Stiftung (2016.123.1 to SM-B).

SUPPLEMENTARY MATERIAL

The Supplementary Material for this article can be found online at https://www.frontiersin.org/articles/10.3389/fimmu.2018.01425/full#supplementary-material.

REFERENCES

1. Bingle L, Brown NJ, Lewis CE. The role of tumour-associated macrophages in tumour progression: implications for new anticancer therapies. *J Pathol* (2002) 196(3):254–65. doi:10.1002/path.1027
2. Condeelis J, Pollard JW. Macrophages: obligate partners for tumor cell migration, invasion, and metastasis. *Cell* (2006) 124:263–6. doi:10.1016/j.cell.2006.01.007
3. Santin AD, Bellone S, Ravaggi A, Roman J, Smith CV, Pecorelli S, et al. Increased levels of interleukin-10 and transforming growth factor-β in the plasma and ascitic fluid of patients with advanced ovarian cancer. *BJOG* (2001) 108:804–8. doi:10.1111/j.1471-0528.2001.00206.x
4. Worzfeld T, Pogge von Strandmann E, Huber M, Adhikary T, Wagner U, Reinartz S, et al. The unique molecular and cellular microenvironment of ovarian cancer. *Front Oncol* (2017) 7:24. doi:10.3389/fonc.2017.00024
5. Reinartz S, Schumann T, Finkernagel F, Wortmann A, Jansen JM, Meissner W, et al. Mixed-polarization phenotype of ascites-associated macrophages in human ovarian carcinoma: correlation of CD163 expression, cytokine levels and early relapse. *Int J Cancer* (2013) 134(1):32–42. doi:10.1002/ijc.28335
6. Finkernagel F, Reinartz S, Lieber S, Adhikary T, Wortmann A, Hoffmann N, et al. The transcriptional signature of human ovarian carcinoma macrophages is associated with extracellular matrix reorganization. *Oncotarget* (2016) 7(46):75339–52. doi:10.18632/oncotarget.12180
7. Adhikary T, Wortmann A, Finkernagel F, Lieber S, Nist A, Stiewe T, et al. Interferon signaling in ascites-associated macrophages is linked to a favorable clinical outcome in a subgroup of ovarian carcinoma patients. *BMC Genomics* (2017) 18(1):243. doi:10.1186/s12864-017-3630-9
8. Yuan X, Zhang J, Li D, Mao Y, Mo F, Du W, et al. Prognostic significance of tumor-associated macrophages in ovarian cancer: a meta-analysis. *Gynecol Oncol* (2017) 147(1):181–7. doi:10.1016/j.ygyno.2017.07.007
9. Schneemann M, Schoedon G, Hofer S, Blau N, Guerrero L, Schaffner A. Nitric oxide synthase is not a constituent of the antimicrobial armature of human mononuclear phagocytes. *J Infect Dis* (1993) 167(6):1358–63. doi:10.1093/infdis/167.6.1358
10. Konur A, Krause SW, Rehli M, Kreutz M, Andreesen R. Human monocytes induce a carcinoma cell line to secrete high amounts of nitric oxide. *J Immunol* (1996) 157(5):2109–15.
11. Fang FC. Antimicrobial reactive oxygen and nitrogen species: concepts and controversies. *Nat Rev Microbiol* (2004) 2:820–32. doi:10.1038/nrmicro1004
12. Schneemann M, Schoeden G. Macrophage biology and immunology: man is not a mouse. *J Leukoc Biol* (2007) 81:579; discussion 580. doi:10.1189/jlb.1106702
13. Gross TJ, Kremens K, Powers LS, Brink B, Knutson T, Domann FE, et al. Epigenetic silencing of the human NOS2 gene: rethinking the role of nitric oxide in human macrophage inflammatory responses. *J Immunol* (2014) 192(5):2326–38. doi:10.4049/jimmunol.1301758

14. Balakrishnan A, Schnare M, Chakravortty D. Of men not mice: bactericidal/permeability-increasing protein expressed in human macrophages acts as a phagocytic receptor and modulates entry and replication of Gram-negative bacteria. *Front Immunol* (2016) 7:455. doi:10.3389/fimmu.2016.00455
15. Anzai R, Seki S, Ogasawara K, Hashimoto W, Sugiura K, Satoh M, et al. Interleukin-12 induces cytotoxic NK1 Ag+ αβ T cells in the lungs of euthymic and athymic mice. *Immunology* (1996) 88:82–9. doi:10.1046/j.1365-2567.1996.d01-638.x
16. Takeda K, Seki S, Ogasawara A, Anzai R, Hashimoto W, Sugiura K, et al. Liver NK1.1+CD4+ T cells activated by IL-12 as a major effector in inhibition of experimental tumor metastasis. *J Immunol* (1996) 156:3366–73.
17. Cui J, Shin T, Kawano T, Sato H, Kondo E, Toura I, et al. Requirement for Vα14 NKT cells in IL-12-mediated rejection of tumors. *Science* (1997) 278:1623–6. doi:10.1126/science.278.5343.1623
18. Kawamura T, Takeda K, Mendiratta SK, Kawamura H, Kaer LV, Yagita H, et al. Critical role of NK1+ T cells in IL-12-induced immune responses in vivo. *J Immunol* (1998) 160:16–9.
19. Kodama T, Takeda K, Shimozato O, Hayakawa Y, Atsuta M, Kobayashi K, et al. Perforin-dependent NK cell cytotoxicity is sufficient for anti-metastatic effect of IL-12. *Eur J Immunol* (1999) 29:1390–6. doi:10.1002/(SICI)1521-4141(199904)29:04<1390::AID-IMMU1390>3.0.CO;2-C
20. Gotlieb WH, Abrams JS, Watson JM, Velu TJ, Berek JS, Martinez-Maza O. Presence of interleukin 10 (IL-10) in the ascites of patients with ovarian and other intra-abdominal cancers. *Cytokine* (1992) 4(5):385–90. doi:10.1016/1043-4666(92)90082-3
21. Reinartz S, Finkernagel F, Adhikary T, Rohnalter V, Schumann T, Schober Y, et al. A transcriptome-based global map of signaling pathways in the ovarian cancer microenvironment associated with clinical outcome. *Genome Biol* (2016) 17:108. doi:10.1186/s13059-016-0956-6
22. Sica A, Saccani A, Bottazzi B, Polentarutti N, Vecchi A, van Damme J, et al. Autocrine production of IL-10 mediates defective IL-12 production and NF-kappa B activation in tumor-associated macrophages. *J Immunol* (2000) 164(2):762–7. doi:10.4049/jimmunol.164.2.762
23. Aste-Amezaga M, Ma X, Sartori A, Trinchieri G. Molecular mechanisms of the induction of IL-12 and its inhibition by IL-10. *J Immunol* (1998) 160:5936–44.
24. Smith A, Qualls J, O'Brien K, Balouzian L, Johnson P, Schultz-Cherry S, et al. A distal enhancer in Il12b is the target of transcriptional repression by the STAT3 pathway and requires the basic leucine zipper (B-ZIP) protein NFIL3. *J Biol Chem* (2011) 286(26):23582–90. doi:10.1074/jbc.M111.249235
25. D'Andrea A, Rengaraju M, Valiante NM, Chehimi J, Kubin M, Aste M, et al. Production of natural killer cell stimulatory factor (NKSF/IL-12) by peripheral blood mononuclear cells. *J Exp Med* (1992) 176(5):1387–98. doi:10.1084/jem.176.5.1387
26. Segal BM, Dwyer BK, Shevach EM. An interleukin (IL)-10/IL-12 immunoregulatory circuit controls susceptibility to autoimmune disease. *J Exp Med* (1998) 187(4):537–46. doi:10.1084/jem.187.4.537
27. Ma X, Yan W, Zheng H, Du Q, Zhang L, Ban Y, et al. Regulation of IL-10 and IL-12 production and function in macrophages and dendritic cells. *F1000Res* (2015) 4:1465. doi:10.12688/f1000research.7010.1
28. Buechler C, Ritter M, Orsó E, Langmann T, Klucken J, Schmitz G. Regulation of scavenger receptor CD163 expression in human monocytes and macrophages by pro- and antiinflammatory stimuli. *J Leukoc Biol* (2000) 67(1):97–103. doi:10.1002/jlb.67.1.97
29. Sulahian TH, Högger P, Wahner AE, Wardwell K, Goulding NJ, Sorg C, et al. Human monocytes express CD163, which is upregulated by IL-10 and identical to p155. *Cytokine* (2000) 12(9):1312–21. doi:10.1006/cyto.2000.0720
30. Philippidis P, Mason JC, Evans BJ, Nadra I, Taylor KM, Haskard DO, et al. Hemoglobin scavenger receptor CD163 mediates interleukin-10 release and heme oxygenase-1 synthesis. *Circ Res* (2004) 94:119–26. doi:10.1161/01.RES.0000109414.78907.F9
31. Hsieh CS, Macatonia SE, Tripp CS, Wolf S, O'Garra A, Murphy KM. Development of CD4+ T cells through IL-12 production by *Listeria*-induced macrophages. *Science* (1993) 260:547–9. doi:10.1126/science.8097338
32. Handel-Fernandez ME, Cheng X, Herbert LM, Lopez DM. Down-regulation of IL-12, not a shift from a T helper-1 to a T helper-2 phenotype, is responsible for impaired IFN-gamma production in mammary tumor-bearing mice. *J Immunol* (1997) 158(1):280–6.
33. Michel T, Hentges F, Zimmer J. Consequences of the crosstalk between monocytes/macrophages and natural killer cells. *Front Immunol* (2013) 3:403. doi:10.3389/fimmu.2012.00403
34. Duluc D, Corvaisier M, Blanchard S, Catala L, Descamps P, Gamelin E, et al. Interferon-gamma reverses the immunosuppressive and protumoral properties and prevents the generation of human tumor-associated macrophages. *Int J Cancer* (2009) 125(2):367–73. doi:10.1002/ijc.24401
35. Beatty G, Chiorean E, Fishman M, Saboury B, Teitelbaum U, Sun W, et al. CD40 agonists alter tumor stroma and show efficacy against pancreatic carcinoma in mice and humans. *Science* (2011) 331:1612–6. doi:10.1126/science.1198443
36. Rosenzweig S, Holland S. Defects in the interferon-γ and interleukin-12 pathways. *Immunol Rev* (2005) 203:38–47. doi:10.1111/j.0105-2896.2005.00227.x
37. Bustamante J, Picard C, Boisson-Dupuis S, Abel L, Casanova J-L. Genetic lessons learned from X-linked Mendelian susceptibility to mycobacterial diseases. *Ann N Y Acad Sci* (2011) 1246:92–101. doi:10.1111/j.1749-6632.2011.06273.x
38. Bustamante J, Boisson-Dupuis S, Abel L, Casanova J-L. Mendelian susceptibility to mycobacterial disease: genetic, immunological, and clinical features of inborn errors of IFN-γ immunity. *Semin Immunol* (2014) 26:454–70. doi:10.1016/j.smim.2014.09.008
39. Ma X, Chow J, Gri G, Carra G, Gerosa G, Wolf S, et al. The interleukin 12 p40 gene promoter is primed by interferon γ in monocytic cells. *J Exp Med* (1996) 183:147–57. doi:10.1084/jem.183.1.147
40. Mason N, Aliberti J, Caamano JC, Liou H-C, Hunter CA. Identification of *c*-Rel-dependent and -independent pathways of IL-12 production during infectious and inflammatory stimuli. *J Immunol* (2002) 168:2590–4. doi:10.4049/jimmunol.168.6.2590
41. Visekruna A, Volkov A, Steinhoff U. A key role for NF-κB transcription factor *c*-Rel in T-lymphocyte-differentiation and effector functions. *Clin Dev Immunol* (2012) 2012:239368. doi:10.1155/2012/239368
42. Sanjabi S, Williams K, Saccani S, Zhou L, Hoffmann A, Ghosh G, et al. A *c*-Rel subdomain responsible for enhanced DNA-binding affinity and selective gene activation. *Genes Dev* (2005) 19:2138–51. doi:10.1101/gad.1329805
43. Rahim SS, Khan N, Boddupalli CS, Hasnain SE, Mukhopadhyay S. Interleukin-10 (IL-10) mediated suppression of IL-12 production in RAW 264.7 cells also involves c-rel transcription factor. *Immunology* (2005) 114(3):313–21. doi:10.1111/j.1365-2567.2005.02107.x
44. Saccani A, Schioppa T, Porta C, Biswas SK, Nebuloni M, Vago L, et al. p50 nuclear factor-kappaB overexpression in tumor-associated macrophages inhibits M1 inflammatory responses and antitumor resistance. *Cancer Res* (2006) 66:11432–40. doi:10.1158/0008-5472.CAN-06-1867
45. Wang P, Wu P, Siegel MI, Egan RW, Billah MM. IL-10 inhibits transcription of cytokine genes in human peripheral blood mononuclear cells. *J Immunol* (1994) 153(2):811–6.
46. Schottelius AJG, Mayo MW, Balfour Sartor R, Baldwin ASJ. Interleukin-10 signaling blocks inhibitor of kB kinase activity and nuclear factor kB DNA binding. *J Biol Chem* (1999) 274:31868–74. doi:10.1074/jbc.274.45.31868
47. Lentsch AB, Shanley TP, Sarma V, Ward PA. In vivo suppression of NF-kappa B and preservation of I kappa B alpha by interleukin-10 and interleukin-13. *J Clin Invest* (1997) 100(10):2443–8. doi:10.1172/JCI119786
48. Guescini M, Sisti D, Rocchi M, Stocchi L, Stocchi V. A new real-time PCR method to overcome significant quantitative inaccuracy due to slight amplification inhibition. *BMC Bioinformatics* (2008) 9:326. doi:10.1186/1471-2105-9-326
49. Adhikary T, Wortmann A, Schumann T, Finkernagel F, Lieber S, Roth K, et al. The transcriptional PPARβ/δ network in human macrophages defines a unique agonist-induced activation state. *Nucleic Acids Res* (2015) 43(10):5033–51. doi:10.1093/nar/gkv331
50. Adhikary T, Müller R. In vivo studies of PPAR-chromatin interactions: chromatin immunoprecipitation for single-locus and genomewide analyses. *Methods Mol Biol* (2013) 952:175–85. doi:10.1007/978-1-62703-155-4_12
51. Saccani S, Pantano S, Natoli G. Two waves of nuclear factor κb recruitment to target promoters. *J Exp Med* (2001) 193(12):1351. doi:10.1084/jem.193.12.1351
52. Worzfeld T, Finkernagel F, Reinartz S, Konzer A, Adhikary T, Nist A, et al. Proteotranscriptomics reveal signaling networks in the ovarian cancer microenvironment. *Mol Cell Proteomics* (2018) 17(2):270–89. doi:10.1074/mcp.RA117.000400
53. Brown K, Park S, Kanno T, Franzoso G, Siebenlist U. Mutual regulation of the transcriptional activator NF-kappa B and its inhibitor, I kappa B-alpha. *Proc Natl Acad Sci U S A* (1993) 90(6):2532–6. doi:10.1073/pnas.90.6.2532

54. Bunting K, Rao S, Hardy K, Woltring D, Denyer GS, Wang J, et al. Genome-wide analysis of gene expression in T cells to identify targets of the NF-kB transcription factor c-Rel. *J Immunol* (2007) 178:7097–109. doi:10.4049/jimmunol.178.11.7097
55. Chin M, Herscovitch M, Zhang N, Waxman DJ, Gilmore TD. Overexpression of an activated REL mutant enhances the transformed state of the human B-lymphoma BJAB cell line and alters its gene expression profile. *Oncogene* (2009) 28:2100–11. doi:10.1038/onc.2009.74
56. van Essen D, Zhu Y, Saccani S. A feed-forward circuit controlling inducible NF-κB target gene activation by promoter histone demethylation. *Mol Cell* (2010) 39(5):750–60. doi:10.1016/j.molcel.2010.08.010
57. Clarke DL, Clifford RL, Jindarat S, Proud D, Pang L, Belvisi M, et al. TNFα and IFN-γ synergistically enhance transcriptional activation of *CXCL10* in human airway smooth muscle cells via STAT-1, NF-κB, and the transcriptional coactivator CREB-binding protein. *J Biol Chem* (2020) 285:29101–10. doi:10.1074/jbc.M109.099952
58. Piunti A, Shilatifard A. Epigenetic balance of gene expression by polycomb and COMPASS families. *Science* (2016) 352(6290):aad9780. doi:10.1126/science.aad9780
59. Kim T-Y, Shiekhattar R. Diverse regulatory interactions of long noncoding RNAs. *Curr Opin Genet Dev* (2016) 36:73–82. doi:10.1016/j.gde.2016.03.014
60. Huang D-B, Chen Y-Q, Ruetsche M, Phelps CB, Ghosh G. X-ray crystal structure of proto-oncogene product c-Rel bound to the CD28 response element of IL-2. *Structure* (2001) 9(8):669–78. doi:10.1016/S0969-2126(01)00635-9
61. Barski A, Cuddapah S, Cui K, Roh T-Y, Schones DE, Wang Z, et al. High-resolution profiling of histone methylations in the human genome. *Cell* (2007) 129:823–37. doi:10.1016/j.cell.2007.05.009
62. Jung M, Kadam S, Xiong W, Rauch TA, Jin S-G, Pfeifer GP. MIRA-seq for DNA methylation analysis of CpG islands. *Epigenomics* (2015) 7(5):695–706. doi:10.2217/epi.15.33
63. Kuo H-C, Lin P-Y, Chung T-C, Chao C-M, Lai L-C, Tsai M-H, et al. DBCAT: database of CpG islands and analytical tools for identifying comprehensive methylation profiles in cancer cells. *J Comput Biol* (2011) 18(8):1013–7. doi:10.1089/cmb.2010.0038
64. Hilliard BA, Mason N, Xu L, Sun J, Lamhamedi-Cherradi S-E, Liou H-C, et al. Critical roles of c-Rel in autoimmune inflammation and helper T cell differentiation. *J Clin Invest* (2002) 110(6):843–50. doi:10.1172/JCI0215254
65. Sanjabi S, Hoffmann A, Liou H-C, Baltimore D, Smale ST. Selective requirement for c-Rel during IL-12 P40 gene induction in macrophages. *Proc Natl Acad Sci U S A* (2000) 97(23):12705–10. doi:10.1073/pnas.230436397
66. Stearns M, Kim G, Garcia F, Wang M. Interleukin-10 induced activating transcription factor 3 transcriptional suppression of matrix metalloproteinase-2 gene expression in human prostate CPTX-1532 cells. *Mol Cancer Res* (2004) 2(7):403–16.
67. Gilchrist M, Thorsson V, Li B, Rust A, Korb M, Roach J, et al. Systems biology approaches identify ATF3 as a negative regulator of toll-like receptor 4. *Nature* (2006) 441:173–8. doi:10.1038/nature04768
68. Whitmore M, Iparraguirre A, Kubelka L, Weninger W, Hai T, Williams B. Negative regulation of TLR-signaling pathways by activating transcription factor-3. *J Immunol* (2007) 179:3622–30. doi:10.4049/jimmunol.179.6.3622
69. Lang R, Patel D, Morris JJ, Rutschman RL, Murray P. Shaping gene expression in activated and resting primary macrophages by IL-10. *J Immunol* (2002) 169:3353–63. doi:10.4049/jimmunol.169.5.2253
70. Ramana CV, Gil MP, Han Y, Ransohoff R, Schreiber RD, Stark GR. Stat1-independent regulation of gene expression in response to IFN-γ. *Proc Natl Acad Sci U S A* (2001) 98(12):6674–9. doi:10.1073/pnas.111164198
71. de Paus RA, Kilic SS, van Dissel JT, van de Vosse E. Effect of amino acid substitutions in the human IFN-γR2 on IFN-γ responsiveness. *Genes Immun* (2011) 12:136–44. doi:10.1038/gene.2010.74
72. Tamassia N, Calzetti F, Ear T, Cloutier A, Gasperini S, Bazzoni F, et al. Molecular mechanisms underlying the synergistic induction of CXCL10 by LPS and IFN-γ in human neutrophils. *Eur J Immunol* (2007) 37:2627–34. doi:10.1002/eji.200737340
73. van der Pouw Kraan TC, Boeije LC, Smeenk RJ, Wijdenes J, Aarden LA. Prostaglandin-E2 is a potent inhibitor of human interleukin 12 production. *J Exp Med* (1995) 181:775–9. doi:10.1084/jem.181.2.775
74. Link A, Kino T, Worth JA, McGuire JL, Crane ML, Chrousos GP, et al. Ligand-activation of the adenosine A2a receptors inhibits IL-12 production by human monocytes. *J Immunol* (2000) 164(1):436–42. doi:10.4049/jimmunol.164.1.436
75. Haskó G, Kuhel DG, Chen JF, Schwarzschild MA, Deitch EA, Mabley JG, et al. Adenosine inhibits IL-12 and TNF-α production via adenosine A2a receptor-dependent and independent mechanisms. *FASEB J* (2000) 14(13):2065–74. doi:10.1096/fj.99-0508com
76. Panther E, Idzko M, Corinti S, Ferrari D, Herouy Y, Mockenhaupt M, et al. The influence of lysophosphatidic acid on the functions of human dendritic cells. *J Immunol* (2002) 169(8):4129–35. doi:10.4049/jimmunol.169.8.4129
77. Zhang M, Fritsche KL. Fatty acid-mediated inhibition of IL-12 production by murine macrophages is independent of PPARgamma. *Br J Nutr* (2004) 91(5):733–9. doi:10.1079/BJN20041096
78. Um SH, Mulhall C, Alisa A, Ives AR, Karani J, Williams R, et al. α-Fetoprotein impairs APC function and induces their apoptosis. *J Immunol* (2004) 173(3):1772–8. doi:10.4049/jimmunol.173.3.1772
79. Yamamoto M, Tatsumi T, Miyagi T, Tsunematsu H, Aketa H, Hosui A, et al. α-Fetoprotein impairs activation of natural killer cells by inhibiting the function of dendritic cells. *Clin Exp Immunol* (2011) 165(2):211–9. doi:10.1111/j.1365-2249.2011.04421.x
80. Xing J, Weng L, Yuan B, Wang Z, Jia L, Jin R, et al. Identification of a role for TRIM29 in the control of innate immunity in the respiratory tract. *Nat Immunol* (2016) 17(12):1373–80. doi:10.1038/ni.3580
81. Ghisletti S, Huang W, Jepsen K, Benner C, Hardiman G, Rosenfeld MG, et al. Cooperative NCoR/SMRT interactions establish a corepressor-based strategy for integration of inflammatory and anti-inflammatory signaling pathways. *Genes Dev* (2009) 23(6):681–93. doi:10.1101/gad.1773109
82. Cao S, Liu J, Chesi M, Bergsagel PL, Ho I-C, Donnelly RP, et al. Differential regulation of IL-12 and IL-10 gene expression in macrophages by the basic leucine zipper transcription factor c-Maf fibrosarcoma. *J Immunol* (2002) 169(19):5715–25. doi:10.4049/jimmunol.169.10.5715
83. Unger A. *Suppression proinflammatorischer Gene in Makrophagen durch Aszites des Ovarialkarzinoms [PhD thesis]*. Marburg: Philipps University of Marburg (2017).

Conflict of Interest Statement: The authors declare that the research was conducted in the absence of any commercial or financial relationships that could be construed as a potential conflict of interest.

Supplementary Material: Chromatin binding of *c*-REL and p65 is not limiting for macrophage *IL12B* transcription during immediate suppression by ovarian carcinoma ascites

FIGURE CAPTIONS

1. Pretreatment with IFNγ does not lead to elevated p40 synthesis by MDMs cultivated in RPMI supplemented with adult human serum. MDMs were differentiated for 6–7 d in RPMI 1640 media supplemented with 5 % adult human AB serum (R5) and treated with IFNγ for the indicated periods of time prior to stimulation with LPS and IFNγ together or with vehicle for 24 h. IL-12p40 concentrations in culture supernatants were measured by ELISA. Two biological replicates denoted by colored symbols are shown.
2. Kinetics of *IL12B* induction and REL nuclear translocation in MDMs. MDMs were differentiated for 6–7 d in R5 media and incubated with vehicle or LPS and IFNγ for the indicated periods of time. **(A)** RT-qPCR was used to measure *IL12B* transcript levels (N=2). Dots represent mean values. **(B)** REL localisation was detected by immunoblotting after subcellular fractionation. LDH and acetylated histone H3 were used as both loading and fractionation controls. CE, cytoplasmic extract; NE, nuclear extract.
3. Macrophage M2 surface markers do not reflect immediate suppression of *IL12B* by ascites. MDM cultures (N=6) were differentiated in R5 media, in ascites, in ascites in the presence of 50 ng/ml recombinant for 7 d, or in R5 media for 6 d followed by ascites for 1 d. Cells were analysed by flow cytometry using α-CD163 **(A)** and α-CD206 **(B)** as probes. Data were plotted as percentage of positive cells or MFI (mean fluorescence index) as indicated. Each color denotes an individual donor, and donor MDMs were randomly combined with different ascites samples. Horizontal bars denote median values.
4. Degradation and translocation of NFκB pathway components (representative immunoblots). MDMs were differentiated in R5 media or in ascites and cultivated consecutively as indicated. Cells were incubated with vehicle or LPS and IFNγ for 2.5 h. **(A)** Whole-cell lysates were blotted, and membranes were probed with antibodies against IκB proteins as indicated. β-actin was used as a loading control. Relative calculated protein amounts are included in the panel. One representative blot is shown. **(B,C)** Cellular fractions were blotted, and membranes were probed with antibodies against REL or p65. LDH and acetylated histone H3 were used as both loading and fractionation controls. Relative calculated protein amounts are included in the panel. One representative blot is shown. CE, cytoplasmic extract; NE, nuclear extract.
5. Stimulus-dependent protein levels of IκBα, β and ε are not differentially affected upon exposure to ascites. **(A–C)** MDMs were differentiated in R5 media or in ascites and cultivated consecutively as indicated. Cells were incubated with or without LPS and IFNγ for 2.5 h, harvested and lysed. After immunoblotting of whole cell lysates, levels of IκB family members α (**A**, two biological replicates),

β (**B**, three biological replicates) and ε (**C**, three biological replicates) relative to the corresponding unstimulated sample were determined. Mean values are indicated by horizontal bars.

6. Induction of *CXCL10* expression is not prevented in the presence of ascites. *CXCL10* expression was measured by qRT-PCR in a subset of samples shown in fig. 2. MDMs were differentiated in R5 media or in ascites and cultivated consecutively as indicated. Stimulation was with LPS and IFNγ for 24 h prior to harvesting. Each symbol denotes a biological replicate (MDM donor). **(A)** Induction after differentiation in normal media, after short-term exposure to ascites, and after short-term exposure and withdrawal as indicated (N=4), samples correspond to fig. 2A. **(B)** Induction after differentiation in normal media, after long-term exposure to ascites, and after long-term exposure and withdrawal as indicated (N=3; cells from each donor were exposed to 1–3 different ascites samples as indicated; samples correspond to fig. 2C). Colors encode ascites samples from four (panel A) or three (panel B) different patients; shapes encode different healthy donors. The code is consistent with fig. 2A,C. Median values are indicated by horizontal bars. Statistical significances were calculated with paired t tests; *, $p<0.05$; ns, not significant.
7. MDMs differentiated in R5 media for 6–7 d (N=3) were transfected with siRNA as indicated, incubated for 24 h, stimulated with or without LPS and (+) or their respective solvents (vehicle; −) for an additional 24 h, and *IL12B* expression was measured by RT-qPCR. Black dots, Viromer transfection reagent; blue and green dots, Trans-IT X2 transfection reagent. Median values are indicated by horizontal bars. Each dot denotes a biological replicate. Statistical significances were calculated with paired t tests; ns, not significant ($p>0.05$).
8. Functionality of siRNA sequences on protein level (representative immunoblots). MDMs were differentiated for 6–7 d in R5 media. Cells were transfected with siRNA as indicated and incubated for 48 h. After immunoblotting of whole cell lysates, relative REL and p65 levels were calculated using LDH as a loading control. Relative calculated protein amounts are included in the panel. One representative blot is shown.
9. Chromatin marks at the *IL2* and *CXCL10* loci in TAMs and MDMs. **(A,B)** Genome browser snapshots including ChIP-seq tracks for α-H3K4me3, α-H3K4me1, α-H3K9me3, α-H3K27me3, α-C/EBPβ, α-H3K27ac, α-H3K36me3, IgG (unspecific polyclonal rabbit IgG pool) and MIRA from a TAM sample freshly isolated from ovarian carcinoma ascites encompassing the *IL2* (**A**) and *CXCL10* (**B**) genes. Regions of interest are highlighted with rectangles. **(C,D)** ChIP-qPCR analyses of the indicated histone marks in MDMs differentiated in normal media, in ascites, or in normal media followed by ascites for 1 d (the same samples as in figs. 6 and 7 are shown). Primers for the *CXCL10* 5000 bp upstream region (**C**) or the *CXCL10* TSS (**D**) were used, respectively. Each dot denotes a biological replicate ($N\geq3$); for each replicate, MDMs from six donors were pooled after harvesting of the cells. Median values are indicated by horizontal bars. Colors encode ascites samples from individual patients, and colors are consistent between panels within this figure and figs. 6 and 7.
10. Original immunoblot images used for compilation of fig. 3. Please note that some of the blots are also shown in fig. S4. MDMs were differentiated in R5 media or in ascites and cultivated consecutively as indicated. Cells were incubated with vehicle or LPS and IFNγ for 2.5 h. Cellular fractions were blotted, and membranes were probed with antibodies against REL or p65. LDH and acetylated histone H3 or lamin B were used as both loading and fractionation controls. Relative calculated protein amounts are included in the panel. CE, cytoplasmic extract; NE, nuclear extract.

0.1 Figures

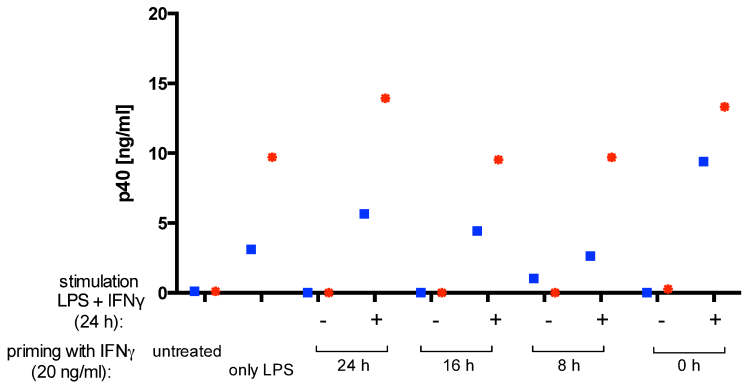

Figure S1: Pretreatment with IFNγ does not lead to elevated p40 synthesis by MDMs cultivated in RPMI supplemented with adult human serum.

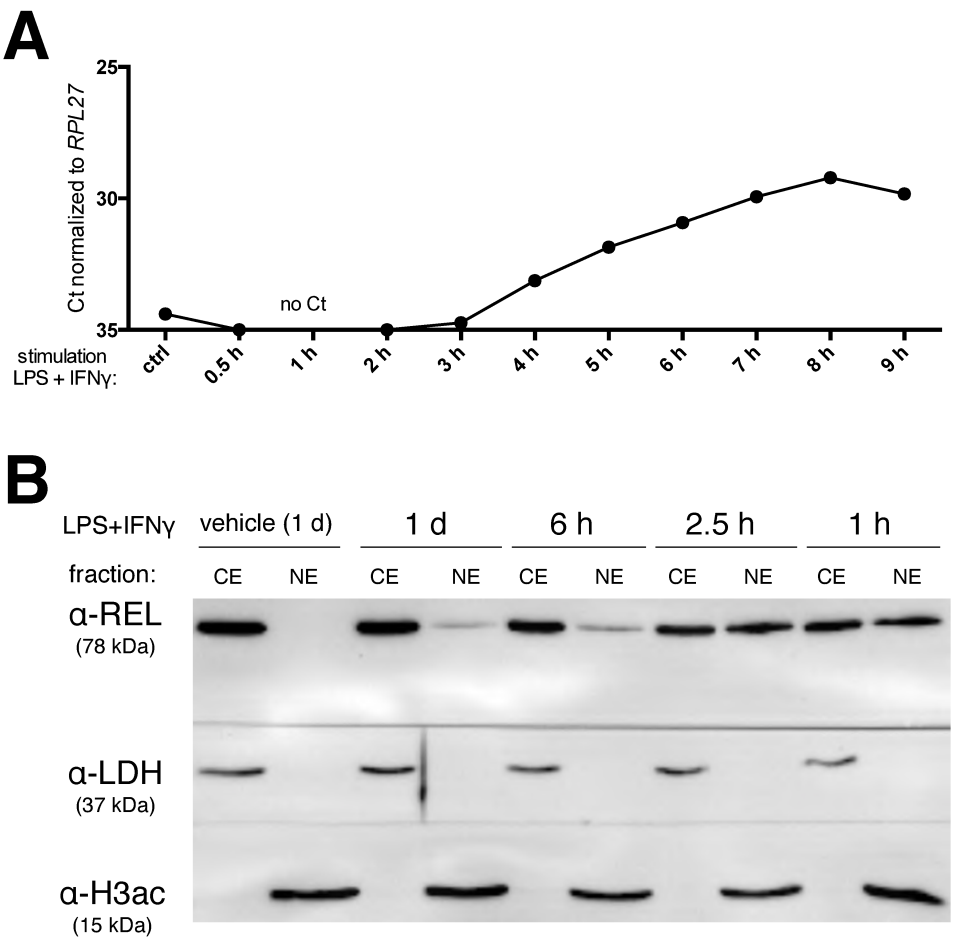

Figure S2: Kinetics of *IL12B* induction and REL nuclear translocation in MDMs.

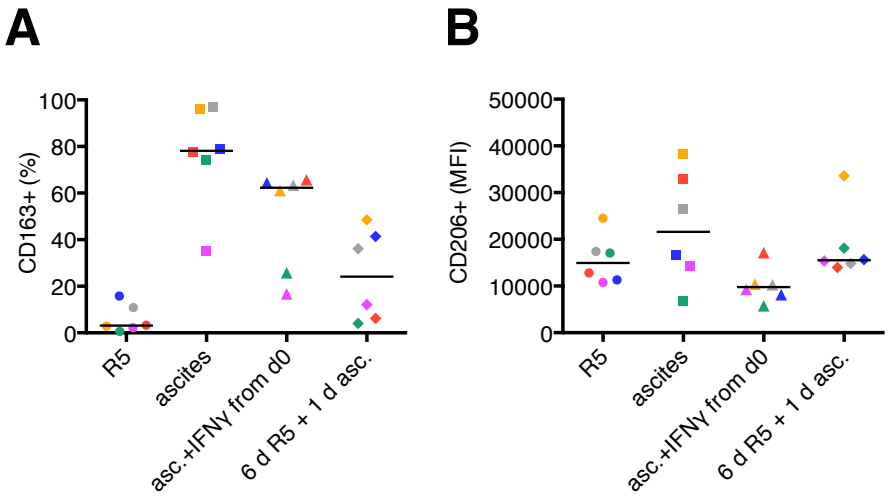

Figure S3: Macrophage M2 surface markers do not reflect immediate suppression of *IL12B* by ascites.

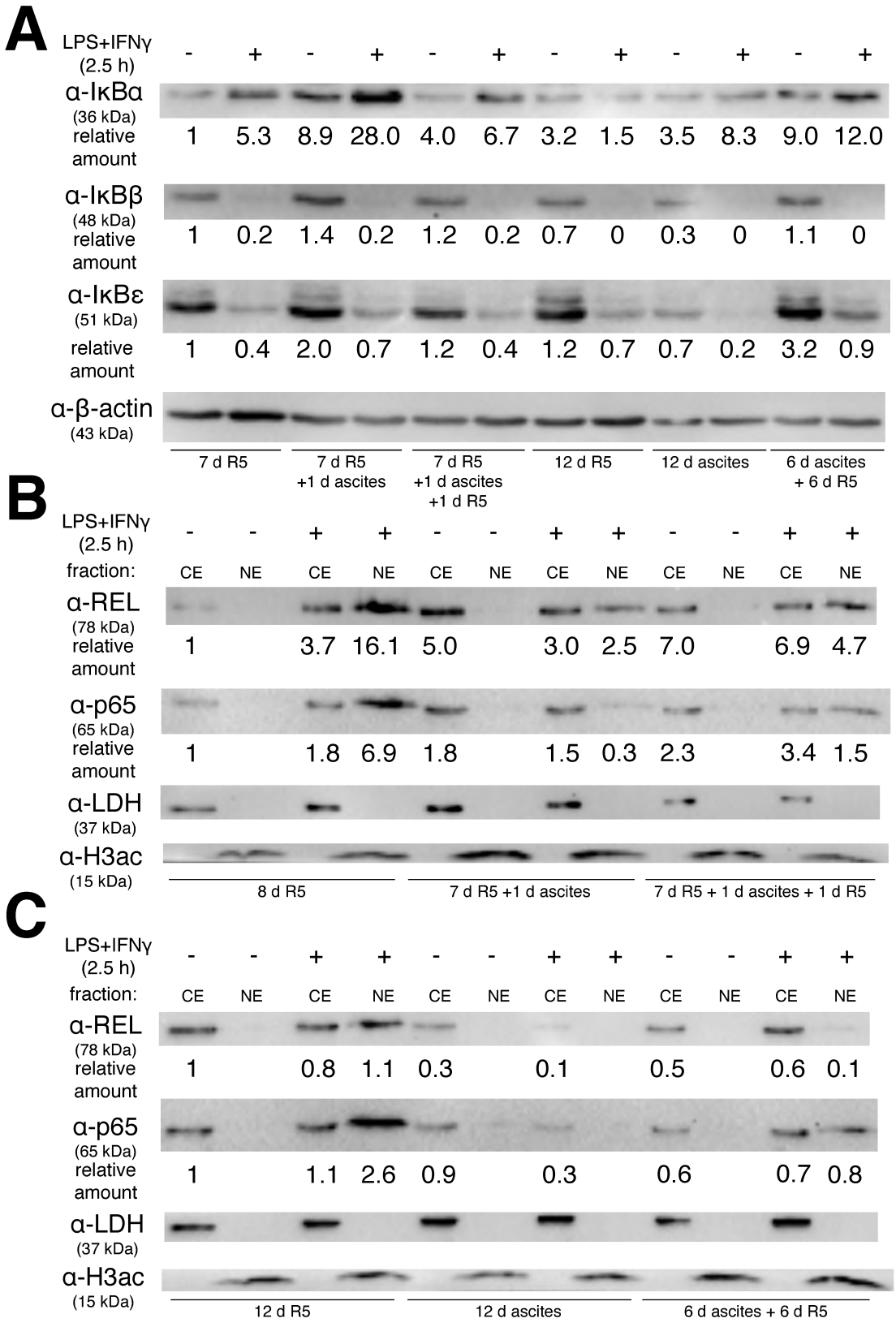

Figure S4: Degradation and translocation of NFκB pathway components (representative immunoblots).

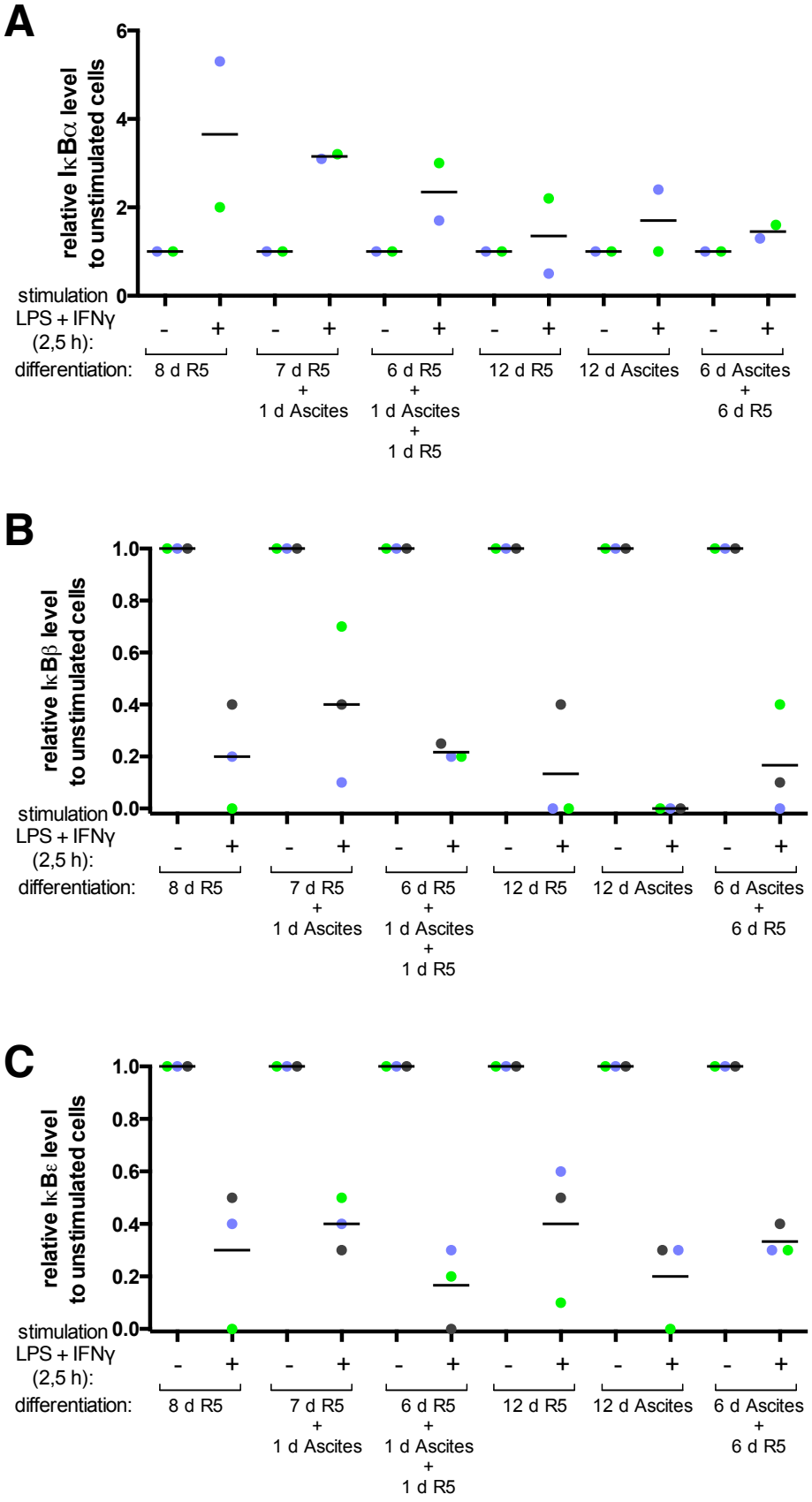

Figure S5: Stimulus-dependent protein levels of IκBα, β and ε are not differentially affected upon exposure to ascites.

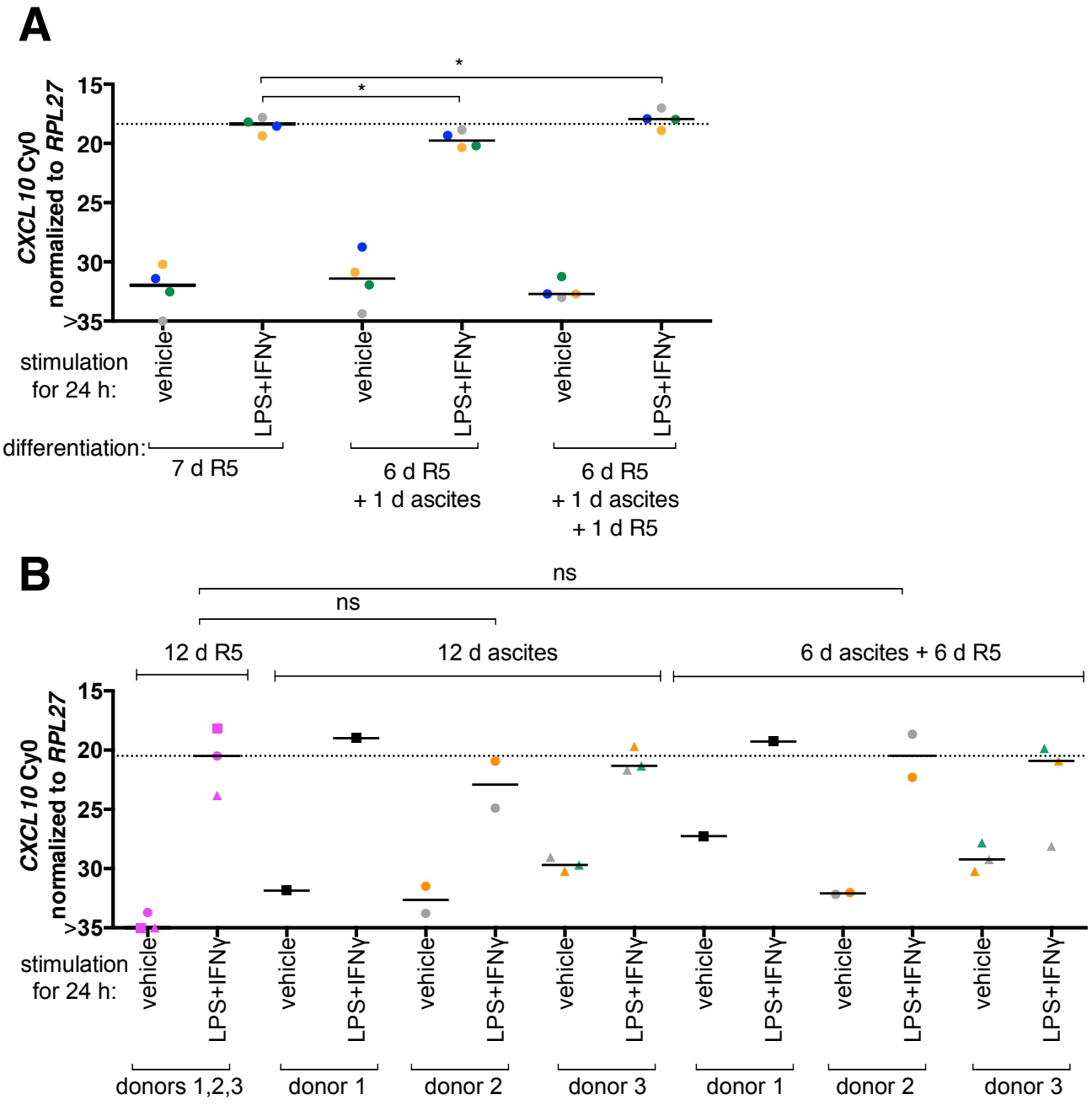

Figure S6: Induction of *CXCL10* expression is not prevented in the presence of ascites.

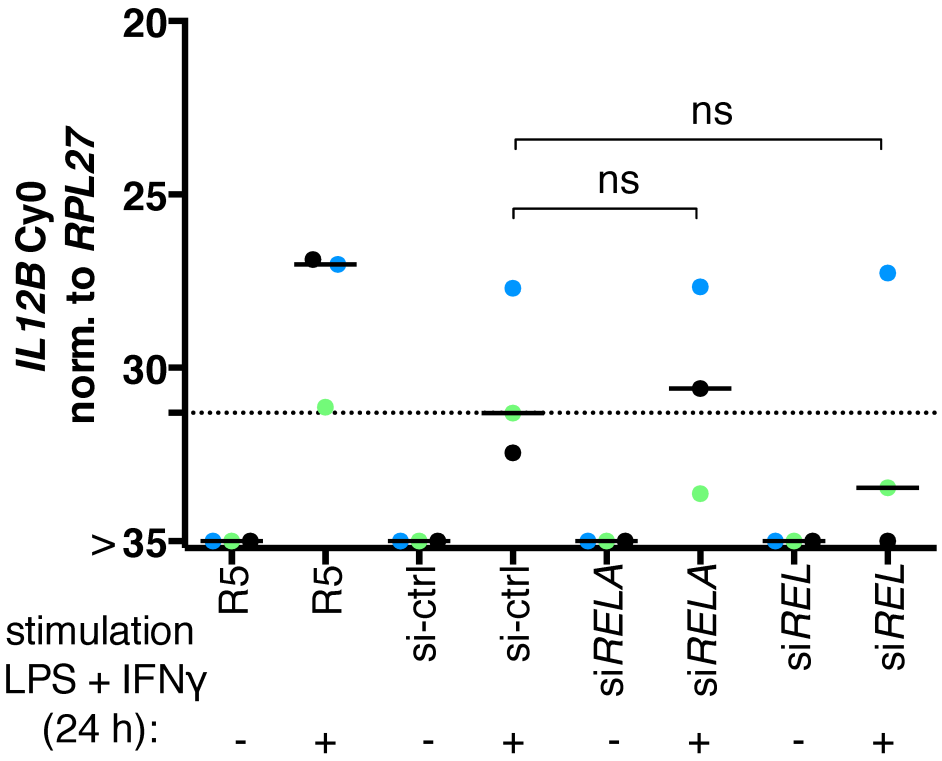

Figure S7: Induction of IL-12p40 expression after *REL* knockdown.

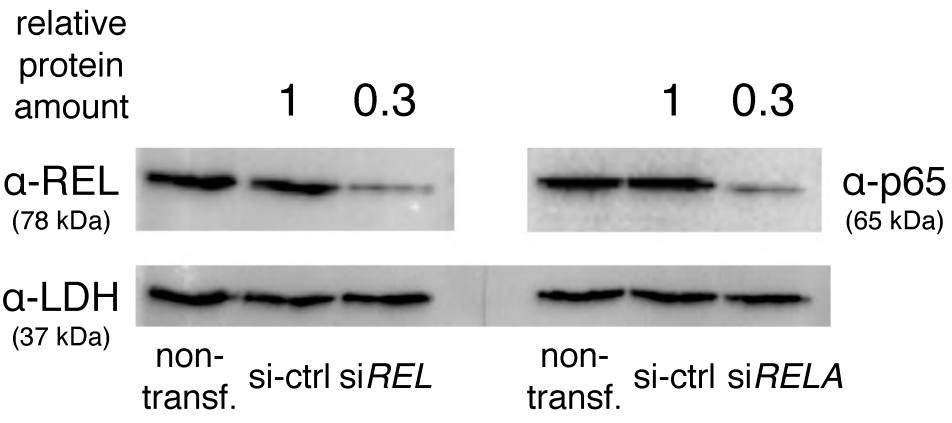

Figure S8: Functionality of siRNA sequences on protein level (representative immunoblots).

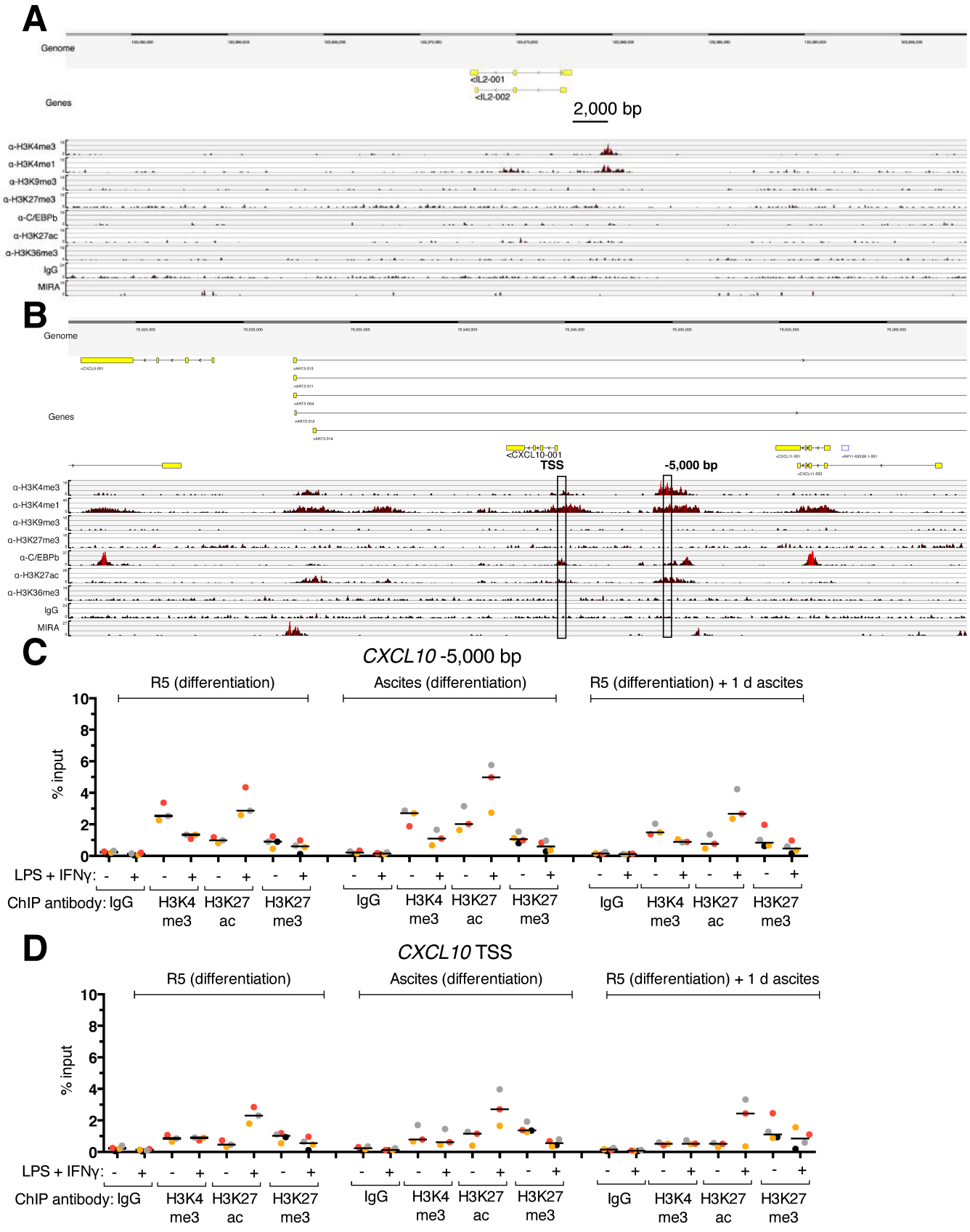

Figure S9: Chromatin marks at the *IL2* and *CXCL10* loci in TAMs and MDMs.

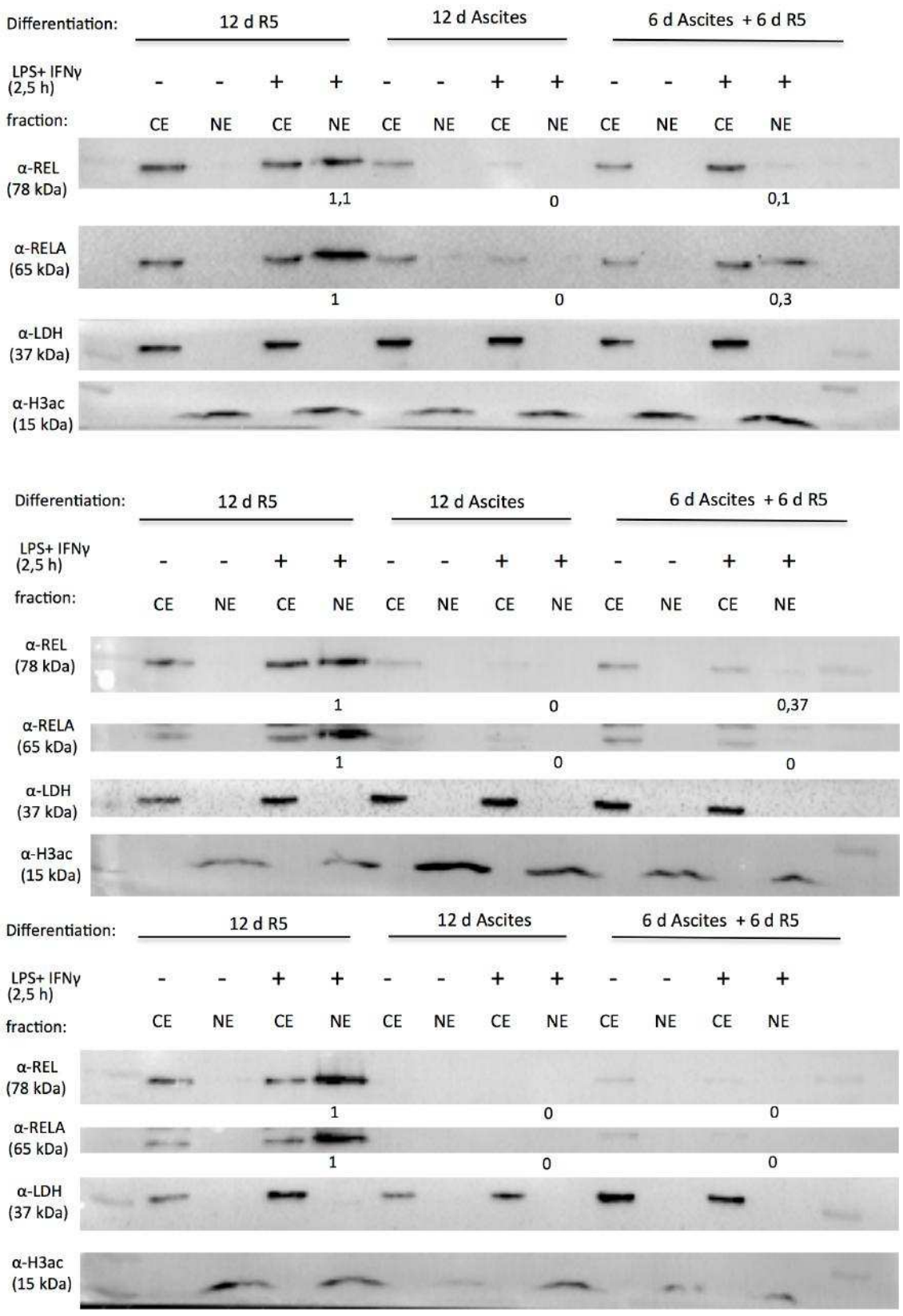

Figure S10: Original immunoblot images used for compilation of fig. 3.

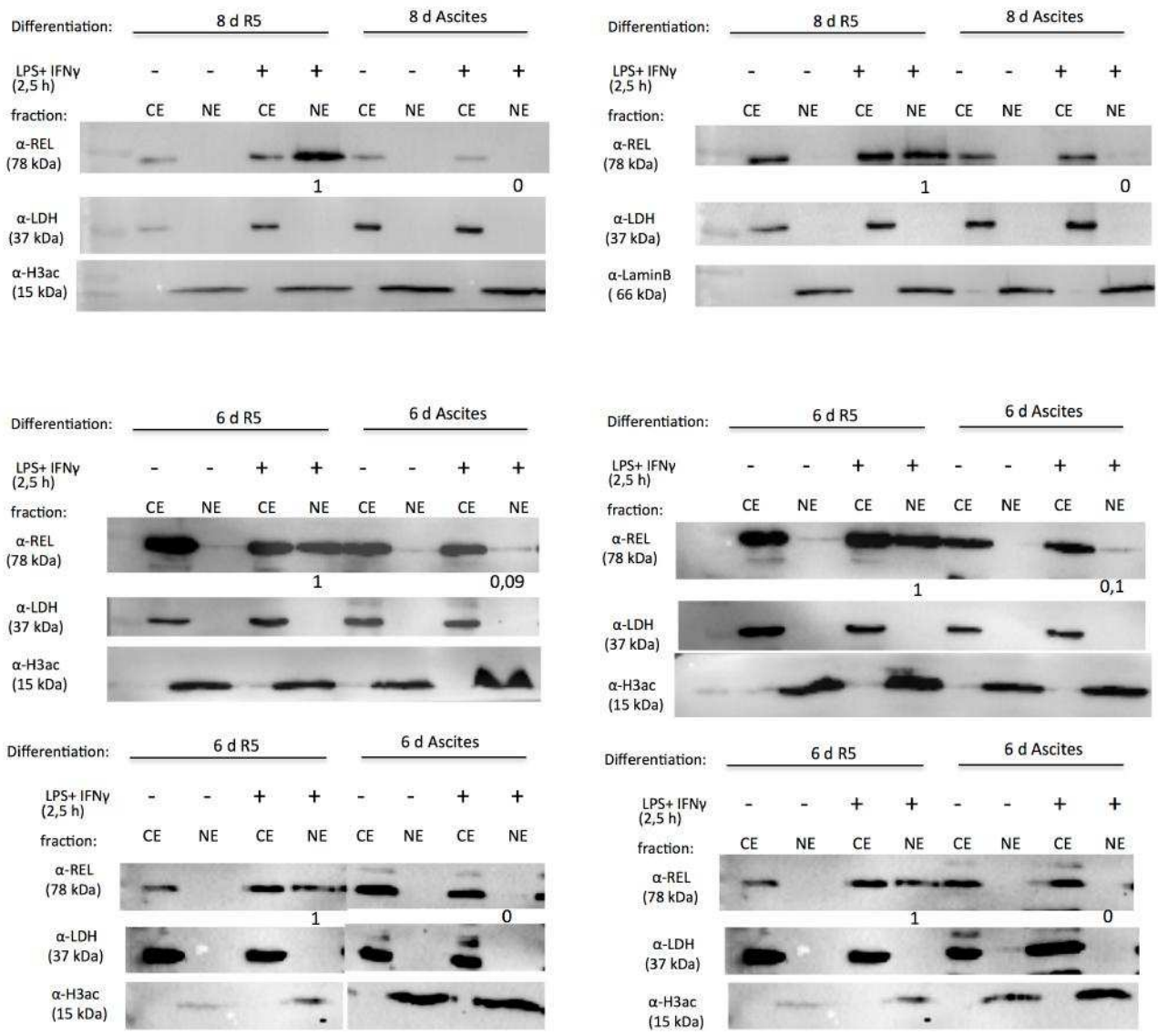

Figure S10: Original immunoblot images used for compilation of fig. 3.

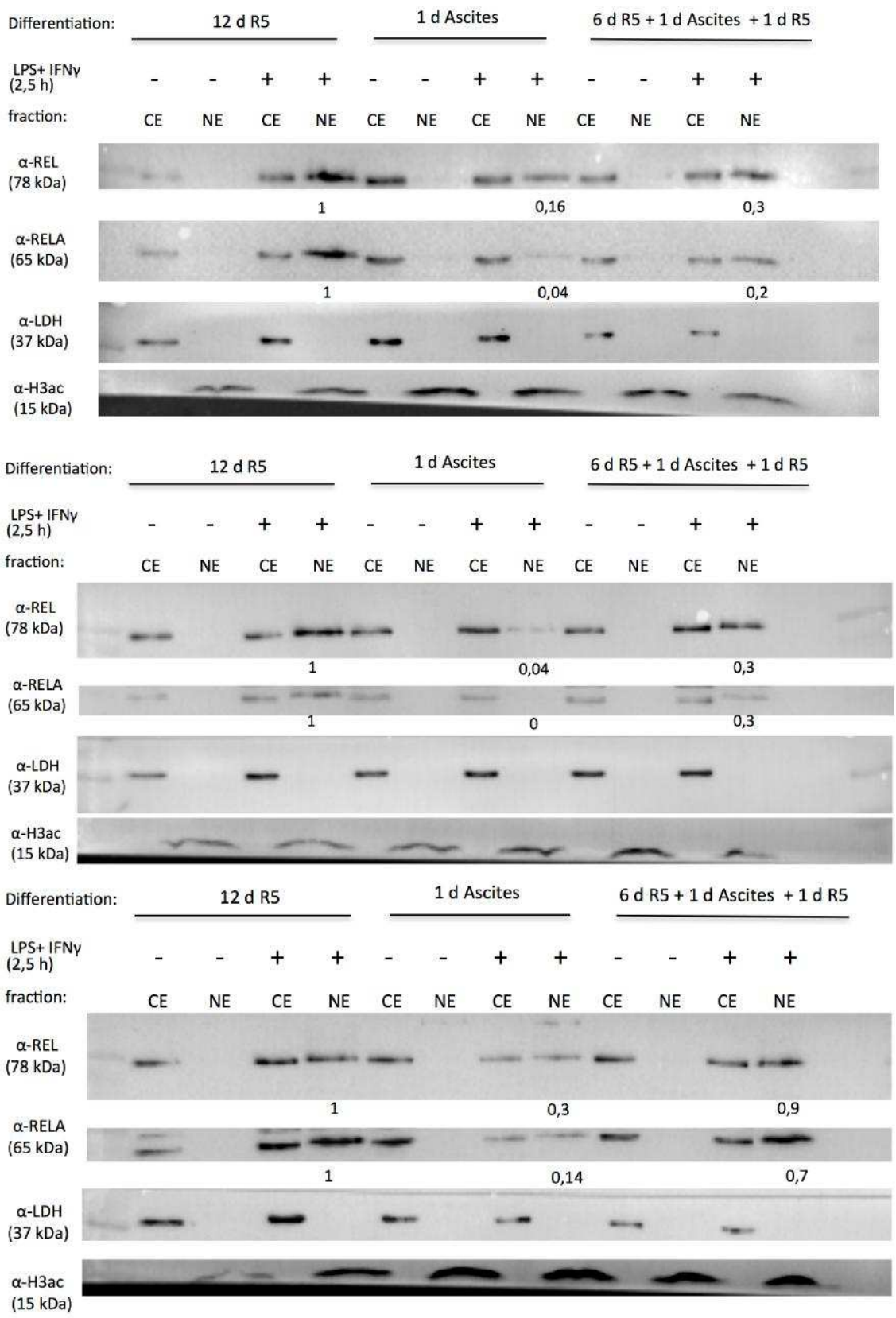

Figure S10: Original immunoblot images used for compilation of fig. 3.

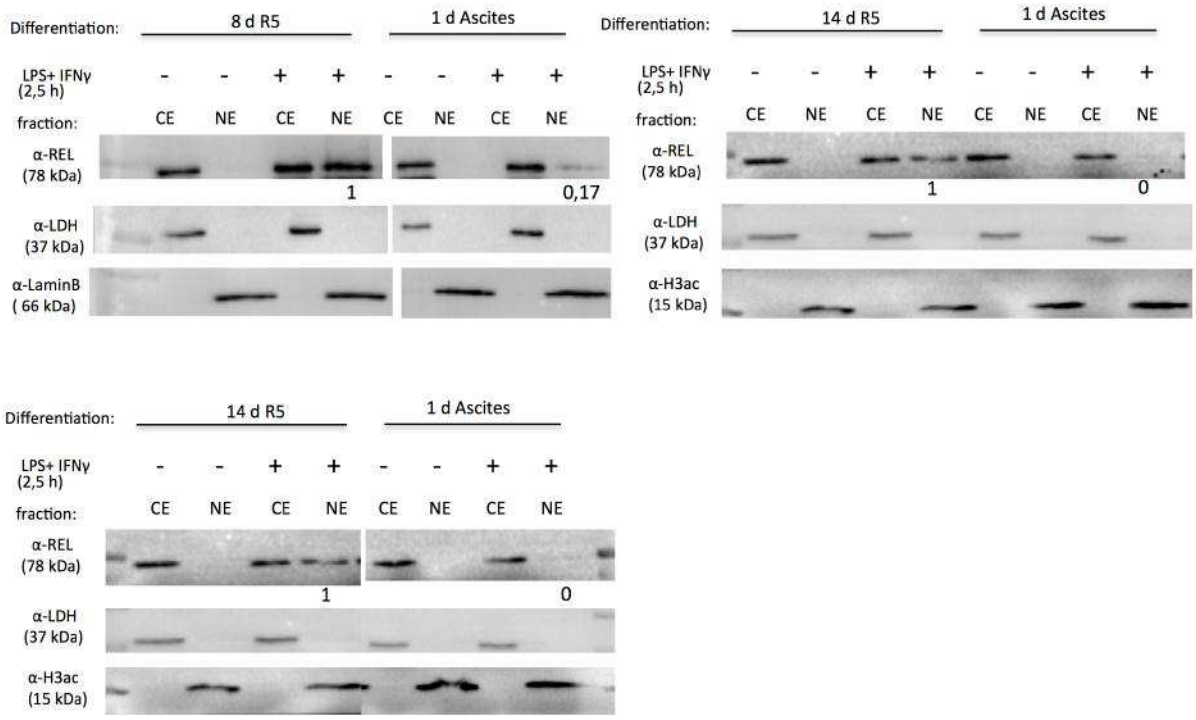

Figure S10: Original immunoblot images used for compilation of fig. 3.